

CHARLES UNIVERSITY IN PRAGUE

FACULTY OF SCIENCE

Dissertation



**TARGETING MITOCHONDRIA TO OVERCOME RESISTANCE OF
BREAST CANCER TO THERAPY**
**MITOCHONDRIE JAKO CÍL PŘI REZISTENCI RAKOVINY PRSU K
TERAPII**

Mgr. Kateřina Rohlenová

Supervisor: Prof. Ing. Jiří Neužil, CSc.

INSTITUTE OF BIOTECHNOLOGY, CZECH ACADEMY OF SCIENCES

PRAGUE, 2016

This thesis was composed at the Institute of Biotechnology, Czech Academy of Sciences, in the Laboratory of Molecular Therapy. Experimental data included herein were published in three original research articles, two review articles, and one book chapter.

I hereby declare that I have written this thesis independently, and all resources as well as co-authors were properly indicated. I also declare that I did not submit this thesis or a part of it, to obtain any other academic degree.

Prague, 2016 Kateřina Rohlenová

Here, I would like to express my gratitude to my supervisor professor Jiří Neuzil for his guidance, encouragement and advice. With his help I was able to step into the fascinating world of science, for which I will always be grateful. My thanks go also to all my colleagues from Laboratory of Molecular Therapy.

More generally, I am thankful to my alma mater, the Charles University, Faculty of Science, where I learned the principles and obtained the support to try to discover a piece of knowledge by my own.

TABLE OF CONTENTS

Table of Contents.....	4
Abstract (EN).....	7
Keywords.....	8
Abstract (CZ).....	9
Klíčová slova.....	10
List of Abbreviations.....	11
1. Introduction.....	13
1.1. HER2/ERBB2.....	15
1.2. Tumour heterogeneity.....	16
1.2.1. Genomic heterogeneity.....	16
1.2.2. Cancer stem cells.....	17
1.2.3. Metabolic heterogeneity.....	20
1.3. Mitochondria and cancer.....	21
1.3.1. Oxidative phosphorylation.....	24
1.3.2. Reactive oxygen species (ROS).....	31
1.3.3. Mitochondria in cell death induction.....	33
1.3.4. Mitochondrially targeted anti-cancer compounds.....	38
1.3.5. Mitochondrially localised HER2 oncogene.....	41
2. Aims.....	44

3. List of methods	45
4. Publications.....	47
4.1. List of publications.....	47
4.1.1. Rohlenova K, Sachaphibulkij K, Stursa J, Bezework-Geleta A, Blecha J, Endaya B, Werner L, Cerny J, Zobalova R, Goodwin J, Spacek T, Pesdar EA, Yan B, Nguyen MN, Vondrusova M, Sobol M, Jezek P, Hozak P, Truksa J, Rohlena J, Dong LF, Neuzil J. Selective disruption of respiratory supercomplexes as a new strategy to suppress Her2^{high} breast cancer. Antioxid Redox Sign. 2016 Jul 8.....	47
4.1.2. Rohlenova K, Neuzil J, Rohlena J. The role of Her2 and other oncogenes of the PI3K/AKT pathway in mitochondria. Biol Chem. 2016 Jul 1;397:607-15... 	48
4.1.3. Yan B, Stantic M, Zobalova R, Bezawork-Geleta A, Stapelberg M, Stursa J, Prokopova K, Dong LF, Neuzil J. Mitochondrially targeted vitamin E succinate efficiently kills breast tumour-initiating cells in a complex II-dependent manner. BMC Cancer. 2015 May 15:401.....	49
4.1.4. Stapelberg M, Zobalova R, Nguyen MN, Walker T, Stantic M, Goodwin J, Pasdar EA, Thai T, Prokopova K, Yan B, Hall S, de Pennington N, Thomas SR, Grant G, Stursa J, Bajzikova M, Meedeniya ACB, Truksa J, Ralph SJ , Ansorge O, Dong LF, Neuzil J. Indoleamine-2,3-dioxygenase elevated in tumor-initiating cells is suppressed by mitocans. Free Radic Biol Med. 2013 Oct 18;67C:41-50.....	50
4.1.5. Zobalova R, Prokopova K, Stantic M, Stapelberg M, Dong L, Ralph S, Akporiaye E, Neuzil J. The potential role of CD133 in immune surveillance and	

apoptosis: A mitochondrial connection? Antioxid Redox Signal. 2011 Dec 15;15(12):2989-3002.	51
4.1.6. Zobalova R, Stantic M, Stapelberg M, Prokopova K , Dong LF, Truksa J, Neuzil J. Drugs that kill cancer stem-like cells. 2011. In Cancer Stem Cells, ed. Stanley Shostak, p. 361-377, InTech, Rijeka, Croatia. Book chapter.	51
4.2. Publications <i>in extenso</i>	53
5. Discussion	176
6. Conclusions.....	183
7. References.....	185

ABSTRACT (EN)

Tumours are heterogeneous and consist of multiple populations of cells. The population of cells with tumour-initiating capability is known as cancer stem cells (CSC). Cells with increased stemness properties and elevated resistance to anti-cancer treatment have been shown to be highly affected upon decline of mitochondrial respiration, linking the concept of CSCs to deregulated bioenergetics. Consistently, functional electron transport chain (ETC) is crucial in tumorigenesis. Expression of *HER2* oncogene, associated with resistance to treatment in breast cancer, has been connected with regulation of mitochondrial function. We therefore investigated the possibility that manipulation of mitochondrial bioenergetics via disruption of ETC eliminates the conventional therapy-resistant populations of tumour, such as CSCs and *HER2*^{high} cells.

We demonstrate that *HER2*^{high} cells and tumours have increased complex I-driven respiration and increased assembly of respiratory supercomplexes (SC). These cells are highly sensitive to MitoTam, a novel mitochondria-targeted derivative of tamoxifen, acting as a CI inhibitor and SC disruptor. MitoTam was able to overcome resistance to tamoxifen, and to reduce the metastatic potential of *HER2*^{high} cells. Higher sensitivity of *HER2*^{high} cells to MitoTam is dependent on the mitochondrial fraction of *HER2*. Another ETC disrupting anti-cancer agent MitoVES efficiently eliminates breast CSCs and, via suppression of tryptophan uptake machinery in CSC, exposes CSCs to the immune system.

In summary, we show that mitochondrially targeted agents directed at ETC act by several mechanisms that in combination are able to overcome resistance of breast cancer to therapy.

Keywords

Breast cancer, cancer stem cells, electron transport chain, HER2, respiratory supercomplexes, reactive oxygen species.

ABSTRACT (CZ)

Nádory jsou heterogenní a sestávají z několika buněčných populací. Populace buněk, se schopností iniciovat nádor je známá jako rakovinné kmenové buňky (RKB). Rakovinné buňky s kmenovými vlastnostmi a se zvýšenou rezistencí k protirakovinné léčbě, jsou nejvíce postiženy při zásahu do mitochondriální respirace, což koncept RKB spojuje s deregulovanou bioenergetikou. V souladu s tím bylo prokázáno, že funkční elektron transportní řetězec (ETC) je nezbytný pro vznik nádoru. Exprese onkogenu *HER2* v rakovině prsu je spojována s rezistencí k léčbě a byla též spojena s regulací mitochondriální funkce. Proto jsme zkoumali možnost, zda manipulací s mitochondriální bioenergetikou prostřednictvím narušení ETC je možné eliminovat buněčné populace rezistentní vůči zavedené léčbě, jako jsou RKB a buňky exprimující *HER2*.

Zjistili jsme, že buňky a nádory s vysokou expresí *HER2* vykazují zvýšenou respiraci přes komplex I a mají více respiračních superkomplexů (SK). Tyto buňky jsou citlivé k látce MitoTam (mitochondriálně cílený derivát tamoxifenu), která působí jako inhibitor komplexu I a narušuje SK. MitoTam překonává rezistenci k tamoxifenu a snižuje metastatický potenciál buněk s vysokou expresí *HER2*. Zvýšená citlivost buněk exprimujících *HER2* k látce MitoTam je závislá na mitochondriální frakci *HER2*. Další protirakovinná látka narušující ETC, MitoVES, účinně eliminuje RKB rakoviny prsu a prostřednictvím potlačení příjmu tryptofanu v RKB, vede k vystavení RKB imunitnímu systému.

V závěru můžeme konstatovat, že mitochondriálně cílené látky ovlivňující ETC působí pomocí několika mechanismů, jež jsou v kombinaci schopné překonat rezistenci rakoviny prsu k terapii.

Klíčová slova

Rakovina prsu, rakovinné kmenové buňky, dýchací řetězec, HER2, respirační superkomplexy, reaktivní sloučeniny kyslíku.

LIST OF ABBREVIATIONS

α -TOS	α -tocopheryl succinate
ABCG2	ATP-binding cassette sub-family G member 2
ALDH1	aldehyde dehydrogenase 1
ANT	adenine nucleotide translocase
ATP	adenosine triphosphate
ADP	adenosine diphosphate
BAX	Bcl-2-associated X protein
BAK	Bcl-2 homologous antagonist killer
CoQ	coenzyme Q
CSC	cancer stem cell
Cyt c	cytochrome c
EGFR	epidermal growth factor receptor
ER	oestrogen receptor
EpCAM	epithelial cell adhesion molecule
ESA	epithelial-specific antigen
FADD	FAS-associated death domain protein
HER2	human epidermal growth factor receptor 2
IDO1	indoleamine-2,3-dioxygenase 1
IMM	inner mitochondrial membrane
IMS	inter membrane space
MEK	mitogen-activated protein kinase kinase

MitoTam	mitochondrially targeted tamoxifen
MitoVES	mitochondrially targeted vitamin E succinate
MnSOD	manganese superoxide dismutase
mtDNA	mitochondrial DNA
mTOR	mammalian target of rapamycin
OMM	outer mitochondrial membrane
OXPHOS	oxidative phosphorylation
PARP	poly ADP ribose polymerase
PDX	patient derived xenograft
PI3K	phosphatidylinositol-3-kinase
PTEN	phosphatase and tensin homologue
PR	progesterone receptor
SC	supercomplex
SDH	succinate dehydrogenase
SQR	succinate ubiquinone reductase
TCA	tricarboxylic acid cycle
TNF	tumour necrosis factor
TPP ⁺	triphenyl phosphonium cation
TRAIL	TNF-related apoptosis inducing ligand

1. INTRODUCTION

Despite considerable advances in molecular oncology, cancer remains a disease with high level of mortality. Breast cancer, a prevailing type of neoplasia in women, accounts for one third of all estimated new cancer diagnoses and is the second most prevalent cause of expected cancer deaths in the coming years (Siegel et al., 2016). The reasons for high number of fatalities in breast cancer are its metastatic potential and common development of resistance to treatment (DeSantis et al., 2014). The major subtypes of breast cancer according to gene expression profiling are shown in Table 1.

Table 1. Major molecular subtypes of breast cancer.

Molecular subtype	Gene expression profile	Outcome and therapy
Luminal A	ER ⁺ and/or PR ⁺ , HER2 ⁻	Endocrine therapy (tamoxifen, aromatase inhibitors). Prognosis is
Luminal B	ER ⁺ and/or PR ⁺ , HER2 ⁺ or high Ki67	better for luminal A than for luminal B subtype.
HER2	ER ⁻ , PR ⁻ , HER2 ⁺	Anti-HER2 monoclonal antibody trastuzumab (Herceptin), pertuzumab. HER2 inhibitor lapatinib. Poor prognosis.
Basal-like	ER ⁻ , PR ⁻ , HER2 ⁻	Platinum-based chemotherapy, PARP inhibitors. Poor prognosis.

Adapted from Schnitt (2010)

Certain subtypes of breast cancer are very hard to manage. Besides the basal-like subtype, where the lack of targetable markers makes the prognosis rather grim, *HER2* oncogene overexpression is a common complicating factor for therapy. HER2-positive cancers are treated with anti-HER2 monoclonal antibody (trastuzumab), and/or tyrosine kinase inhibitors (such as lapatinib), that brought a considerable improvement in the therapy of this pathology. However, resistance to trastuzumab, either acquired or *de novo*, is common, and as many as 50% of patients develop resistance after 5 years of treatment. Luminal A and B subtypes, characterized by high expression of oestrogen receptor (ER), are commonly treated with ER antagonists, such as tamoxifen or aromatase inhibitors. Also in this case, HER2 overexpression is a complicating factor for therapy, causing resistance to tamoxifen treatment.

1.1.HER2/ERBB2

HER2 (ERBB2/neu) is a receptor tyrosine kinase from the family of epidermal growth factor receptors, together with EGFR (ERBB1), HER3 (ERBB3) and HER4 (ERBB4) (Hynes and Lane, 2005). HER2 is a trans-membrane protein that lacks a specific ligand and remains in a constitutively active conformation. In heterodimers with other EGFR family members, HER2 serves as an enhancer of signalling. HER2 is an upstream component of several pathways including those of SRC kinases, STAT3 transcription factor, PI3K/AKT/mTOR and RAS/RAF/MEK/ERK. Through these pathways HER2 regulates various cellular functions including cell growth and survival, proliferation, migration, and resistance to apoptosis.

Under physiological conditions and with proper regulation, HER2 has a role in the development of breast tissue. HER2 is also necessary for proliferation of cardiomyoblasts in the neonate and for maintenance of heart integrity (D'Uva et al., 2015). This relates to the major side effect of anti-HER2 antibody treatment, which is a cardiotoxicity (Cardinale et al., 2010; Keefe, 2002). Pathological hyper-activation of HER2 and its downstream signalling partners, however, often leads to cancer initiation. Therefore, improved modalities of treatment effective in HER2-high cases are needed.

1.2. Tumour heterogeneity

It is widely accepted that tumours consist of heterogeneous populations of cells. The complexity is even higher when tumour microenvironment, consisting of various non-malignant cell types such as immune cells, endothelial cells and cancer-associated fibroblasts, is taken into account. The intra-tumour heterogeneity can be seen from several perspectives.

1.2.1. Genomic heterogeneity

By sequencing multiple regions of renal carcinoma and its metastases, Gerlinger et al. (2012) showed that different mutations are present in distinct sites of the same tumour. Gene signatures of both 'good' and 'poor' prognosis were found in these various sites indicative of co-existence of multiple dominant clones. Based on that, authors proposed the branched evolution model of a growing tumour, as opposed to the traditionally accepted linear evolution model, where the successful driver mutation arises within a single clone, which completely replaces the original, less advantageous clone. The branched evolution pattern was also found in chronic lymphocytic leukaemia (Schuh et al., 2012) as well as in other solid tumours, such as ovarian (Khalique et al., 2007) and pancreatic cancer (Campbell et al., 2010). In breast cancer, alterations of ER and HER2 status have been demonstrated during multiple consecutive relapses of the disease (Lindstrom et al., 2012). This underlines the relevance of such a phenomenon in clinical practice and points to a need for multiple biopsies for both first diagnosis and a re-evaluation after relapse of the disease. Targeted treatment can select for up-regulation of an adjacent oncogenic pathway

leading to therapeutic resistance developed during the course of treatment. Such feature of tumours complicates the efficacy of targeted therapeutics and may at least partially explain why targeted treatments so often fails to protect against relapse of a disease in a long term. Therefore, alternative, broader modes of treatment are needed to complement targeted therapy.

Although this area, based on whole genome sequencing of tumours and personalized treatment, is undoubtedly one of the important topics in the field, its complexity is beyond the scope of this thesis.

1.2.2. Cancer stem cells

Almost a decade ago, cancer stem cells (CSC, also called tumour-initiating cells) attracted the attention of investigators. CSCs were defined as a relatively rare sub-population (<1%) of a tumour, expressing specific cell-surface markers with the enhanced ability to form a tumour after limiting dilution transplantation, usually into immune-deficient mice. CSCs therefore represent a minor population of tumorigenic cells as opposed to the major population forming the bulk of the tumour. CSC presence was first identified in acute myeloid leukaemia in 1994 (Lapidot et al., 1994), and the paradigm was soon applied also to solid tumours. The defining markers of CSC population have been suggested for many tumour types, e.g. CD44⁺/CD24⁻ (Al-Hajj et al., 2003) or ALDH1^{high} (Ginestier et al., 2007) for breast cancer, CD44⁺/CD117⁺ for ovarian cancer (Zhang et al., 2008), CD133⁺ for lung cancer (Eramo et al., 2008), CD44⁺/CD24⁺/ESA⁺ for pancreatic cancer (Li et al., 2007), CD44⁺/α2β1^{high}/CD133⁺ for prostate cancer (Collins et al., 2005) or CD24⁺/ABCG2^{high} for malignant mesothelioma (Pasdar et al., 2015). However, no

universal or broadly applicable marker has been found, and in some cases conflicting results were published with several, often non-overlapping, populations claimed as CSCs. For example, in breast cancer, the widely used CD44⁺/CD24⁻ population does not possess CSC properties in ER-negative and triple-negative tumours (Meyer et al., 2010). Ginestier et al. (2007) showed that the two most commonly used populations of CSCs in breast cancer, the CD44⁺/CD24⁻ and ALDH^{high} subsets, barely overlap within the same specimen. Similarly, in colorectal cancer, CD133⁺ and EpCAM^{high}CD44⁺ sub-populations of CSCs did not overlap (Dalerba et al., 2007).

The CD133 marker, first discovered as a surface marker of hematopoietic stem cells (Miraglia et al., 1997), was proposed as a marker of a broad range of tumours such as brain (Singh et al., 2003), colorectal (Ricci-Vitiani et al., 2007) and breast tumours (Wright et al., 2008). However, others reported that CD133-negative population shows the same tumorigenic potential as its CD133-positive counterpart, and that it exerts even greater potential to metastasize (Shmelkov et al., 2008; Stewart et al., 2011). Although CD133 was shown to participate in the CSC characteristics (Zobalova et al., 2008; Zobalova et al., 2011), its usefulness as a universal CSC marker is unclear.

The phenotypic heterogeneity revealed between CSCs isolated from the same tumour type may suggest a co-existence of multiple clones of CSCs but at the same time it may be an argument against the CSC hypothesis (Quintana et al., 2010). In addition to challenges with identification of CSCs, experimental manipulation with this population is rather complicated. CSCs can be enriched by fluorescence- or magnetic-activated cell sorting for a marker of choice, but the resulting population reverts the relative expression patterns of the markers back to the situation before enrichment when placed into serum-containing media for further study (Zobalova et al., 2008). More promising approach, allowing long-

term maintenance of CSCs in culture, is based on a method originally developed for the cultivation of stem cells of neural origin in the form of spheroids (Singh et al., 2003; Uchida et al., 2000). For this, cancer cells are seeded in serum-free conditions, which does not allow them to adhere, and are supplemented with growth factors. Cells that survive and proliferate under such conditions are considered a model of CSCs. In our research we evaluated this approach by microarray analysis, which confirmed the enrichment of stemness-related genes in resulting population of spheres of breast, prostate and mesothelioma origin (Stapelberg et al., 2014).

It is to be noted however, that spheres of tumour cells may not represent homogenous structures. Rather, they may contain cells in various states of differentiation, with variable expression levels of differentiation markers (Smart et al., 2013). Therefore, caution is needed when CSCs are evaluated experimentally. Simultaneous analysis of multiple CSC markers or the broad expression patterns may provide more robust identification (Li et al., 2011; Silva et al., 2011; Stapelberg et al., 2014) of the CSC fraction. Furthermore, studies in immune-deficient mice may suffer from a bias due to the lack of natural immune stimuli, excluding the formation of pre-tumorigenic niche (Stewart et al., 2011). The percentage of CSCs in tumour cell population may also be largely underestimated due to the residual immune reaction against the xenograft in most widely used nude mice (Quintana et al., 2010). And finally, many published studies were based exclusively on cancer cell line material, where the expression patterns may differ substantially when compared to the freshly isolated tumour samples.

In summary, the research on CSCs struggles due to the lack of specific markers and experimental methods to precisely define and separate this sub-population of tumour cells, preventing a broader implementation of these results into the clinic. The author of this

thesis believes that definition of CSCs based mainly on the surface markers remains a topic of considerable controversy.

1.2.3. Metabolic heterogeneity

Recently, a research of oxidative phosphorylation (OXPHOS) utilization in slow-dividing population of tumour cells shed a new light at the CSCs area. Rather than classification according to the surface markers, tumour cells have been differentiated according to their metabolic needs. Several studies document that cells in the tumour, which show the stemness properties, are the ones most affected upon decline of mitochondrial respiration (Lonardo et al., 2013; Roesch et al., 2013; Viale et al., 2014). This is consistent with a notion that quiescent cells employ OXPHOS to a higher degree than the rapidly proliferating cells, which rely more on glycolysis (Vander Heiden et al., 2009). Tumours therefore consist of at least two populations of cells, the slowly proliferating cells with stemness properties and tumorigenic potential, which are dependent on OXPHOS, and the rapidly proliferating bulk of the tumour, mostly employing aerobic glycolysis (Sancho et al., 2015).

Such heterogeneity may seriously complicate the treatment of cancer by traditional approaches targeting rapidly proliferating cells of the bulk tumour, sparing the CSCs at the same time and allowing them to successfully establish second line tumours.

1.3.Mitochondria and cancer

Until recently, tumours have been considered defective in mitochondrial respiration and the role of mitochondria in cancer was largely neglected. This notion stemmed from the work of a German physiologist, Otto Warburg. Almost a century ago Warburg observed that even in conditions of oxygen access, proliferating tumour cells convert majority of their glucose into lactate in a process called ‘aerobic glycolysis’, instead of the full conversion into CO₂ in oxidative phosphorylation that yields many more molecules of ATP per molecule of glucose than glycolysis (Warburg, 1925). This paradoxical phenomenon has been successfully exploited in the clinic for tumour imaging as ¹⁸F-deoxyglucose positron emission tomography (FDG-PET, Figure 1). Warburg later proposed a theory that dysfunctional mitochondria stand at the origin of tumorigenesis (Warburg, 1956). This notion together with the discovery of oncogenes and tumour suppressors diverted, for a long time, the main focus of cancer biology away from mitochondria.

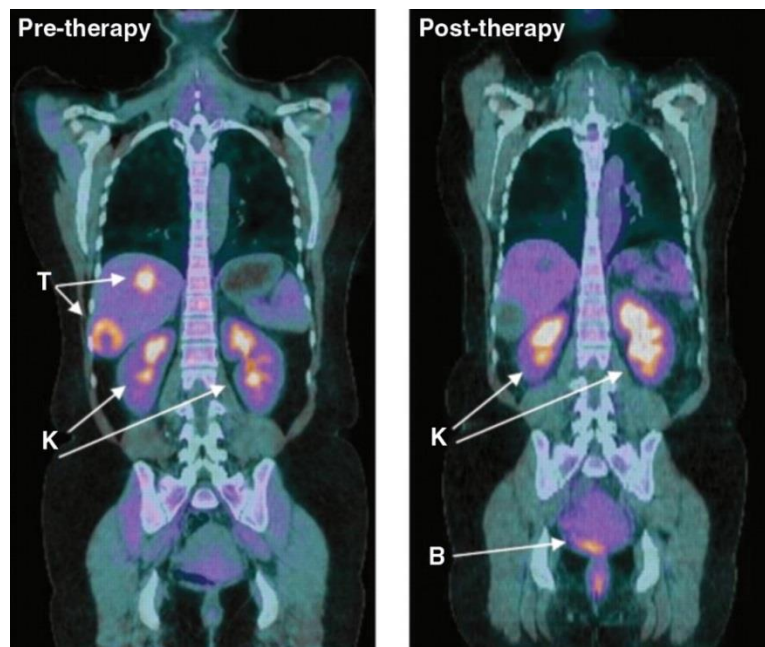


Figure 1. FDG-PET imaging. Merged picture of FDG-PET and computer tomography shows a decreased metabolism of glucose by malignant sarcoma tumour after FDG infusion in patient. While tumour (T) is clearly positive for FDG before therapy (left), it shows no uptake of FDG after 4 weeks of therapy (right). The excess FDG is excreted by urine, therefore kidney (K) and bladder (B) are also stained. Adapted from Vander Heiden et al. (2009).

It is now clear that, in contrast to Warburg’s theory, mitochondrial function in most cancers is not compromised (Zu and Guppy, 2004). Instead, in proliferating tumour cells the observed increase in aerobic glycolysis is based on high biosynthetic demands associated with the rapid growth and related modulation of cell’s metabolism (Ward and Thompson, 2012).

While aerobic glycolysis is a very inefficient process in terms of ATP yield, it is able to produce ATP at a much faster rate than respiration (Koppenol et al., 2011; Pfeiffer et al., 2001). This could be important in situations where glucose supply is abundant and energy demand for fast proliferating cells is high. Nevertheless, along with aerobic glycolysis, most cancer cells maintain active mitochondrial respiration, implicating that these two main

sources of energy are not simply interchangeable (Zu and Guppy, 2004). Respiration is essential for cell proliferation, and recent research indicates that the main reason for sustained respiration in rapidly proliferating cells is the need for biosynthesis of aspartate and pyrimidine nucleotides (Birsoy et al., 2015; Sullivan et al., 2015), not ATP generation. This illustrates, that mitochondria in cancer are not irrelevant bystanders, but appear to be central to the metabolic management.

Consistently, a growing body of evidence shows that functional OXPHOS is essential for tumour initiation, progression and metastasis (Tan et al., 2015; Weinberg et al., 2010), and a reliance on OXPHOS is considered as one of the major characteristics of the treatment-resistant population of cancer cells (Roesch et al., 2013; Viale et al., 2014; Zhang et al., 2014). An example of functional dependence of cancer cells on OXPHOS is a recent study of Tan et al (2015). They used tumour cells depleted of mitochondrial DNA (mtDNA), the so called ρ^0 cells, which lack mitochondrially encoded subunits of OXPHOS and are therefore unable to engage in mitochondrial respiration. These cells were only capable of tumour formation in syngeneic mice once repopulated with functional mitochondria transferred from a surrounding tissue of the host (Tan et al., 2015). Another study showed the essential role of OXPHOS in tumorigenesis using a model of TFAM deficiency (mitochondrial transcription factor A), a protein required to maintain, replicate and transcribe mtDNA. The loss of TFAM protein abolished the tumorigenicity in an oncogenic Kras-driven mouse model (Weinberg et al., 2010).

These results underscore the need for re-evaluation of the role of mitochondria in cancer and for updating the Warburg's fundamental observations based on the recent, new discoveries (Pavlova and Thompson, 2016; Ward and Thompson, 2012).

1.3.1. Oxidative phosphorylation

Embedded in the inner mitochondrial membrane (IMM), the oxidative phosphorylation (OXPHOS) system plays a prominent role in the energy metabolism of the cell. The OXPHOS system, consisting of five multi-subunit complexes and two mobile carriers, couples respiration to ATP synthesis (Figure 2).

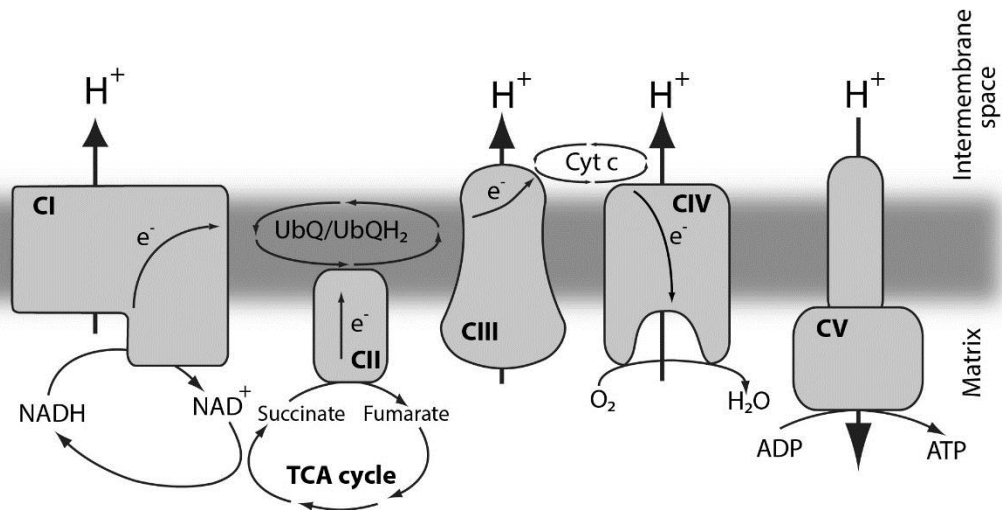


Figure 2. The OXPHOS system. Thick arrows indicate the direction of proton pumping by CI, CIII and CIV. The resulting proton gradient is used by CV to generate ATP. Electrons transferred through the ETC originate at CI, which oxidises NADH from the TCA cycle, or at CII, which directly converts succinate to fumarate. Electrons are then transferred, via CIII and two mobile carriers UbQ and cyt c, to CIV, where they reduce molecular oxygen to form water. Adapted from Rohlena et al. (2013).

Electrons retrieved from nutrient compounds are transferred through a chain of oxidoreductase reactions leading to the reduction of the final electron acceptor, molecular oxygen, to water. Complexes I (CI, NADH:ubiquinone oxidoreductase), III (CIII, ubiquinol:ferricytochrome C oxidoreductase) and IV (CIV, cytochrome c oxidoreductase) act as proton pumps, using the redox energy to transfer protons across the IMM. This

generates proton gradient resulting in electro-chemical potential across the IMM. Complex V (F₁F_o-ATP synthase) uses this membrane potential to catalyse condensation of ADP and inorganic phosphate into ATP.

From a genetic point of view, the OXPHOS system is under unique control of two distinct genomes, the nuclear and the mitochondrial genome. All complexes, with the exception of complex II (CII, succinate:ubiquinone oxidoreductase) consist of protein subunits encoded by nuclear as well as mitochondrial genes (Table 2). The precise regulation of biogenesis and interaction between the two genomes is therefore essential to avoid biochemical and metabolic aberrations. Mutations in OXPHOS complexes and its assembly factors are implicated in many hereditary and degenerative disorders (Koopman et al., 2012).

Table 2. Subunit composition of OXPHOS complexes.

OXPHOS complex	Molecular weight	Total number of subunits	Mitochondrial encoded subunits	Citation
Complex I	~1 MDa	44	7 (ND1-6, ND4L)	Zickermann et al. (2015), Balsa et al. (2012)
Complex II	~140 kDa	4	0	Sun et al. (2005)
Complex III	~240 kDa	11	1 (cytochrome b)	Iwata et al. (1998)
Complex IV	~200 kDa	14	3 (COI, COII, COIII)	Balsa et al. (2012), Tsukihara et al. (1996)
Complex V	~ 600 kDa	17	2 (ATP6, ATP8)	Meyer et al. (2007)

Complex I is the first and largest enzyme of the respiratory chain. It consists of 44 different subunits (45 subunits in total), and forms an L-shaped structure with combined mass of ~1 MDa. The complex is organized in four functional modules (Figure 3). The N module oxidizes NADH, the Q module reduces ubiquinone, and the proximal (P_P) and distal (P_D) pump modules translocate protons across the IMM (Vinothkumar et al., 2014; Zickermann et al., 2015). CI transfers two electrons provided by oxidation of NADH to flavin mononucleotide (FMN), the primary electron acceptor of CI. Electrons are then conveyed through redox centres (eight iron-sulphur [FeS] clusters) to the final acceptor ubiquinone (UbQ, also known as coenzyme Q), reducing it to ubiquinol (UbQH₂). This process is coupled to the transport of four protons across the IMM, from the negative matrix side to the positive intermembrane space side (Figure 4). Transfer of protons via CI accounts for approximately 40% of the proton-motive force generation for the ATP synthesis.

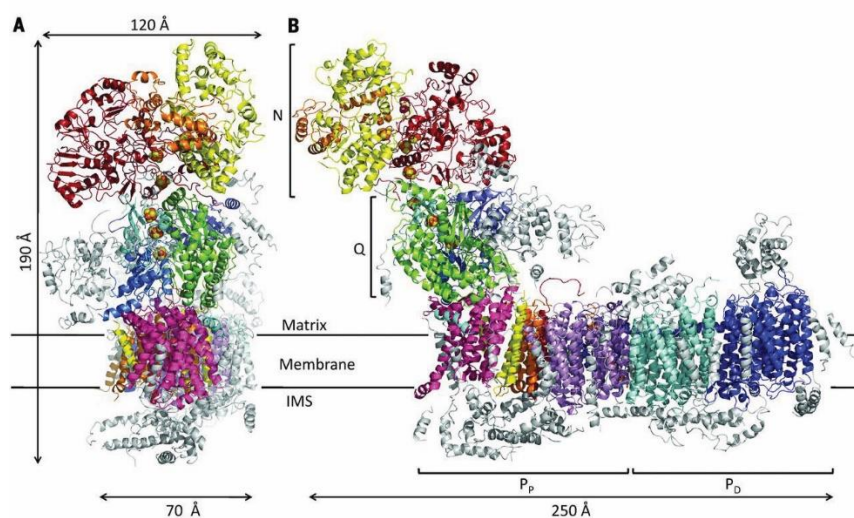


Figure 3. The structure of CI. The view from peripheral arm (A) and at 90° rotation (B). N module, Q module, and proximal and distal pump modules are shown. Adapted from Zickermann et al. (2015).

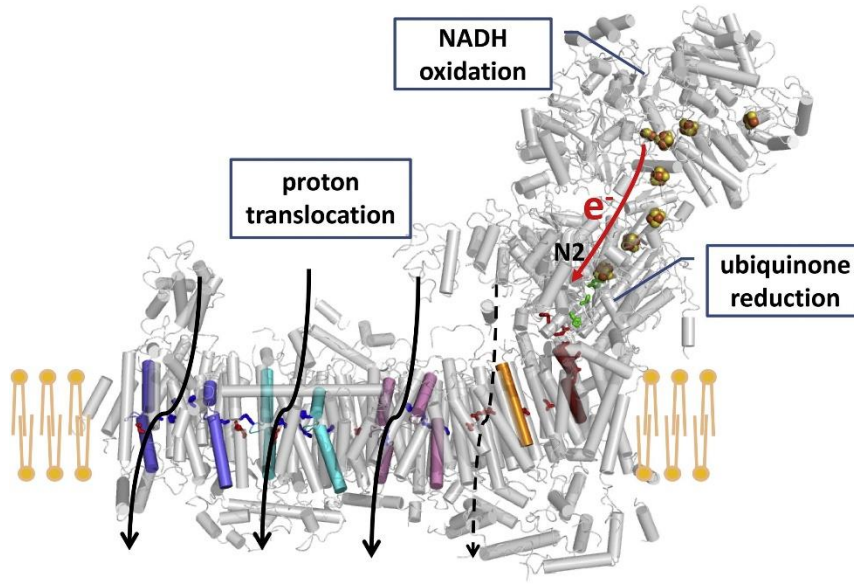


Figure 4. Proton translocation by CI. Electrons are transferred from NADH oxidation site to ubiquinone, where they are reduced (shown in red). Black arrows depict position of three potential proton translocation sites, forth putative proton pathway is showed in dashed arrow. Adapted from Wirth et al. (2016).

CII is the second entry point for electrons into the ETC. CII has a dual role in mitochondria. It is not only a part of the OXPHOS system, but also a key enzyme in the tricarboxylic acid cycle (TCA). By employing the succinate dehydrogenase (SDH) activity it catalyses oxidation of succinate to fumarate. Within the CII, then electrons are transferred from succinate through flavin adenine dinucleotide (FAD) and three [Fe-S] clusters to ubiquinone (Sun et al., 2005). This is coupled with the reduction of ubiquinone to ubiquinol in the ETC, which is known as the succinate ubiquinone reductase (SQR) activity (Cecchini, 2003).

Ubiquinol produced from CI and CII is oxidized by CIII, where the electrons from ubiquinol are transferred to cytochrome c (cyt c). Electrons from cyt c are subsequently transferred to CIV, and finally reduce oxygen into two molecules of H₂O. CIV then

generates the trans-membrane proton gradient, used by CV as a proton-motive force to generate ATP.

The complexity of the OXPHOS system demands for higher structural organization of the individual complexes, and this topic has been a matter of a lively debate for years. Initial concept, the so called oxysome model, was proposed by Chance and Williams (1955). The OXPHOS system in this model was envisioned as a rigid higher-order assembly holding together to maximize its catalytic activity.

This original model was later replaced by the random collision or fluid model postulated by Hackenbrock et al. (1986). In this model, the individual complexes were viewed as independent entities laterally diffusing between the IMM, communicating via the two mobile electron carrier molecules UbQ and cyt c. Transfer of electrons within the individual OXPHOS complexes would occur randomly at the moment of their collision.

The fluid model was generally accepted until 2000 when Schagger and Pfeiffer showed the experimental evidence for the existence of higher-order assemblies of OXPHOS. Those structures were called supercomplexes (SCs), and although reminiscent of the oxysome structures proposed by Chance and Williams, SCs differed substantially as they did not contain CV. Schagger and Pfeiffer formulated the solid model which allowed for more efficient transfer of electrons than the previous random collision model (Schagger and Pfeiffer, 2000).

When the solid model was proposed, the scientific community split into two fractions, the defenders of the solid model versus the defenders of the fluid model. The main argument against the solid model was based on the doubt whether SCs are genuinely present in an *in vivo* system, or whether they are an artefact of sample processing, especially due to the use of detergents. Experimentally, the presence of SCs was detected

using very mild solubilisation, solely by the detergent digitonin. Individual SCs were resolved under non-denaturing conditions by blue native electrophoresis (Schagger et al., 1994). Proteins from the individual bands were then extracted from the gel and analysed by electrophoresis under denaturing conditions, processed for mass spectrometric analysis or subjected to functional assays.

The functional consequences of the organization into SCs were first confirmed in *Paracoccus denitrificans* (Stroh et al., 2004). SC assembly comprising CI, CIII and CIV referred to as the respirasome, since it represents the minimal unit needed to perform complete respiration from NADH to oxygen. Later, functional respirasome was reported also in mammalian cells, and detergents other than digitonin, such as triton X-100, were shown to preserve SC composition (Acin-Perez et al., 2008), supporting the integrity of SCs. Now it is widely accepted that SCs serve as functional assemblies of respiratory complexes that enable channelling of substrates during OXPHOS, prevent competition with other enzymes, optimize sequestration of reactive intermediates (see below) and stabilize individual OXPHOS complexes, especially CI (Acin-Perez et al., 2004; Stroh et al., 2004). It is of note that in mammalian mitochondria, CI almost exclusively associates with respirasome consisting of monomeric CI, dimeric CIII and up to four units of CIV (Schagger, 2002).

The solid model as it stands was not able to fully describe all the experimental data, and therefore other models have been proposed. The plasticity model by the group of J. Enriquez (Acin-Perez and Enriquez, 2014; Acin-Perez et al., 2008) stress the need for dynamic re-arrangement of OXPHOS to achieve an optimum performance in the changing environment in response to stress or nutrient availability. Using metabolic labelling of mtDNA-encoded proteins, the authors found a delay between formation of individual

complexes and their incorporation into an SC. They observed not only SC comprising of CI/CIII/CIV but also assemblies made from CI/CIII and CIII/CIV, as well as free complexes. Based on these results, the authors established a model of dynamic balance distribution between free respiratory complexes and SCs. According to the plasticity model, the solid and fluid models represent extreme phases of the highly dynamic OXPHOS organization.

This hypothesis was questioned by the group of C. Ugalde (Moreno-Lastres et al., 2012). In their study they employed doxycycline, a reversible inhibitor of mitochondrial translation, for simulating the course of re-assembly of complexes and formation of SCs. In their model, the authors document the existence of a ‘pre-respirasome’. CI, according to this hypothesis, is only partially assembled, and completed only by association with the pre-assembled pre-respirasome complex of CIII/CIV. By this the authors preclude the existence of free complexes and explicitly provide support to the solid model.

In summary, the structural organization of the OXPHOS system and dynamics of SC assembly remains a field of active investigation. The discrepancy between the two latest concepts of SC assembly details may be, however, a matter of different experimental set up. For the plasticity model the authors used functionally respiring cells, as opposed to the Ugalde’s research employing cells with dysfunctional respiration after withdrawal of mitochondria-encoded subunits. Despite the considerable ongoing debate on the principles of OXPHOS system organization, the role of higher molecular assembly of OXPHOS in cancer and its utilization for potential cancer therapy are starting to emerge (Rohlenova et al., 2016b).

In addition to the supramolecular organization of the OXPHOS system, another layer of complexity is provided by the dynamic nature of mitochondrial network and the sub-

compartmentalization of the organelle. Mitochondria consist of the outer mitochondria membrane (OMM) and the inner membrane which encloses the matrix compartment, and the inter-membrane space. The IMM is further sub-compartmentalized into the inner boundary membrane facing the OMM, and the cristae separated by cristae junctions. While the cristae part of the IMM is considered to be the prime site of OXPHOS localization, it is preserved even during fusion/fission events. The overall IMM morphology and the formation of sub-compartments within the IMM is dictated by CV, which is apparent from the recently published structure of the ATP synthase dimer (Hahn et al., 2016). CV is organised in rows of dimers along the cristae vesicles forming tubular cristae structures (Davies et al., 2012). Interestingly, individual OXPHOS complexes differ in mobility and localization within the IMM. CII, localized in close proximity to cristae junction, moves very rapidly, in contrast to other complexes, whose mobility within IMM is relatively slow (Wilkens et al., 2013). CII and CV form another type of supramolecular assembly. This so called ATP synthasome consists of CV associated with adenine nucleotide translocase (ANT) (Wittig and Schagger, 2008) and CII (Acin-Perez et al., 2008; Kovarova et al., 2013), but the exact nature and function of this assembly remains to be elucidated.

1.3.2. Reactive oxygen species (ROS)

In addition to the central role in cellular bioenergetics, mitochondria are major producers of reactive oxygen species.

Under physiological conditions, ROS act as second messengers, participating in regulation of various cellular functions such as growth, survival and proliferation (Holmstrom and Finkel, 2014; Sundaresan et al., 1995), hypoxia adaptation (Chandel et al.,

2000) and differentiation (Tormos et al., 2011; Zhang et al., 2011). Under pathological conditions, ROS contribute to initiation of the cancerous phenotype (Weinberg et al., 2010) and to metastasis (Ishikawa et al., 2008). The effect is facilitated by oxidation of proteins and lipids, which changes the phosphorylation pattern of important oncoproteins, such as those from mitogen-activated protein kinase (MAPK), extracellular signal-regulated kinase (ERK), or the PI3K/AKT pathway (Martindale and Holbrook, 2002). AKT (protein kinase B) was shown to be activated by oxidative stress (Higaki et al., 2008), and the negative regulator of PI3K/AKT pathway, the PTEN phosphatase, is inactivated by hydrogen peroxide, leading to further enhancement of PI3K/AKT signalling (Lee et al., 2002). Low doses of ROS stimulate cell proliferation in cancer cells (Okoh et al., 2015), metastatic properties, independence on extracellular matrix and genomic instability (Fruehauf and Meyskens, 2007; Chiarugi and Fiaschi, 2007). On the other hand, cancer cells possess elevated basal ROS levels which makes them vulnerable to therapies that further increase the ROS stress (Nogueira et al., 2008; Toyokuni et al., 1995).

Eleven distinct sites associated with substrate and oxidative phosphorylation have been shown to produce ROS by the leak of electrons from donor redox centres to molecular oxygen within mitochondria. From these, sites at CI and CIII are considered the major sources of ROS, although CII has also been implicated (Adam-Vizi and Chinopoulos, 2006; Brand, 2016; Kluckova et al., 2015; Moreno-Sanchez et al., 2013; Siebels and Drose, 2013). Inhibition of respiratory complexes has been shown to trigger excessive ROS generation (Dong et al., 2011a; Kluckova et al., 2015; Quinlan et al., 2013; St-Pierre et al., 2002). The rate of electron leakage depends primarily on the relative position within the electron flow where the inhibitor binds. If the inhibitor acts predominantly at a downstream site in the ETC, then most of the up-stream redox sites will become reduced leading to

increased electron leak. On the other hand, inhibitor acting upstream would lead to the oxidation of the redox sites that are more downstream in the ETC and decreased electron leak. Similarly, increase in the respiration rate may cause increased ROS production, in a case when increase in respiration is driven by higher substrate supply. Increased respiratory rate, however, would lead to a decrease of ROS production when driven by the ATP demand, i.e. the ETC redox centres become more oxidized (Brand, 2016).

When a particular site leaks one electron, it generates superoxide, two electrons that leak then generate hydrogen peroxide. Although certain sites generate exclusively superoxide, many others may generate both superoxide and hydrogen peroxide. Since superoxide is negatively charged, it cannot freely cross the mitochondrial membrane, but it can potentially pass through anion channels (Han et al., 2003). The majority of superoxide is converted by manganese superoxide dismutase (MnSOD) to hydrogen peroxide. In contrast to superoxide, hydrogen peroxide can move to the cytosol via free diffusion, and it can also be transported via aquaporin channels (Bienert et al., 2007). Agents may therefore be designed to stimulate ROS production from the ETC, which may be applicable for anti-cancer therapy.

1.3.3 Mitochondria in cell death induction

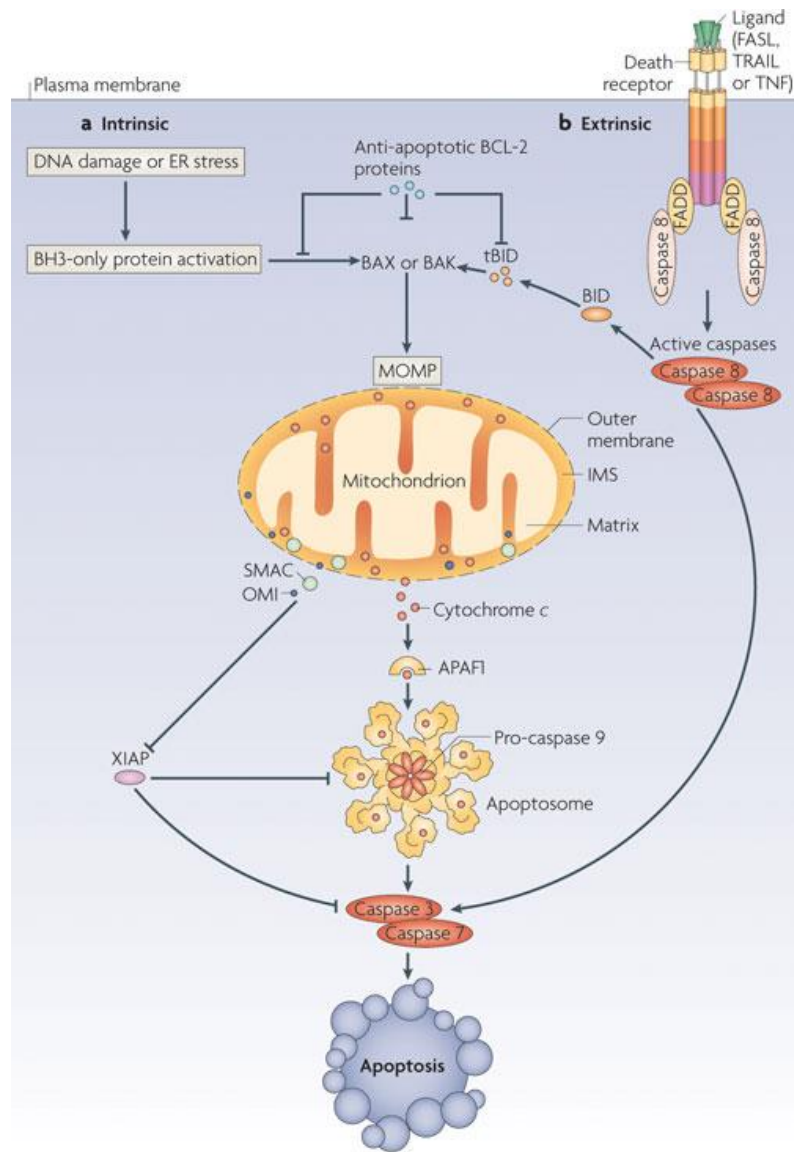
Mitochondria play a dual role in the fate of a cell. They are the source of energy under aerobic conditions, maintaining life, but they also promote death by inducing apoptosis. Apoptosis, a form of controlled cell death program dependent on ATP, is essential during development. It serves as a defence mechanism against pathogens, and is one of the important barriers against tumorigenesis.

Mitochondria act as points of convergence of many apoptosis-inducing signals, containing key regulators of apoptosis. According to the site of induction, apoptosis is divided into intrinsic and extrinsic pathways, both of which converge on activating the executioner caspase-3 and -7. The extrinsic pathway is initiated at the extracellular death receptors by binding of death ligands (FASL, TRAIL or TNF). This leads to the formation of complex of adaptor proteins, such as FAS-associated death domain protein (FADD), which binds the initiator caspase-8. Activated caspase-8 then cleaves executioner caspase-3 and -7.

The intrinsic apoptotic pathway is initiated as a response to the apoptotic stimuli coming from inside of the cell, and involves the induction of mitochondrial outer membrane permeabilization (MOMP). The induction of MOMP is a highly regulated process, which leads to a release of pro-apoptotic proteins from the IMS. The release of the cyt c protein into the cytosol is one of the first events in apoptosis initiation (Liu et al., 1996). The release of second mitochondrial activator of caspases, the SMAC/DIABLO neutralizes the IAP ('inhibitors of apoptosis proteins') family of caspase inhibitors. Cyt c binds the apoptotic protease-activating factor-1 (APAF1). APAF1 oligomerizes and forms the apoptosome. The apoptosome then recruits the initiator caspase-9, which in turn activates the executioner caspase-3 and -7.

Caspases act as major proteases responsible for the cleavage of numerous cellular proteins. In addition, the cell exposes phosphatidylserine on the outer side of the plasma membrane and its DNA is fragmented and degraded by endonuclease G released from the IMS; these features are utilized for experimental detection of apoptosis by flow cytometry and TUNEL assays, respectively. MOMP is tightly controlled by anti-apoptotic members of the B cell lymphoma 2 (BCL-2) family of proteins, and is recognized as a 'point of no

return' even in the situation when caspases are de-activated, as it leads to the decline of mitochondrial function caused by dissipation of $\Delta\Psi_{m,i}$, perturbations in OXPHOS and the ensuing production of ROS (Ricci et al., 2004). Both extrinsic and intrinsic pathways of apoptosis are schematically depicted in Figure 5. Details on apoptotic cell death have recently been reviewed (Bhola and Letai, 2016; Galluzzi et al., 2015; Tait and Green, 2012).



Nature Reviews | Molecular Cell Biology

Figure 5. Intrinsic and extrinsic pathways of apoptosis. (A) Intrinsic apoptotic stimuli activate BH3-only proteins leading to activation of BAX and BAK, and MOMP induction. Normally, MOMP is prevented by binding of the BCL2 proteins to BAX and BAK. Following MOMP, cyt c and other proteins are released to cytoplasm leading to formation of apoptosome, activation of caspases, and apoptosis. SMAC and OMI activate caspases by inactivating the X-linked inhibitor of apoptosis protein. (B) The extrinsic apoptotic pathway is initiated upon binding of death ligands to the extracellular death receptors. Subsequently, the adaptor protein FADD and caspase-8 are recruited, resulting in activation of caspase-8 which cleaves and activates executioner caspases. In some cell types, truncated product of BH3-interacting domain death agonist (BID), tBID, is required for the induction of extrinsic apoptotic pathway. Adapted from Tait and Green (2010).

Of all the protein players participating in the execution and regulation of apoptosis, the BCL-2 family of proteins is probably the most complex and important. The family members can be divided into three groups. (i) The pro-apoptotic effectors (BAX and BAK) which oligomerize at the OMM, forming a channel that eventually leads to MOMP formation, (ii) the anti-apoptotic guardians (e.g. BCL-2, BCL-X_L, MCL-1) and (iii) the pro-apoptotic BH3-only proteins (e.g. BAD, BID, PUMA, NOXA). Members of the anti-apoptotic group, bind and neutralize the BH3-only proteins and BAX and BAK effectors, preventing their oligomerization. Excess of BH-3 only proteins, however, can activate BAK and BAX even in the presence of the anti-apoptotic members of the family.

BCL-2 is overexpressed in ~75% of breast cancer cases, particularly in ER-positive tumours (Dawson et al., 2010; Vaillant et al., 2013). Accordingly, the small molecule inhibitors of BCL-2 and/or other members BCL-X_L and MCL-1, the BH3-mimetics (such as ABT-737, ABT-199) are tested for use as a combinatorial therapy. Although high expression of BCL-2 in tumours has been correlated with better clinical outcome in some studies, BCL-2 has been shown to be expressed in CSCs (Madjd et al., 2009) and ~50% of circulating tumour cells were found positive for BCL-2 (Smerage et al., 2013). Moreover, BCL-2 overexpression was found in HER2-positive tumour cells resistant to trastuzumab (Wang et al., 2011). *BCL2* is an ER-responsive gene, which may be a reason for these contradictory findings, as high BCL-2 could reflect an intact oestrogen signalling pathway (Perillo et al., 2000).

ROS derived from both CI and CII (Kluckova et al., 2015; Lemarie et al., 2011) have been implicated in cell death induction. In case of CI, NDUFS1 subunit has been shown to be directly cleaved by effector caspase 3, leading to excessive ROS generation (Ricci et al., 2004). The mechanism of cell death induced by ROS, although not entirely clear, includes

oxidative damage to DNA. Mitochondrial DNA lacks introns and is therefore prone to DNA damage, at the same time damage in mtDNA-encoded genes causes perturbations in OXPHOS and further ROS. In the nucleus, DNA damage activates poly-ADP-ribose polymerase (PARP) as a repair mechanism. Activated PARP depletes the NAD^+ pool in the cell, leading to bioenergetic stress and cell death (Schriewer et al., 2013). Moreover, ROS in mitochondria interact with VDAC, ANT and cyclophilin D, the constituents of the permeability transition pore, leading to increased permeability for cyt c and perturbations in $\Delta\Psi_{m,i}$, which will eventually attract the BAX and BAK proteins to the membrane (Tsujimoto and Shimizu, 2007). Large decrease of cyt c in mitochondria then leads to further increase in ROS production (Chen and Lesnefsky, 2006). Cyt c was also shown to interact with mitochondrial phospholipid cardiolipin (CL). The high affinity interaction complex of CL and cyt c acts as a potent oxidant. Moreover, interaction with CL withdraw cyt c from its function in ETC (Bayir and Kagan, 2008; Yanamala et al., 2014).

1.3.4 Mitochondrially targeted anti-cancer compounds

Given the pivotal role of mitochondria in ROS generation as well as cell death induction, these organelles may be a promising target for anti-cancer agents. Agents acting directly on mitochondria have been termed mitocans, and their classification has been proposed in Neuzil et al. (2013). It can be expected that accumulation of mitocans in mitochondria would increase their efficacy. Due to the highly negative charge at the IMM that creates an electrostatic and pH gradient, the IMM potential ($\Delta\Psi_{m,i}$), molecules can be targeted to mitochondria via conjugation with lipophilic delocalized cations (Murphy, 2008). One of the best-studied of these cations is the triphenyl phosphonium (TPP^+), which accumulates

in the mitochondrial matrix up to the several hundred fold due to -140 to -180 mV $\Delta\Psi_{m,i}$. The mitochondrial accumulation is further aided by a 10 fold 'pre-concentration' of TPP⁺-tagged compounds in the cytosol of the cells (compared to the extracellular compartment), based on negative membrane potential across the plasma membrane, usually between -30 and -60 mV. Once in mitochondria, the TPP⁺ compounds localize into the mitochondrial matrix, with TPP⁺ at the interphase of the IMM and matrix and the linker with the tagged molecule positioned within the IMM (Smith et al., 2003).

Pioneers of TPP⁺ based mitochondrial targeting, M. Murphy and R. Smith, employed the method for the development of series of mitochondrially targeted antioxidants/redox-active agents. One of them, the mitochondrially targeted ubiquinone, mitoquinone (MitoQ), was successfully tested in a clinical study of hepatitis C-induced liver disease (Gane et al., 2010). Its efficacy was also examined in experimental animal models of neurodegenerative diseases (Orsucci et al., 2011), ischemia-reperfusion injury (Adlam et al., 2005) or diabetes (Chacko et al., 2010), where excessive ROS are involved in the pathologies.

In contrast to mitochondrially targeted antioxidants, different mitochondrially targeted compounds could exert strong pro-oxidant properties. Several compounds were modified by tagging with TPP⁺, resulting in pro-oxidants with anti-cancer properties superior to those of the parental, untargeted compounds. From these, mitochondrially targeted vitamin E succinate (MitoVES) is a prototypic compound, developed in the laboratory of J. Neuzil. MitoVES is derived from the redox-silent analogue of vitamin E, α -tocopheryl succinate (α -TOS), and it exhibits greatly increased anti-cancer properties in comparison to α -TOS. MitoVES was shown to act as an anti-cancer agent via inhibition of CII-related activity and by the ensuing production of ROS (Dong et al., 2011a; Dong et al., 2011b; Kluckova et al., 2015).

The anti-cancer efficacy of TPP⁺-modified compounds is dependent on several aspects: (i) Hydrophobicity of the attached compound, which determines the effectivity and rate of its transport across the lipid bilayer. (ii) The length of a carbon chain linker and its spatial properties are instrumental for a compound to reach the active sites of the interacting molecules within the IMM, the longer carbon chain being also more hydrophobic. (iii) Cancer cell mitochondria possess higher negative $\Delta\Psi_{m,i}$ compared to that of normal cells (Bonnet et al., 2007; Modica-Napolitano and Aprille, 1987), which ensures accumulation of the anti-cancer compound preferentially in the tumour, and lowers possible negative side effects.

The transport of TPP⁺-tagged anti-cancer compounds to mitochondria of cancer cell is driven by the $\Delta\Psi_{m,i}$ and does not employ any other ‘transporter machinery’, which may undergo mutational changes during the course of a treatment. In this way a mitochondrially targeted compound may overcome resistance developed towards an untargeted compound. This was documented for MitoVES, which was effective in A549 lung cancer cells made resistant to the parental untargeted compound, α -TOS. The authors showed that the reason for acquired resistance to α -TOS was due to up-regulation of the ABCA1 transporter. In that case MitoVES, which is targeted directly to mitochondria, bypasses the protein, by means of which it will ‘escape’ being excluded from the cell. Therefore, the efficacy of MitoVES was not compromised even in the situation of ABCA1 overexpression (Prochazka et al., 2013).

1.3.5 Mitochondrially localised HER2

Canonically, the mitochondrial proteome comprises ~1.200 proteins. The vast majority of these proteins are encoded by nuclear DNA. They are imported into mitochondria after translation, based on the presence of the mitochondrial targeting sequence, usually located at the N-terminus of a nascent polypeptide (Neupert and Herrmann, 2007; Wallace, 2012). Besides the canonical mitochondrial import, proteins comprising non-canonical inner mitochondrial targeting sequences have been found in mitochondria, including a number of important oncogenes. Those proteins are not included in the classical catalogues of mitochondrial proteins, such as mitocarta (Calvo et al., 2016). The reason may be that in normal cells, from which these lists are derived, expression of oncogenes is negligible. Therefore, the whole extent of this phenomenon is largely unknown. However, it has already brought an additional complexity to the well-known signalling pathways by introducing a new determinant, the precise localization within the cell compartments. Mitochondrially localized oncogenes have been to date implicated in regulation of multiple processes such as bioenergetics and sensitivity/resistance to cell death. Localized in close proximity to the OXPHOS machinery and cell death inducers in mitochondria, it is feasible to speculate that these oncogenes could be relevant in tumorigenesis and are therefore of interest for cancer research.

In the epidermal growth factor family of receptors almost all members have been reported in mitochondria, with the only exception being HER3. *HER4 (ERBB4)* is not considered an oncogene, and some reports document its tumour suppressor function. The intracellular domain of HER4 (4ICD) has been found in mitochondria and in the nucleus, where it serves as an ER- α co-activator. Tamoxifen treatment disrupts binding to ER- α ,

leading to translocation of the 4ICD to mitochondria, where it acts as an effector of tamoxifen induced cell death as a pro-apoptotic BH3-only protein (Naresh et al., 2008; Vidal et al., 2005).

EGFR (ERBB1) was found to reside in the IMM (Demory et al., 2009). Mitochondrial EGFR interacts with prohibitin-2 and participates in mitochondrial fusion (Bollu et al., 2014). EGFR in mitochondria was reported to phosphorylate Cox2 subunit of CIV (Boerner et al., 2004; Demory et al., 2009). This inhibits the CIV activity and leads to decrease in cellular ATP. Interestingly, in this study the overexpression of non-mitochondrial EGFR had an opposite, stimulatory effect on cellular ATP (Demory et al., 2009). This documents that mitochondrial fractions of proteins might have unique roles which may lead to completely different outcomes when compared to the plasma membrane fraction.

HER2 (ERBB2) has also been reported in mitochondria of HER2-overexpressing cancer cells, connected to the regulation of mitochondrial bioenergetics and resistance to trastuzumab treatment (Ding et al., 2012). Like EGFR, mitochondrial HER2 was localized at the IMM (Rohlenova et al., 2016b). CIV has been implicated as an interaction partner of HER2 (Ding et al., 2012). Our data indicates a role for mitochondrial HER2 in respiratory SC assembly (Rohlenova et al., 2016b). In contrast to Ding et al. (2012), we have consistently observed a stimulatory effect of mitochondrial HER2 on respiration, especially via CI. Nonetheless, the interaction with CI may not be conflicting with previously reported CIV interaction, as both CI and CIV participate in the formation of respirasome. As mitochondrial HER2 has been shown to shift the resistance/sensitivity pattern to cancer therapy as well as regulate bioenergetics, it may represent a so far unexploited target for cancer therapy.

The precise mechanism of mitochondrial import is not well-known for majority of these oncoproteins found in the organelle. Clathrin-mediated endocytosis has been implicated in case of EGFR, and an inner mitochondrial targeting sequence was detected in both EGFR and HER2. This corresponds to a part of the transmembrane domain and juxta-membrane region (Demory et al., 2009; Ding et al., 2012). Moreover, HER2 has been shown to employ the mitochondrial HSP70 chaperon import machinery.

In summary, the specific mitochondrial role of kinases canonically present at plasma membrane represents an intriguing, so far underexplored area of cancer research.

2. AIMS

The aim of this research was to find new approaches to overcome the resistance of breast cancer cells to therapy by targeting mitochondria. This was pursued by studying two different causes of the resistant phenotype. First the cancer stem cells, which possess characteristics that enable them to survive traditional therapy. Second, cancer cells expressing the *HER2* oncogene, which confers resistance and poor prognosis. Various mitochondrial parameters and sensitivity/resistance were studied in these models. Ultimately, the efficacy of mitochondrially targeted treatment was investigated.

Specific aims of this thesis were:

- To validate an *in vitro* model of cancer stem cells using sphere culture under serum-free conditions, and to test mitochondrially targeted vitamin E succinate (MitoVES) as an experimental compound specifically eliminating CSCs.
- To characterize the mechanism of action of mitochondrially targeted tamoxifen (MitoTam) in HER2-positive breast cancer.
- To evaluate the effect of mitochondrial HER2 on OXPHOS and the mitochondrial function.

3. LIST OF METHODS

Below is a list of methods used by the author while preparing the publications included in the thesis.

Cell culture

- Cancer cell lines
- Sphere culture

Cell fractionation

- Isolation of mitochondrial, nuclear and cytosolic fractions

Cloning

Preparation of cellular sublines

- Transfection with expressing vectors
- RNA interference (shRNA, siRNA)

Quantitative real-time PCR

Electrophoretic methods and western blotting

- SDS-PAGE
- Blue native-PAGE

Microscopy

- Fluorescent microscopy
- Confocal microscopy
- Live-cell imaging
- STED microscopy

Image analysis using ImageJ and Hyugens software

Flow cytometry

- Detection of cell death
- Fluorescent probes (ROS, glucose uptake, $\Delta\Psi_{m,i}$)
- Immunodetection

Respiration measurement

- Oroboros oxygraph measurement

Mice work

- Xenografts of tumour cells
- Intra-peritoneal and sub-cutaneous administrations
- Detection of metastases

4. PUBLICATIONS

The presented thesis consists of a total of six publications: three original research articles, two review articles and one book chapter. During her PhD studies, the author of this thesis was involved also in another study concerning the role of microRNA126 in autophagy induction in mesothelioma cancer cells. This study, however, only partially matches with the presented research project and therefore was not included in the thesis.

Below is a summary of the thesis constituent publications with stated contributions of the author, followed by all publications *in extenso*.

4.1.List of publications

4.1.1. **Rohlenova K**, Sachaphibulkij K, Stursa J, Bezework-Geleta A, Blecha J, Endaya B, Werner L, Cerny J, Zobalova R, Goodwin J, Spacek T, Pesdar EA, Yan B, Nguyen MN, Vondrusova M, Sobol M, Jezek P, Hozak P, Truksa J, Rohlena J, Dong LF, Neuzil J. **Selective disruption of respiratory supercomplexes as a new strategy to suppress Her2^{high} breast cancer**. *Antioxid Redox Sign.* 2016 Jul 8.

Impact factor at the time of publishing = 7.1

In this study we demonstrate that breast cancer cells overexpressing *HER2* oncogene comprise higher level of respiration through mitochondrial complex I and increasingly organized respiratory supercomplexes. We demonstrate that this feature is targetable by a novel inhibitor of respiration based on tamoxifen tagged with triphenylphosphonium

(MitoTam). MitoTam is highly effective in killing of HER2^{high} breast cancer cells, which are otherwise resistant to tamoxifen. We show that MitoTam acts by generation of ROS and disruption of supercomplexes specifically in HER2^{high} background, and the susceptibility is connected with mitochondrial fraction of HER2 protein. MitoTam passed official pre-clinical testing and will continue to phase I clinical trial.

Contribution to the publication: Study design. Experimental part (confocal microscopy, time-lapse confocal microscopy, STED microscopy, apoptosis measurements, ROS measurements, $\Delta\Psi_{m,i}$ measurements, glucose uptake measurements, RNA interference, stable and transient transfections and selection of sublines, western blotting, SDS-PAGE, BN-PAGE, mice experiments, detection of metastases, cell culture, culture and treatment of mammospheres). Data analysis, manuscript writing.

4.1.2. **Rohlenova K, Neuzil J, Rohlena J. The role of Her2 and other oncogenes of the PI3K/AKT pathway in mitochondria.** Biol Chem. 2016 Jul 1;397:607-15.

Impact factor at the time of publishing = 3.3

Recently a number of important cytoplasmic and plasma membrane proteins have been reported to translocate to mitochondria. Among these, many oncoproteins and tumour suppressors were found in the organelle. This may have functional consequences for cancer treatment, as mitochondria are central to cellular metabolism and cell death induction. In this review, we summarized the current knowledge about the function of mitochondrially localized HER2, and of other mitochondria-localised oncoproteins signalling via the

PI3K/AKT pathway, and discuss the evidence for/ and against their localisation on the organelle.

Contribution to the publication: The review is partially based on our results published in Rohlenova et al (2016b). Manuscript design and writing.

4.1.3. Yan B, Stantic M, Zobalova R, Bezawork-Geleta A, Stapelberg M, Stursa J, **Prokopova K**, Dong LF, Neuzil J. **Mitochondrially targeted vitamin E succinate efficiently kills breast tumour-initiating cells in a complex II-dependent manner.** BMC Cancer. 2015 May 15:401.

Impact factor at the time of publishing = 3.4

In this study we document that mitochondrially targeted vitamin E succinate (MitoVES) is efficient in killing breast CSCs, which are believed to be a reason for high level of resistance to established cancer therapy. Using RNA interference approach and homologues of MitoVES differing in the length of the aliphatic chain, we showed that mitochondrial complex II is a target of MitoVES in CSCs. This research establishes novel link between mitochondrial complex II and killing of CSCs. Based on this we propose a combinatorial therapy of MitoVES with established agents targeting fast proliferating cells as a strategy to treat breast cancer and minimize a risk of relapse.

Contribution to the publication: Experimental part (cell culture, sphere culture, apoptosis measurements, qPCR), revision of the manuscript.

4.1.4. Stapelberg M, Zobalova R, Nguyen MN, Walker T, Stantic M, Goodwin J, Pasdar EA, Thai T, **Prokopova K**, Yan B, Hall S, de Pennington N, Thomas SR, Grant G, Stursa J, Bajzikova M, Meedeniya ACB, Truksa J, Ralph SJ , Ansorge O, Dong LF, Neuzil J. **Indoleamine-2,3-dioxygenase elevated in tumor-initiating cells is suppressed by mitocans**. Free Radic Biol Med. 2013 Oct 18;67C:41-50.

Impact factor at the time of publishing = 5.7

In this study we validated the sphere culture of three cancer cell lines of breast, prostate and mesothelioma origin as a plausible model of CSCs. Using microarray analysis we confirmed increased expression of genes related to stemness in spheres of all three cell lines. Moreover, we were first to detect Trp metabolism pathway significantly up-regulated in sphere cells originating from the cell lines and primary biopsies. We found that indoleamine-2,3-dioxygenase-1 (IDO1), the rate-limiting enzyme, as well as constituents of Trp uptake system are up-regulated in spheres. This phenomenon may play an important role in escape of CSCs from immune surveillance. Surprisingly, analogues of vitamin E, α -tocopheryl succinate and especially mitochondrially-targeted derivate MitoVES, suppressed IDO1 in CSCs, pointing to its translational potential.

Contribution to the publication: Experimental part (cell culture, sphere culture, qPCR, verification of the results in an independent microarray analysis), revision of the manuscript.

4.1.5. Zobalova R, **Prokopova K**, Stantic M, Stapelberg M, Dong L, Ralph S, Akporiaye E, Neuzil J. **The potential role of CD133 in immune surveillance and apoptosis: A mitochondrial connection?** Antioxid Redox Signal. 2011 Dec 15;15(12):2989-3002.

Impact factor at the time of publishing = 8.5

In this review we summarized a recent knowledge about the role of the CSC marker CD133 in the acquisition of stemness properties and escape of CSCs from immune surveillance. As we reported earlier, CD133^{high} Jurkat T lymphoma cells possess high expression of anti-apoptotic FLICE-inhibitory protein (FLIP), which makes them resistant to apoptosis-mediated by TNF-related apoptosis-inducing ligand (TRAIL). According to our results and those of others, CD133 protein may thus be considered as a marker which selects cells resistant to increased stress conditions in the tumour and helps to evade the immune surveillance.

Contribution to the publication: From experimental part behind this review (cell culture, sphere culture, validation of stem-like characteristics of sphere cells, RT-PCR, flow cytometry). Manuscript writing.

4.1.6. Zobalova R, Stantic M, Stapelberg M, **Prokopova K**, Dong LF, Truksa J, Neuzil J. **Drugs that kill cancer stem-like cells.** 2011. In Cancer Stem Cells, ed. Stanley Shostak, p. 361-377, InTech, Rijeka, Croatia. Book chapter.

In this book chapter we reviewed cancer therapy approaches focused on CSCs, the resistant sub-population of the tumour. To date not many compounds exist with known effect towards CSCs; this is of high importance for finding effective ways to treat cancer and avoiding relapses.

Contribution to the publication: From experimental part behind this book chapter (cell culture, sphere culture, validation of stem-like characteristics of sphere cells, RT-PCR, flow cytometry). Manuscript writing.

4.2. Publications *in extenso*

Original Research Communication

Selective disruption of respiratory supercomplexes as a new strategy to suppress Her2^{high} breast cancer

Katerina Rohlenova,^{1,#,*} Karishma Sachaphibulkij,^{2,#} Jan Stursa,^{2,3,4} Ayenachew Bezework-Geleta,² Jan Blecha¹, Berwini Endaya,² Lukas Werner,⁴ Jiri Cerny,¹ Renata Zobalova,^{1,2} Jacob Goodwin,² Tomas Spacek,⁵ Elham Alizadeh Pesdar,² Bing Yan,² Maria Nga Nguyen,² Magdalena Vondrusova,¹ Margaryta Sobol,⁶ Petr Jezek,⁵ Pavel Hozak,⁶ Jaroslav Truksa,¹ Jakub Rohlena,^{1,*} Lan-Feng Dong,^{2,*} Jiri Neuzil^{1,2,*}

¹Institute of Biotechnology, Czech Academy of Sciences, Prague, Czech Republic. ²School of Medical Science, Griffith University, Southport, Qld, Australia. ³Prague Institute of Chemical Technology, Prague, Czech Republic. ⁴Biomedical Research Center, University Hospital, Hradec Kralove, Czech Republic. ⁵Institute of Physiology, Prague, Czech Republic. ⁶Institute of Molecular Genetics, Czech Academy of Sciences, Prague, Czech Republic.

This paper is published in *Antioxidants & Redox Signaling*, doi/10.1089/ars.2016.6677

[#]These authors contributed equally to the work.

Running title: Targeting respiration in Her2^{high} breast cancer

Word count: 4978, excluding methods, references and figure legends

Number of references: 60

Greyscale illustrations: 4

Color illustrations: 5 (online 5)

Online supplementary information: Illustrations 3

***Correspondence:** Jiri Neuzil or Lan-Feng Dong, Mitochondria, Apoptosis and Cancer Research Group, School of Medical Science and Menzies Health Institute Queensland, Griffith University, Southport, 4222 Qld, Australia; phone: +61-755529109; fax: +61-755528444; e-mail: j.neuzil@griffith.edu.au or l.dong@griffith.edu.au; or Katerina Rohlenova or Jakub Rohlena, Molecular Therapy Group, Institute of Biotechnology, Czech Academy of Sciences, BIOCEV, Prumyslova 595, 25220 Vestec, Prague-West, Czech Republic; phone: +420-325873795; e-mail: katerina.rohlenova@ibt.cas.cz or jakub.rohlana@ibt.cas.cz.

ABSTRACT

AIMS: Expression of the *HER2* oncogene in breast cancer is associated with resistance to treatment, and Her2 may regulate bioenergetics. Therefore, we investigated whether disruption of the electron transport chain is a viable strategy to eliminate Her2^{high} disease.

RESULTS: We demonstrate that Her2^{high} cells and tumors have increased assembly of respiratory supercomplexes and increased complex I-driven respiration *in vitro* and *in vivo*.

They are also highly sensitive to MitoTam, a novel mitochondrial-targeted derivative of tamoxifen. Unlike tamoxifen, MitoTam efficiently suppresses experimental Her2^{high} tumors without systemic toxicity. Mechanistically, MitoTam inhibits complex I-driven respiration and disrupts respiratory supercomplexes in Her2^{high} background *in vitro* and *in vivo*, leading to elevated reactive oxygen species production and cell death. Intriguingly, higher sensitivity of Her2^{high} cells to MitoTam is dependent on the mitochondrial fraction of Her2.

INNOVATION: Oncogenes such as *HER2* can restructure electron transport chain, creating a previously unrecognized therapeutic vulnerability exploitable by supercomplex-disrupting agents such as MitoTam.

CONCLUSION: We propose that the electron transport chain is a suitable therapeutic target in Her2^{high} disease.

Key words: Electron transport chain, supercomplexes, tamoxifen, complex I, Her2.

INTRODUCTION

Functional electron transport chain (ETC) is essential for tumorigenesis (51,57). At the same time, ETC is important in normal cells by providing milieu permitting biosynthesis of aspartate and pyrimidine nucleotides, and for ATP generation (3,47,50). Classical pharmacological ETC inhibitors such as rotenone, antimycin A or potassium cyanate have systemic toxicity, while available non-toxic ETC inhibitors such as the anti-diabetic drug metformin are not potent enough and show little benefit for cancer patients in a number of clinical trials (18,23,35). Therefore effective agents that would selectively target ETC in specific subsets of cancer cells are sorely needed.

ETC resides in the cristae region of the inner mitochondrial membrane (IMM). It comprises four respiratory complexes (termed CI-CIV) that further assemble into higher molecular structures called supercomplexes (SCs), increasing ETC efficiency and regulating substrate utilization (1,21). ETC generates electrochemical gradient across the IMM referred to as the IMM potential ($\Delta\Psi_{m,i}$). This is essential for ATP production by mitochondrial ATP synthase, and also allows cargo delivery into mitochondria using cations such as the triphenylphosphonium (TPP⁺) group (28), which can therefore be used to bring ETC inhibitors close to their molecular targets (9). The level of ETC organization in various subsets of cancer cell, while largely unexplored, could be associated with differences in sensitivity to ETC inhibition.

Breast cancer is the prevailing type of neoplasia in women, and certain sub-types like Her2^{high} breast carcinomas are difficult to treat (5,6,42). Her2 (also known as ErbB2) is a receptor tyrosine kinase that may regulate metabolism, for example the pentose phosphate pathway (43). It has been suggested that a fraction of Her2 translocates into mitochondria, where it can affect bioenergetics (7). Tamoxifen, a mixed agonist/antagonist of the estrogen receptor, is used as the first line therapy in hormone-sensitive breast cancer but is inefficient

in the Her2^{high} disease. It was reported that tamoxifen inhibits mitochondrial complex I (CI), albeit at supra-pharmacological doses (25). This inspired us to design, synthesize and test tamoxifen tagged with the TPP⁺ group, with expected accumulation adjacent to CI enhancing its effects on mitochondria.

Here we show that mitochondrially targeted tamoxifen (MitoTam) is far more efficient in killing breast cancer cells than the parental compound. In stark contrast to tamoxifen, MitoTam is highly effective towards cells and tumors with high level of Her2. This is linked to the elevated CI and increased SC assembly selectively disrupted by MitoTam, leading to enhanced ROS production and cell death. Interestingly, the sensitivity of Her2^{high} cells to MitoTam depends on the presence of Her2 in mitochondria at the IMM/matrix interface. We found that in a pre-clinical model MitoTam almost completely cured Her2^{high} breast carcinomas without deleterious side-effects, supporting the potential use of this novel ETC-targeted agent against Her2^{high} breast cancer highly recalcitrant to therapy (5).

RESULTS

Tagging tamoxifen with TPP⁺ leads to mitochondrial targeting and increased cell death.

Tamoxifen, a low-affinity inhibitor of CI (25), was modified by the attachment of a TPP⁺ group, which ensures mitochondrial accumulation based on the electro-chemical gradient across the IMM. This TPP⁺-modified tamoxifen, MitoTam (Fig. 1A), was labelled with fluorescein yielding MitoTam-F for intracellular visualization (Fig. S1). Fig. 1B shows that upon addition to MCF7 cells MitoTam-F accumulates in the mitochondria which become doughnut-shaped and lose MitoTracker FarRed fluorescence. The enlarged color-balanced image of the intermediate state prior to the complete loss of red fluorescence shows green staining of internal structures of mitochondria, indicating that the accumulation of the drug at the IMM likely interferes with mitochondrial function. Fig. 1C documents that MitoTam is more efficient in killing MCF7 cells than tamoxifen. We estimated the IC₅₀ value of MitoTam and tamoxifen for a number of breast cancer cell lines and found that, in all cases, it was at least one order of magnitude lower for the TPP⁺-tagged variant. On the other hand, IC₅₀ values for non-cancerous cell lines were more than one order of magnitude higher than for cancer cell lines, indicating a pharmaceutical window of opportunity (Table 1). As expected for a compound originating from an estrogen receptor antagonist, MitoTam was found more efficient in killing the ER-positive MCF7 cells than their triple-negative counterparts, MDA-MB-231 cells (Fig. 1D). MitoTam also eliminated Her2^{high} ER-negative SKBR3 and MDA-MB-453 cells with high efficacy (Fig. 1E). Importantly, when the TPP⁺ group of MitoTam was disabled by the removal of its positive charge, the efficiency of the resulting compound (Tam-DPPO, for structure see Fig. S1) was greatly reduced (Fig. 1F). Similarly, the TPP targeting group alone (Fig. S1) had little effect (Fig. 1G). This illustrates the importance of mitochondrial targeting of the tamoxifen moiety for increased biological activity.

We next tested the effect of MitoTam on tamoxifen-resistant cells using MCF7 cells made resistant to tamoxifen by long-term exposure to escalating doses of the agent (TAM-R cells) (Fig. 1H). Fig. 1I documents that TAM-R cells were slightly more susceptible to MitoTam. On the other hand, Tam-DPPO that lacks the delocalized cationic group was less efficient towards TAM-R cells than to parental MCF7 cells (Fig. 1J). We also attempted to prepare MitoTam-resistant MCF7 cells in a similar manner as we did for TAM. However, we were not able to obtain any surviving population upon long term culture (>6 months), suggesting that resistance to MitoTam may not develop, similarly as we documented before for MitoVES (33). Collectively, these data indicate that MitoTam exhibits superior structure-dependent killing activity that is not compromised in cells resistant to the parental compound.

MitoTam effectively kills cells with high levels of Her2 and efficiently suppresses Her2^{high} breast carcinomas. Breast cancer with high level of expression of the oncogene *HER2* is particularly difficult to manage. Therefore, we next investigated the effect of MitoTam on Her2^{high} breast cancer cells prepared by genetic manipulation. For this we used MCF7 cells with relatively low level of Her2 and Her2-null MDA-MB-231 cells that were both transfected with a Her2 plasmid to achieve Her2 expression levels similar to those found in natural Her2^{high} breast cancer cell lines (Fig. 2A). We also knocked down Her2 using shRNA in MCF7 cells, further reducing its level (Fig. 2A). As expected, MCF7 Her2^{high} cells were more resistant to tamoxifen than the parental cells (Fig. 2B). In stark contrast, Her2^{high} MCF7 and MDA-MB-231 cells were more susceptible to MitoTam than parental or Her2^{null} cells (Fig. 2C-E), while this preference was absent for Tam-DPPO (Fig. 2F). Consistently with the higher level of cell death induction, MitoTam treatment resulted in a stronger activation of the apoptotic pathway in MCF7 Her2^{high} cells compared to mock MCF7 cells (Fig. 2G). Western blotting (WB) revealed accelerated cleavage of pro-caspase-9 and Parp1/2 in

Her2^{high} cells as well as an increase of pro-apoptotic Bax and decrease of the anti-apoptotic Bcl-2 protein. Interestingly, the level of Her2 decreased in MCF7 Her2^{high} cells upon exposure to MitoTam. In a colony-forming assay, tamoxifen was proficient in suppressing formation of colonies in MCF7 and MCF7 mock cultures (Fig. 2H), while MitoTam was more efficient in MCF7 Her2^{high} cultures, corroborating anti-cancer efficacy of MitoTam against Her2^{high} breast cancer. Finally, MitoTam showed an additive effect with inhibitors of Her2 signaling in Her2^{high}, but not in parental MCF7 cells (Fig. 2I,J), indicating that MitoTam targets sites or pathways distinct from the canonical Her2 signaling. In summary, these results show that high Her2 expression is associated with increased sensitivity to MitoTam.

To see whether Her2 sensitizes breast tumors to MitoTam *in vivo*, we used the FVB/N *c-neu* mouse strain subcutaneously (s.c.) injected with NeuTL cells derived from spontaneous Her2^{high} breast carcinoma (13). Fig. 3A (and Fig. S2A with representative images) documents a strong effect of MitoTam (0.54 $\mu\text{mol}/\text{mouse}/\text{dose}$), inhibiting growth of syngeneic tumors by ~80%, while tamoxifen (applied at 2.69 $\mu\text{mol}/\text{mouse}/\text{dose}$, i.e. at ~5-times higher dose than MitoTam) was much less efficient.

We next tested another tumor model, in which Balb/c nude mice were s.c. injected with MCF7 mock or MCF7 Her2^{high} cells. Tamoxifen, which had a modest effect on parental MCF7 mock tumors (2 $\mu\text{mol}/\text{mouse}/\text{dose}$), was even less efficient in suppressing Her2^{high} carcinomas, where it did not prevent reaching the ethical endpoint (Fig. 3B and Fig. S2C, D). On the other hand, MitoTam at 8-times lower dose (0.25 $\mu\text{mol}/\text{mouse}/\text{dose}$) prevented reaching the ethical endpoint in all situations (Fig. S2C, D). It slowed down the growth of the MCF7 mock tumors (featuring relatively low level of Her2) and, after two doses, tumor progression stopped (Fig. 3B). Most importantly, MitoTam suppressed Her2^{high} carcinomas such that their volume decreased 3-fold from the original size with complete disappearance in

two of the treated animals (Fig. 3B, and Fig. S2B with representative images). These animals stayed tumor-free for 8 months following cessation of MitoTam administration, indicating complete eradication of the Her2^{high} breast carcinomas in these particular cases.

Immunohistochemistry (IHC) analysis of control and treated tumors document increased TUNEL-positive cells in particular in Her2^{high} tumors (Fig. 3C). This is supported by WB showing high level of pro-caspase-9 cleavage in MitoTam-treated Her2^{high} tumors, increased Bax and decreased Bcl-2 protein levels. WB also documents high level of the Her2 protein in Her2^{high} tumors and its decrease upon MitoTam treatment (Fig. 3D).

MitoTam effectively suppressed tumors induced by mammary expression of the HER2 transgene in FVB/N *c-neu* mice (13) (Fig. 3E, S2E), demonstrating effectiveness in a more natural situation where a tumor appears in its native environment, without the initial presence of homogenous Her2^{high} cell population. MitoTam also reduced invasiveness in a zone exclusion assay (Fig. S3A), and was effective in a Her2^{high} mammosphere model (Fig. S3B) that generates cells with cancer stem-like properties resistant to conventional therapy (12,49). In addition, MitoTam, but not Tamoxifen, interfered with sphere formation in this situation (Fig. S3C,D). Importantly, MitoTam suppressed not only the primary tumor growth (Fig. 3F, Fig. S2F) but also the metastatic burden in blood, lung and liver (Fig. 3G) in the experimental 4T1 model of Her2^{high} metastatic breast carcinoma in Balb/c mice.

Collectively, these data clearly demonstrate that MitoTam efficiently suppresses growth and progression of Her2^{high} carcinomas.

MitoTam induces ROS, dissipates mitochondrial potential ($\Delta\Psi_{m,i}$), and suppresses mitochondrial respiration via complex I. Since MitoTam showed efficacy superior to that of tamoxifen, in particular in suppressing Her2^{high} tumors, we further investigated its mode of action. We first tested its effect on generation of ROS, as mitochondrial targeting can

improve the efficacy of ROS generation (9,10,37). Clearly, MitoTam induced ROS within a short period of treatment, while no ROS was induced with tamoxifen even at much higher doses. The effect of MitoTam was more profound for Her2^{high} cells (Fig. 4A) when mitochondrial ROS-specific probe (MitoSOX) was used. This was linked to cell death induction, since the ROS scavenger N-acetyl cysteine (NAC) suppressed the killing activity of the agent (Fig. 4B). We next tested the effect of MitoTam on $\Delta\Psi_{m,i}$. Using confocal microscopy and flow cytometry with TMRM probe, we found that MitoTam was very efficient in $\Delta\Psi_{m,i}$ dissipation, while tamoxifen had no effect (Fig. 4C, D). $\Delta\Psi_{m,i}$ is important for ROS generation in response to MitoTam and in cell death induction by the agent, as pre-treatment with the uncoupler FCCP suppressed both events (Fig. 4E, F). Interestingly, MCF7 Her2^{low} cells showed higher basal $\Delta\Psi_{m,i}$, although this was not followed by increased activity of MitoTam. Finally, we show that MitoTam, in contrast to tamoxifen, decreased $\Delta\Psi_{m,i}$ almost to the same level as FCCP (Fig. 4G). These data support the notion that ROS generation is mediating the killing activity of MitoTam and that this is more profound in Her2^{high} cells.

Since MitoTam is targeted to mitochondria (more specifically, to the interface of the IMM and matrix), we tested its effect on mitochondrial respiration. Using high-resolution respirometry, we found that MitoTam suppressed CI-dependent respiration more efficiently than CII-dependent respiration and that this effect was stronger for MitoTam than for tamoxifen (Fig. 5A,B Table 2). In addition, MitoTam inhibited NADH-cytochrome c (CI-CIII), but not succinate-cytochrome c (CII-CIII) oxidoreductase activity in MCF7 cells (Fig. 5C,D), suggesting that CI is the likely target. To support a role of CI in the anti-cancer activity of MitoTam, we used Chinese hamster lung fibroblast cells with functional and mutant CI (46) transformed with H-Ras (8). Interestingly, the CI-dysfunctional B10_{H-Ras} cells (Fig. 5E) were more resistant to MitoTam than the parental B1_{H-Ras} cells (Fig. 5F). We next

tested MCF7 cells and their Her2^{high} counterparts for respiration, and found that the latter respired more, in particular via CI (Fig. 5G). In addition, the CI-CIII activity was higher in mitochondria from Her2^{high} cells (Fig. 5C). We also found that MitoTam suppressed respiration of Her2^{high} cells more profoundly than that of parental MCF7 cells (Fig. 5G). In this case we used a different set-up than that used in Fig. 5A, B. Rather than titrating cells placed in the respirometer chamber with MitoTam, they were cultured with the agent for 1 h, after which respiration was assessed.

The *in vitro* results were recapitulated by assessing *in vivo* effects of MitoTam (*c.f.* Fig. 3B). Tumors derived from Her2^{high} cells had unchanged leak respiration, but increased maximal respiratory capacity (Fig. 5H) and higher CI-dependent respiration (Fig. 5I), which was strongly suppressed in response to MitoTam treatment of the animals, while CII-dependent respiration was unchanged (Fig. 5I). These effects were tumor-specific, as there was no difference in respiration and no effect of MitoTam in the liver tissue from the same animals (Fig. 5J).

Concerning glycolysis, neither glucose uptake (Fig. 5K), nor lactate production (Fig. 5L) and ATP levels (Fig. 5M) were affected differentially in parental and Her2^{high} cells by MitoTam. This suggests that alteration in glycolytic compensation is not responsible for increased sensitivity of Her2^{high} cells to MitoTam.

Collectively, these data document that MitoTam suppresses respiration via CI both in cultured cells *in vitro* and in breast carcinomas *in vivo*, resulting in ROS generation and cell death.

MitoTam disrupts respiratory supercomplexes elevated in Her2^{high} cells and tumors. The increased respiration of Her2^{high} cells via CI might be related to a more efficient assembly of respiratory complexes (RCs). We therefore evaluated MCF7 Her2^{high} and MCF7 mock cells

for expression of components of mitochondrial RCs using WB. Of these, subunits of CI and, to some extent those of CIII and CIV, were more expressed (Fig. 6A). The level of respiratory SCs including the respirasome, an SC composed of CI, CIII and CIV (1,2), was also increased in MCF7 Her2^{high} cells, as determined by native blue gel electrophoresis (NBGE) (Fig. 6B, D). Interestingly, treatment of MCF7 Her2^{high} cells with MitoTam disrupted the SC (Fig. 6C, E) in the Her2^{high} background. To see if MCF7 and their Her2^{high} counterparts maintain these features also *in vivo*, we analyzed tumors from control and MitoTam-treated mice. NBGE analysis documents that tumors derived from MCF7 Her2^{high} cells contain higher level of SCs than tumors derived from parental cells and that the respirasome was disrupted by MitoTam treatment in the Her2^{high} situation (Fig. 6F, H). This effect was not secondary to the suppression of individual protein subunits of ETC complexes, as no change in expression of these subunits was detected by WB after SDS-PAGE in tumors from MitoTam-treated and control mice (Fig. 6G). These data suggests that MitoTam directly disrupts respiration via CI and the respirasome, an effect that is much more prominent in Her2-high cells.

To gain insight into the interaction of MitoTam with CI, we performed molecular modelling of MitoTam association with CI, using the recently published crystal structure of *Yarrowia lipolytica* CI resolved at 3.6-3.9 Å (60). Among the 20 poses with predicted highest binding affinity, we identified 3 preferred binding regions: inside the ubiquinone (UbQ)-binding pocket, at its entrance, and at the surface of the transmembrane region of the P_P module. The internal poses share the same binding cavity as well as orientation of the tamoxifen moiety with the predicted position of UbQ (Fig. 7), while the external poses are in close proximity to the cavity's entrance. This suggests that MitoTam could affect UbQ interaction with CI and in this way stimulate ROS generation, consistent with observed experimental results.

Her2 is localized at the inner mitochondrial membrane. The Her2 protein was recently shown to localize also into mitochondria using GFP-tagged Her2 fragments and biochemical means (7), but this unexpected report has not been confirmed. We therefore studied localization of Her2 in our cellular models using several approaches. STED confocal microscopy of MCF7 Her2^{high} cells revealed co-localization of a fraction of the Her2 protein with the IMM protein ATP synthase. As expected, Her2 was also detected in the cytoplasm and on the plasma membrane (Fig. 8A). This is consistent with WB of fractionated cells, showing high levels of Her2 in mitochondria in MCF7 Her2^{high} cells as well as in a number of other breast cancer cell lines (Fig. 8B). We then performed immuno-gold transmission electron microscopy (IG-TEM). Fig. 8C reveals that MCF7 Her2^{high} cells contain more Her2 than their parental counterparts at the IMM (light blue arrow-heads) and that some Her2 signal is also associated with stress fibers in the cytoplasm (green arrow-heads). The super-resolution Biplane FPALM/dSTORM technique (Fig. 8D) documents that in MCF7 Her2^{high} cells Her2 is primarily associated with the outer surface of the mitochondrial matrix mtHsp70-stained region, highly indicative of localization at the IMM. This was further documented by WB analysis of sub-mitochondrial fractions, where Her2 was detected in intact mitochondria and isolated mitoplasts but not in the intermembrane space (IMS) and outer mitochondrial membrane (OMM) fractions (Fig. 8E). Moreover, using the ‘protease protection’ assay, Her2 remained unchanged upon addition of trypsin to intact mitochondria isolated from MCF7 Her2^{high} cells while the OMM marker VDAC was almost completely digested; both proteins were sensitive to trypsin treatment in mitochondria solubilized with Triton-X100 (Fig. 8F).

We also fractionated MCF7 and MCF7 Her2^{high} cell-derived tumors treated with MitoTam and assessed them for Her2 (Fig. 8G). Consistently with cultured cells, Her2 was

present primarily in the mitochondrial fraction of Her2^{high} tumors. Collectively, these findings confirm mitochondrial localization of Her2 and document its presence at the IMM.

Mitochondrial Her2 determines susceptibility to MitoTam. We speculated that the fraction of Her2 in mitochondria may promote the increased sensitivity of Her2^{high} MCF7 cells to MitoTam. According to a recent report, mtHsp70 is needed for mitochondrial localization of Her2 (7), and we also detected Her2-mtHsp70 interaction using immunoprecipitation (Fig. 9A). We knocked down mtHsp70 in MCF7 cells by siRNA (Fig. 9B), and this reduced MitoTam-induced cell death selectively in MCF7 Her2^{high} cells while having no effect in mock-transfected or Her2^{low} cells, completely abrogating the increased sensitivity of Her2^{high} cells to MitoTam (Fig. 9C). Cells transfected with mtHsp70 siRNA showed lower levels of Her2, mtHsp70 and NDUFA9 in whole cell lysate (Fig. 9D) and, in particular, in the mitochondrial fraction (Fig. 9E). NBGE also documents reduced SC levels in mtHsp70 knockdown cells using an antibody to a CI and CIII subunits, while no effect on CII was observed (Fig. 9F). To evaluate the involvement of mitochondrial Her2 in the susceptibility of Her2^{high} cells to MitoTam, we used a set of modified Her2 constructs with increased or decreased ability to translocate to mitochondria. Upon transient transfection in MCF7 cells the construct comprising Her2 tagged with the mitochondrial targeting sequence of Cox8 (MTS) made the cells more susceptible to MitoTam than the construct where the inner MTS of Her2, described earlier (7) was deleted (Δ MTS) (Fig. 9G). The insert in Fig. 9G shows different levels of mitochondrial Her2 expression in MTS- and Δ MTS-transfected cells, while the total Her2 expression was similar in wild-type, MTS and Δ MTS cells (Fig. 9H). These results strongly indicate that the mitochondrial Her2 pool determines the sensitivity of MCF7 cells to MitoTam.

DISCUSSION

Despite considerable advances in molecular oncology, cancer remains one of the leading causes of premature death (44). Breast cancer is the most frequent carcinoma in females, responsible for a high number of fatalities, and some sub-types are very hard to manage (6). Tamoxifen is commonly used as a first-line therapy of estrogen receptor (ER)-positive breast cancer. However, almost 50% of patients develop resistance caused by multiple molecular reasons. One of these is the overexpression of the *HER2/neu* (also referred to as *ERBB2*) oncogene (45). Taking the high percentage of relapsed patients and possible side effects into consideration (5,6), there is a demand for new generation of efficient drugs.

Based on the above, we designed and synthesized MitoTam, a tamoxifen derivative where the original tamoxifen moiety is conjugated to the mitochondria-targeting TPP⁺ group (*cf* Fig. 1A). As predicted, this caused substantial accumulation of the modified compound at the matrix/IMM interface and led to a number of striking functional consequences. We found that MitoTam i) kills a variety of breast cancer cells with a much higher efficacy than tamoxifen; ii) in stark contrast to tamoxifen, is more efficient in killing Her2^{high} than Her2^{low} cells; iii) very efficiently suppresses experimental Her2^{high} breast carcinomas; iv) acts by suppression of CI-dependent respiration and disruption of respiratory SCs, which is particularly apparent in the Her2^{high} background; v) relies on the presence of mitochondrial fraction of Her2 protein for high efficacy in Her2^{high} cells/tumors.

TPP⁺-tagging of tamoxifen makes it ideally suited for interaction with the ETC located at the matrix/IMM interface. We have shown recently that TPP⁺ modification accentuates the propensity of medium affinity CII inhibitors to generate ROS (9,17). In the current study we detected substantial ROS generation upon MitoTam treatment, whereas very little or no ROS were induced by tamoxifen. ROS were functionally relevant, as application of antioxidants protected from MitoTam-induced cell death. Given the previously published report that

tamoxifen at supra-pharmacological concentrations inhibits CI (25), we considered the possibility that TPP⁺-driven accumulation of the inhibitor in the vicinity of the ETC might result in accelerated CI inhibition. Indeed, MitoTam avidly and instantaneously suppressed CI-dependent respiration and CI-CIII oxidoreductase activity in cultured cells and in tumors (but not in the liver demonstrating selectivity), while its effect on CII-driven respiration or CII-CIII oxidoreductase activity was low. In addition, cell death induced by MitoTam was significantly reduced in a cellular model of CI deficiency, and molecular modelling suggested that MitoTam interacts within the UbQ-binding cavity of CI. Importantly, such interaction would induce ROS in CI functioning in the forward manner expected to occur in intact cells (19,52), explaining the experimental observations. Even though we cannot completely discount a contribution of downstream ETC components such as CIII and CIV to MitoTam-induced ROS formation and cell death, based on the available evidence we propose that CI is the molecular target of MitoTam in mitochondria.

In contrast to tamoxifen, MitoTam proved very efficient in eliminating Her2^{high} breast cancer cells and tumors in multiple Her2^{high} models. In some instances, MitoTam application in mice led to complete regression of Her2^{high} tumors (*c.f.* Fig. 3), with no detectable relapse over the 8 month period after cessation of treatment. In addition, MitoTam suppressed invasiveness and metastasis formation, in line with reports that elevated oxidative stress reduces metastases (32,59). Her2 overexpression sensitized both MCF7 and MDA-MB-231 cell lines to MitoTam, even though these cell lines differ in their estrogen receptor status. This indicates that the Her2-associated sensitivity is independent of estrogen signaling. Interestingly, we discovered that Her2^{high} cells and tumors express more CI and that they have higher level of SCs including the respirasome (1,21,24,51), and that Her2^{high} cells and tumors feature higher oxygen consumption with CI substrates. In addition, we found that MitoTam treatment of Her2^{high} cells and mice bearing Her2^{high} tumors disrupted ETC SCs,

which was much less apparent in cells with low Her2. MitoTam also induced more mitochondrial ROS in Her2^{high} cells. Taken together, with more CI available, Her2^{high} cells may have higher capacity to generate ROS upon CI inhibition. This effect might be further amplified in a positive feed-back loop by the MitoTam-mediated disruption of ETC SCs. This is consistent with the notion that SCs are viewed as conduits facilitating passage of reduced electron carriers such as UbQ within the ETC (21,24) and prevent premature escape of electrons, limiting ROS formation. Hence, disruption of SCs, possibly by direct MitoTam binding or by initial ROS produced from CI, could amplify the overall rate of ROS generation specifically in Her2^{high} background and push the Her2^{high} cells over the threshold to cell death.

The results discussed above raise the possibility that Her2 overexpression could directly sensitize mitochondria to MitoTam. Several oncogenes have been reported in mitochondria (40), and one study recently suggested that a fraction of cellular Her2 also translocates into that organelle and stimulates glycolysis (7). We detect Her2 in mitochondria in our experimental breast cancer *in vitro* and *in vivo* models using several independent techniques, and document that a significant portion of the cellular Her2 is localized at the cristae region of the IMM. In contrast to Ding et al (7), we consistently find increased respiration in Her2^{high} cells and tumors, in line with increased SC assembly. Two pieces of evidence indicate that the mitochondrial fraction of Her2 is functionally relevant for the sensitization to MitoTam. First, the knockdown of mtHSP70, which mediates mitochondrial Her2 import (7), de-sensitized Her2^{high} cells to MitoTam, while no effect was observed in parental cells. Second, overexpression of Her2 constructs with increased and decreased ability to localize into mitochondria increased and decreased, respectively, sensitivity to MitoTam. The reason why mitochondrial Her2 sensitizes to MitoTam is not entirely clear, but is very likely connected to the IMM localization of Her2 in the proximity of ETC. The reduction of

mitochondrial Her2 upon mtHSP70 knock down reduced the SCs including the respirasome, and Ding and colleagues reported Her2 interaction with complex IV of ETC (7). Because the assembly of the respirasome occurs only in the presence of CIII and CIV (21,26,51), Her2 could affect this process by facilitating respirasome assembly at the level of CIV, even though our data suggest that MitoTam interacts directly with CI.

In summary, we show that mitochondrial targeting of tamoxifen enhances its efficacy and broadens its applicability by imparting an additional biological activity directed at the ETC. This introduces MitoTam into the family of mitocans, anti-cancer agents acting directly on mitochondria, as first shown for the selective agent α -tocopheryl succinate (29,30) targeting CII (8,11). The role of CI in cancer is undoubtedly complex and context-dependent (15,41), but its pharmacological modulation might represent an effective approach to cancer therapy as demonstrated in this report. A novel finding that oncogenes such as *HER2* might modulate the supramolecular organization of ETC and in this way determine the amount of ROS produced upon CI inhibition strengthens the paradigm of ETC targeting as a relevant approach for selective suppression of cancer (20,38,39,54,58). Interestingly, various treatment-resistant and metastatic subpopulations of cancer cells show a high dependence on mitochondrial respiratory function, even though the information about ETC supramolecular organization into SCs in this context is limited (14,22,36,51,55). Accordingly, ETC-targeting agents such as MitoTam might provide means to eradicate these resistant populations, as documented in this report by the efficient suppression of the hard-to-manage Her2^{high} breast carcinomas. MitoTam already passed the preclinical testing where it showed a very favorable toxicity profile and continues to phase I clinical trials.

INNOVATION

Despite the promise of targeted therapeutics, Her2^{high} breast cancer is still difficult to control. Here we show that Her2^{high} cells and tumors have increased respiratory supercomplex assembly, which can be selectively disrupted *in vitro* and *in vivo* by MitoTam, a mitochondrially-targeted tamoxifen. This results in substantial reactive oxygen species generation in Her2^{high} background and efficient induction of apoptotic cell death. Hence, disruption of respiratory supercomplexes in specific subsets of cancer cells represents a viable therapeutic strategy that avoids toxicity associated with conventional electron transport chain inhibitors. MitoTam has now passed preclinical testing and proceeds to phase I clinical trial.

MATERIALS AND METHODS

Reagents. All reagents were from Sigma Aldrich (St. Louis, MO, USA), unless stated otherwise.

Cell culture. Human breast cancer cell lines MCF7 and MDA-MB-453 were obtained from the ATCC. BT474, MDA-MB-231, MDA-MB-436, SK-BR-3 and T47D human breast cancer cell lines were from J. A. López (Griffith University, Australia). The mouse NeuTL breast cancer cell line was originally derived from spontaneous breast carcinomas of FVB/N *c-neu* mice (13). The cells were cultured in DMEM (Lonza, Basel, Switzerland) with 10% FBS, 1% antibiotics in a 5% CO₂, 37°C incubator. The 6-thioguanine resistant mouse 4T1 cell line, from ATCC was maintained in RPMI1640 (Lonza). Tamoxifen-resistant MCF7 cells were prepared by cultivation of MCF7 cells in the presence of escalating doses of tamoxifen for over one year. Chinese hamster lung fibroblasts B1 and B10 were from Prof. I. Scheffler (46). Human foreskin fibroblasts A014578, rat cardioblasts H9c2 and human immortalized endothelial EAhy926 cells were from the ATCC. All cell lines were authenticated. Mammospheres were generated and cultured as described (49).

Primary Antibodies. The primary antibodies used were: Her2 (OP-15, Calbiochem, San Diego, CA, USA or Ab-1221/1222, Sigma Aldrich), mtHsp70 (MA3-028, Thermo Scientific, Waltham, MA, USA), Actin-HRP (5125, Cell Signaling, Danvers, MA, USA), Caspase-9 (9501, Cell Signaling), Procaspase-9 (9508, Cell Signaling), Parp 1/2 (sc7150, Santa Cruz, Dallas, TX, USA), Bax (2772, Cell Signaling), Bcl-2 (sc7382, Santa Cruz), Hsp60 (4870, Cell Signaling), NDUFA9 (459100, Life Technologies), NDUFS3 (459103, Life Technologies), NDUFV1 (ab5535, Abcam, Cambridge, UK), SDHA(ab14715, Abcam), SDHA (ab14715, Abcam), SDHB (ab14714, Abcam), CoreI (459140, Life Technologies), Cox5a (453120, Life Technologies), CoxIV (4844, Cell Signaling), Atpβ (14730, Abcam; or kind gift from J. Houstek, Institute of Physiology CAS, used for imaging), mt-ND1 (74257,

Abcam), Cyt c (sc13156, Santa Cruz), SOD1 (sc-11407, Santa Cruz), VDAC (4866, Cell Signaling), β -tubulin-HRP (ab40742, Abcam).

DNA constructs and cell transfections. MCF7 cells with silenced expression of *HER2* oncogene were prepared by stable transfection with shRNA vectors (KH00209N, SA Biosciences, Frederick, MD, USA). Full length human Her2 construct was produced by PCR amplification of cDNA isolated from MDA-MB-453 cells using proofreading PFU DNA polymerase (Fermentas, Waltham, MA, USA) and primers 5'-ATA AAG CTA GCC TCG AGC ACC ATG GAG CTG GCG G-3' (forward) and 5'-ATA AAT CTA GAG AAT TCT CAC ACT GGC ACG TCC AGA C-3' (reverse). The PCR product was gel-purified, digested with XhoI/XbaI (Takara, Mountain View, CA, USA), re-purified and ligated between the XhoI and XbaI sites of pEF/IRES/Puro plasmid. MCF7 and MDA-MB-231 cells overexpressing Her2 were prepared by electroporation. Empty vectors were used as a control (mock transfection). Stable clones were selected by puromycin and verified by WB. Transient transfections with modified Her2-containing vectors were done using Lipofectamine 3000 (Thermo Scientific). To obtain the Her2-MTS construct, Cox8-derived mitochondrial targeting sequence was PCR-amplified from the pTagGFP2-mito vector (Evrogen, Moscow, Russia) using primers 5'-ATA AAG CTA GCC ACC ATG TCC GTC CTG ACG CCG CTG-3' (forward) and 5'-ATA AAC TCG AGC TTG GAT CCC CCA ACG AAT G-3' (reverse), gel-purified, digested by NheI/XhoI fast digestion enzymes (Thermo Scientific), re-purified and ligated between the NheI and XhoI sites in front of the full-length *HER2* cDNA in the pEF/IRES/Puro plasmid. The Her2- Δ MTS construct was prepared by deletion of the internal mitochondria-targeting sequence reported by Ding et al (7) from the full length *HER2* cDNA in the pEF/IRES/Puro plasmid by inverse PCR using Q5 high fidelity DNA polymerase in the presence of a GC enhancer (New England Biolabs, Ipswich, MA, USA). The PCR product was agarose gel-purified and self-ligated by T4 ligase (Thermo Scientific).

Primers for the inverse PCR reaction were phosphorylated by T4 oligonucleotide kinase (Thermo Scientific) prior to use, and their sequences were 5'-CTG CAG GAA ACG GAG CTG GTG GAG-3' and 5'-GCA TGC GCC CTC CTC ATC TGG-3'. All constructs were verified by DNA sequencing. MCF7 cells with GFP-labelled mitochondria were prepared by stable transfection with pTagGFP2-mito vector using Fugene transfection reagent (Promega, Madison, WI, USA). Transfections with siRNAs, where indicated in the figure legends, were performed using DharmaFect 1 reagent (Thermo Scientific). siRNAs for mtHsp70 (SASI_Hs01_00216924) and universal non-silencing control siRNA were purchased from Sigma Aldrich.

Cell death and viability assays. Cell death was quantified by using the annexin V-FITC/propidium iodide (PI) method and assessed by flow cytometry (FACSCalibur or FACSCanto, Becton Dickinson, Franklin Lakes, NJ, USA). Proliferation was estimated using the crystal violet staining. Cell death in the mammosphere model was assessed by propidium iodide (5 ng/ml, 5 min) staining and visualized by wide-field fluorescent microscopy (Nikon Ti-E, 10x lense).

Detection of ROS levels and mitochondrial inner membrane potential. The levels of ROS were evaluated using 2',7'-dichlorodihydrofluorescein diacetate (DCF) or MitoSOX (Life Technologies, Carlsbad, CA, USA). Mitochondrial inner membrane potential was detected using tetramethylrhodamine methyl ester (TMRM). Cells were incubated with both probes under normal culture conditions for the times indicated followed by evaluation using flow cytometry (50 nM TMRM, 5 μ M DCF, 0.5 μ M MitoSOX) or time-lapse confocal microscopy (10 nM TMRM).

Glucose uptake, lactate production and ATP measurements. Glucose uptake was measured after 24 h incubation in low glucose DMEM and 15 min pre-incubation with 50 μ M 2-nitrobenzodeoxyglucose (2-NBDG; Life Technologies) by flow cytometry. For lactate

production and ATP measurements, the cells were seeded in a 96 well format (10^4 per well) and the assays were performed as described (51).

Assessment of respiration of cells and tissue. Routine respiration and respiration via CI and CII was assessed using the high-resolution Oxygraph-2k respirometer (O2k; Oroboros Instruments, Innsbruck, Austria) according to the standard procedure (16,31). For CI- and CII-dependent respiration, digitonin-permeabilized cells suspended in mitochondrial respiration medium MiR05 were used in all experiments. The total oxygen concentration and consumption were monitored in the presence of specific inhibitors and substrates of CI (rotenone or glutamate/malate, respectively) or CII (malonate or succinate, respectively) in the presence of increasing concentrations of tamoxifen or MitoTam. Tissue respiration was assessed in an analogous manner using freshly excised tumor or liver homogenized in a dedicated tissue shredder. Respiration was monitored within 1 h after mice were sacrificed to avoid deterioration of the tissue.

Enzymatic assays. Isolated mitochondria were used after freeze-thaw treatment and hypotonic lysis. For NADH-cytochrome c oxidoreductase (CI-CIII) activity, 20 μ g of mitochondria were incubated with 50 mM Tris (pH 8.0), 1 mM KCN and 2.5 mg/ml BSA and 1 mM NADH at 30°C. Reaction (1 ml volume) was started by the addition of 40 μ M cytochrome c, absorbance at 550 nm was followed for 90 s, and rotenone (5 μ g/ml) was added for another 90 s. Rotenone insensitive rate was subtracted. Succinate-cytochrome c (CII-CIII) oxidoreductase activity was measured similarly, only NADH was replaced by 10 mM succinate, and rotenone by 3 μ M antimycin. Citrate synthase was measured as described (48), but the reaction was scaled down into a 96 well plate format (200 μ l volume).

Cellular and sub-cellular fractionation. Cells were washed twice with PBS, harvested by scrapping and suspended in STE buffer (250 mM sucrose, 10 mM Tris, 1 mM EDTA) containing protease inhibitors. Suspension was homogenized on ice using a glass-Teflon

homogenizer, mitochondrial fraction was isolated by differential centrifugation as detailed before (51). For preparation of mitoplasts, isolated mitochondria were re-centrifuged at 10,000 x g, the pellet re-suspended in the hypotonic buffer (10 mM MOPS-KOH, pH 7.2, 1 mM EDTA) and incubated on ice for 30 min with occasional pipetting. The efficiency of the swelling reaction was confirmed by WB for selected IMM, IMS and matrix proteins with parallel reaction of intact mitochondria incubated in the SEM buffer (10 mM MOPS-KOH, pH 7.2, 250 mM sucrose, 1 mM EDTA).

Protease protection assay. To determine mitochondrial residence of Her2, crude mitochondria were pelleted via centrifugation (10,000 x g, 10 min, 4°C), re-suspended to 0.5 mg/ml in the SEM buffer and treated with 50 µg/ml trypsin in the presence or absence of 1% Triton X-100. The protease was inhibited by addition of 1 mg/ml soybean trypsin inhibitor at indicated times and the sample was processed for WB analysis.

Electrophoresis and western blot analysis. SDS-PAGE, native blue gel electrophoresis (NBGE) and western blot (WB) analysis were performed according to standard protocols as detailed elsewhere (51).

TUNEL assay. Excised tumors were mounted into paraffin blocks and sectioned. Tissue slices were de-paraffinized and rehydrated. Apoptosis was detected using Click-iT TUNEL AlexaFluor 488 assay (Invitrogen, Carlsbad, CA, USA) according to manufacturer's instructions.

Animal studies. Balb-c *nu/nu* mice were implanted with a slow-release estradiol pellet (60-day release of 12 µg per day; Innovative Research of America, Sarasota, FL, USA) and injected sub-cutaneously (s.c.) with MCF7 mock or MCF7 Her2^{high} cells at 2x10⁶ cells/animal. When tumors reached the volume of 30-50 mm³ (quantified by ultrasound imaging, USI), mice were treated with either tamoxifen (2 µmol/mouse/dose), MitoTam (0.25 µmol/mouse/dose) or solvent control (4% ethanol in corn oil, 100 µl per dose) given

intraperitoneally (i.p.) twice per week. FVB/N *c-neu* mice were s.c. injected with syngeneic NeuT1 cells (13) at 2×10^6 cells/animal and treated as above with tamoxifen (2.69 $\mu\text{mol}/\text{mouse}/\text{dose}$) or MitoTam (0.54 $\mu\text{mol}/\text{mouse}/\text{dose}$). Tumor volume was monitored by the USI instrument Vevo770 (VisualSonics, Toronto, Canada). For spontaneous Her2^{high} tumor treatment, FVB/N *c-neu* mice that developed tumors (450 mm^3 on average) were treated with MitoTam (0.54 $\mu\text{mol}/\text{mouse}/\text{dose}$) or solvent as above. For metastasis measurements, Balb/c mice were s.c. injected with 1×10^6 4T1 cells. After 1 week (when tumors reached on average 100 mm^3), MitoTam (0.25 $\mu\text{mol}/\text{mouse}/\text{dose}$) or solvent were administered as above for two weeks. The mice were sacrificed, blood, lungs and liver were collected, single cells suspension was prepared and the metastatic cells were selected with 6-thioguanine for 10 days as described (34). The number of 6-thioguanine-resistant colonies was counted and expressed on per-organ bases. Animal weight was regularly monitored. Individual experimental groups contained at least 5 mice. All experiments were approved by the Czech academy of Sciences or Griffith University Ethics Committee and performed according to the Czech or the Australian and New Zealand Council guidelines for the Care and Use of Animals in Research and Teaching.

Zone exclusion assay. 7×10^4 cells were seeded into glass-bottom microscopy plates using 2 well silicone inserts (Ibidi, Martinsried, Germany). 3 days after seeding the inserts were removed, and MitoTam (0.5 μM) or solvent control were added. The plates were inspected by Nikon Ti-E wide field microscope using a 10x lens at the time of insert removal, and after 24 and 48 hours.

Time-lapse confocal microscopy. Cells were seeded on glass bottom microscopy dishes coated with poly-L-lysine. Images were recorded the third day after seeding using 63x oil immersion lens of the SP5 confocal microscope (Leica Microsystems, Wetzlar, Germany) equipped with a heated CO₂ incubator as described in detail before (53). Time-lapse images

were recorded every 5 min with the first image taken 5 min before adding the drug. The maximal projection of 2 μm z-stack is shown.

STED microscopy. Cells were grown on cover-slips coated with poly-L-lysine, fixed with 4% paraformaldehyde the third day after seeding, permeabilized with 0.05 % Triton X-100, 0.05 % Tween-20 in PBS, blocked with 5% FBS and incubated with primary antibodies against ATP β and Her2 (OP-15, Calbiochem) and secondary antibodies conjugated with Alexa Fluor 488 or Alexa Fluor 555 (Life Technologies). The cover-slips were mounted in a glycerol medium containing N-propyl gallate, and single focal plane images were recorded with 100x oil immersion lens of SP8 confocal microscope equipped with STED module with 660 nm depletion laser (Leica Microsystems) and white laser.

Double channel BiplaneFPALM/dSTORM. Cells were grown on glass cover-slips coated with poly-L-lysine. Immunocytochemistry of Her2 and mtHSP70 proteins was performed using respective primary antibodies and secondary antibodies conjugated with Alexa Fluor 647 and Cy3b (Life Technologies). Samples were mounted in the dSTORM buffer (10% glucose, 50 mM cysteamine, 169 units of glucose oxidase, 1.4 units of catalase; all in 10 mM NaCl, 50 mM Tris-HCl, pH 8.0). Images were obtained using the BiplaneFPALM instrument (Vutara, Salt Lake City, UT, USA) equipped with 60x water immersion objective.

Immunogold transmission electron microscopy (IG-TEM). Cells were grown on cover-slips and fixed with 3% paraformaldehyde, 0.1% glutaraldehyde in Sorensen's buffer (SB; pH 7.2-7.4). After washing in the SB buffer, cells were dehydrated in ethanol series and embedded in LR white resin by a standard procedure. Ultrathin sections (70-90 nm) mounted on gilded copper grids, blocked with 10% NGS in PBS with 0.1% Tween 20, 1% BSA, pH 7.4, were incubated with primary antibody against Her2 diluted 1:50 (mouse monoclonal IgG, OP-15) and then with secondary antibody diluted 1:30 (goat anti-mouse conjugated with

12 nm colloidal gold particles, Jackson ImmunoResearch Laboratories, West Grove, PA, USA). Observations and acquisition were done using the FEI Morgagni 268 transmission electron microscope operated at 80 kV (Fei Morgagni, Hillsboro, OR, USA). The images were captured with Mega View III CCD camera (Olympus, Tokyo, Japan). Multiple sections of at least three independent immunogold labelling experiments were analyzed.

Molecular modelling. The pre-released crystal structure of yeast complex I from *Yarrowia lipolytica* (PDB ID 4wz7) was kindly provided by the authors (60). The geometry of MitoTam was optimized using the DFT-D method (4). MitoTam was then allowed to sample docking poses in a box (90x90x90 grid points, 1.0 Å spacing) covering the lower part of the peripheral arm (Q module) and the transmembrane P_P module of the membrane arm. The Python Molecular Viewer (PMV 1.5. genetic algorithm steps each were collected employing AutoDock version 4.2 (27). The program 3V (56) was used to identify internal cavities connecting the iron-sulfur clusters with the ubiquinone-binding site in the crystal structure.

Synthesis of tamoxifen derivatives. The synthesis of MitoTam and the derivatives used in this study (Fig. S1) will be described in a separate publication (J.S. et al., under preparation).

Statistical analysis. Data were analyzed in GraphPad Prism 5.04 software (GraphPad Software, La Jolla, CA, USA) using unpaired Student's t-test analysis or two-way ANNOVA for comparisons of more than two parameters. Data shown are mean values ± S.E.M. of at least three independent experiments (unless stated otherwise). A statistical difference of $p < 0.05$ was considered significant.

ACKNOWLEDGEMENTS

This research was supported in part by grants from the Australian Research Council (DP110105009) to J.N. and L.F.D., from the National and Health Medical Research Council of Australia (APP1011955), the Australian Research Council (DP130101651, DP15010280) the Cancer Council Queensland (APP1049104) to J.N., by the Czech Science Foundation grants to J.N. (16-12719S), J.R. (16-22823S) and J.T. (P305/13-28830S), by the Technology Agency of the Czech Republic (TE01020118), Ministry of Industry and Trade of the Czech Republic (FR-TI3/588), and Institutional Research Support (RVO: 68378050) to M.S. and P.H., and by LQ1604 NPU II provided by MEYS and CZ.1.05/1.1.00/02.0109 BIOCEV provided by ERDF and MEYS.

AUTHOR'S DISCLOSURE STATEMENT

J.N. and J.S. are inventors of a patent 'Tamoxifen analogues for treatment of neoplastic diseases, especially with high Her2 protein level'. The authors declare no additional competing financial interests.

AUTHOR'S CONTRIBUTIONS

K. R., L. D. and J. N. designed the study; K. R., K. S., J. S., A. B., J. B., B. E., R. Z., J. G., T. S., E. A. P., B. Y., M. N. N., M. V., M. S., J. T., J. R. and L. D. performed experiments; J. S. and L. W. designed, synthesized and analyzed compounds used in the study; J. C. performed molecular modelling; P. J. and P. H. supervised PALM and TEM studies; K. R., K. S., J. R., L. D. and J. N. analyzed and interpreted data; K. R., J. R. and J. N. wrote the manuscript; J. N. supervised the study.

LIST OF ABBREVIATIONS

$\Delta\Psi_{m,i}$ – mitochondrial inner membrane potential

CI, CII, CIII, CIV, CV – respiratory complex I, II, III, IV, V

ETC – electron transport chain

FCCP – carbonyl cyanide 4-(trifluoromethoxy)phenylhydrazone

IMM – inner mitochondrial membrane

IMS – intermembrane space

MitoTam- mitochondrially-targeted tamoxifen

NAC - N-acetyl cysteine

NBGE – native blue gel electrophoresis

OMM – outer mitochondrial membrane

RC – respiratory complex

ROS – reactive oxygen species

SC – respiratory supercomplex

Tam-DPPO – Diphenylphosphine oxide tamoxifen

TMRM – tetramethylrhodamine methyl ester

TPP⁺ - triphenylphosphonium

UbQ – ubiquinone

WB – western blotting

REFERENCES

1. Acin-Perez R, Fernandez-Silva P, Peleato ML, Perez-Martos A, Enriquez JA. Respiratory active mitochondrial supercomplexes. *Mol Cell* 32: 529-39, 2008.
2. Althoff T, Mills DJ, Popot JL, Kuhlbrandt W. Arrangement of electron transport chain components in bovine mitochondrial supercomplex I1III2IV1. *EMBO J* 30: 4652-64, 2011.
3. Birsoy K, Wang T, Chen WW, Freinkman E, Abu-Remaileh M, Sabatini DM. An Essential Role of the Mitochondrial Electron Transport Chain in Cell Proliferation Is to Enable Aspartate Synthesis. *Cell* 162: 540-51, 2015.
4. Cerny J, Jurecka P, Hobza P, Valdes H. Resolution of identity density functional theory augmented with an empirical dispersion term (RI-DFT-D): a promising tool for studying isolated small peptides. *J Phys Chem A* 111: 1146-54, 2007.
5. Dawood S, Broglio K, Buzdar AU, Hortobagyi GN, Giordano SH. Prognosis of women with metastatic breast cancer by HER2 status and trastuzumab treatment: an institutional-based review. *J Clin Oncol* 28: 92-8, 2010.
6. DeSantis CE, Lin CC, Mariotto AB, Siegel RL, Stein KD, Kramer JL, Alteri R, Robbins AS, Jemal A. Cancer treatment and survivorship statistics, 2014. *CA Cancer J Clin* 64: 252-71, 2014.
7. Ding Y, Liu Z, Desai S, Zhao Y, Liu H, Pannell LK, Yi H, Wright ER, Owen LB, Dean-Colomb W, Fodstad O, Lu J, LeDoux SP, Wilson GL, Tan M. Receptor tyrosine kinase ErbB2 translocates into mitochondria and regulates cellular metabolism. *Nat Commun* 3: 1271, 2012.
8. Dong LF, Freeman R, Liu J, Zabalova R, Marin-Hernandez A, Stantic M, Rohlena J, Valis K, Rodriguez-Enriquez S, Butcher B, Goodwin J, Brunk UT, Witting PK, Moreno-Sanchez R, Scheffler IE, Ralph SJ, Neuzil J. Suppression of tumor growth in vivo by the mitocan alpha-tocopheryl succinate requires respiratory complex II. *Clin Cancer Res* 15: 1593-600, 2009.
9. Dong LF, Jameson VJ, Tilly D, Cerny J, Mahdavian E, Marin-Hernandez A, Hernandez-Esquivel L, Rodriguez-Enriquez S, Stursa J, Witting PK, Stantic B, Rohlena J, Truksa J, Kluckova K, Dyason JC, Ledvina M, Salvatore BA, Moreno-Sanchez R, Coster MJ, Ralph SJ, Smith RA, Neuzil J. Mitochondrial targeting of vitamin E succinate enhances its pro-apoptotic and anti-cancer activity via mitochondrial complex II. *J Biol Chem* 286: 3717-28, 2011.
10. Dong LF, Jameson VJ, Tilly D, Prochazka L, Rohlena J, Valis K, Truksa J, Zabalova R, Mahdavian E, Kluckova K, Stantic M, Stursa J, Freeman R, Witting PK, Norberg E, Goodwin J, Salvatore BA, Novotna J, Turanek J, Ledvina M, Hozak P, Zhivotovsky B, Coster MJ, Ralph SJ, Smith RA, Neuzil J. Mitochondrial targeting of alpha-tocopheryl

succinate enhances its pro-apoptotic efficacy: a new paradigm for effective cancer therapy. *Free Radic Biol Med* 50: 1546-55, 2011.

11. Dong LF, Low P, Dyason JC, Wang XF, Prochazka L, Witting PK, Freeman R, Swettenham E, Valis K, Liu J, Zobalova R, Turanek J, Spitz DR, Domann FE, Scheffler IE, Ralph SJ, Neuzil J. Alpha-tocopheryl succinate induces apoptosis by targeting ubiquinone-binding sites in mitochondrial respiratory complex II. *Oncogene* 27: 4324-35, 2008.
12. Dontu G, Abdallah WM, Foley JM, Jackson KW, Clarke MF, Kawamura MJ, Wicha MS. In vitro propagation and transcriptional profiling of human mammary stem/progenitor cells. *Genes Dev* 17: 1253-70, 2003.
13. Guy CT, Webster MA, Schaller M, Parsons TJ, Cardiff RD, Muller WJ. Expression of the neu protooncogene in the mammary epithelium of transgenic mice induces metastatic disease. *Proc Natl Acad Sci U S A* 89: 10578-82, 1992.
14. Haq R, Shoag J, Andreu-Perez P, Yokoyama S, Edelman H, Rowe GC, Frederick DT, Hurley AD, Nellore A, Kung AL, Wargo JA, Song JS, Fisher DE, Arany Z, Widlund HR. Oncogenic BRAF regulates oxidative metabolism via PGC1alpha and MITF. *Cancer Cell* 23: 302-15, 2013.
15. Kim EM, Park JK, Hwang SG, Kim WJ, Liu ZG, Kang SW, Um HD. Nuclear and cytoplasmic p53 suppress cell invasion by inhibiting respiratory Complex-I activity via Bcl-2 family proteins. *Oncotarget* 5: 8452-8465, 2014.
16. Kluckova K, Dong LF, Bajzikova M, Rohlena J, Neuzil J. Evaluation of respiration of mitochondria in cancer cells exposed to mitochondria-targeted agents. *Methods Mol Biol* 1265: 181-94, 2015.
17. Kluckova K, Sticha M, Cerny J, Mracek T, Dong L, Drahota Z, Gottlieb E, Neuzil J, Rohlena J. Ubiquinone-binding site mutagenesis reveals the role of mitochondrial complex II in cell death initiation. *Cell Death Dis* 6: e1749, 2015.
18. Kordes S, Pollak MN, Zwinderman AH, Mathot RA, Weterman MJ, Beeker A, Punt CJ, Richel DJ, Wilmink JW. Metformin in patients with advanced pancreatic cancer: a double-blind, randomised, placebo-controlled phase 2 trial. *Lancet Oncol* 16: 839-47, 2015.
19. Kussmaul L, Hirst J. The mechanism of superoxide production by NADH:ubiquinone oxidoreductase (complex I) from bovine heart mitochondria. *Proc Natl Acad Sci U S A* 103: 7607-12, 2006.
20. Kwong JQ, Henning MS, Starkov AA, Manfredi G. The mitochondrial respiratory chain is a modulator of apoptosis. *J Cell Biol* 179: 1163-77, 2007.
21. Lapuente-Brun E, Moreno-Loshuertos R, Acin-Perez R, Latorre-Pellicer A, Colas C, Balsa E, Perales-Clemente E, Quiros PM, Calvo E, Rodriguez-Hernandez MA, Navas P, Cruz R, Carracedo A, Lopez-Otin C, Perez-Martos A, Fernandez-Silva P, Fernandez-Vizarra E,

Enriquez JA. Supercomplex assembly determines electron flux in the mitochondrial electron transport chain. *Science* 340: 1567-70, 2013.

22. LeBleu VS, O'Connell JT, Gonzalez Herrera KN, Wikman H, Pantel K, Haigis MC, de Carvalho FM, Damascena A, Domingos Chinen LT, Rocha RM, Asara JM, Kalluri R. PGC-1 α mediates mitochondrial biogenesis and oxidative phosphorylation in cancer cells to promote metastasis. *Nat Cell Biol* 16: 992-1003, 1-15, 2014.

23. Lega IC, Austin PC, Gruneir A, Goodwin PJ, Rochon PA, Lipscombe LL. Association between metformin therapy and mortality after breast cancer: a population-based study. *Diabetes Care* 36: 3018-26, 2013.

24. Maranzana E, Barbero G, Falasca AI, Lenaz G, Genova ML. Mitochondrial respiratory supercomplex association limits production of reactive oxygen species from complex I. *Antioxid Redox Signal* 19: 1469-80, 2013.

25. Moreira PI, Custodio J, Moreno A, Oliveira CR, Santos MS. Tamoxifen and estradiol interact with the flavin mononucleotide site of complex I leading to mitochondrial failure. *J Biol Chem* 281: 10143-52, 2006.

26. Moreno-Lastres D, Fontanesi F, Garcia-Consuegra I, Martin MA, Arenas J, Barrientos A, Ugalde C. Mitochondrial complex I plays an essential role in human respirasome assembly. *Cell Metab* 15: 324-35, 2012.

27. Morris GM, Huey R, Lindstrom W, Sanner MF, Belew RK, Goodsell DS, Olson AJ. AutoDock4 and AutoDockTools4: Automated docking with selective receptor flexibility. *J Comput Chem* 30: 2785-91, 2009.

28. Murphy MP, Smith RA. Targeting antioxidants to mitochondria by conjugation to lipophilic cations. *Annu Rev Pharmacol Toxicol* 47: 629-56, 2007.

29. Neuzil J, Weber T, Gellert N, Weber C. Selective cancer cell killing by alpha-tocopheryl succinate. *Br J Cancer* 84: 87-9, 2001.

30. Neuzil J, Weber T, Schroder A, Lu M, Ostermann G, Gellert N, Mayne GC, Olejnicka B, Negre-Salvayre A, Sticha M, Coffey RJ, Weber C. Induction of cancer cell apoptosis by alpha-tocopheryl succinate: molecular pathways and structural requirements. *FASEB J* 15: 403-15, 2001.

31. Pesta D, Gnaiger E. High-resolution respirometry: OXPHOS protocols for human cells and permeabilized fibers from small biopsies of human muscle. *Methods Mol Biol* 810: 25-58, 2012.

32. Piskounova E, Agathocleous M, Murphy MM, Hu Z, Huddleston SE, Zhao Z, Leitch AM, Johnson TM, DeBerardinis RJ, Morrison SJ. Oxidative stress inhibits distant metastasis by human melanoma cells. *Nature* 527: 186-91, 2015.

33. Prochazka L, Koudelka S, Dong LF, Stursa J, Goodwin J, Neca J, Slavik J, Ciganek M, Masek J, Kluckova K, Nguyen M, Turanek J, Neuzil J. Mitochondrial targeting overcomes ABCA1-dependent resistance of lung carcinoma to alpha-tocopheryl succinate. *Apoptosis* 18: 286-99, 2013.
34. Pulaski BA, Ostrand-Rosenberg S. Mouse 4T1 breast tumor model. *Curr Protoc Immunol* Chapter 20: Unit 20 2, 2001.
35. Reni M, Dugnani E, Cereda S, Belli C, Balzano G, Nicoletti R, Liberati D, Pasquale V, Scavini M, Maggiora P, Sordi V, Lampasona V, Ceraulo D, Di Terlizzi G, Doglioni C, Falconi M, Piemonti L. (Ir)relevance of metformin treatment in patients with metastatic pancreatic cancer: an open-label, randomized phase 2 trial. *Clin Cancer Res*: 10.1158/1078-0432.ccr-15-1722, 2015.
36. Roesch A, Vultur A, Bogeski I, Wang H, Zimmermann KM, Speicher D, Korbel C, Laschke MW, Gimotty PA, Philipp SE, Krause E, Patzold S, Villanueva J, Krepler C, Fukunaga-Kalabis M, Hoth M, Bastian BC, Vogt T, Herlyn M. Overcoming intrinsic multidrug resistance in melanoma by blocking the mitochondrial respiratory chain of slow-cycling JARID1B(high) cells. *Cancer Cell* 23: 811-25, 2013.
37. Rohlena J, Dong LF, Kluckova K, Zobalova R, Goodwin J, Tilly D, Stursa J, Pecinova A, Philimonenko A, Hozak P, Banerjee J, Ledvina M, Sen CK, Houstek J, Coster MJ, Neuzil J. Mitochondrially targeted alpha-tocopheryl succinate is antiangiogenic: potential benefit against tumor angiogenesis but caution against wound healing. *Antioxid Redox Signal* 15: 2923-35, 2011.
38. Rohlena J, Dong LF, Neuzil J. Targeting the mitochondrial electron transport chain complexes for the induction of apoptosis and cancer treatment. *Curr Pharm Biotechnol* 14: 377-89, 2013.
39. Rohlena J, Dong LF, Ralph SJ, Neuzil J. Anticancer drugs targeting the mitochondrial electron transport chain. *Antioxid Redox Signal* 15: 2951-74, 2011.
40. Rohlenova K, Neuzil J, Rohlena J. The role of Her2 and other oncogenes of the PI3K/AKT pathway in mitochondria. *Biol Chem* 397: 607-15, 2016.
41. Santidrian AF, Matsuno-Yagi A, Ritland M, Seo BB, LeBoeuf SE, Gay LJ, Yagi T, Felding-Habermann B. Mitochondrial complex I activity and NAD⁺/NADH balance regulate breast cancer progression. *J Clin Invest* 123: 1068-81, 2013.
42. Saura C, Bendell J, Jerusalem G, Su S, Ru Q, De Buck S, Mills D, Ruquet S, Bosch A, Urruticoechea A, Beck JT, Di Tomaso E, Sternberg DW, Massacesi C, Hirawat S, Dirix L, Baselga J. Phase Ib study of Buparlisib plus Trastuzumab in patients with HER2-positive advanced or metastatic breast cancer that has progressed on Trastuzumab-based therapy. *Clin Cancer Res* 20: 1935-45, 2014.

43. Schafer ZT, Grassian AR, Song L, Jiang Z, Gerhart-Hines Z, Irie HY, Gao S, Puigserver P, Brugge JS. Antioxidant and oncogene rescue of metabolic defects caused by loss of matrix attachment. *Nature* 461: 109-13, 2009.
44. Siegel RL, Miller KD, Jemal A. Cancer statistics, 2015. *CA Cancer J Clin* 65: 5-29, 2015.
45. Slamon DJ, Clark GM, Wong SG, Levin WJ, Ullrich A, McGuire WL. Human breast cancer: correlation of relapse and survival with amplification of the HER-2/neu oncogene. *Science* 235: 177-82, 1987.
46. Soderberg K, Mascarello JT, Breen GA, Scheffler IE. Respiration-deficient Chinese hamster cell mutants: genetic characterization. *Somatic Cell Genet* 5: 225-40, 1979.
47. Soderberg KL, Ditta GS, Scheffler IE. Mammalian cells with defective mitochondrial functions: a Chinese hamster mutant cell line lacking succinate dehydrogenase activity. *Cell* 10: 697-702, 1977.
48. Spinazzi M, Casarin A, Pertegato V, Salviati L, Angelini C. Assessment of mitochondrial respiratory chain enzymatic activities on tissues and cultured cells. *Nat Protoc* 7: 1235-46, 2012.
49. Stapelberg M, Zabalova R, Nguyen MN, Walker T, Stantic M, Goodwin J, Pasdar EA, Thai T, Prokopova K, Yan B, Hall S, de Pennington N, Thomas SR, Grant G, Stursa J, Bajzikova M, Meedeniya AC, Truksa J, Ralph SJ, Ansorge O, Dong LF, Neuzil J. Indoleamine-2,3-dioxygenase elevated in tumor-initiating cells is suppressed by mitocans. *Free Radic Biol Med* 67: 41-50, 2014.
50. Sullivan LB, Gui DY, Hosios AM, Bush LN, Freinkman E, Vander Heiden MG. Supporting Aspartate Biosynthesis Is an Essential Function of Respiration in Proliferating Cells. *Cell* 162: 552-63, 2015.
51. Tan AS, Baty JW, Dong LF, Bezawork-Geleta A, Endaya B, Goodwin J, Bajzikova M, Kovarova J, Peterka M, Yan B, Pesdar EA, Sobol M, Filimonenko A, Stuart S, Vondrusova M, Kluckova K, Sachaphibulkij K, Rohlena J, Hozak P, Truksa J, Eccles D, Haupt LM, Griffiths LR, Neuzil J, Berridge MV. Mitochondrial genome acquisition restores respiratory function and tumorigenic potential of cancer cells without mitochondrial DNA. *Cell Metab* 21: 81-94, 2015.
52. Treberg JR, Quinlan CL, Brand MD. Evidence for two sites of superoxide production by mitochondrial NADH-ubiquinone oxidoreductase (complex I). *J Biol Chem* 286: 27103-10, 2011.
53. Truksa J, Dong LF, Rohlena J, Stursa J, Vondrusova M, Goodwin J, Nguyen M, Kluckova K, Rychtarcikova Z, Lettlova S, Spacilova J, Stapelberg M, Zoratti M, Neuzil J. Mitochondrially targeted vitamin E succinate modulates expression of mitochondrial DNA transcripts and mitochondrial biogenesis. *Antioxid Redox Signal* 22: 883-900, 2015.

54. Viale A, Corti D, Draetta GF. Tumors and Mitochondrial Respiration: A Neglected Connection. *Cancer Res* 75: 3687-3691, 2015.
55. Viale A, Pettazzoni P, Lyssiotis CA, Ying H, Sanchez N, Marchesini M, Carugo A, Green T, Seth S, Giuliani V, Kost-Alimova M, Muller F, Colla S, Nezi L, Genovese G, Deem AK, Kapoor A, Yao W, Brunetto E, Kang Y, Yuan M, Asara JM, Wang YA, Heffernan TP, Kimmelman AC, Wang H, Fleming JB, Cantley LC, DePinho RA, Draetta GF. Oncogene ablation-resistant pancreatic cancer cells depend on mitochondrial function. *Nature* 514: 628-32, 2014.
56. Voss NR, Gerstein M. 3V: cavity, channel and cleft volume calculator and extractor. *Nucleic Acids Res* 38: W555-62, 2010.
57. Weinberg F, Hamanaka R, Wheaton WW, Weinberg S, Joseph J, Lopez M, Kalyanaraman B, Mutlu GM, Budinger GR, Chandel NS. Mitochondrial metabolism and ROS generation are essential for Kras-mediated tumorigenicity. *Proc Natl Acad Sci U S A* 107: 8788-93, 2010.
58. Wolf DA. Is reliance on mitochondrial respiration a "chink in the armor" of therapy-resistant cancer? *Cancer Cell* 26: 788-95, 2014.
59. Zhang Q, Raje V, Yakovlev VA, Yacoub A, Szczepanek K, Meier J, Derecka M, Chen Q, Hu Y, Sisler J, Hamed H, Lesnfsky EJ, Valerie K, Dent P, Larner AC. Mitochondrial localized Stat3 promotes breast cancer growth via phosphorylation of serine 727. *J Biol Chem* 288: 31280-8, 2013.
60. Zickermann V, Wirth C, Nasiri H, Siegmund K, Schwalbe H, Hunte C, Brandt U. Structural biology. Mechanistic insight from the crystal structure of mitochondrial complex I. *Science* 347: 44-9, 2015.

Table 1. IC₅₀ values for killing of breast cancer cell lines and non-malignant cells with tamoxifen and MitoTam.

Cell line [*]	IC ₅₀ (tamoxifen) [†]	IC ₅₀ (MitoTam)
BT474	29.8	2.4
MCF7	15.2	1.25
MCF7 Her2 ^{high}	21.6	0.65
MCF7 Her2 ^{low}	14.1	1.45
MDA-MB-231	35.8	6.2
MDA-MB-436	12.6	3.4
MDA-MB-453	17.5	2.5
SK-BR-3	28.3	3.5
T47D	17.3	3.4
NeuTL	35.6	4.5
EAhy926 [§]	40.3	10.9
A014578	n.d. [‡]	55.9
H9c2	n.d. [‡]	48.4

^{*}Cells were treated at ~60% confluence.

[†]The IC₅₀ values were derived from viability curves using the crystal violet staining and are expressed in $\mu\text{mol/l}$.

[‡]n.d., not determined.

[§]EAhy926 cells were evaluated for the effect of MitoTam after reaching complete confluence.

Table 2. Inhibition of respiration via complex I and complex II.

Complex	IC₅₀ (tamoxifen)*	IC₅₀ (MitoTam)
CI	30	11.5
CII	47.2	30.6

*IC₅₀ values were estimated from the inhibition of respiration of MCF7 cells grown to 60-70% confluence in the Oxygraph using the CI (glutamate/malate) and CII substrates (succinate) under increasing concentration of tamoxifen or MitoTam.

FIGURE LEGENDS

Figure 1. MitoTam associates with mitochondria and efficiently kills breast cancer cells. **(A)** Structures of tamoxifen and tamoxifen tagged with the TPP⁺ group (MitoTam). **(B)** MCF7 cells were pre-loaded with MitoTracker FarRed, exposed to FITC labelled MitoTam (5 μ M) and inspected by time-lapse confocal microscopy for the times shown. The last panel presents the magnified and color-balanced view of the region highlighted at 40 minutes time point. Size bar = 5 μ m. **(C)** MCF7 cells were exposed to tamoxifen and MitoTam at the concentrations (μ M) and times shown, and cell death was evaluated using the annexin V-FITC/PI method using flow cytometry. **(D)** MCF7 and MDA-MB-231 cells were exposed to MitoTam for 24 h at the concentrations shown and cell death was evaluated by annexin V/PI. **(E)** MCF7, MDA-MB-453 and SKBR3 cells were exposed to MitoTam for 20 h at the concentrations shown and cell death was evaluated by annexin V/PI staining. **(F)** MCF7 cells were exposed to MitoTam, Tam-DPPO and tamoxifen or **(G)** MitoTam and C11-TPP for 24 h and cell death was evaluated by annexin V/PI staining. **(H)** Parental and tamoxifen-resistant MCF7 cells (MCF7 and TAM-R cells, respectively) were exposed to tamoxifen, **(I)** MitoTam or **(J)** Tam-DPPO for 24 h at the concentrations shown and cell death was evaluated by annexin V/PI staining. Images in **(B)** are representative of 3 independent experiments; data in all other panels are mean values ($n \geq 3$) \pm SEM. The symbol ‘*’ indicates statistically significant difference ($p < 0.05$). (To see this illustration in color the reader is referred to the web version of this article at www.liebertonline.com/ars).

Figure 2. MitoTam is more efficient in killing Her2^{high} cells than their Her2^{low} counterparts. **(A)** MCF7 parental, Her2^{low} (shRNA-transfected), mock (empty plasmid-transfected) and Her2^{high} cells (Her2 plasmid-transfected), and MDA-MB-231 parental, mock and Her2^{high}

cells were assessed for the Her2 protein in whole cell lysate using WB with actin as a loading control. MCF7, MCF7 Her2^{low} and MCF7 Her2^{high} cells were exposed to (B) tamoxifen or (C) MitoTam at the concentrations shown for 16 h and cell viability assessed using the crystal violet method. (D) MCF7, MCF7 Her2^{low} and MCF7 Her2^{high} cells and (E) MDA-MB-231, MDA-MB-231 mock and MDA-MB-231 Her2^{high} cells were exposed to MitoTam at the concentrations shown for 24 h and cell death was evaluated using annexin V/PI staining. (F) MCF7, MCF7 Her2^{low} and MCF7 Her2^{high} cells were exposed to TAM-DPPO at the concentrations shown for 24 h and cell was death evaluated using annexin V/PI staining. (G) MCF7 mock and MCF7 Her2^{high} cells were exposed to 2.5 μ M MitoTam for the times shown and the levels of procaspase-9, caspase-9, Parp 1/2 (both the intact and cleaved forms, indicated by arrows), Bax, Bcl2 and Her2, with actin as loading control were estimated by WB. (H) MCF7, MCF7 mock and MCF7 Her2^{high} cells were seeded in Petri dishes in soft agar, cultured for 14 days after 16-h treatment with 20 μ M tamoxifen or 2.5 μ M MitoTam and stained with crystal violet to visualize individual colonies. (I) MCF7 and (J) MCF7 Her2^{high} cells were exposed to 2.5 μ M MitoTam or solvent control in the presence of lapatinib (0.5 μ M) or mubritinib (0.5 μ M) for 24 h and cell death was evaluated. Images in (A), (G) and (H) are representative of three independent experiments. Data in all other panels are mean values ($n \geq 3$) \pm S.E.M. The symbol ‘*’ indicates statistically significant differences ($p < 0.05$).

Figure 3. MitoTam efficiently suppresses Her2^{high} breast carcinomas. (A) FVB/N *c-neu* mice s.c. injected with syngeneic NeuTL cells (2×10^6 cells per animal) were treated twice a week with tamoxifen (2.69 μ mol/mouse/dose) or MitoTam (0.54 μ mol/mouse/dose) dissolved in 4 % EtOH in corn oil, 100 μ l per dose, and tumor volume evaluated by USI. (B) Balb-c *nu/nu*

mice were implanted with a slow-release estradiol pellet and injected s.c. with 2×10^6 MCF7 mock or MCF7 Her2^{high} cells per animal. As soon as USI-detectable tumors appeared ($\sim 50 \text{ mm}^3$), the mice were treated with i.p. injection with 100 μl of tamoxifen (2 $\mu\text{mol}/\text{mouse}/\text{dose}$) or MitoTam (0.25 $\mu\text{mol}/\text{mouse}/\text{dose}$) dissolved in 4% EtOH in corn oil on days 3 and 7 of every week, and tumor volume was visualized and evaluated using USI. (C) Control and MitoTam-treated MCF7 mock and MCF7 Her2^{high} cell derived tumors, excised at the end of the experiment, were fixed, paraffin-embedded and stained using the TUNEL technique. The arrows indicate TUNEL-positive cells. Size bar = 50 μm . (D) Control and treated tumors as shown in panel B were lysed and evaluated for the level of pro-caspase-9 and caspase-9, Bax, Bcl-2 and Her2 with actin as loading control using WB. (E) FVB/N *c-neu* mice with spontaneous tumors were treated twice a week with MitoTam (0.54 $\mu\text{mol}/\text{mouse}/\text{dose}$) or solvent control, and tumor volume was evaluated. (F) Balb/c mice were s.c. injected with syngeneic 4T1 cells (1×10^6 cells per animal) and treated with MitoTam (0.25 $\mu\text{mol}/\text{mouse}/\text{dose}$) or solvent control twice a week, and tumor volume was evaluated. (G) Blood, lung and liver harvested from animals in (F) were homogenized and subjected to selection in the presence of 6-thioguanine for 10 days and colonies were counted. Data in (A) and (B) are mean values ($n=6$) \pm S.E.M, in (E) and (F) are mean values ($n \geq 5$) \pm S.E.M. The symbols ‘*’, ‘**’ and ‘#’ indicates statistically significant differences ($p < 0.05$). (To see this illustration in color the reader is referred to the web version of this article at www.liebertonline.com/ars).

Figure 4. MitoTam induces generation of ROS and dissipation of $\Delta\Psi_{\text{m,i}}$. (A) MCF7, MCF7 Her2^{low} and MCF7 Her2^{high} cells exposed to 5 μM MitoTam and 15 μM tamoxifen were assessed for ROS using DCF or MitoSOX. (B) Cells were pre-treated with 10 μM NAC,

exposed to 2.5 μ M MitoTam for 24 h and evaluated for viability. (C) MCF7 Her2^{high} cells were stably transfected with mtGFP, pre-loaded with TMRM and exposed to 5 μ M MitoTam, followed by time-lapse confocal microscopy. Size bar = 5 μ m. (D) Cell lines exposed to 5 μ M MitoTam and 15 μ M tamoxifen were assessed for $\Delta\Psi_{m,i}$ using TMRM. (E) MCF7 cells exposed to 10 μ M MitoTam or 30 μ M tamoxifen in the absence or presence of 10 μ M FCCP were assessed for ROS using DCF (60-min treatment) or (F) cell death (4-h treatment). (G) MCF7 cells, control or exposed to 10 μ M MitoTam or 30 μ M tamoxifen for 60 min, were evaluated for $\Delta\Psi_{m,i}$ in the absence or presence of 10 μ M FCCP. The symbol ‘*’ indicates statistically significant differences ($p < 0.05$) between MCF7 Her2^{high} and MCF7/MCF7 Her2^{low} cells/tumors (A, D), cells treated in the absence and presence of NAC (B) or MitoTam (G). The symbol ‘**’ indicates statistically significant difference in the absence and presence of FCCP (G). (To see this illustration in color the reader is referred to the web version of this article at www.liebertonline.com/ars).

Figure 5. Respiration is elevated in Her2^{high} cells and tumors and is efficiently suppressed by MitoTam. MCF7 cells respiration (10^6 cells/ml) was evaluated in the presence of CI (glutamate/malate) and CII substrate (succinate) with titrated (A) MitoTam or (B) tamoxifen. (C) NADH-cytochrome c (CI-CIII) and (D) succinate-cytochrome c (CII-CIII) oxidoreductase activity was measured in mitochondria isolated from MCF7 and MCF7 Her2^{high} cells and corrected for citrate synthase. (E) B1_{H-Ras} and B10_{H-Ras} cells were evaluated for routine, leak and ETS respiration and respiration via CI and CII, and (F) for cell death upon exposure to MitoTam for 12 h. (G) MCF7 and MCF7 Her2^{high} cells were treated with 2.5 μ M MitoTam for 1 h, harvested and evaluated for respiration via CI and CII. (H) MCF7 mock and MCF7 Her2^{high} tumors were evaluated for ETC and leak respiration and (I) CI and

CII respiration. **(J)** Liver from the same control and MitoTam-treated mice as in **(I)** were evaluated for CI and CII respiration. **(K)** Glucose uptake in MCF7 and MCF7 Her2^{high} cells was measured after 1 h incubation with MitoTam (2 μ M and 5 μ M) or solvent control. **(L)** Lactate production and **(M)** ATP level and were measured in MCF7 and MCF7 Her2^{high} cells after incubation with MitoTam (5 μ M) for the times indicated. The symbols ‘*’ and ‘***’ indicate statistically significant differences ($p < 0.05$).

Figure 6. Increased supercomplex assembly in Her2^{high} cells and tumors is disrupted by MitoTam. **(A)** Whole cell lysate from MCF7 mock and MCF7 Her2^{high} cells was assessed for the expression of subunits of CI, CII, CIII, CIV and CV as shown, using SDS-PAGE followed by WB, with actin as loading control. **(B)** Mitochondrial fraction was probed for respiratory complexes and SCs by WB following NBGE with the following antibodies: CI, NDUFA9; CII, SDHA; CIII, Core I; CIV, Cox5a; CV, ATP β ; Hsp60 was used as loading control. **(C)** MCF7 mock and MCF7 Her2^{high} cells were exposed to 2.5 μ M MitoTam for the time periods indicated, and isolated mitochondrial fractions were evaluated for the CI complex and SC by WB following NBGE. **(D)** Densitometric evaluation of NBGE blots shown in **(B)**. **(E)** Densitometric evaluation of NBGE blots shown in **(C)**. **(F)** Control and MitoTam-treated tumors derived from MCF7 mock and MCF7 Her2^{high} cells were evaluated for complexes and SCs as described above for panel **B**. **(G)** Control and MitoTam-treated tumors derived from MCF7 mock and MCF7 Her2^{high} cells were homogenized and evaluated for subunits of mitochondrial complexes by WB following SDS-PAGE with actin as loading control. **(H)** Densitometric evaluation of NBGE blots shown in **(G)**. Images in **(A, B, C, F and G)** are representative of 3 independent experiments. Data in **(D, E and H)** are mean values \pm S.E.M from 3 independent experiments.

Figure 7. Molecular modeling of MitoTam interaction with complex I. Left: Molecular structure of complex I with indicated N, Q, PD and PP modules. The broken red line indicates movement of electrons from the catalytic center of CI to their acceptor, UbQ. Right: The structure of CI is showed using its lateral views with the boxed area containing the cavity into which MitoTam can bind. The boxed area is enlarged, indicating two most probable positions of MitoTam inside the cavity, with the potential effect on electron flow. (To see this illustration in color the reader is referred to the web version of this article at www.liebertonline.com/ars).

Figure 8. Her2 is localized at the inner mitochondrial membrane. **(A)** MCF7 Her2^{high} cells stained using anti-ATP β IgG followed by Alexa Fluor 488 stained secondary IgG and anti-Her2 IgG followed by Alexa Fluor 555 secondary IgG were inspected by STED confocal microscopy. White arrows show co-localization of anti-ATP β and anti-Her2 signals. Size bar = 5 μ m. **(B)** Breast cancer cell lines as shown were fractionated into the cytosolic + plasma membrane fraction and the mitochondrial fraction, and assessed for the level of Her2 by WB following SDS-PAGE. Mitochondrial marker COXIV, and cytosolic markers SOD1 and actin were used as loading controls. **(C)** MCF7 and MCF7 Her2^{high} cells were assessed for localization of Her2 using IG-TEM. The light blue arrow-heads show position of gold particles associated with Her2 in mitochondria, the green ones outside mitochondria, often pointing to stress fibers. Size bar = 0.5 μ m. The two images on the right hand side are enlarged boxed regions in the middle images. **(D)** MCF7 Her2^{high} cells were subjected to double-staining with anti-Her2 IgG followed by Alexa Fluor 647 stained secondary IgG and anti-mtHsp70 IgG followed by Cy3b stained secondary IgG and inspected using the super-resolution PALM microscopy. The left and bottom images are enlarged boxed images in the

top right hand micrograph. Size bar = 10 μm . (E) MCF7 Her2^{high} cell lysate, their cytosolic + plasma membrane fraction (C+PMF), mitochondria, mitoplasts and inter-membrane space + outer membrane (IMS+OMM) fraction were assessed for Her2 using WB after SDS-PAGE with actin, NDUFA9, VDAC, Cyt c and SDHA as loading controls and preparation markers. (F) Mitochondrial fraction of MCF7 Her2^{high} cells was exposed to trypsin in the absence or presence of Triton X-100 for the periods indicated, at which time the preparations were assessed for Her2 by WB following SDS-PAGE. VDAC, ATP β , NDUFS3, COXIV and Cyt c were used as markers of different mitochondrial compartments. (G) Cytosolic + plasma membrane fraction and mitochondria of MCF7 mock or MCF7 Her2^{high} tumors, excised from either control or MitoTam-exposed mice, were evaluated for Her2 by WB following SDS-PAGE with COXIV and actin as fraction markers and loading controls. All images represent at least three independent experiments. (To see this illustration in color the reader is referred to the web version of this article at www.liebertonline.com/ars).

Figure 9. Mitochondrial fraction of Her2 determines sensitivity to MitoTam. (A)

Mitochondrial fractions of MCF7 Her2^{high} and BT474 cells were immunoprecipitated with anti-Her2 IgG and the immunoprecipitate, input and flow-through inspected for Her2 and mtHsp70 by WB after SDS-PAGE. (B) MCF7 Her2^{high} cells transfected with mtHSP70 siRNA or NS siRNA were assessed for Her2 using qPCR. (C) MCF7, MCF7 Her2^{low} and MCF7 Her2^{high} cells were transfected with siRNA against mtHSP70 or with NS siRNA, left to recover for 24 h and then exposed to 2 μM MitoTam for 24 h and assessed for cell death. (D) MCF7 Her2^{high} cells were transfected with mtHSP70 siRNA or NS siRNA and the whole cell lysates were assessed for Her2, NDUFA9 and mtHSP70 by WB, Actin was used as a loading control. (E) MCF7 Her2^{high} cells were transfected with mtHSP70 siRNA or NS siRNA, and cytoplasmic and mitochondrial fractions were assessed for Her2 and NDUFA9

by WB. VDAC and tubulin- α were used as a loading controls. **(F)** MCF7 Her2^{high} cells were transfected with mtHSP70 siRNA or NS siRNA, and the solubilized mitochondria were assessed for NDUFA9, SDHA (probed after NDUFA9 using the same membrane) and UQCRC2 by WB after NBGE. VDAC was used as a loading control. **(G)** MCF7 cells transiently transfected with empty vector, wild-type Her2, Her2-MTS or Her2- Δ MTS, were exposed to 2 μ M MitoTam for 24 h and assessed for cell death. Insert shows the protein level of Her2 in mitochondrial fraction in MTS- and Δ MTS-transfected cells. SDHB was used as a loading control. **(H)** Whole cell lysates of transiently transfected cells shows an even level of Her2. Actin and VDAC were used as loading controls. The symbol ‘*’ indicates statistically significant difference between cells transfected with NS and mtHSP70 siRNA **(B)**, between MCF7, MCF7 Her2^{high} and MCF7 Her2^{low} cells transfected with NS or mtHsp70 and MCF7 Her2^{high} cells transfected with NS and mtHsp70 cells **(C)**, and MCF7 cells transfected with wt, MTS or Δ MTS plasmids **(G)**. Images in panels **A, D, E, F, G** and **H** are representatives of at least three independent experiments.

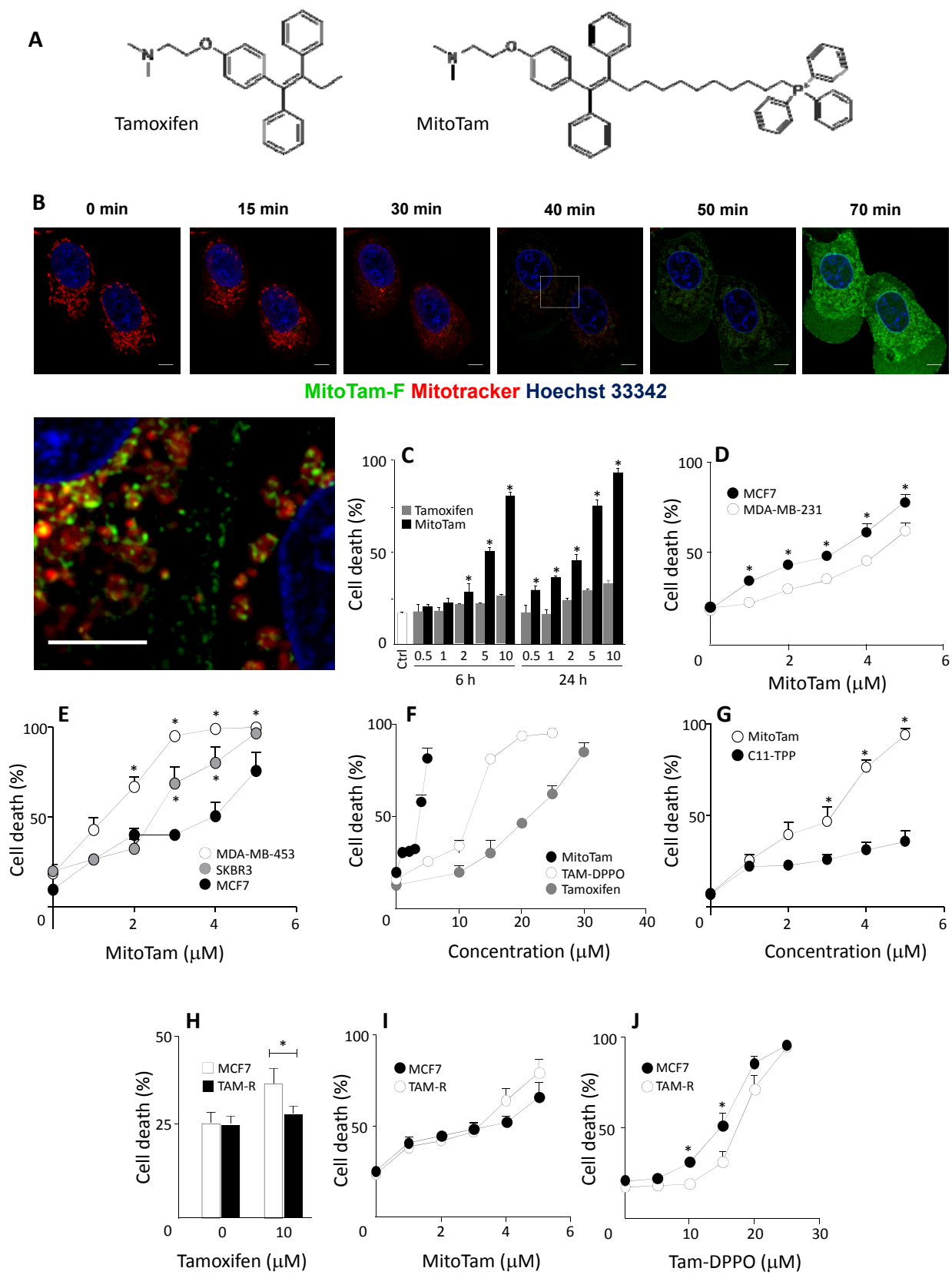


Figure 1

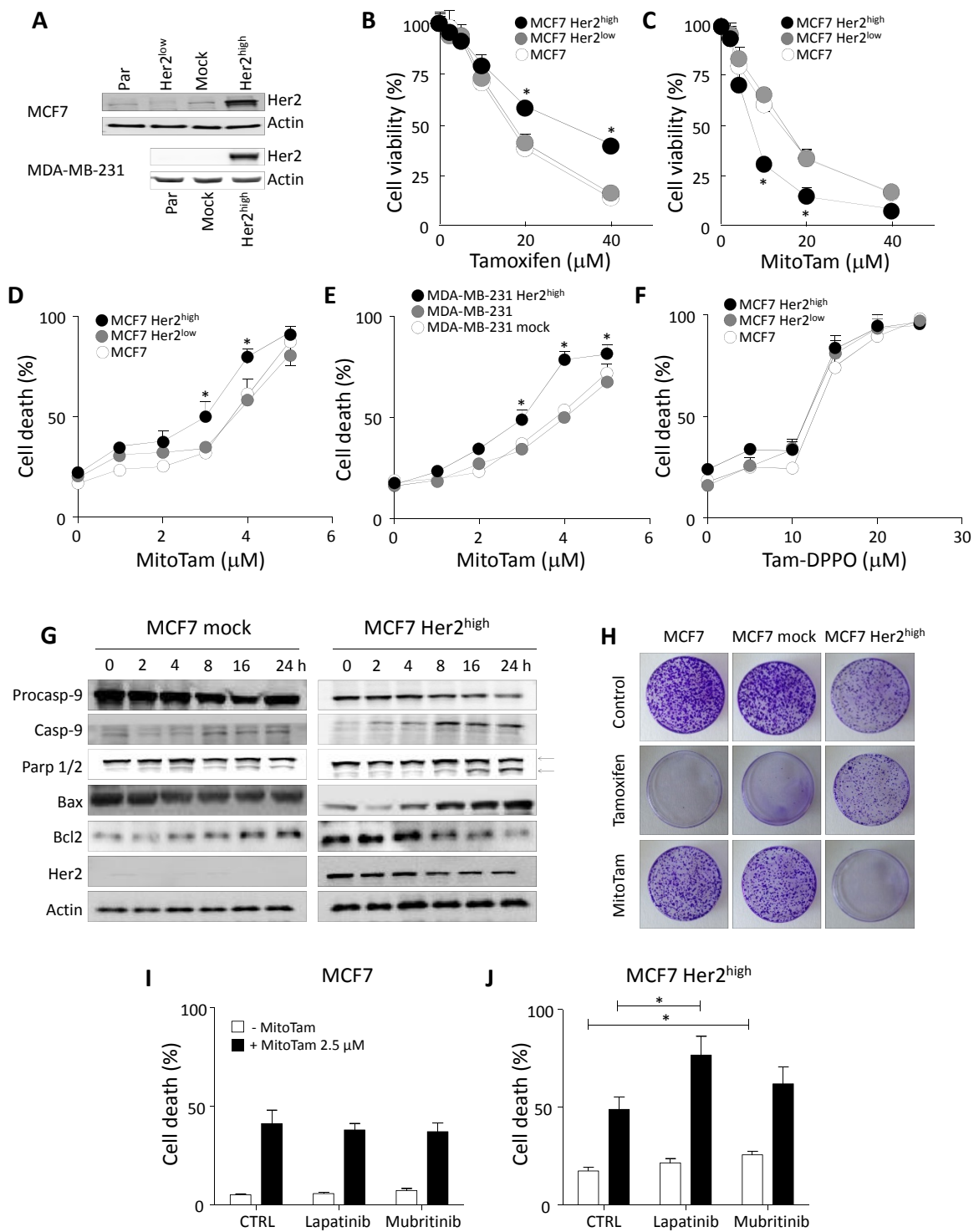


Figure 2

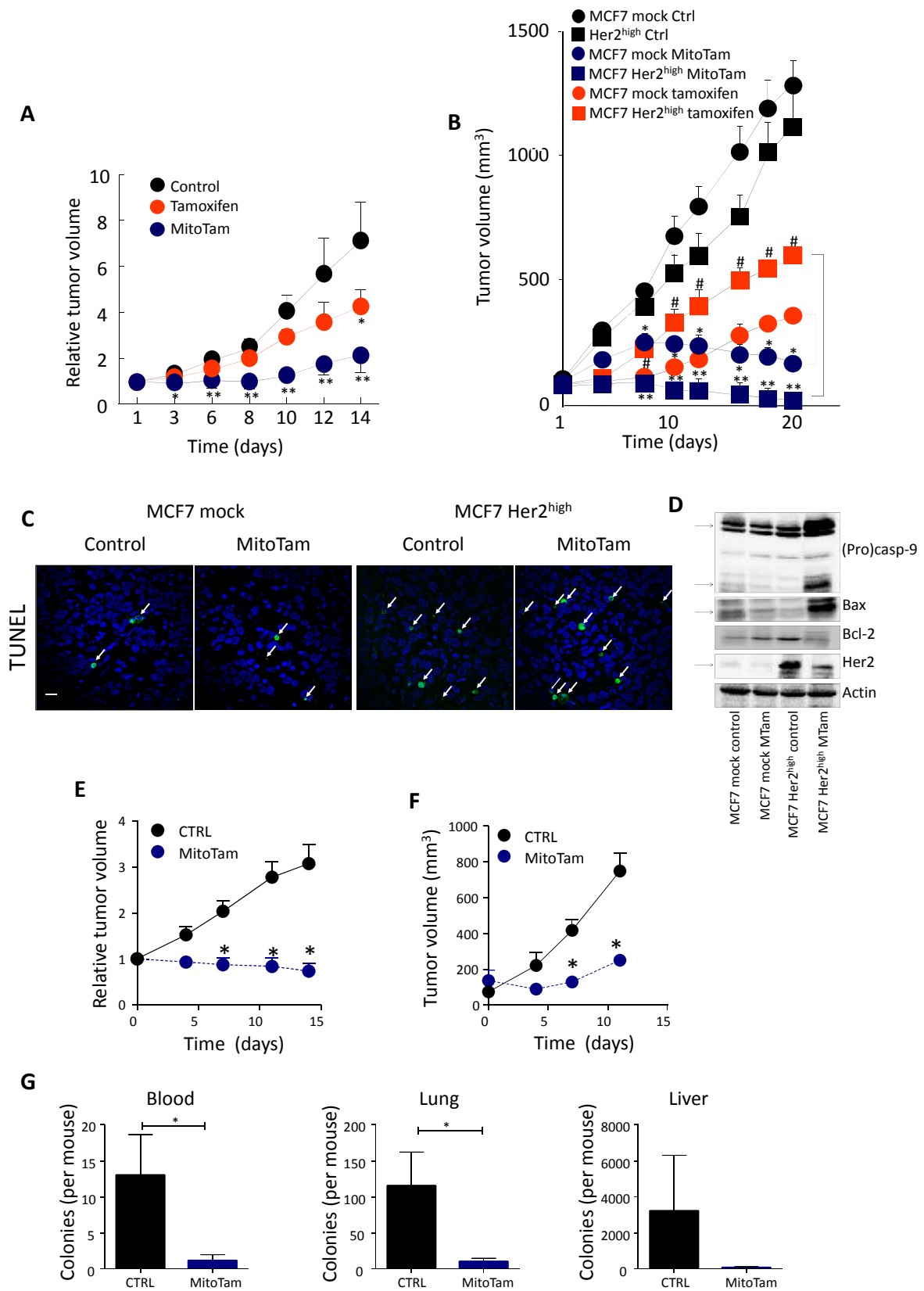


Figure 3

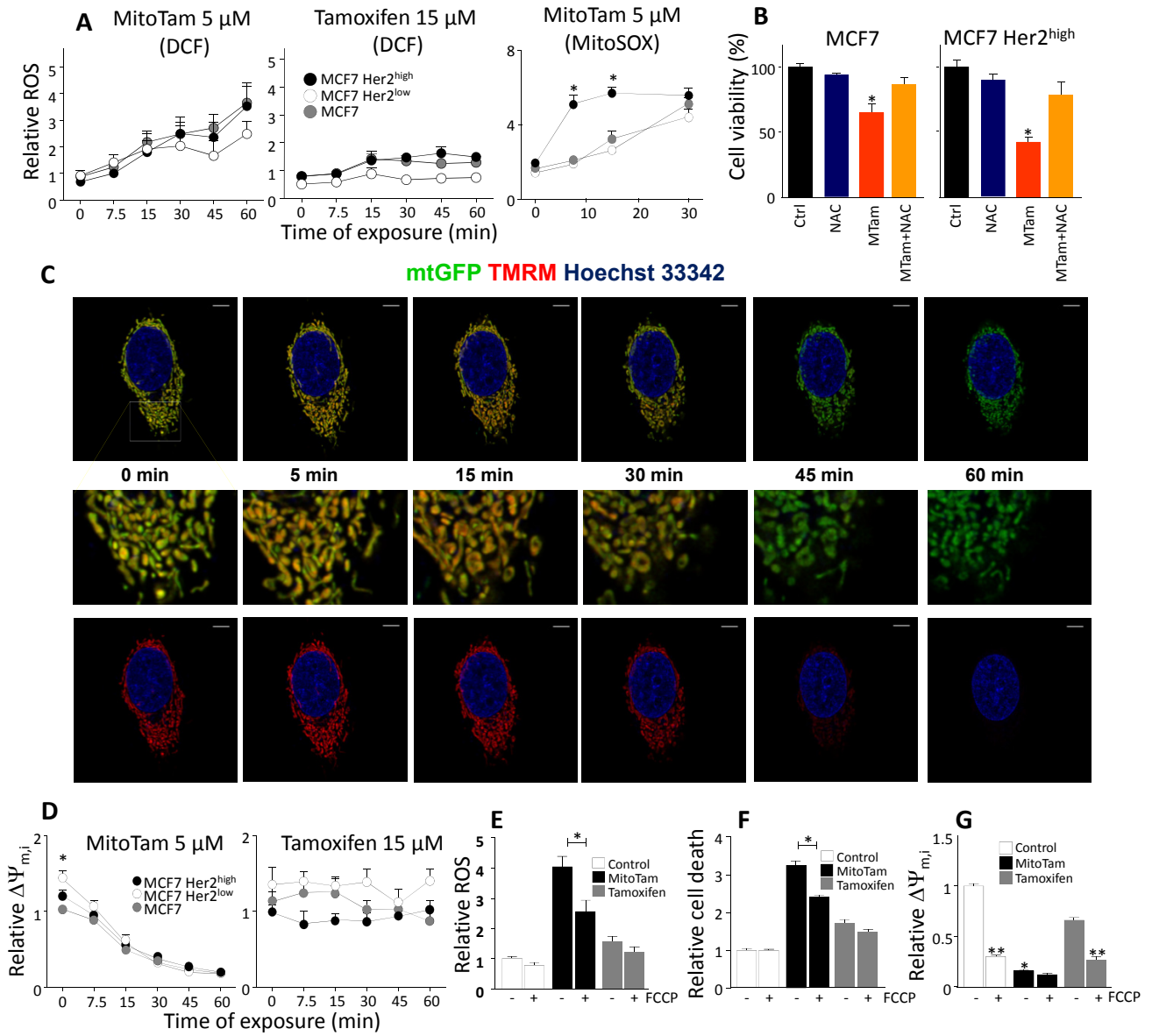


Figure 4

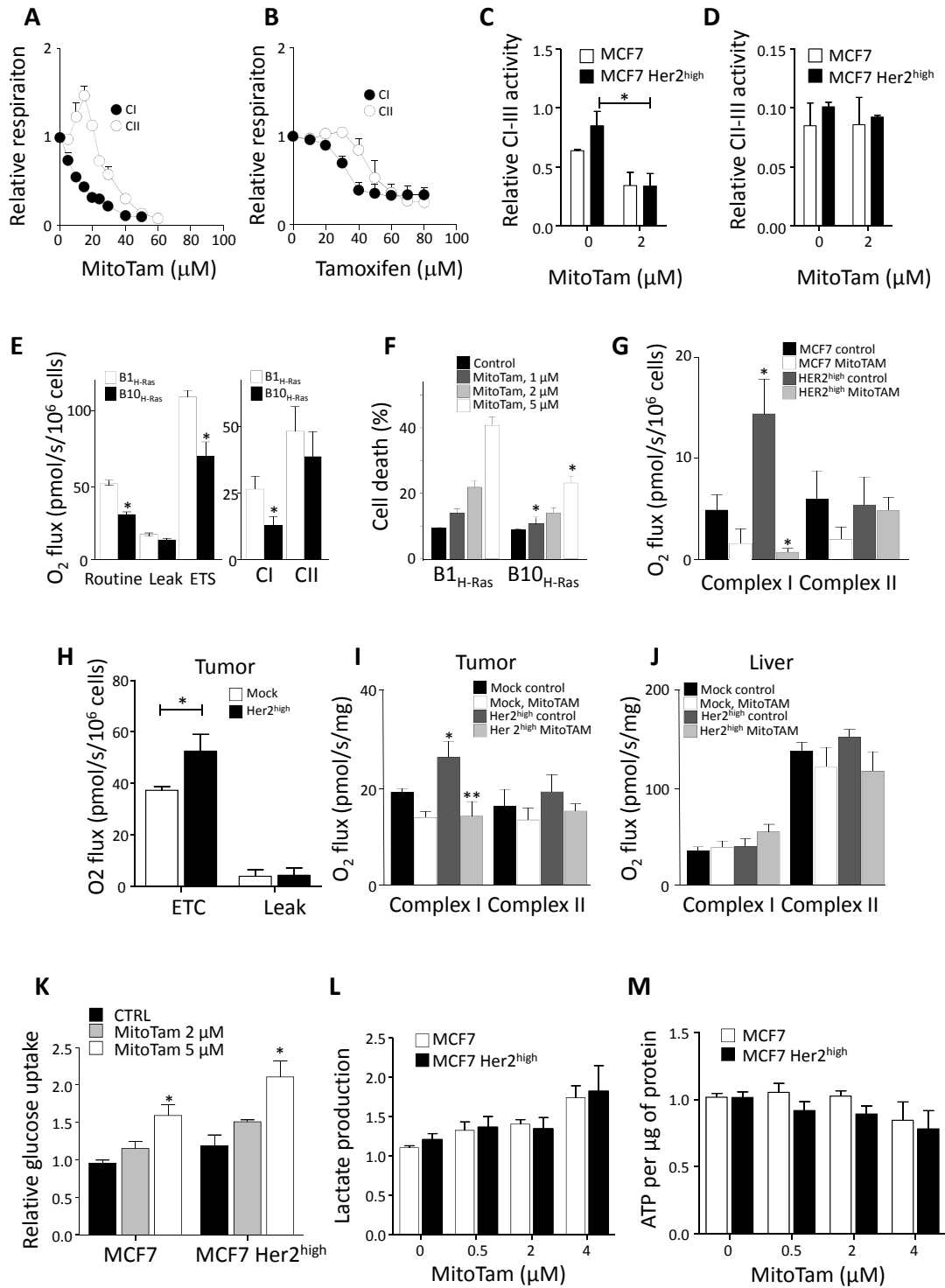


Figure 5

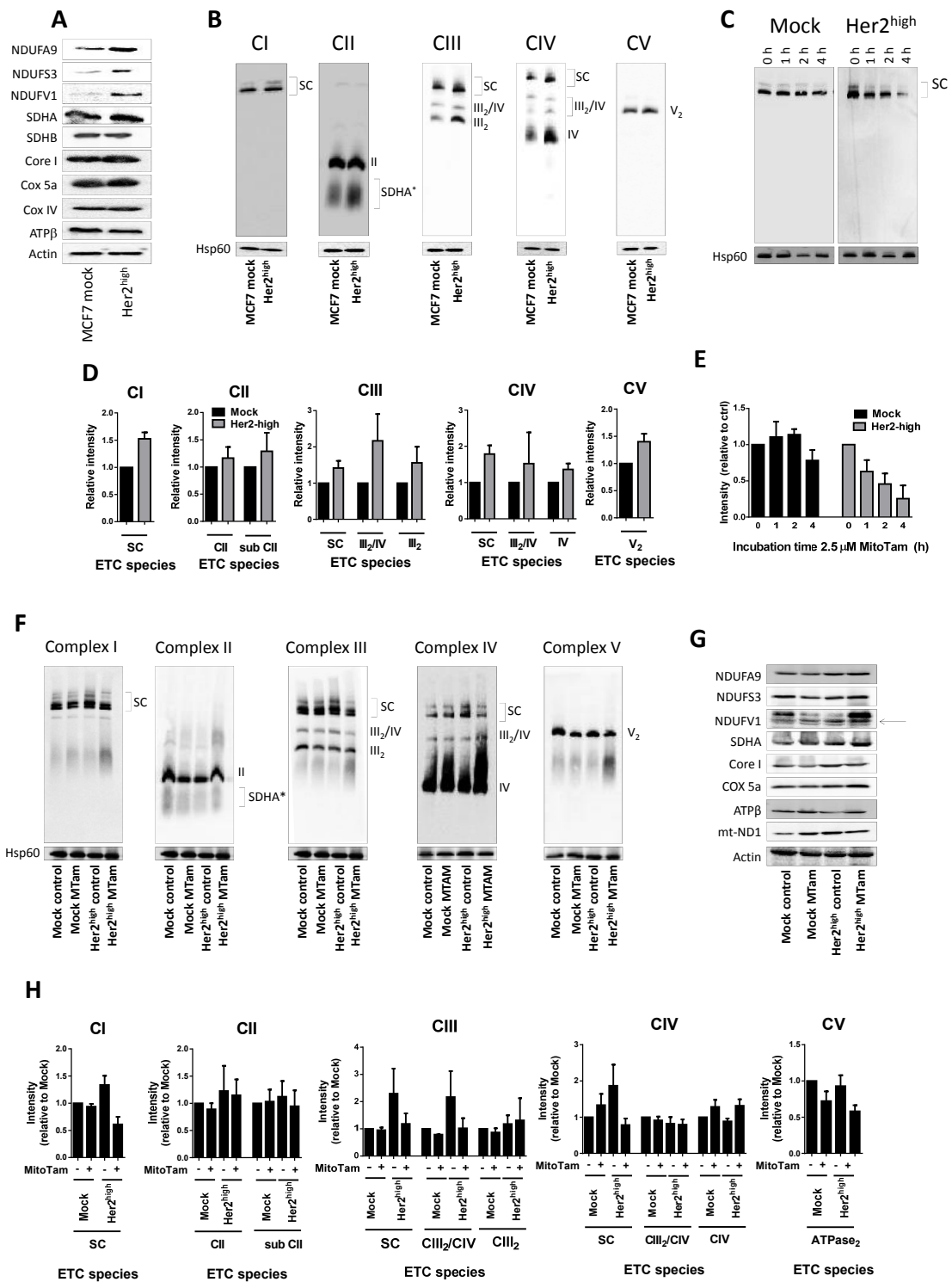


Figure 6

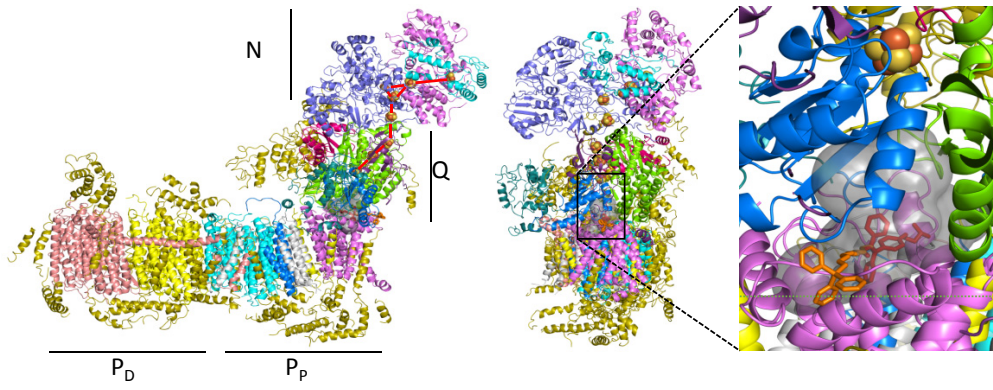


Figure 7

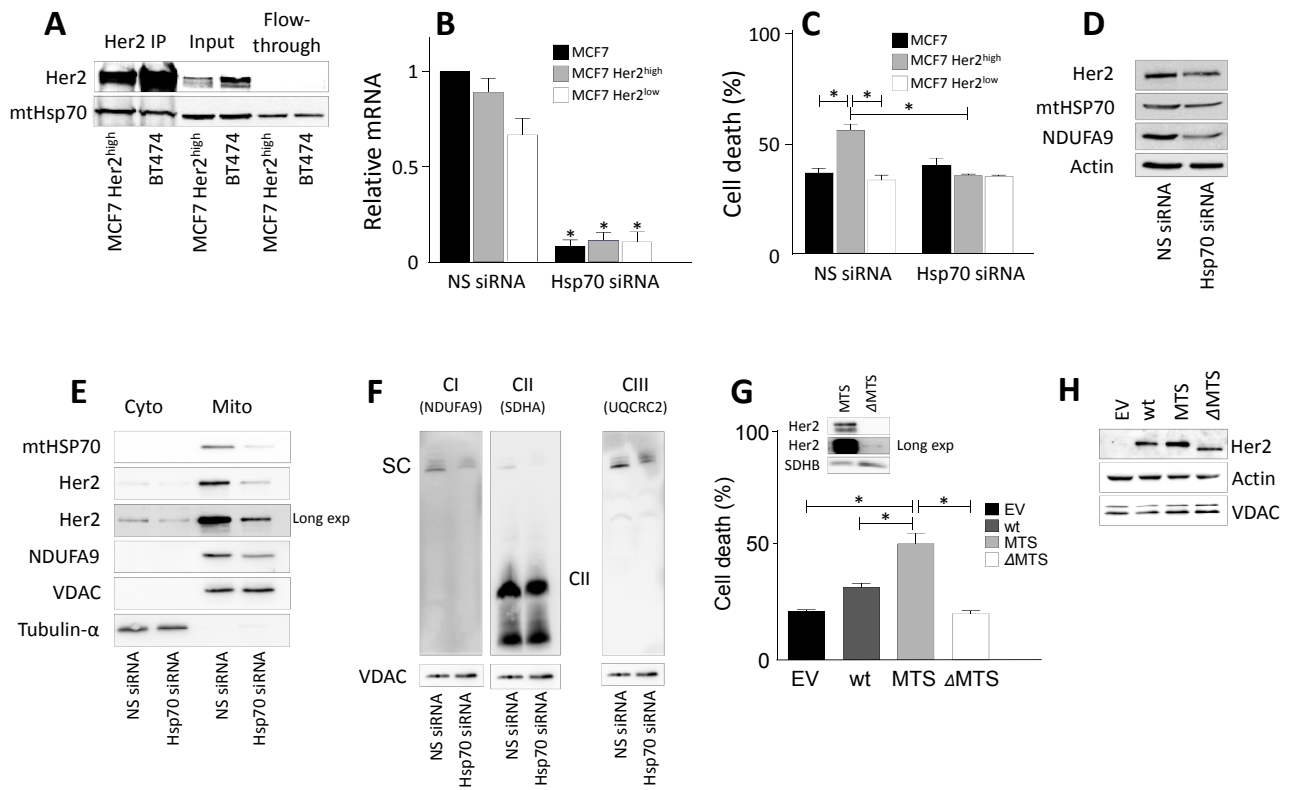


Figure 9

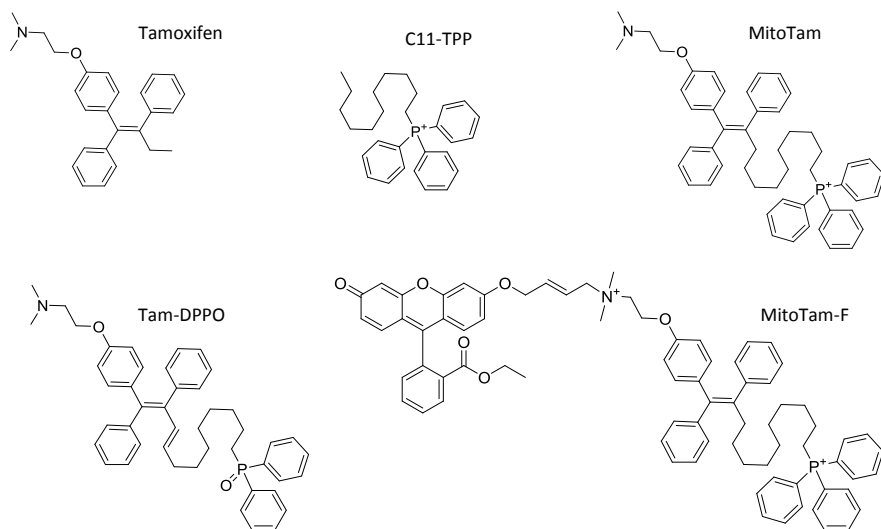


Figure S1. Structures of compounds used in the current study. The mitochondria-targeting TPP⁺ group is disabled in Tam-DPPO, whereas fluorescein group attached to MitoTam (MitoTam-F) allows direct visualization.

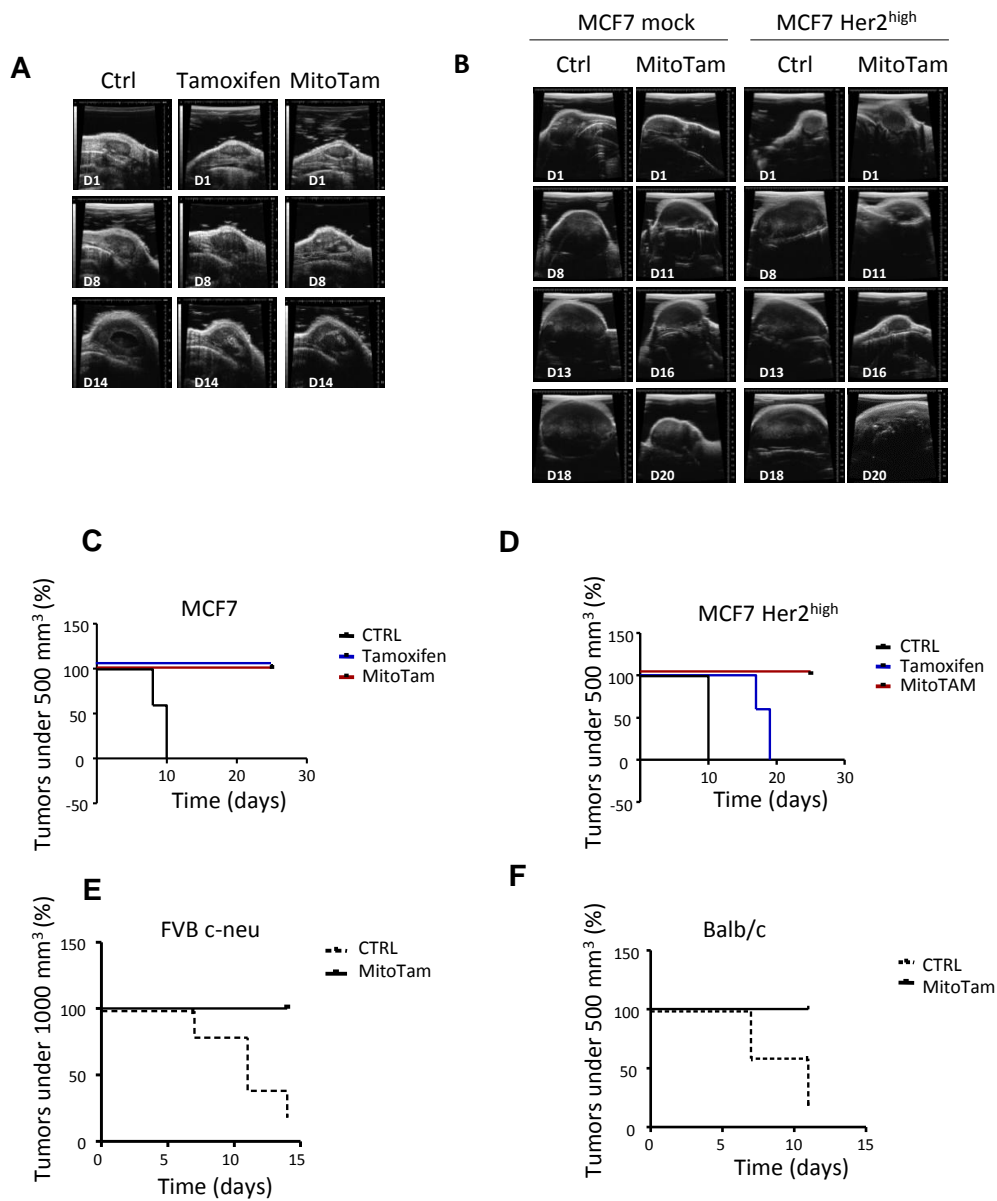
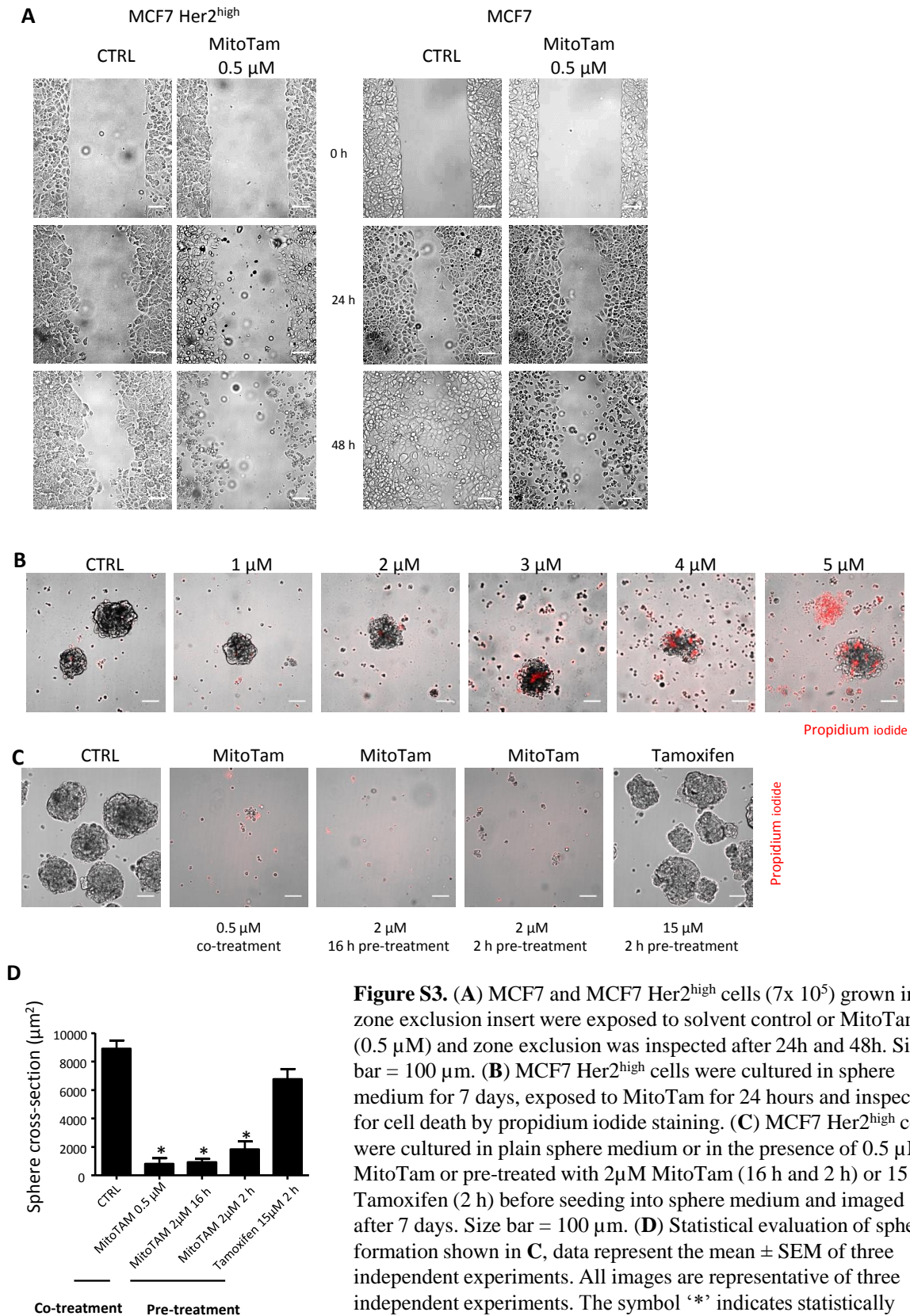


Figure S2. (A) Representative USI images of tumors from Fig. 3A. (B) Representative USI images of tumors from Fig. 3B. Percentage of animals reaching the ethical end-point (tumor volume over 500 mm³ (C), (D) and (F) or 1000 mm³ (E)). Data in (C) and (D) corresponds to the experiment shown in Fig. 3B, data in (E) corresponds to the experiment in Fig. 3E and graph in (F) corresponds to the experiment shown in Fig. 3F.



Review

Katerina Rohlenova, Jiri Neuzil and Jakub Rohlena*

The role of *Her2* and other oncogenes of the PI3K/AKT pathway in mitochondria

DOI 10.1515/hsz-2016-0130

Received February 1, 2016; accepted April 13, 2016; previously published online April 14, 2016

Abstract: Altered metabolism and resistance to cell death are typical hallmarks of cancer phenotype. Mitochondria are organelles central to cellular metabolism as well as to cell death induction. Hyperactivation of pro-survival and proliferative pathways such as PI3K/AKT leads to cancer initiation, which affects mitochondria. Growing body of evidence indicates that oncogenes such as *HER2*, *EGFR* and *RAS*, as well as the downstream members of the PI3K/AKT signaling pathway, directly regulate mitochondria by translocating to the organelle. Here we discuss evidence of this scenario and consider mechanisms for direct regulation of mitochondrial function. Being in close proximity to mitochondrial bioenergetics machinery as well as to the regulators/executors of programmed cell death, oncogenes in mitochondria may be ideally placed to perform this task. This represents a thus far under-explored area, which may be relevant to better understanding of cancer initiation, progression and treatment.

Keywords: cancer; *EGFR*; *HER2*; mitochondria; PI3K/AKT; *RAS*.

Introduction: mitochondria, oncogenic signaling and cancer

Cancer is a complex, multifactorial disease. This complexity derives from diverse genetic and environmental

cues often unique to a given cancer subtype, site of origin and target organs of metastatic dissemination. Nevertheless, certain unifying features typical for cancer behavior can be defined (Hanahan and Weinberg, 2011). These ‘hallmarks of cancer’ broadly cover the cancer-associated phenotypes, irrespective of the underlying genetic cause, and include phenomena such as deregulation of the cell cycle, unlimited proliferation, resistance to cell death and invasive behavior. Accumulating evidence indicates that one of these hallmarks is cancer-associated adaptation of cellular metabolism (Pavlova and Thompson, 2016). This is not an entirely new idea (reviewed in Koppenol et al., 2011), but the interpretation of this phenomenon has recently been revised. Today, the altered metabolism of cancer cells is considered a consequence of increased capacity of these cells to proliferate and survive in nutrient-poor conditions. With respect to the former, it is assumed that increased glycolytic rates allow for efficient activity of essential biosynthetic routes branching off the main glycolytic pathway (Vander Heiden et al., 2009). Concerning the latter, cancer cells maintain functional oxidative phosphorylation within mitochondria to retain metabolic flexibility, use opportunistic substrates such as pyruvate and acetate to support their metabolic activity, and can utilize external sources of proteins to maintain biomass (Commisso et al., 2013; Cardaci et al., 2015; Lussey-Lepoutre et al., 2015; Schug et al., 2015; Tan et al., 2015).

The metabolic adaptations described above are intricately connected with deregulated oncogenic signaling typical for cancer cells. One of the major signaling pathways relevant in cancer is the PI3K-AKT pathway (Engelman, 2009), schematically depicted in Figure 1. Activation of this pathway is linked to increased proliferation and glycolysis as well as resistance to cell death. The core of the pathway consists of two kinases, phosphatidylinositol tris-phosphate kinase (PI3K) and AKT, also known as protein kinase B. Through a series of phosphorylations, the pathway ultimately regulates the mTORC1 and mTORC2 complexes, signaling hubs that control cell growth and biomass utilization (Betz and Hall, 2013). Conversely, the activity of the core PI3K-AKT

*Corresponding author: **Jakub Rohlena**, Institute of Biotechnology, Czech Academy of Sciences, BIOCEV, Prumyslova 595, CZ-25250 Vestec, Prague-West, Czech Republic, e-mail: jakub.rohlena@ibt.cas.cz, <http://orcid.org/0000-0001-5427-6502>.

Katerina Rohlenova: Institute of Biotechnology, Czech Academy of Sciences, BIOCEV, Prumyslova 595, CZ-25250 Vestec, Prague-West, Czech Republic

Jiri Neuzil: Institute of Biotechnology, Czech Academy of Sciences, BIOCEV, Prumyslova 595, CZ-25250 Vestec, Prague-West, Czech Republic, and School of Medical Science, Griffith University, Southport 4222, Qld, Australia

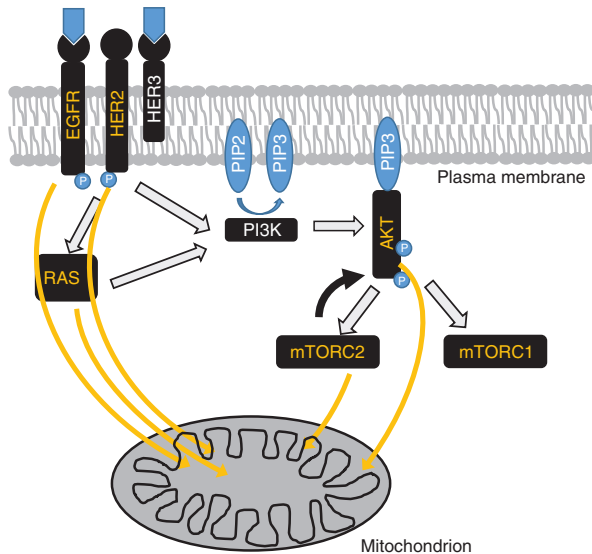


Figure 1: Schematic representation of the PI3K/AKT pathway. Signaling events are depicted by open arrows, the filled arrow indicates the feedback activation of AKT by mTORC2. Members of the pathway that have been observed to translocate to mitochondria are indicated by yellow and the non-translocating members by white letters. The yellow lines indicate mitochondrial translocation.

pathway is regulated by a number of upstream signaling components often deregulated in cancer. These include members of the receptor tyrosine kinases (RTK) such as HER2 (ERBB2) and epithelial growth factor receptor (EGFR, *aka* ERBB1), and GTPases of the RAS family, which are frequently mutated in cancer (Hynes and Lane, 2005; Pylayeva-Gupta et al., 2011).

Cellular metabolism is to a large degree organized around mitochondria (Wallace, 2012). In addition, these unique organelles also perform other important functions such as participating in cell death induction (Galluzzi et al., 2012). The inside of a mitochondrion (the mitochondrial matrix) is separated from the rest of the cell by a

double membrane (Scheffler, 2008). The inner mitochondrial membrane (IMM) is relatively impermeable, and the activity of the electro transport chain (ETC) residing in this membrane creates an electrostatic and pH gradient (referred to as the mitochondrial inner transmembrane potential) propelling the mitochondrial ATP synthase to produce ATP. The outer mitochondrial membrane (OMM), by contrast, is relatively permeable for small molecules. The space enclosed between the inner and outer membrane is referred to as the inter-membrane space. In principle, this double barrier allows compartmentalization of metabolic and signaling events inside the mitochondrion, separating to a large degree the action inside mitochondria from what is happening elsewhere in the cell. Given the importance of metabolic adaptation to cancer progression and the central role of mitochondria therein (Frezza, 2014), it is conceivable that oncogenic components of the PI3K-AKT signaling pathway influence the mitochondrial behavior directly by translocating into the organelle.

Over the past decade, the number of mitochondrial proteins increased as certain cytosolic and plasma membrane proteins were also found in the organelle. This brought a new level of complexity to the canonical view of protein signaling pathways by introducing another determinant, the precise localization of proteins into cellular sub-compartments. A number of well-known oncogenes have been detected in mitochondria (Table 1, Figure 1). They have been shown to regulate multiple processes such as mitochondrial bioenergetics or sensitivity/resistance to cell death induction. As such, they could be relevant for the molecular mechanisms of tumorigenesis and cancer progression, and should be considered in the context of cancer management. Below, we review the current knowledge about the presence of *HER2* and other oncogenes signaling via the PI3K-AKT pathway in mitochondria including its functional consequences.

Table 1: Overview of mitochondrial localization for RTKs and RAS proteins.

Family	Member	Mitochondrial sub-compartment	References
RTK	EGFR	IMM	Boerner et al., 2004; Demory et al., 2009; Bollu et al., 2014
	HER2	IMM	Ding et al., 2012; Rohlenova et al., submitted
	HER3	No report	
	HER4	Not specified	Vidal et al., 2005; Naresh et al., 2006
AKT		IMM, OMM, Matrix	Bijur and Jope, 2003; Yang et al., 2013; Iskandar et al., 2016
RAS	KRAS	OMM/IMM	Wolfman et al., 2006; Bivona et al., 2006; Hu et al., 2012; Iskandar et al., 2016
		IMM, OMM	Wolfman et al., 2006
	HRAS	Not specified	Rimessi et al., 2014

HER2/ERBB2

HER2 (ERBB2) is a receptor tyrosine kinase from the epidermal growth factor family of receptors, along with EGFR/ERBB1, HER3/ERBB2 and HER4/ERBB4 (Hynes and Lane, 2005). This trans-membrane protein acts as an up-stream component for several pathways including SRC kinases, STAT3 transcription factors, PI3K/AKT/mTOR and RAS/RAF/MEK/ERK signaling. HER2-related pathways regulate various cellular functions including cell growth and survival, proliferation and migration and resistance to apoptosis. Therefore, hyper-activation of these pathways often leads to cancer initiation. HER2 overexpression is found in ~20% of breast cancer patients and is associated with poor prognosis (Slamon et al., 1987). Currently, therapeutic strategies for HER2-overexpressing cancers involve the use of specific kinase inhibitors (e.g. lapatinib) and monoclonal antibodies (e.g. trastuzumab/herceptin, pertuzumab). These approaches, despite providing substantial benefit to patients, suffer from frequent instances of *de novo* or acquired resistance involving alternative signaling routes (so called ‘bypass track’ type resistance), or up-regulation of anti-apoptotic proteins or cell cycle regulators (Niederst and Engelman, 2013; Arteaga and Engelman, 2014).

The presence of a fraction of the *HER2* oncogene in mitochondria has been reported, and was linked to the regulation of mitochondrial bioenergetics and resistance to treatment (Ding et al., 2012). Mitochondrial HER2 was shown to localize to the IMM both by electron microscopy and by biochemical means. Positioned at IMM, HER2 would reside in a close proximity to components of oxidative phosphorylation, and the interaction of mitochondrial HER2 with complex IV (CIV) of the electron transport chain (ETC) was proposed (Ding et al., 2012). Mitochondrial HER2 in this study was connected to increased resistance to trastuzumab treatment, and the authors suggested that HER2 in mitochondria is shielded from this antibody. The role for HER2 in the regulation of CIV has also been suggested in another report, where in unstimulated cells HER2 expression inversely correlated with COX2 levels (Sun et al., 2002). This study considered only plasma membrane HER2, pointing to transcriptional regulation; this may differ in its activity from that of the mitochondrial fraction of HER2. Our own data also strongly point to the presence of HER2 in mitochondria, which was documented by several independent techniques. These data imply mitochondrial HER2 in the regulation of mitochondrial bioenergetics, particularly at the level of respiratory supercomplexes (SCs). These macromolecular structures are formed by the association of

respiratory complexes I, III and IV (CI, CIII and CIV) of the ETC, and they are believed to increase the efficacy of electron flow and to minimize formation of ROS during OXPHOS (Acin-Perez et al., 2008; Lapuente-Brun et al., 2013; Maranzana et al., 2013; Tan et al., 2015). In contrast to the above mentioned report, we found that HER2 correlates with increased level of SC assembly and increased protein levels of individual subunits of respiratory CI, CIII and CIV. This has functional consequences, as HER2^{high} cells and *ex vivo* tumors exert increased respiration via CI compared to HER2^{low} cells and tumors (Rohlenova et al., submitted). Importantly, there are practical implications for treatment of HER2^{high} cancers, as we observed increased sensitivity towards a CI inhibitor, mitochondrially-targeted tamoxifen (MitoTam), in HER2^{high} cells and tumors, stemming from the capacity of this compound to selectively disrupt the SC and to induce ROS in HER2^{high} cells. Accordingly, mitochondrial HER2-related re-structuring of the ETC and mitochondrial bioenergetics dictates altered sensitivity/resistance to therapy. As we have shown in case of MitoTam, this change is targetable by drugs acting as OXPHOS inhibitors.

Epithelial growth factor receptor, EGFR/ERBB1

Similar to HER2, EGFR was shown to localize to IMM (Demory et al., 2009; Bollu et al., 2014). Mitochondrial EGFR interacts with the mitochondrial protein prohibitin-2 (PHB2). PHB2 then stabilizes the optic atrophy-1 protein (OPA1) and promotes mitochondrial fusion (Bollu et al., 2014). EGFR in mitochondria was shown to phosphorylate the COX2 subunit of CIV (Boerner et al., 2004; Demory et al., 2009), which is the complex also implicated in the interaction with HER2 (Ding et al., 2012). After stimulation by EGF, mitochondrial EGFR causes inhibition of CIV activity, leading to a decrease in cellular ATP. The effect is transient as after attenuation of EGF stimulation, ATP returned to normal levels. Signaling pathways downstream of EGFR may also be involved. For example, c-SRC has been shown to translocate to mitochondria at the same time as EGFR, where it also phosphorylates COX2. Interestingly, an opposite, stimulatory effect on cellular ATP levels was shown when non-mitochondrial EGFR was overexpressed (Demory et al., 2009). Therefore, by spatial distribution in cellular sub-compartments, a single protein may be involved in various signaling pathways leading to completely different outcomes.

HER3/ERBB3 and HER4/ERBB4

Contrary to other EGFR family members, *HER4* is not considered an oncogene; it was reported to be selectively lost in aggressive cancers. Some reports show tumor suppressor functions of *HER4*, and the loss of *HER4* has been connected with resistance to tamoxifen. Intracellular domain of *HER4* (4ICD), which acts as a pro-apoptotic BH3-only protein, translocates to the nucleus, where it serves as a potent estrogen receptor- α (ER- α) co-activator. Tamoxifen, a selective estrogen receptor modulator, disrupts 4ICD/ER α binding, with ensuing translocation of 4ICD to mitochondria (Vidal et al., 2005; Naresh et al., 2006; Gallo et al., 2013), where it acts as an effector of tamoxifen-induced cell death (Naresh et al., 2008).

Interestingly, to the best of our knowledge, mitochondrial localization of *HER3* has not been documented. This is rather intriguing, as *HER3* serves as an important heterodimerization partner of *HER2* and *EGFR* (Lee-Hoeflich et al., 2008) and all members of *EGFR* family are structurally similar.

RAS oncogenes

RAS proteins, frequently mutated in cancer, serve as transducers and amplifiers of growth signals relayed towards the MAPK/ERK and PI3K/AKT pathways. The RAS family consists of four highly homologous members, HRAS, NRAS, KRAS4A and KRAS4B, the last two being splice variants of the *KRAS* gene (Pylayeva-Gupta et al., 2011). Their activity is regulated by cycling between the 'on' GTP-bound and 'off' GDP-bound state, and their cancer-associated mutations lock them in the active, GTP-bound state. An interaction with PI3K is required for KRAS to initiate and maintain tumors, suggesting that PI3K/AKT pathway represents an essential route for RAS-mediated oncogenesis (Gupta et al., 2007; Castellano et al., 2013). Mutated RAS proteins affect proliferation, cell death resistance and metabolism, and there are number of reports describing RAS family members in mitochondria. It was found that a distinct fraction of RAS proteins translocates into mitochondria in an IL2-dependent T cell line, where it interacts with the OMM-resident anti-apoptotic protein BCL2. Mitochondrial localization of RAS family members, except for HRAS, depends on isoprenylation, a post-translational modification essential for tethering at the plasma membrane and activity of the proteins (Rebollo et al., 1999). Mitochondrial localization of NRAS was later confirmed in an independent report (Matallanas et al., 2003), and was also described in association with BCL2 in a murine model

of acute myelogenous leukemia, MRP8[BCL-2/NRASD12] mice. The authors speculated that this protects these particular leukemic cells from apoptosis (Omidvar et al., 2007). Another study then pinpointed NRAS mitochondrial localization into both IMM and OMM, while KRAS4B was found only in the outer membrane (Wolfman et al., 2006). Interestingly, targeted delivery of NRAS into mitochondria could alleviate mitochondrial defects observed in NRAS null mouse embryonic fibroblasts (Wolfman et al., 2006).

Little is known about the mechanism of NRAS and HRAS targeting to mitochondria. In contrast, the mechanism for the translocation of KRAS4B has been described. This oncoprotein dissociates from the plasma membrane and moves to mitochondria in response to phosphorylation of its C-terminal polybasic region by protein kinase C (PKC). At the OMM, it binds to BCL-XL, another anti-apoptotic protein. Association with BCL-XL triggers apoptosis; translocation of KRAS to the OMM induced by the PKC agonist bryostatin-1 limits the growth of KRAS-dependent tumors in mice (Bivona et al., 2006). This translocation mechanism is specific to KRAS, as other RAS homologues lack the polybasic region amenable to PKC-mediated phosphorylation. In addition, KRAS^{G12V} translocation into mitochondria in HEK293 cells was shown to reduce the mitochondrial membrane potential and oxygen consumption via CI, gradually leading to the establishment of typical cancer phenotype of reduced mitochondrial respiration and elevated glycolysis (Hu et al., 2012). Using the inducible KRAS system, these authors proposed that KRAS translocation into mitochondria is the initial event that is responsible for bioenergetics alteration associated with KRAS expression. Based on a protease protection assay they placed KRAS into the IMM, and speculated that it might directly interact with CI. The reduction of mitochondrial membrane potential was eliminated by the application of the PKC inhibitor H-7, implicating a functional relevance of this kinase in the translocation of KRAS into mitochondria. Finally, HRAS^{G12V} was reported to localize into mitochondria and mitochondria-associated membranes, affecting calcium homeostasis in a caveolin-1-dependent manner (Rimessi et al., 2014).

In summary, basically all RAS homologues have been detected in mitochondria, with best evidence available for NRAS and KRAS4B. Precise mitochondrial location of RAS homologues is a matter of debate. The effect of mitochondrial RAS on bioenergetics is complex; endogenous NRAS was necessary to maintain mitochondrial morphology and function, while the overexpression of KRAS^{G12V} compromised it. Similarly, mitochondrial NRAS in association with BCL2 reduced susceptibility to cell death, while the mitochondrial KRAS4B complexed with BCL-XL increased

it. In addition, pharmacological hyper-activation of mutant KRAS resulted in its mitochondrial translocation, ROS generation and cell death (Iskandar et al., 2016).

The core PI3K/AKT/mTOR pathway

The signaling input from the proteins described above comes together at the core PI3K/AKT signaling pathway. While there is ample evidence for the role of this pathway in the regulation of metabolism and cell death (Depez et al., 1997; Kennedy et al., 1997, 1999; Barthel et al., 1999; Cerniglia et al., 2015), much less is known about the possible mitochondrial localization of its members. For example, we could not find any report describing mitochondrial localization of PI3K. While the downstream target mTOR is not considered a mitochondrial protein, it is known that its precise intracellular localization is important for mTOR activation and function (Betz and Hall, 2013). Contrary to mTORC1 localized in the cytosol, on lysosomes and on peroxisomes, mTORC2 has been reported in mitochondria and endoplasmic reticulum at mitochondria-associated membranes. It was speculated that here, mTORC2 may directly interact with its substrate AKT (Betz et al., 2013), which was also found in this compartment. Because the subcellular localization of mTORC1/2 complexes has been extensively reviewed before (Betz and Hall, 2013), we will focus on AKT, for which ample evidence exists for its mitochondrial localization and its functional significance.

The role for the serin/threonin kinase AKT in the regulation of cellular metabolism has been well described. AKT stimulates ATP production via glycolysis (Elstrom et al., 2004) as well as via OXPHOS (Gottlob et al., 2001; Nogueira et al., 2008; Goo et al., 2012), and serves as a regulator of both glycolytic and oxidative energy metabolism. It has been established that AKT decreases the sensitivity to cell death by stimulating the association of hexokinase II (HKII) with VDAC at the OMM (Gottlob et al., 2001; Majewski et al., 2004a,b). With respect to mitochondrial localization of AKT itself, it has been detected within OMM, IMM and mitochondrial matrix, which indicates relatively fast shuttling between sub-organelle structures. AKT accumulates in mitochondria rapidly after activation by mTORC2 phosphorylation at Ser473 (Sarbasov et al., 2005) in a mitochondrial membrane potential-dependent manner (Bijur and Jope, 2003), and participates in regulation of cell death and mitochondrial bioenergetics. In mitochondria, AKT is further phosphorylated at Thr308 by PDK1 (Alessi et al., 1997), with ensuing translocation to the nucleus and support of proliferation (Antico Arciuch

et al., 2009). Whether AKT proceeds to the nucleus or remains in mitochondria depends on the concentration of H_2O_2 . At low H_2O_2 , AKT translocates to the nucleus and triggers a pro-proliferative program. At high H_2O_2 , AKT is retained in mitochondria and participates in apoptosis induction (Antico Arciuch et al., 2009). Similarly, it has been reported that AKT and KRAS translocate into mitochondria upon pharmacological hyper-activation of mutant KRAS, stimulating ROS generation and cell death (Iskandar et al., 2016). Incidentally, it has been reported that AKT sensitizes to ROS-induced cell death by increasing oxygen consumption and related production of ROS (Nogueira et al., 2008), even though the mitochondrial fraction of AKT has not been addressed in that study. Mitochondrial AKT also negatively phosphorylates GSK-3 β at Ser9. This protects from cell death, because the uninhibited GSK-3 β would otherwise phosphorylate VDAC, prevent HKII binding and increase sensitivity to cell death (Bijur and Jope, 2003; Pastorino et al., 2005). HKII itself contains a phosphorylation site at T473, which is amenable to phosphorylation by mitochondrial AKT (Miyamoto et al., 2008; Roberts et al., 2013). This stabilizes HKII association with VDAC and protects from cell death. Furthermore, GSK-3 β stimulates phosphorylation of the anti-apoptotic protein MCL-1, leading to its degradation. Therefore, by inhibition of GSK-3 β , mitochondrial AKT maintains MCL-1 stability and exerts an additional anti-apoptotic effect (Maurer et al., 2006). Finally, it has been shown that overexpression of mitochondria-targeted AKT protects from cell death (Su et al., 2012).

With respect to bioenergetics, the β -subunit of ATP synthase was identified as another AKT interaction partner in mitochondria. Upon phosphorylation by AKT, the activity of ATP synthase is increased (Yang et al., 2013). However, in this case, AKT substrate consensus motif in ATP synthase has not been found. Similarly, mitochondrial AKT may stimulate respiratory activity indirectly through the above mentioned inhibition of GSK-3 β , which phosphorylates and inactivates the pyruvate dehydrogenase complex. In this way, mitochondrial AKT may stimulate the synthesis of acetyl-coenzyme A, a tricarboxylic acid cycle substrate (Hoshi et al., 1996). In summary, it appears that mitochondrial AKT may stimulate OXPHOS and ATP production in addition to its complex pro- and anti-apoptotic activity.

Mechanism of mitochondrial import

The mechanism of mitochondrial import is not well defined for most of the above mentioned proteins.

Clathrin-mediated endocytosis has been shown critical for mitochondrial import of EGFR (Demory et al., 2009). The authors also detected inner mitochondrial targeting sequence between residues 622 and 666 of EGFR, which corresponds to the combined trans-membrane domain (residues 622-644) and juxta-membrane hydrophobic region (residues 645-666) of the receptor. In addition, EGFR co-immunoprecipitated with TOM40, an OMM import protein (Demory et al., 2009). For HER2, a similar scenario of mitochondria translocation has been suggested. Ding et al. (2012) proposed an inner mitochondrial targeting sequence between residues 623 and 689 of HER2, which again corresponds to the trans-membrane plus juxta-membrane domain regions. HER2 was detected by immune-gold electron microscopy staining on cytoskeletal structures, suggesting the involvement of endocytosis (Rohlenova et al, submitted). Mitochondrial HSP70 chaperon is required for HER2 import (Ding et al., 2012) implicating the TIM23 IMM translocase complex, which needs mitochondrial HSP70 for proper function (Schneider et al., 1994). AKT was shown to translocate to mitochondria upon phosphorylation by mTORC2 (Bijur and Jope, 2003), and KRAS translocates to mitochondria upon phosphorylation by PKC (Bivona et al., 2006). Plasma membrane may therefore be a possible source of the mitochondrial fraction of these proteins. Other routes, such as *de novo* protein import cannot be ruled out at present, but the fast kinetics of mitochondrial enrichment (found for EGFR) make this scenario less likely (Demory et al., 2009). The mechanistic details of translocation into mitochondria from the plasma membrane are poorly understood. Even though it appears that the canonical TOM/TIM mitochondrial import machinery could be involved, it is unclear whether phosphorylated proteins can be handled in this way. In addition, most studies into the mechanism of TOM/TIM-mediated mitochondrial import have been done in yeast (Dudek et al., 2013), where RTKs discussed in this review are not present. Additional studies are therefore needed to clarify this issue.

The mitochondrial import of proteins is likely a regulated process. EGFR, AKT and KRAS translocation into mitochondria is induced by specific stimuli, and can occur in a coordinated manner. For example, mutant oncogenic KRAS along with AKT have been reported to enter mitochondria upon KRAS hyper-activation by a compound selective for the mutated form of RAS, leading to ROS production and ROS-induced cell death (Iskandar et al., 2016). Even though the mechanism of translocation has not been defined in this case, it suggests that it can be actively induced by pharmacological intervention.

The question arises whether the distinct lipid environment of mitochondria can accommodate the plasma membrane proteins that often reside in lipid rafts. The IMM contains a substantial percentage of the lipid cardiolipin and lacks cholesterol, enriched in the lipid rafts of the plasma membrane. However, proteins that tend to be recruited into rafts on the plasma membrane, such as caspase eight during apoptosis induction, can translocate to mitochondria and bind to raft-like structures formed by cardiolipin in the OMM (Gonzalvez et al., 2008; Sorice et al., 2009). Cardiolipin contains four acyl chains, most of them highly unsaturated, and could therefore represent an interaction partner capable of substituting cholesterol within both IMM and OMM for proteins naturally localizing into lipid rafts. Similar phenomenon was reported in *Escherichia coli* membranes, where cardiolipin concentrates in regions of high curvature and selectively recruits specific proteins (Renner and Weibel, 2011). Therefore, in our opinion the absence of cholesterol is not necessarily incompatible with the translocation of plasma membrane proteins into mitochondria.

Conclusions and perspectives

The oncogenes of the PI3K/AKT pathway in mitochondria play a complex role. Both metabolic parameters and sensitivity to cell death are affected by their presence, but the reported findings are sometime difficult to interpret. This may be related to different tissues, cell lines and samples investigated. The studies may also be confusing by not differentiating between the mitochondrial fraction of the studied protein and signaling events initiated by that protein at other cellular compartments. Furthermore, the presence in mitochondria should be verified by several independent techniques, which is sometimes not the case. For these reasons, to define the specific role of the mitochondrial fraction of a given protein may be challenging, and its effect may easily be over- or underestimated.

Naturally, one may wonder whether complete signaling cascades of these receptor/adaptor proteins may be initiated and transmitted within mitochondria. We think that this is an unlikely scenario, because we believe that essential signaling partners for both RTKs and RAS are absent in these organelles. RTKs in mitochondria lack HER3 to initiate signaling events (Lee-Hoeflich et al., 2008), and little is known about the multiple RAS adaptor proteins and other partners in mitochondria. In addition, there are no reports on mitochondrial location of PI3K. Hence, it appears more likely that RTKs and RAS proteins translocate to mitochondria in their active,

phosphorylated form, even though, as discussed above, the mechanism of this transport is unknown at present. The exception to the rule may be the mTORC2-AKT interaction at the mitochondria-endoplasmic reticulum contact sites, where several members of this signaling route have been located together (Betz et al., 2013).

It is not surprising that the proteins discussed here are not present in the catalogues of canonical mitochondrial proteins such as the mitocarta (Calvo et al., 2016). These classifications are derived from normal healthy tissue, where expression of oncogenes is negligible. Mitochondrial composition of cancer cells and tissue is not well classified/understood, and functional significance of these oncogenes in mitochondria cannot be easily obtained from available genomics data. It is possible, therefore, that oncogenes in mitochondria could be enriched in populations of cancer cells that are resistant to treatment, where they may promote metabolic plasticity by modulating OXPHOS and responses to the pro-apoptotic stimuli. For example, it was suggested for HER2 that it can be shielded in mitochondria from the effect of targeted drugs (Ding et al., 2012). The same mitochondrial localization might make the cell susceptible to mitochondrial targeted agents such as MitoTam (Rohlenova et al, submitted) or MitoVES (Dong et al., 2011b; Yan et al., 2015) that increase mitochondrial ROS (Dong et al., 2011a; Rohlena et al., 2011; Kluckova et al., 2015). As such, oncogenes in mitochondria may alter responses to specific modes of anti-cancer therapy, which is also interesting from a translational point of view.

Acknowledgments: The authors' work is in part supported by grants from the Czech Science Foundation 16-22823S to J. R., the Australian Research Council (DP110105009, DP130101651, DP15010280), the National and Health Medical Research Council of Australia (APP1011955), the Queensland Cancer Council (APP1049104), the Czech Science Foundation 16-12719S to J.N. and by LQ1604 NPU II provided by MEYS and CZ.1.05/1.1.00/02.0109 BIOCEV provided by ERDF and MEYS.

References

- Acin-Perez, R., Fernandez-Silva, P., Peleato, M.L., Perez-Martos, A., and Enriquez, J.A. (2008). Respiratory active mitochondrial supercomplexes. *Mol. Cell* 32, 529–539.
- Alessi, D.R., Deak, M., Casamayor, A., Caudwell, F.B., Morrice, N., Norman, D.G., Gaffney, P., Reese, C.B., MacDougall, C.N., Harbison, D., et al. (1997). 3-Phosphoinositide-dependent protein kinase-1 (PKD1): structural and functional homology with the *Drosophila* DSTPK61 kinase. *Curr. Biol.* 7, 776–789.
- Antico Arciuch, V.G., Galli, S., Franco, M.C., Lam, P.Y., Cadenas, E., Carreras, M.C., and Poderoso, J.J. (2009). Akt1 intramitochondrial cycling is a crucial step in the redox modulation of cell cycle progression. *PLoS One* 4, e7523.
- Arteaga, C.L. and Engelman, J.A. (2014). ERBB receptors: from oncogene discovery to basic science to mechanism-based cancer therapeutics. *Cancer Cell* 25, 282–303.
- Barthel, A., Okino, S.T., Liao, J., Nakatani, K., Li, J., Whitlock, J.P., Jr., and Roth, R.A. (1999). Regulation of *GLUT1* gene transcription by the serine/threonine kinase Akt1. *J. Biol. Chem.* 274, 20281–20286.
- Betz, C. and Hall, M.N. (2013). Where is mTOR and what is it doing there? *J. Cell Biol.* 203, 563–574.
- Betz, C., Stracka, D., Prescianotto-Baschong, C., Frieden, M., Demaurex, N., and Hall, M.N. (2013). mTOR complex 2-Akt signaling at mitochondria-associated endoplasmic reticulum membranes (MAM) regulates mitochondrial physiology. *Proc. Natl. Acad. Sci. USA* 110, 12526–12534.
- Bijur, G.N. and Jope, R.S. (2003). Rapid accumulation of Akt in mitochondria following phosphatidylinositol 3-kinase activation. *J. Neurochem.* 87, 1427–1435.
- Bivona, T.G., Quatela, S.E., Bodemann, B.O., Ahearn, I.M., Soskis, M.J., Mor, A., Miura, J., Wiener, H.H., Wright, L., Saba, S.G., et al. (2006). PKC regulates a farnesyl-electrostatic switch on K-Ras that promotes its association with Bcl-XL on mitochondria and induces apoptosis. *Mol. Cell* 21, 481–493.
- Boerner, J.L., Demory, M.L., Silva, C., and Parsons, S.J. (2004). Phosphorylation of Y845 on the epidermal growth factor receptor mediates binding to the mitochondrial protein cytochrome c oxidase subunit II. *Mol. Cell. Biol.* 24, 7059–7071.
- Bollu, L.R., Ren, J., Blessing, A.M., Katreddy, R.R., Gao, G., Xu, L., Wang, J., Su, F., and Weihua, Z. (2014). Involvement of *de novo* synthesized palmitate and mitochondrial EGFR in EGF induced mitochondrial fusion of cancer cells. *Cell Cycle* 13, 2415–2430.
- Calvo, S.E., Clauser, K.R., and Mootha, V.K. (2016). MitoCarta2.0: an updated inventory of mammalian mitochondrial proteins. *Nucleic Acids Res.* 44, D1251–1257.
- Cardaci, S., Zheng, L., MacKay, G., van den Broek, N.J., MacKenzie, E.D., Nixon, C., Stevenson, D., Tumanov, S., Bulusu, V., Kamphorst, J.J., et al. (2015). Pyruvate carboxylation enables growth of SDH-deficient cells by supporting aspartate biosynthesis. *Nat. Cell Biol.* 17, 1317–1326.
- Castellano, E., Sheridan, C., Thin, M.Z., Nye, E., Spencer-Dene, B., Diefenbacher, M.E., Moore, C., Kumar, M.S., Murillo, M.M., Gronroos, E., et al. (2013). Requirement for interaction of PI3-kinase p110alpha with RAS in lung tumor maintenance. *Cancer Cell* 24, 617–630.
- Cerniglia, G.J., Dey, S., Gallagher-Colombo, S.M., Daurio, N.A., Tuttle, S., Busch, T.M., Lin, A., Sun, R., Esipova, T.V., Vinogradov, S.A., et al. (2015). The PI3K/Akt pathway regulates oxygen metabolism via pyruvate dehydrogenase (PDH)-E1 α phosphorylation. *Mol. Cancer Ther.* 14, 1928–1938.
- Commisso, C., Davidson, S.M., Soydaner-Azeloglu, R.G., Parker, S.J., Kamphorst, J.J., Hackett, S., Grabocka, E., Nofal, M., Drebin, J.A., Thompson, C.B., et al. (2013). Macropinocytosis of protein is an amino acid supply route in Ras-transformed cells. *Nature* 497, 633–637.
- Demory, M.L., Boerner, J.L., Davidson, R., Faust, W., Miyake, T., Lee, I., Huttemann, M., Douglas, R., Haddad, G., and Parsons, S.J. (2009). Epidermal growth factor receptor translocation to

- the mitochondria: regulation and effect. *J. Biol. Chem.* **284**, 36592–36604.
- Deprez, J., Vertommen, D., Alessi, D.R., Hue, L., and Rider, M.H. (1997). Phosphorylation and activation of heart 6-phosphofructo-2-kinase by protein kinase B and other protein kinases of the insulin signaling cascades. *J. Biol. Chem.* **272**, 17269–17275.
- Ding, Y., Liu, Z., Desai, S., Zhao, Y., Liu, H., Pannell, L.K., Yi, H., Wright, E.R., Owen, L.B., Dean-Colomb, W., et al. (2012). Receptor tyrosine kinase ErbB2 translocates into mitochondria and regulates cellular metabolism. *Nat. Commun.* **3**, 1271.
- Dong, L.F., Jameson, V.J., Tilly, D., Cerny, J., Mahdavian, E., Marin-Hernandez, A., Hernandez-Esquivel, L., Rodriguez-Enriquez, S., Stursa, J., Witting, P.K., et al. (2011a). Mitochondrial targeting of vitamin E succinate enhances its pro-apoptotic and anti-cancer activity via mitochondrial complex II. *J. Biol. Chem.* **286**, 3717–3728.
- Dong, L.F., Jameson, V.J., Tilly, D., Prochazka, L., Rohlena, J., Valis, K., Truksa, J., Zabalova, R., Mahdavian, E., Kluckova, K., et al. (2011b). Mitochondrial targeting of alpha-tocopheryl succinate enhances its pro-apoptotic efficacy: a new paradigm for effective cancer therapy. *Free Radic. Biol. Med.* **50**, 1546–1555.
- Dudek, J., Rehling, P., and van der Laan, M. (2013). Mitochondrial protein import: common principles and physiological networks. *Biochim. Biophys. Acta* **1833**, 274–285.
- Elstrom, R.L., Bauer, D.E., Buzzai, M., Karnauskas, R., Harris, M.H., Plas, D.R., Zhuang, H., Cinalli, R.M., Alavi, A., Rudin, C.M., et al. (2004). Akt stimulates aerobic glycolysis in cancer cells. *Cancer Res.* **64**, 3892–3899.
- Engelman, J.A. (2009). Targeting PI3K signalling in cancer: opportunities, challenges and limitations. *Nat. Rev. Cancer* **9**, 550–562.
- Frezza, C. (2014). The role of mitochondria in the oncogenic signal transduction. *Int. J. Biochem. Cell Biol.* **48**, 11–17.
- Gallo, R.M., Bryant, I.N., Mill, C.P., Kaverman, S., and Riese, D.J., 2nd (2013). Multiple functional motifs are required for the tumor suppressor activity of a constitutively-active ErbB4 mutant. *J. Cancer. Res. Ther. Oncol.* **1**, 10.
- Galluzzi, L., Kepp, O., Trojel-Hansen, C., and Kroemer, G. (2012). Mitochondrial control of cellular life, stress, and death. *Circ. Res.* **111**, 1198–1207.
- Gonzalvez, F., Schug, Z.T., Houtkooper, R.H., MacKenzie, E.D., Brooks, D.G., Wanders, R.J., Petit, P.X., Vaz, F.M., and Gottlieb, E. (2008). Cardiolipin provides an essential activating platform for caspase-8 on mitochondria. *J. Cell Biol.* **183**, 681–696.
- Goo, C.K., Lim, H.Y., Ho, Q.S., Too, H.P., Clement, M.V., and Wong, K.P. (2012). PTEN/Akt signaling controls mitochondrial respiratory capacity through 4E-BP1. *PLoS One* **7**, e45806.
- Gottlob, K., Majewski, N., Kennedy, S., Kandel, E., Robey, R.B., and Hay, N. (2001). Inhibition of early apoptotic events by Akt/PKB is dependent on the first committed step of glycolysis and mitochondrial hexokinase. *Genes Dev.* **15**, 1406–1418.
- Gupta, S., Ramjaun, A.R., Haiko, P., Wang, Y., Warne, P.H., Nicke, B., Nye, E., Stamp, G., Alitalo, K., and Downward, J. (2007). Binding of ras to phosphoinositide 3-kinase p110alpha is required for ras-driven tumorigenesis in mice. *Cell* **129**, 957–968.
- Hanahan, D. and Weinberg, R.A. (2011). Hallmarks of cancer: the next generation. *Cell* **144**, 646–674.
- Hoshi, M., Takashima, A., Noguchi, K., Murayama, M., Sato, M., Kondo, S., Saitoh, Y., Ishiguro, K., Hoshino, T., and Imahori, K. (1996). Regulation of mitochondrial pyruvate dehydrogenase activity by tau protein kinase I/glycogen synthase kinase 3 β in brain. *Proc. Natl. Acad. Sci. USA* **93**, 2719–2723.
- Hu, Y., Lu, W., Chen, G., Wang, P., Chen, Z., Zhou, Y., Ogasawara, M., Trachootham, D., Feng, L., Pelicano, H., et al. (2012). K-rasG12V transformation leads to mitochondrial dysfunction and a metabolic switch from oxidative phosphorylation to glycolysis. *Cell Res.* **22**, 399–412.
- Hynes, N.E. and Lane, H.A. (2005). ERBB receptors and cancer: the complexity of targeted inhibitors. *Nat. Rev. Cancer* **5**, 341–354.
- Iskandar, K., Rezlan, M., Yadav, S.K., Foo, C.H., Sethi, G., Qiang, Y., Bellot, G.L., and Pervaiz, S. (2016). Synthetic lethality of a novel small molecule against mutant KRAS-expressing cancer cells involves AKT-dependent ROS production. *Antioxid. Redox. Signal.*, Epub ahead of print, DOI: 10.1089/ars.2015.6362.
- Kennedy, S.G., Wagner, A.J., Conzen, S.D., Jordan, J., Bellacosa, A., Tschlis, P.N., and Hay, N. (1997). The PI 3-kinase/Akt signaling pathway delivers an anti-apoptotic signal. *Genes Dev.* **11**, 701–713.
- Kennedy, S.G., Kandel, E.S., Cross, T.K., and Hay, N. (1999). Akt/Protein kinase B inhibits cell death by preventing the release of cytochrome c from mitochondria. *Mol. Cell. Biol.* **19**, 5800–5810.
- Kluckova, K., Sticha, M., Cerny, J., Mracek, T., Dong, L., Drahota, Z., Gottlieb, E., Neuzil, J., and Rohlena, J. (2015). Ubiquinone-binding site mutagenesis reveals the role of mitochondrial complex II in cell death initiation. *Cell Death Dis.* **6**, e1749.
- Koppenol, W.H., Bounds, P.L., and Dang, C.V. (2011). Otto Warburg's contributions to current concepts of cancer metabolism. *Nat. Rev. Cancer* **11**, 325–337.
- Lapiente-Brun, E., Moreno-Loshuertos, R., Acin-Perez, R., Latorre-Pellicer, A., Colas, C., Balsa, E., Perales-Clemente, E., Quiros, P.M., Calvo, E., Rodriguez-Hernandez, M.A., et al. (2013). Supercomplex assembly determines electron flux in the mitochondrial electron transport chain. *Science* **340**, 1567–1570.
- Lee-Hoeflich, S.T., Crocker, L., Yao, E., Pham, T., Munroe, X., Hoeflich, K.P., Sliwkowski, M.X., and Stern, H.M. (2008). A central role for HER3 in HER2-amplified breast cancer: implications for targeted therapy. *Cancer Res.* **68**, 5878–5887.
- Lussey-Lepoutre, C., Hollinshead, K.E., Ludwig, C., Menara, M., Morin, A., Castro-Vega, L.J., Parker, S.J., Janin, M., Martinelli, C., Ottolenghi, C., et al. (2015). Loss of succinate dehydrogenase activity results in dependency on pyruvate carboxylation for cellular anabolism. *Nat. Commun.* **6**, 8784.
- Majewski, N., Nogueira, V., Bhaskar, P., Coy, P.E., Skeen, J.E., Gottlob, K., Chandel, N.S., Thompson, C.B., Robey, R.B., and Hay, N. (2004a). Hexokinase-mitochondria interaction mediated by Akt is required to inhibit apoptosis in the presence or absence of Bax and Bak. *Mol. Cell* **16**, 819–830.
- Majewski, N., Nogueira, V., Robey, R.B., and Hay, N. (2004b). Akt inhibits apoptosis downstream of BID cleavage via a glucose-dependent mechanism involving mitochondrial hexokinases. *Mol. Cell. Biol.* **24**, 730–740.
- Maranzana, E., Barbero, G., Falasca, A.I., Lenaz, G., and Genova, M.L. (2013). Mitochondrial respiratory supercomplex association limits production of reactive oxygen species from complex I. *Antioxid. Redox. Signal.* **19**, 1469–1480.
- Matallanas, D., Arozarena, I., Berciano, M.T., Aaronson, D.S., Pellicer, A., Lafarga, M., and Crespo, P. (2003). Differences on the inhibitory specificities of H-Ras, K-Ras, and N-Ras (N17) dominant negative mutants are related to their membrane microlocalization. *J. Biol. Chem.* **278**, 4572–4581.

- Maurer, U., Charvet, C., Wagman, A.S., DeJardin, E., and Green, D.R. (2006). Glycogen synthase kinase-3 regulates mitochondrial outer membrane permeabilization and apoptosis by destabilization of MCL-1. *Mol. Cell* 21, 749–760.
- Miyamoto, S., Murphy, A.N., and Brown, J.H. (2008). Akt mediates mitochondrial protection in cardiomyocytes through phosphorylation of mitochondrial hexokinase-II. *Cell Death Differ.* 15, 521–529.
- Naresh, A., Long, W., Vidal, G.A., Wimley, W.C., Marrero, L., Sartor, C.I., Tovey, S., Cooke, T.G., Bartlett, J.M., and Jones, F.E. (2006). The ERBB4/HER4 intracellular domain 4ICD is a BH3-only protein promoting apoptosis of breast cancer cells. *Cancer Res.* 66, 6412–6420.
- Naresh, A., Thor, A.D., Edgerton, S.M., Torkko, K.C., Kumar, R., and Jones, F.E. (2008). The HER4/4ICD estrogen receptor coactivator and BH3-only protein is an effector of tamoxifen-induced apoptosis. *Cancer Res.* 68, 6387–6395.
- Niederst, M.J. and Engelman, J.A. (2013). Bypass mechanisms of resistance to receptor tyrosine kinase inhibition in lung cancer. *Sci. Signal.* 6, re6.
- Nogueira, V., Park, Y., Chen, C.C., Xu, P.Z., Chen, M.L., Tonic, I., Unterman, T., and Hay, N. (2008). Akt determines replicative senescence and oxidative or oncogenic premature senescence and sensitizes cells to oxidative apoptosis. *Cancer Cell* 14, 458–470.
- Omidvar, N., Kogan, S., Beurlet, S., le Pogam, C., Janin, A., West, R., Noguera, M.E., Reboul, M., Soulie, A., Leboeuf, C., et al. (2007). BCL-2 and mutant NRAS interact physically and functionally in a mouse model of progressive myelodysplasia. *Cancer Res.* 67, 11657–11667.
- Pastorino, J.G., Hoek, J.B., and Shulga, N. (2005). Activation of glycogen synthase kinase 3beta disrupts the binding of hexokinase II to mitochondria by phosphorylating voltage-dependent anion channel and potentiates chemotherapy-induced cytotoxicity. *Cancer Res.* 65, 10545–10554.
- Pavlova, N.N. and Thompson, C.B. (2016). The emerging hallmarks of cancer metabolism. *Cell Metab.* 23, 27–47.
- Pylayeva-Gupta, Y., Grabocka, E., and Bar-Sagi, D. (2011). RAS oncogenes: weaving a tumorigenic web. *Nat. Rev. Cancer* 11, 761–774.
- Rebollo, A., Perez-Sala, D., and Martinez, A.C. (1999). Bcl-2 differentially targets K-, N-, and H-Ras to mitochondria in IL-2 supplemented or deprived cells: implications in prevention of apoptosis. *Oncogene* 18, 4930–4939.
- Renner, L.D. and Weibel, D.B. (2011). Cardiolipin microdomains localize to negatively curved regions of *Escherichia coli* membranes. *Proc. Natl. Acad. Sci. USA* 108, 6264–6269.
- Rimessi, A., Marchi, S., Patergnani, S., and Pinton, P. (2014). H-Ras-driven tumoral maintenance is sustained through caveolin-1-dependent alterations in calcium signaling. *Oncogene* 33, 2329–2340.
- Roberts, D.J., Tan-Sah, V.P., Smith, J.M., and Miyamoto, S. (2013). Akt phosphorylates HK-II at Thr-473 and increases mitochondrial HK-II association to protect cardiomyocytes. *J. Biol. Chem.* 288, 23798–23806.
- Rohlena, J., Dong, L.F., Kluckova, K., Zobalova, R., Goodwin, J., Tilly, D., Stursa, J., Pecinova, A., Philimonenko, A., Hozak, P., et al. (2011). Mitochondrially targeted alpha-tocopheryl succinate is antiangiogenic: potential benefit against tumor angiogenesis but caution against wound healing. *Antioxid. Redox. Signal.* 15, 2923–2935.
- Sarbasov, D.D., Guertin, D.A., Ali, S.M., and Sabatini, D.M. (2005). Phosphorylation and regulation of Akt/PKB by the rictor-mTOR complex. *Science* 307, 1098–1101.
- Scheffler, I. (2008). *Mitochondria*, Second Edition (Hoboken, New Jersey, USA: John Wiley & Sons, Inc.).
- Schneider, H.C., Berthold, J., Bauer, M.F., Dietmeier, K., Guiard, B., Brunner, M., and Neupert, W. (1994). Mitochondrial Hsp70/MIM44 complex facilitates protein import. *Nature* 371, 768–774.
- Schug, Z.T., Peck, B., Jones, D.T., Zhang, Q., Grosskurth, S., Alam, I.S., Goodwin, L.M., Smethurst, E., Mason, S., Blyth, K., et al. (2015). Acetyl-CoA synthetase 2 promotes acetate utilization and maintains cancer cell growth under metabolic stress. *Cancer Cell* 27, 57–71.
- Slamon, D.J., Clark, G.M., Wong, S.G., Levin, W.J., Ullrich, A., and McGuire, W.L. (1987). Human breast cancer: correlation of relapse and survival with amplification of the HER-2/neu oncogene. *Science* 235, 177–182.
- Sorice, M., Manganelli, V., Matarrese, P., Tinari, A., Misasi, R., Malorni, W., and Garofalo, T. (2009). Cardiolipin-enriched raft-like microdomains are essential activating platforms for apoptotic signals on mitochondria. *FEBS Lett.* 583, 2447–2450.
- Su, C.C., Yang, J.Y., Leu, H.B., Chen, Y., and Wang, P.H. (2012). Mitochondrial Akt-regulated mitochondrial apoptosis signaling in cardiac muscle cells. *Am. J. Physiol. Heart Circ. Physiol.* 302, H716–723.
- Sun, Y., Lin, H., Zhu, Y., Ma, C., Ye, J., and Luo, J. (2002). Induction or suppression of expression of cytochrome c oxidase subunit II by heregulin β 1 in human mammary epithelial cells is dependent on the levels of ErbB2 expression. *J. Cell. Physiol.* 192, 225–233.
- Tan, A.S., Baty, J.W., Dong, L.F., Bezawork-Geleta, A., Endaya, B., Goodwin, J., Bajzikova, M., Kovarova, J., Peterka, M., Yan, B., et al. (2015). Mitochondrial genome acquisition restores respiratory function and tumorigenic potential of cancer cells without mitochondrial DNA. *Cell Metab.* 21, 81–94.
- Vander Heiden, M.G., Cantley, L.C., and Thompson, C.B. (2009). Understanding the Warburg effect: the metabolic requirements of cell proliferation. *Science* 324, 1029–1033.
- Vidal, G.A., Naresh, A., Marrero, L., and Jones, F.E. (2005). Presenilin-dependent gamma-secretase processing regulates multiple ERBB4/HER4 activities. *J. Biol. Chem.* 280, 19777–19783.
- Wallace, D.C. (2012). Mitochondria and cancer. *Nat. Rev. Cancer* 12, 685–698.
- Wolfman, J.C., Planchon, S.M., Liao, J., and Wolfman, A. (2006). Structural and functional consequences of c-N-Ras constitutively associated with intact mitochondria. *Biochim. Biophys. Acta* 1763, 1108–1124.
- Yan, B., Stantic, M., Zobalova, R., Bezawork-Geleta, A., Stapelberg, M., Stursa, J., Prokopova, K., Dong, L., and Neuzil, J. (2015). Mitochondrially targeted vitamin E succinate efficiently kills breast tumour-initiating cells in a complex II-dependent manner. *BMC Cancer* 15, 401.
- Yang, J.Y., Deng, W., Chen, Y., Fan, W., Baldwin, K.M., Jope, R.S., Wallace, D.C., and Wang, P.H. (2013). Impaired translocation and activation of mitochondrial Akt1 mitigated mitochondrial oxidative phosphorylation complex V activity in diabetic myocardium. *J. Mol. Cell. Cardiol.* 59, 167–175.

Copyright of Biological Chemistry is the property of De Gruyter and its content may not be copied or emailed to multiple sites or posted to a listserv without the copyright holder's express written permission. However, users may print, download, or email articles for individual use.

RESEARCH ARTICLE

Open Access

Mitochondrially targeted vitamin E succinate efficiently kills breast tumour-initiating cells in a complex II-dependent manner

Bing Yan¹, Marina Stantic¹, Renata Zobalova^{1,3}, Ayenachew Bezawork-Geleta¹, Michael Stapelberg¹, Jan Stursa², Katerina Prokopova³, Lanfeng Dong^{1*} and Jiri Neuzil^{1,3*}

Abstract

Background: Accumulating evidence suggests that breast cancer involves tumour-initiating cells (TICs), which play a role in initiation, metastasis, therapeutic resistance and relapse of the disease. Emerging drugs that target TICs are becoming a focus of contemporary research. Mitocans, a group of compounds that induce apoptosis of cancer cells by destabilising their mitochondria, are showing their potential in killing TICs. In this project, we investigated mitochondrially targeted vitamin E succinate (MitoVES), a recently developed mitocan, for its *in vitro* and *in vivo* efficacy against TICs.

Methods: The mammosphere model of breast TICs was established by culturing murine NeuTL and human MCF7 cells as spheres. This model was verified by stem cell marker expression, tumour initiation capacity and chemotherapeutic resistance. Cell susceptibility to MitoVES was assessed and the cell death pathway investigated. *In vivo* efficacy was studied by grafting NeuTL TICs to form syngeneic tumours.

Results: Mammospheres derived from NeuTL and MCF7 breast cancer cells were enriched in the level of stemness, and the sphere cells featured altered mitochondrial function. Sphere cultures were resistant to several established anti-cancer agents while they were susceptible to MitoVES. Killing of mammospheres was suppressed when the mitochondrial complex II, the molecular target of MitoVES, was knocked down. Importantly, MitoVES inhibited progression of syngeneic HER2^{high} tumours derived from breast TICs by inducing apoptosis in tumour cells.

Conclusions: These results demonstrate that using mammospheres, a plausible model for studying TICs, drugs that target mitochondria efficiently kill breast tumour-initiating cells.

Keywords: Tumour-initiating cells, Mitochondrially targeted vitamin E succinate, Complex II, Mitochondrial potential, Mitochondria, Breast cancer

Background

Breast cancer, a neoplastic disease with high level of incidence and mortality, is the prevalent cancer in females [1, 2]. One reason for high rate of breast cancer, its metastatic potential and, in many cases, resistance to therapy, is the presence of tumour-initiating cells (TICs) [3, 4] that represent a small tumour subpopulation with the ability to self-renew and drive tumour growth [5, 6]. Recent research provides strong evidence for the contribution of TICs to tumour (re-) initiation and progression [7-12].

Therefore, specific therapies targeted at TICs may suppress tumour (re-) growth, perhaps even eliminating the pathology [13, 14]. Development of anti-TIC approaches is an emerging focus of research, and a group of compounds with anti-cancer properties acting by destabilising mitochondria, 'mitocans', appear to be efficient against TICs [15].

Mitocans define small compounds that induce apoptosis of malignant cells via targeting mitochondria. They are classified into several categories according to their molecular target [16]. Mitocans from the vitamin E (VE) group, epitomised by α -tocopheryl succinate (α -TOS), affect the mitochondrial complex II (CII) by interfering

* Correspondence: l.dong@griffith.edu.au; j.neuzil@griffith.edu.au

¹School of Medical Science, Griffith University, Southport, Qld, 4222, Australia
Full list of author information is available at the end of the article

with the function of ubiquinone (UbQ), resulting in leakage of electrons and generation of reactive oxygen species (ROS), which trigger selective apoptosis in cancer cells [17, 18]. To promote its selective mitochondrial uptake driven by mitochondrial potential ($\Delta\Psi_{m,i}$), we tagged α -TOS with the delocalised cation triphenylphosphonium (TPP⁺) to prepare mitochondrially targeted vitamin E succinate (MitoVES). This agent preferentially associates with mitochondria of cancer cells and kills malignant cells more efficiently than the parental compound [19, 20].

Selectivity of agents like MitoVES for malignant cells is based on the relatively high $\Delta\Psi_{m,i}$ of cancer cells [21]. Recent reports document that TICs have higher $\Delta\Psi_{m,i}$ than differentiated cancer cells [22]. Therefore we decided to establish a model of breast cancer TICs and test the anti-cancer efficacy of MitoVES.

Methods

Cell culture and sphere preparation

Breast cancer NeuTL cells derived from tumours of transgenic FVB/N *c-neu* mice [23] and human MCF7 cells obtained from the ATCC were cultured in DMEM with 10 % FBS and antibiotics. Spheres were prepared by seeding cells at the density of 10^5 /ml of 'sphere medium' composed of DMEM-F12 plus cell proliferation supplement (Neurocult), 10 ng/ml mouse or human recombinant EGF, 5 ng/ml recombinant FGF (R&D Systems), and 2 mM L-glutamine.

Quantitative RT-PCR (qPCR)

Total RNA from cells or tissues was extracted using the RNeasy kit (Qiagen). The Revertaid First-Strand Synthesis System plus random hexamer primers (Thermo Fischer Scientific) were used to transcribe total RNA into cDNA. Using specific primers, genes of interest were evaluated with 2xSYBR Green (Qiagen) by means of the Eco qPCR System (Illumina). Target genes were normalised to *GAPDH*, and change in gene expression determined using the $\Delta\Delta$ Ct method (see Additional file 1 for primer sequences).

Cell cycle analysis

Adherent or sphere cells were fixed in 70 % ethanol overnight at -20 °C, pelleted and re-suspended in the staining solution (50 μ g/ml propidium iodide, 100 μ g/ml RNase A, 0.1 % Triton X-100). After 40 min incubation at 37 °C, samples were accessed with the Fortessa flow cytometer (BectonDickonson) and data analysed using the FlowJo software (TreeStar).

Evaluation of mitochondrial membrane potential ($\Delta\Psi_{m,i}$), reactive oxygen species (ROS), cell death and viability

Standard flow cytometric methods were applied utilising the following fluorescent probes. $\Delta\Psi_{m,i}$ was estimated

with tetramethylrhodamine methyl ester (TMRM), and ROS were evaluated using dichlorofluorescein diacetate (DCF) or MitoSOX. Apoptosis was evaluated using annexin V-FITC/propidium iodide. Viability was assessed using the MTT assay.

Succinate dehydrogenase (SDH) and succinate quinone reductase (SQR) activity assays

For SDH activity, cells were seeded in 96 well plates at 10,000 cells per well and allowed to recuperate overnight. They were then incubated with 20 mM succinate for 1 h before 10 μ l MTT reagent (5 mg/ml) was added to each well, followed by 4-h incubation at 37 °C and 5 % CO₂. Media was then removed and formazan dissolved in DMSO, and absorbance was measured at 570 nm [19, 20]. For SQR activity, 40 μ g of protein lysate extracted before the assay (Cell Lysis Buffer, Cell Signaling) were added to 1 ml of the SQR assay buffer (10 mM KH₂PO₄, pH 7.8, 2 mM EDTA, 1 mg/ml BSA, 80 μ M DCPIP, 4 μ M rotenone, 0.2 mM ATP and 10 mM succinate) and incubated at 30 °C for 10 min. Decylubiquinone was added to a final concentration of 80 μ M, and absorbance assessed each minute for 30 min at 600 nm [19, 20].

High-resolution respirometry

Oxygen consumption was assessed using the Oxygraph-2 k high-resolution respirometer (Oroboros). Intact cell respiration was evaluated with cells suspended in the RPMI medium without serum. Oxygen consumption was evaluated for cellular routine respiration, oligomycin-inhibited leak respiration, FCCP-stimulated uncoupled respiration (ETS) and rotenone/antimycin-inhibited residual respiration (ROX). Respiration via mitochondrial complexes was evaluated using saponin-permeabilised cells or shredded tumour tissue, suspended in the mitochondrial respiration medium MiR06. Oxygen consumption was evaluated for routine respiration, CI-linked respiration, (CI + CII)-linked respiration, maximum uncoupled respiration, CII-linked uncoupled respiration as well as residual oxygen consumption [24].

Western blotting (WB)

Cells and homogenised tumour tissue were lysed, and total protein (30 μ g) resolved by SDS-PAGE and transferred to PVDF membranes, which were probed with following antibodies: EpCAM, erbB2 (both from Sigma-Aldrich), caspase-9, caspase-8, cleaved caspase-3, VDAC, COX IV, SDHA (all from Cell Signaling), CD44, HSP60, actin (all from Abcam), CD133, PARP-1/2 (both from Santa Cruz), and SDHC (Novus Biologicals). ECL western blotting substrate (Thermo Scientific) and ChemiDoc™ XRS+ System (BioRad) were used to visualise and evaluate the blots.

Native blue Gel electrophoresis

Mitochondria were isolated following a standard protocol, and protein concentration assessed using the BCA assay. NativePAGE Novex Bis-Tris (4–16 % gradient) gels (Life Technologies) were used for electrophoresis of digitonin-solubilised mitochondria. After electrophoresis, gels were incubated in the SDS-PAGE 1 × running buffer for 5 min, and the protein transferred to a PVDF membrane probed with specific antibodies against mitochondrial complex I (CI) (NUDFA9), CII (SDHA and SDHB), complex III (Core1), complex IV (COX Va) and complex V (ATPase β) (all antibodies from Cell Signaling). HSP60 was used as loading control.

Preparation of SDHC knock-down cells

MCF7 cells were transfected with non-silencing (N.S.) or SDHC shRNA (both SABiosciences) using the FuGENE HD reagent as per standard protocol. Selected clones were tested for SDHC mRNA and protein, and the clone with lowest level of SDHC used in experiments.

Tumour formation and MitoVES treatment

Tumours were established in female FVB/N *c-neu* mice (~2 months old) by subcutaneous grafting of NeuTL adherent or sphere cells at 3×10^6 per animal. Mice were regularly checked by the Vevo770 ultrasound imaging (USI) apparatus equipped with a 30- μ m resolution scan-head (VisualSonics). As soon as tumours reached ~50 mm³, animals were treated by intraperitoneal (i.p.) injection of MitoVES (25 nmol per gram of body weight) in corn oil containing 4 % ethanol every 3–4 d. Control mice were injected with the same volume (100 μ l) of the excipient. Tumour progression was assessed by USI, which enables 3D reconstruction of tumours and precise quantification of their volume. Tumours were harvested, fixed in and paraffin-embedded. The blocks were cut into 1 μ m sections stained with H&E or incubated with primary antibody and biotinylated secondary antibody. The ABC kit (Vector Laboratories) was used to amplify the signal. Mayer's haematoxylin was used for counterstaining the nuclei. All animal experiments were performed according to the guidelines of the Australian and New Zealand Council for the Care and Use of Animals in Research and Teaching and were approved by the Griffith University Animal Ethics Committee.

Statistical analysis

All data are mean values of at least three independent experiments \pm S.D. The unpaired Student's *t* test or one-way ANOVA were used to assess statistical significance. Differences with *p* < 0.05 were regarded as significant. Images are representative of three independent experiments.

Results

NeuTL and MCF7 spheres are enriched in TICs

To establish an *in vitro* model to study breast TICs, we grew NeuTL and MCF7 cells under condition that promotes sphere generation (Fig. 1 A, B). Both cell lines formed mammospheres within 3–5 days, reaching ~50 μ m in diameter. To verify spheres as a model of breast TICs, mRNA level of a series of 'stemness' markers was assessed. As can be seen in Fig. 1 C, NeuTL spheres had higher expression of *CD44*, *ALDH*, *EpCAM*, *CD61*, *CD133*, *CD49* and *CD29f*, and lower expression of *CD24*, compared to their adherent counterparts. MCF7 spheres featured higher level of *CD44*, *CD133*, *OCT4*, *ABCG2*, *ESA* and *c-Kit*, and lower level of *CD24* (Fig. 1 D).

To assess their tumour-propagating efficacy, sphere and adherent cells were grafted into FVB/N *c-neu* mice. As shown in Fig. 1 E, NeuTL spheres initiated USI-detectable tumours within ~1 week, while there was a 2-week delay for adherent cells. Adherent cell-derived tumours progressed at about half the rate of the sphere-derived ones, with an increase by 100 mm³ in 1.4 and 2.7 days, respectively. Morphologically, the two types of tumours were similar, as documented by H&E staining (Fig. 1 F). As assessed by WB and IHC (Fig. 1 G), the receptor tyrosine kinase *erbB2* was highly and similarly expressed in both tumour types.

Breast TICs are resistant to chemotherapeutic drugs but sensitive to MitoVES

Figure 2 A documents that NeuTL spheres are more resistant to doxorubicin and paclitaxel compared to their adherent counterparts, consistent with their TIC nature. α -TOS killed adherent and sphere NeuTL and MCF7 cells with similar efficacy, while MitoVES was more efficient in killing sphere cells (Fig. 2 A, B). The IC₅₀ values were higher for killing sphere cells by doxorubicin and paclitaxel, while they were significantly lower for MitoVES (Table 1). As the MTT assay used for cell viability partially relies on the oxidative capacity of mitochondria, the above results of α -TOS and MitoVES may be affected to some extent. Therefore further cell death assessment was carried on by flow cytometry using PI and Annexin IV staining. We can see that MitoVES also induced more cell death by apoptosis in sphere *vs.* adherent cells, while α -TOS was inefficient (Fig. 2 C–E). At 2 μ M, MitoVES was more efficient in inducing apoptosis in MCF7 sphere cells than 10 μ M parthenolide. While MitoVES at 2 μ M was not very efficient in causing apoptosis in adherent NeuTL cells, it arrested their cell cycle (Fig. 2 F). The apoptotic nature of cell death induced in sphere cells by MitoVES is documented in Fig. 2 G. Apart from apoptotic proteins activated by MitoVES treatment, there were also certain

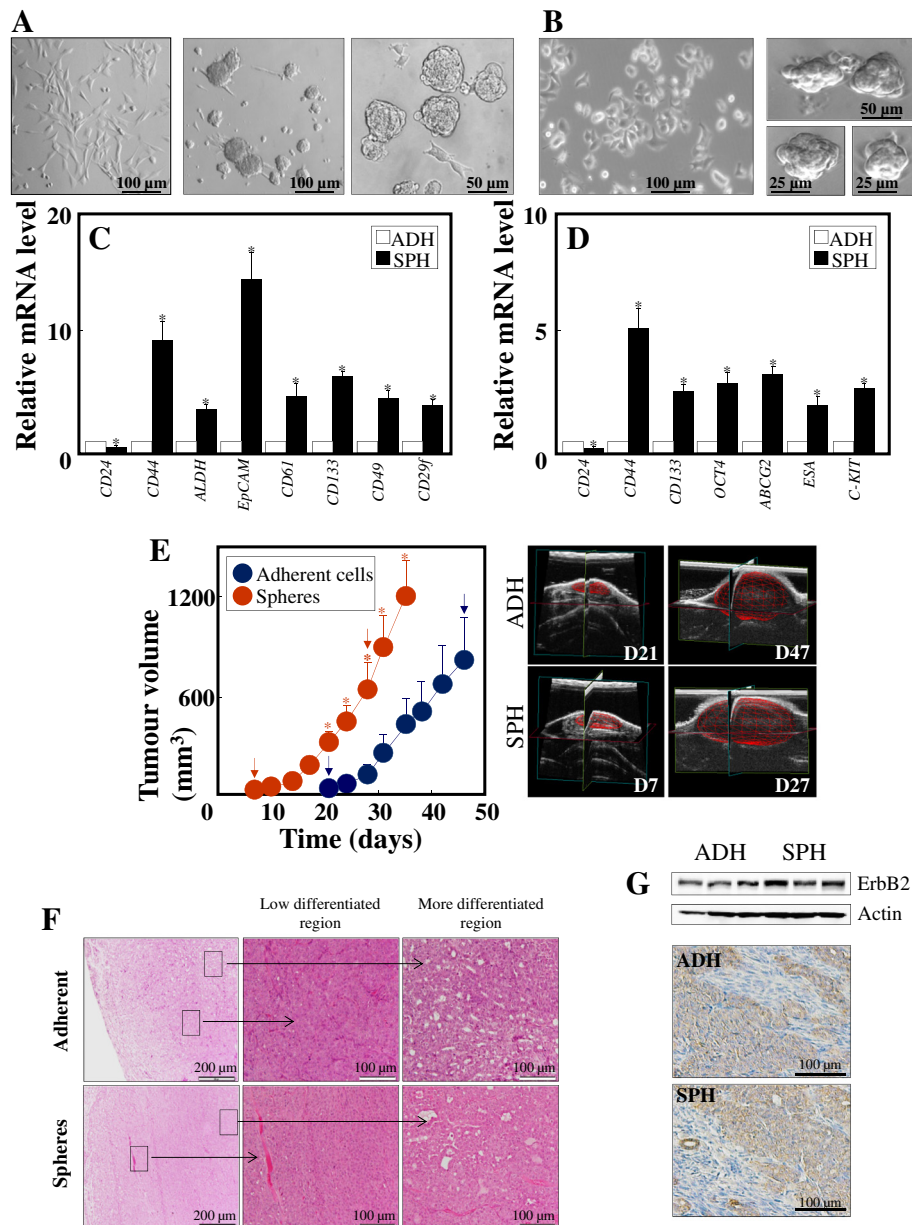


Fig. 1 NeuTL and MCF7 spheres are a plausible model of TICs. Neu TL cells were cultured in serum-containing and sphere medium (A) and assessed for selected stemness genes by qPCR (C). MCF7 cells were cultured in adherent and 'sphere' medium (B) and assessed for selected stemness genes by qPCR (D). (E) NeuTL adherent and sphere cells were grafted s.c. in FVB/N c-neu mice (10⁶ cells per animal) and tumour volume assessed using USI. The images on the right are representative USI scans of tumours taken on the given days (indicated by arrows in the graph on the left). (F) Sections of tumours were stained by H&E for morphology, also showing regions of low and more differentiated cancer cells. (G) Tumour sections were evaluated for the level of erbB2 using WB and IHC. In all cases, the level of stemness genes in sphere cells was related to that in their adherent counterparts, set as 1. Data are mean values ± S.D. (n = 3). The symbol '*' indicates statistically significant differences in the level of mRNA in adherent and sphere cells with p < 0.05. Images in panels A, B, E, F and G are representative of three independent experiments

amounts of cleaved Caspase-8 and cleaved Caspase-9 documented in the control group, which may be due to a small population of cells undergoing apoptosis among the whole cell culture.

Increased killing of breast TICs by MitoVES involves mitochondria

MitoVES was more efficient in ROS generation in sphere than adherent cells, in particular when assessed

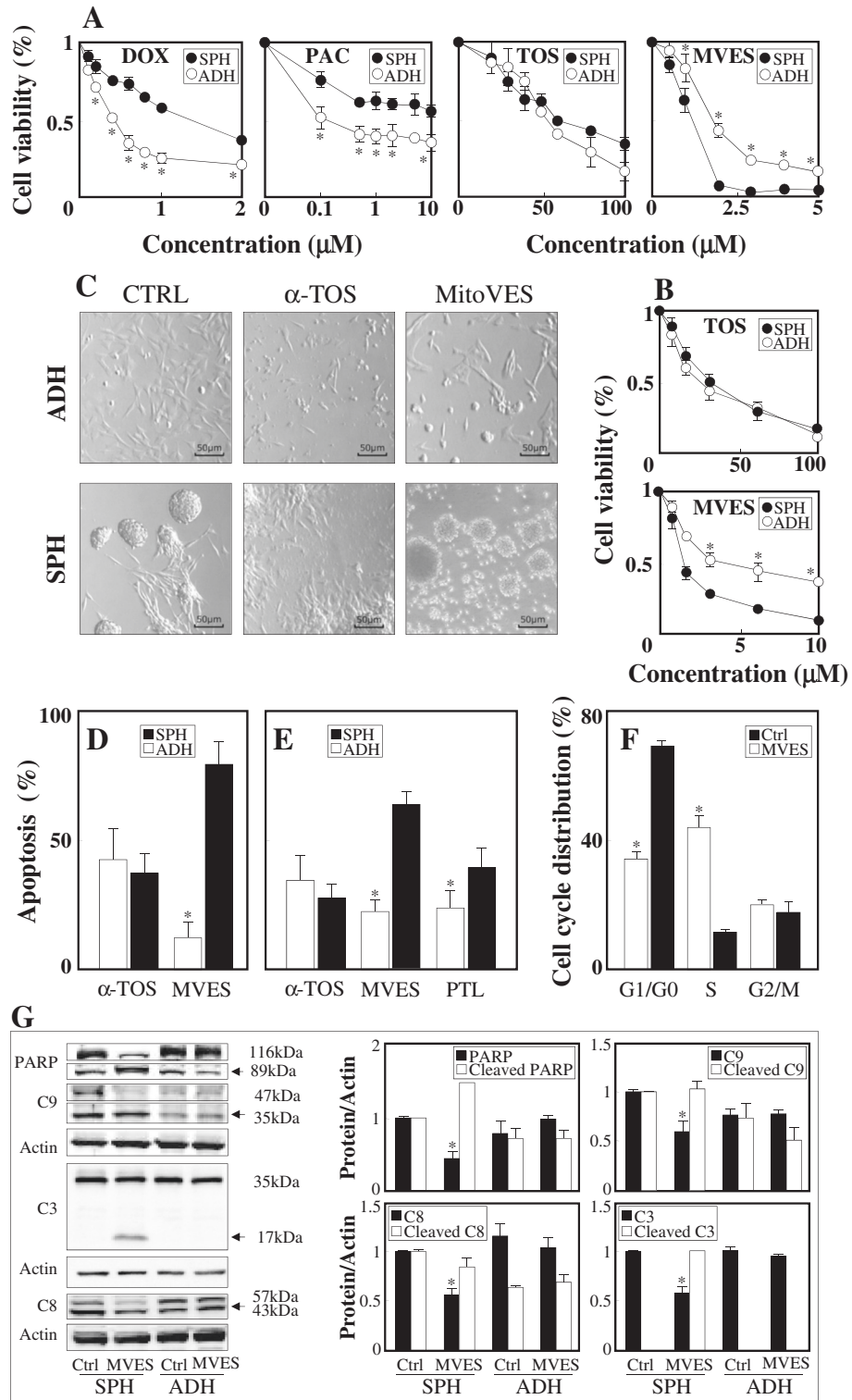


Fig. 2 (See legend on next page.)

(See figure on previous page.)

Fig. 2 Breast TICs are resistant to chemotherapeutic drugs but sensitive to MitoVES. Adherent and sphere NeuTL (**A**) and MCF7 cells (**B**) were exposed to different concentrations of the agents for 24 h and viability assessed by the MTT assay. (**C**) NeuTL adherent and sphere cells were exposed to 50 μ M α -TOS or 2 μ M MitoVES for 24 h and inspected by light microscopy. Adherent or sphere NeuTL (**D**) or MCF7 cells (**E**) were exposed to α -TOS (50 μ M), MitoVES (2 μ M) or parthenolide (PTL; 10 μ M) for 12 h and apoptosis evaluated using the annexin V/PI method. (**F**) Adherent NeuTL cells were exposed to 2 μ M MitoVES for 24 h and evaluated for cell cycle distribution. (**G**) NeuTL sphere and adherent cells were exposed to 5 μ M MitoVES for 12 h and full length and cleaved PARP, caspase-9 (C9), caspase-3 (C3) and caspase-8 assessed using WB with actin as loading control. The level of full length and cleaved proteins was evaluated by densitometry and related to actin. Data are mean values \pm S.D. (n = 3). The symbol ^{*} in panels A, B, D-F indicates statistically significant differences for adherent and sphere cells with p < 0.05. The symbol ^{**} in panel G indicates statistically significant differences in the expression of the full length and cleaved protein with p < 0.05. Images in panel C are representative of three independent experiments

with DCF (Fig. 3 A, B). MitoVES also more efficiently suppressed respiration in sphere compared to adherent cells (Fig. 3 C). That the two types of cells do not differ in mitochondrial mass was confirmed by WB (Fig. 3 D). Both NeuTL and MCF7 spheres showed considerably higher $\Delta\Psi_{m,i}$ potential than their adherent counterparts (Fig. 3 E-G). Important role of $\Delta\Psi_{m,i}$ in apoptosis induction by MitoVES follows from an experiment, in which the mitochondrial uncoupler FCCP inhibited MitoVES-induced killing in NeuTL and MCF7 spheres (Fig. 3 H, I). The higher $\Delta\Psi_{m,i}$ in sphere cells may enrich more MitoVES into their mitochondrial, which contribute to the high susceptibility of spheres upon MitoVES treatment in comparison with their adherent counterparts. Moreover, it is also found that NeuTL sphere cells have higher expression of mitochondrial complexes (unpublished data), some of which function as the molecular targets of MitoVES.

MitoVES affects mitochondrial complexes of breast TICs

We tested the contribution of CI and CII to respiration of breast cancer cells and whether this is affected by MitoVES. As shown in Fig. 4 A & B, oxygen consumption was inhibited more at the level of CII, the target of the agent. This was observed for both coupled and uncoupled state of respiration. Native blue gel electrophoresis using a mild detergent followed by WB was employed to assess the change of mitochondrial respiratory complexes and supercomplexes upon MitoVES treatment. Some decrease in the level of supercomplexes in cells treated with MitoVES was observed after 2 and 4 h of exposure to the drug (Fig. 4 C).

MitoVES efficiently suppresses tumour growth

Adherent and sphere NeuTL cells were subcutaneously injected in FVB/N *c-neu* mice to form syngeneic tumours, after which MitoVES was administered. As revealed by USI, MitoVES efficiently suppressed growth of tumours derived from both types of cells, such that after 7-8 injections, the tumour volume was lower by ~80 % in the treated vs. control mice (Fig. 5 A, B). MitoVES suppressed tumour growth by way of inducing apoptosis, as documented by IHC using an antibody to cleaved caspase-3 (Fig. 5 C, D). Assessment of respiration revealed that MitoVES suppressed both CI- and CII-dependent respiration of tumours (Fig. 5 E, F).

MitoVES kills breast TICs in a complex II-dependent manner

Whether MitoVES induces apoptosis in breast TICs via CII has not been tested. We therefore knocked down the SDHC subunit of CII in MCF7 cells and found that SDHC^{low} MCF7 cells form spheres with low level of SDHC, while SDHA is unaffected (Fig. 6 B). SDH activity of CII, residing in SDHA, was only marginally affected, while SQR activity of CII that requires intact SDHC was suppressed (Fig. 6C). SDHC^{low} MCF7 spheres feature high level of stemness, as documented by several TIC markers (Fig. 6D). Treatment of MCF7 sphere cells with MitoVES homologues differing in the length of the aliphatic chain linking the tocopheryl succinyl group TPP⁺ group revealed that the short-chain homologues are inefficient in ROS generation and apoptosis induction (Fig. 6 E, F), pointing to CII as a target. SDHC^{low} MCF7 spheres showed higher viability in the presence of MitoVES than

Table 1 IC₅₀ values (μ M) for adherent and sphere cells exposed to various anti-cancer agents

Cell line	Doxorubicin		Paclitaxel		α -TOS		MitoVES	
	ADH	SPH	ADH	SPH	ADH	SPH	ADH	SPH
NeuTL	0.45 \pm 0.07 ^a	1.44 \pm 0.17	0.26 \pm 0.06	>10	53 \pm 4.5	58 \pm 6.3	1.9 \pm 0.31	1.1 \pm 0.25
MCF7	n.d. ^b	n.d.	n.d.	n.d.	24.8 \pm 2.2	28.6 \pm 1.9	4.52 \pm 0.29	1.2 \pm 0.25
MCF7 SDHC ^{low}	n.d.	n.d.	n.d.	n.d.	n.d.	n.d.	n.d.	8.2 \pm 1.3

^aIC₅₀ values were calculated from the killing curves of the various adherent and sphere cell cultures exposed to the agents for 24 h. The killing curves were constructed using the MTT assay

^bn.d.: not determined

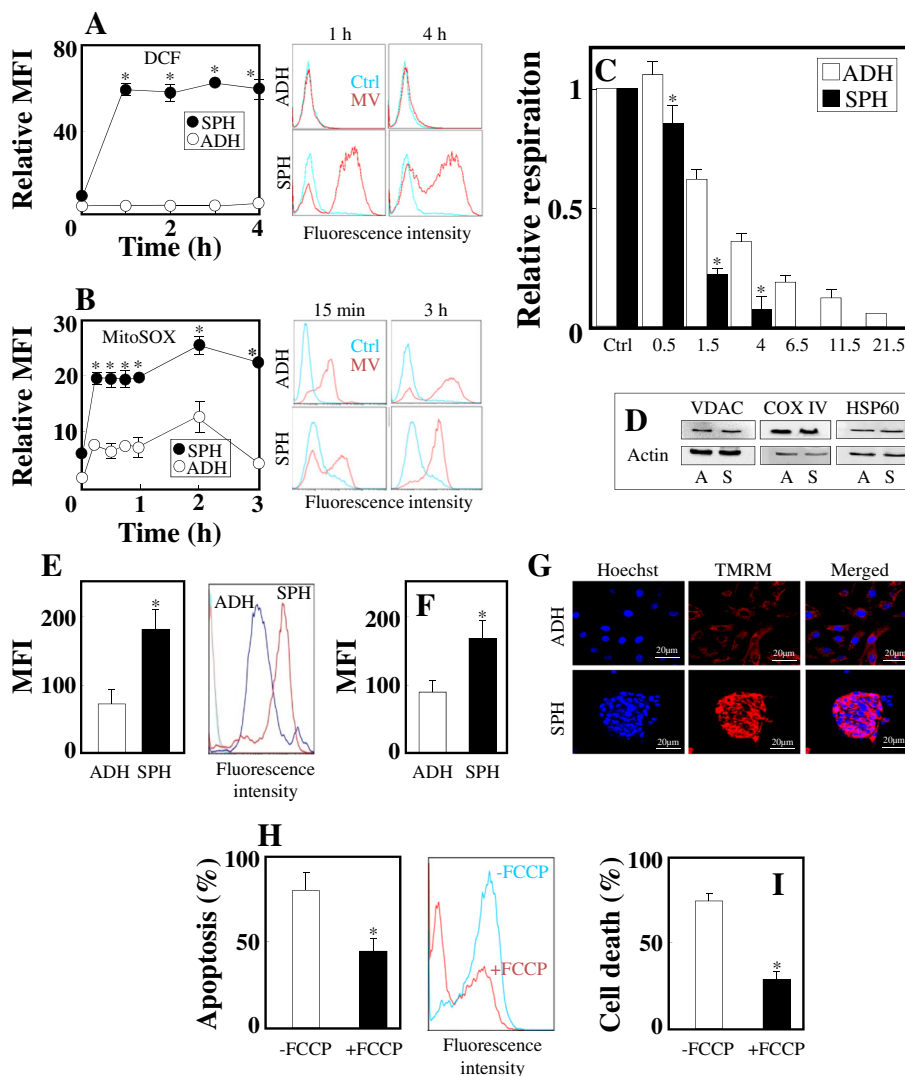


Fig. 3 Mitochondria play a role in high TIC killing activity of MitoVES. NeuTL adherent and sphere cells were exposed to 2 μ M MitoVES for the times shown and ROS evaluated by flow cytometry using DCF (A) or MitoSOX (B), and expressed as relative mean fluorescence intensity (MFI). The histograms on the right are representative of individual readings. (C) Adherent and sphere NeuTL cells were assessed for routine respiration in the absence or presence of MitoVES at the concentrations shown (μ M). (D) Adherent and sphere NeuTL cells were probed by WB for the levels of mitochondrial markers with actin as loading control. Adherent and sphere NeuTL (E) and MCF7 cells (F) were evaluated for $\Delta\Psi_{mj}$ using TMRM and flow cytometry. The histogram in panel E on the right is an example of a reading for NeuTL cells. (G) Adherent and sphere NeuTL cells were labelled with Hoechst to visualise nuclei and TMRM to document $\Delta\Psi_{mj}$, and inspected by confocal microscopy. Sphere NeuTL (H) and MCF7 (I) cells were exposed to 2 μ M MitoVES for 24 h in the absence or presence of 10 μ M FCCP and apoptosis evaluated. The histogram in panel H on the right is an example of reading for NeuTL cells. Data are mean values \pm S.D. (n = 3). The symbol * indicates statistically significant differences for adherent and sphere cells with p < 0.05. The symbol ** indicates statistically significant differences in apoptosis induced in the presence and absence of FCCP with p < 0.05. Images in panels C and D are representative of three independent experiments

MCF7 spheres (Fig. 6G) with the IC_{50} value \sim 4-fold higher (Table 1). SDHC^{low} spheres were also more resistant to MitoVES-induced apoptosis than their parental counterparts (Fig. 6H). Finally, thenoyltrifluoroacetate (TTFA), an agent binding to CII's UbQ site, prevented apoptosis induced by MitoVES.

Discussion

In this communication we describe a sphere model of breast TICs that was adapted from research on neural stem cells isolated from the CNS [25, 26] and that is now accepted as a model for TIC studies in tissue culture [27-29]. The increased level of stemness in NeuTL

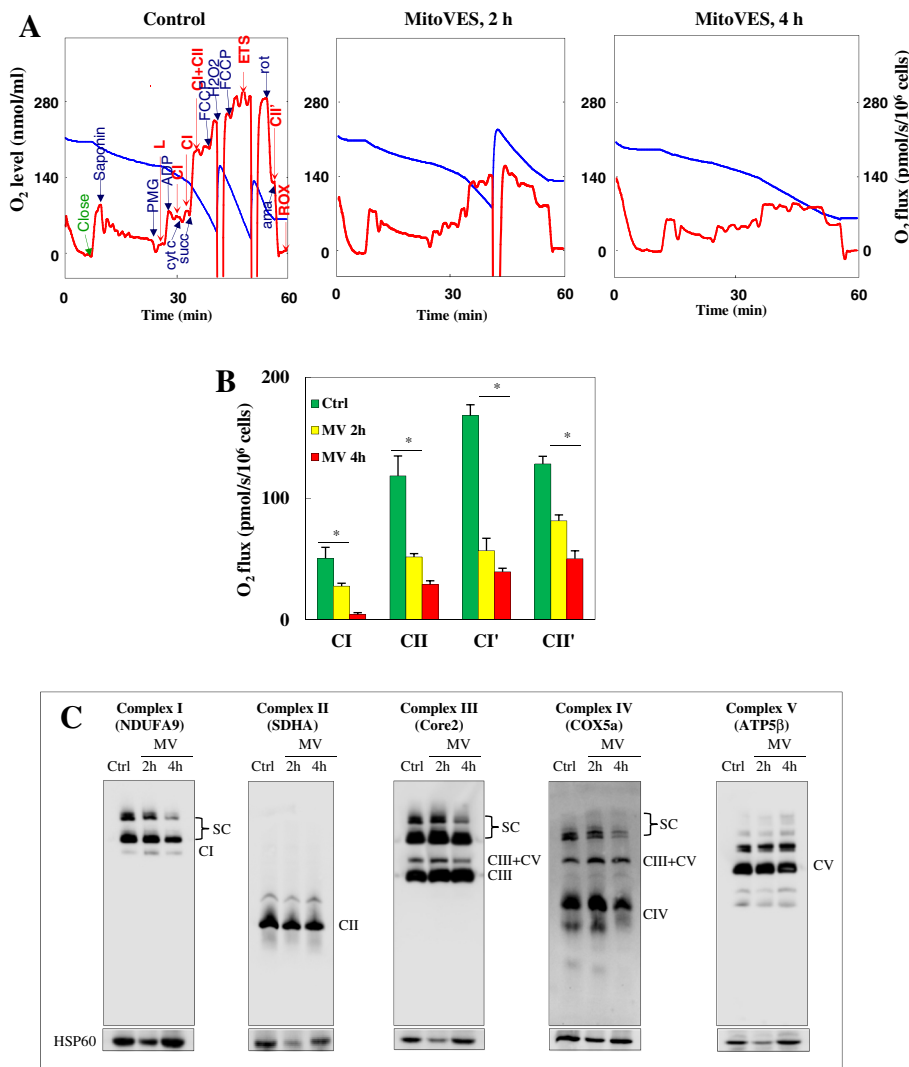


Fig. 4 MitoVES affects mitochondrial complexes. **(A)** NeuTL spheres were treated with 2 μ M MitoVE for and 4 h, before they were harvested, permeabilised with saponin and evaluated for respiration at the presence of substrates specific for CI and CII using the protocol indicated in more detail in Materials and Methods. The abbreviations in the top left line graph are: L, leak; CI, complex I; CII, complex II; ETS, electron transfer system (uncoupled respiration); CI', uncoupled respiration via CI; ROX, residual respiration; PMG, pyruvate, malate and glutamate; cyt c, cytochrome c; succ, succinate; F, FCCP; rot, rotenone; ama, antimycin A. **(B)** The respiration via CI and CII, and the uncoupled respiration via CI (CI') and CII (CII') as derived from results shown in panel A is documented in control cells and cells exposed to 10 μ M MitoVES for 2 and 4 h. **(C)** The mitochondrial fraction, prepared from control NeuTL cells or cells exposed to 10 μ M MitoVES for 2 and 4 h, was lysed in the presence of digitonin and subjected to native blue gel electrophoresis as detailed in Materials and Methods. Specific subunits of individual complexes were detected using the antibodies as shown. HSP60 was used as a loading control. The symbol * in panels indicates statistically significant differences ($p < 0.05$) for the respiration after cells were exposed to MitoVES

and MCF7 spheres documented by expression of specific markers [7, 30-34] is consistent with our recent results using microarray chip approach [35]. Additional evidence for the plausibility of spheres as a TIC model is documented by their higher tumour-initiating/propagating efficacy [7]. Furthermore, the 'sphere' TICs were found resistant to established, first line breast cancer therapeutics, which more efficiently killed adherent breast cancer cells, in line with the notion of general recalcitrant nature of TICs [12, 36, 37].

However, we found that breast TICs are killed more efficiently by the mitocan MitoVES that by pathenolide, an agent that was shown to cause death of TICs [38, 39]. MitoVES accumulates in mitochondria on the basis of high $\Delta\Psi_{m,i}$ due to the presence of the TPP⁺ group [10, 11, 40], and this is consistent with the notion of higher $\Delta\Psi_{m,i}$ in stem cells [41]. MitoVES inhibits the respiration of breast TICs via mitochondrial CI and, even more, CII, causing the generation of ROS, which leads to apoptosis of these cells. The assembly of mitochondrial

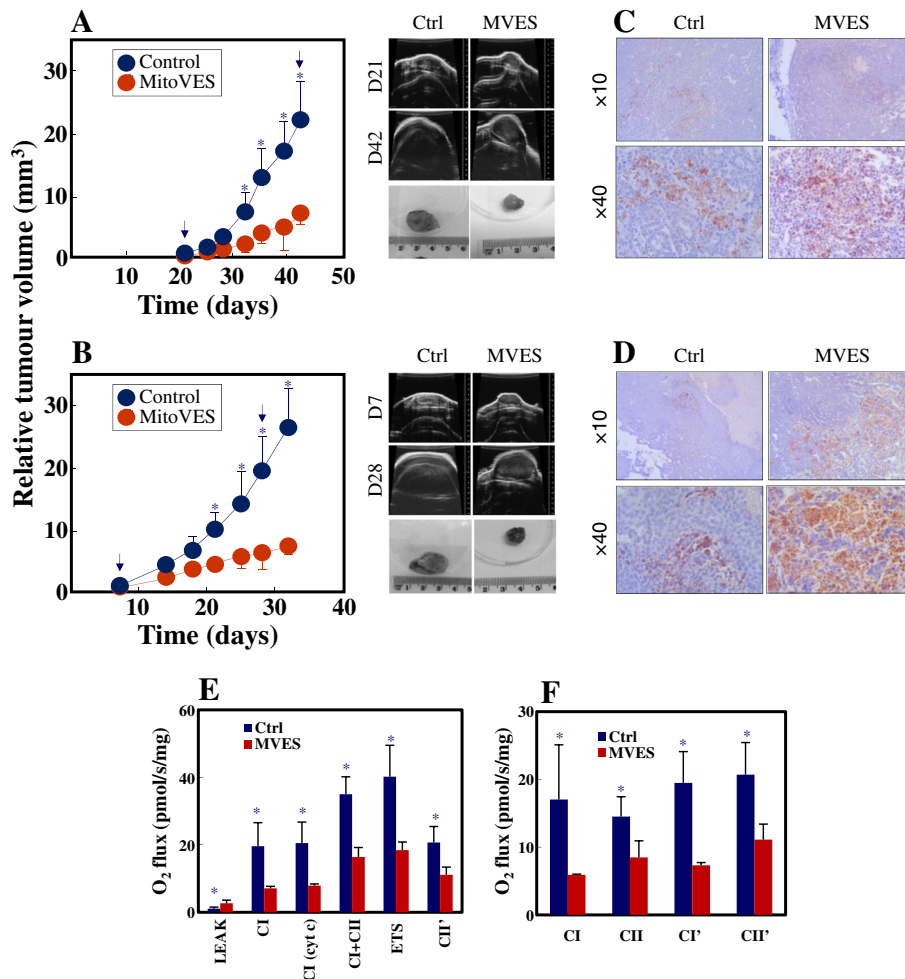
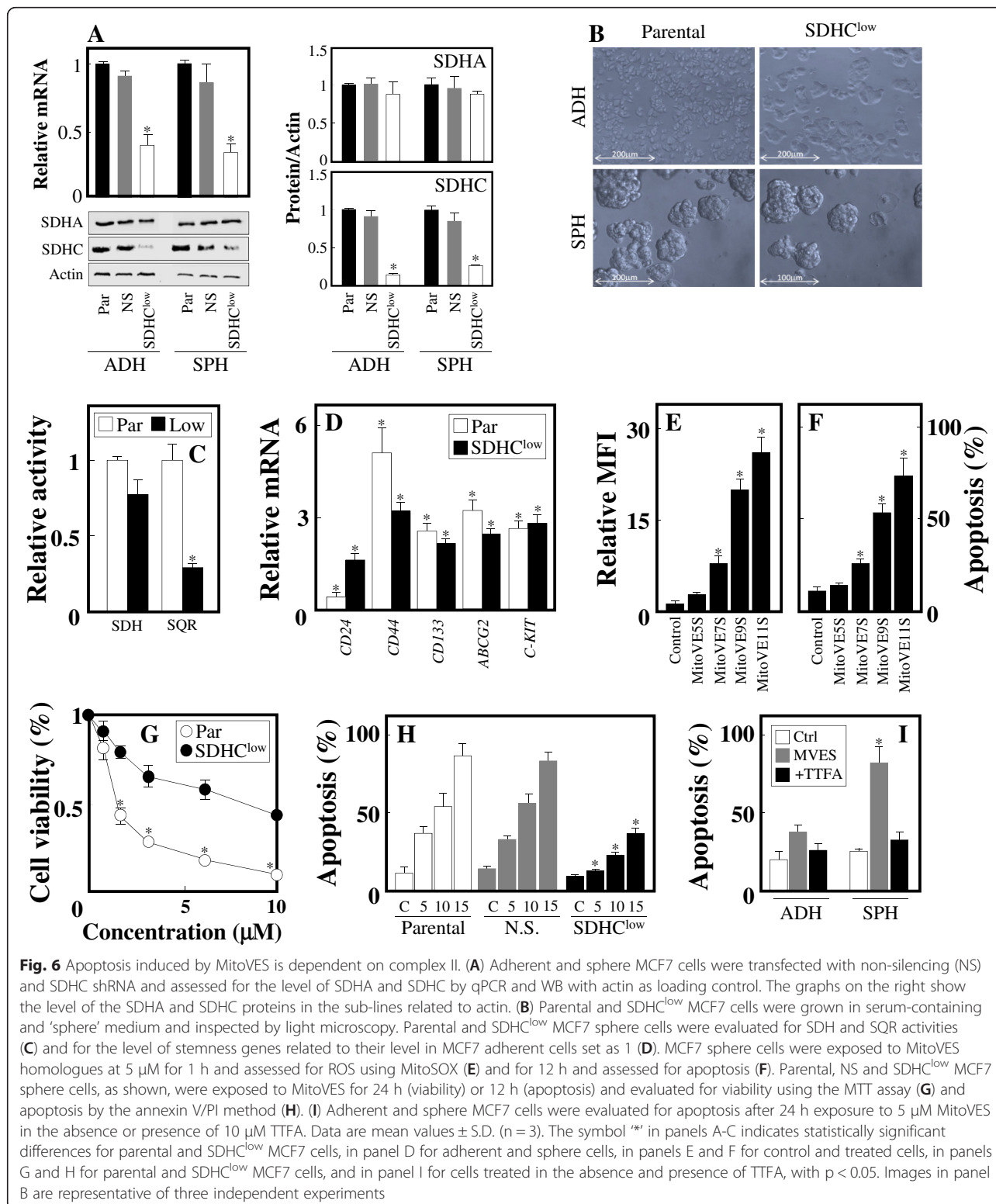


Fig. 5 MitoVES suppresses tumour progression. NeuTL adherent (A) and sphere cells (B) were grafted s.c. in FVB/N c-neu mice (10^6 cells per animal) and tumour volume assessed in control and MitoVES-treated animals using USI. The images on the right are representative USI scans of tumours taken on the given days (indicated by arrows in the graph on the left), the images on the right also show representative tumours excised from mice at the end of the experiment. Tumours derived from adherent (C) and sphere NeuTL cells (D) were paraffin-embedded, sectioned and probed by IHC for cleaved caspase-3. Tumour tissue was shredded and oxygen consumption evaluated using oxygraph. The respiration via mitochondrial complexes was assessed and calculated (E, F). Data are mean values \pm S.D. (n = 3). The symbol '*' in panels A and B indicates statistically significant differences in the volume of control and MitoVES-treated tumours with $p < 0.05$. Images in panels C and D are representative of three independent experiments. The symbol '*' in panel F and G indicates statistically significant differences in the respiration levels of control and MitoVES-treated tumours with $p < 0.05$

supercomplexes was inhibited, to some extent, as well. MitoVES also suppressed progression of tumours derived from both adherent and sphere cells, with similar efficacy. The likely reason for this is that, when grafted, TICs differentiate within the tumour microenvironment into fast-proliferating tumour cells [28]. In tumour tissue, inhibition of cell respiration and induction of apoptosis were also documented. Using the syngeneic FVB/N c-neu mouse model, the drug effect against erbB2^{high} breast tumour was investigated under conditions of functional immune system.

Of interest is the mechanism by which MitoVES kills breast TICs. Our previous data document that the

mitochondrially targeted agent, similarly as the untargeted α -TOS, acts via interacting with the UbQ site of CII [17-20]. That MitoVES acts also by targeting the UbQ site in CII of breast TICs was first indicated by experiments, in which shorter homologues of full length MitoVES (11 carbons in the aliphatic chain linking the tocopheryl succinyl and TPP⁺ groups) were correspondingly less efficient in ROS generation and apoptosis induction. Our recent molecular modelling indicates that this linker has to be of certain length so that the biologically active moiety of MitoVES can reach the UbQ site of CII buried in the inner mitochondrial membrane; the reason being that the TPP⁺ group anchors the



positively charged end of the molecule at the matrix face of the inner mitochondrial membrane [19, 20]. Importantly, spheres derived from MCF7 cells with knocked down SDHC, lacking the UbQ site, were resistant to

MitoVES treatment. Further, we show that the presence of TTFA, a small molecule that is known to bind to CII's UbQ site [42], prevented the killing activity of MitoVES in sphere cells. Collectively, our data convincingly document

that MitoVES targets the UbQ site in CII to efficiently kill breast TICs, and are consistent with the notion of CII as an intriguing, novel target for anti-cancer agents [43]. Importantly, subunits of CII only rarely mutate, such that their mutational frequency is high in neoplasias like familial paraganglioma, but only one in one million breast cancer patients features a CII mutation [44].

Thus, we document a high killing activity of MitoVES towards breast cancer TICs that are resistant to several established anti-cancer agents. While our findings are of translational significance, we also, for the first time, document a link between mitochondrial complex II and killing of tumour-initiating cells. The combination therapy of MitoVES which effectively kills breast TICs and established anti-cancer drugs targeting highly proliferating cells may lead to a better tumour suppression results, which will be further investigated in our future research.

Conclusions

In this project, mammosphere models for studying breast TICs were established and verified. These cells featured altered mitochondrial function. A mitochondrially targeted anti-cancer compound, mitocan, epitomised by mitochondrially targeted vitamin E succinate (MitoVES), was found very efficient in killing TICs, which has a potential translational relevance. Additional studies are needed to explore the clinical value of our study for using MitoVES as an agent that can potentially eradicate cancer stem-like cells alone or in combination with other anti-cancer drugs.

Additional file

Additional file 1: Primers used for qPCR analyses.

Abbreviations

ADH: Adherent; CI: Complex I; CII: Complex II; DCF: Dichlorofluorescein diacetate; H & E: Haematoxylin & eosin; IHC: Immunohistochemistry; MitoVES: Mitochondrially targeted vitamin E succinate; PI: Propidium iodide; ROS: Reactive oxygen species; SPH: Sphere; TICs: Tumour-initiating cells; α -TOS: α -tocopheryl succinate; TMRM: Tetramethylrhodamine methyl ester; TPPP⁺: Triphenylphosphonium; TFFA: Thenoyltrifluoroacetate; UbQ: Ubiquinone; USI: Ultrasound imaging.

Competing interests

The authors declare that they have no competing interests.

Authors' contributions

BY conducted experiments, interpreted the data and wrote the manuscript, MS, RZ, AB, MS and KP conducted experiments, JS synthesised MitoVES, LFD conducted experiments, conceived the study, interpreted data and wrote the manuscript, JN conceived the study, supervised it and wrote the manuscript. All authors read and approved the final manuscript.

Acknowledgements

This work was supported in part by funding from the National Health and Medical Research Council of Australia and Cancer Council Queensland to J.N. and L.F.D., and IGA (NT14078) to J.N., and by the BIOCEV European Regional Development Fund CZ.1.05/1.1.00/02.0109. B.Y. was supported by Griffith University International PhD Scholarship.

Author details

¹School of Medical Science, Griffith University, Southport, Qld, 4222, Australia. ²The Department of Chemistry of Natural Compounds, University of Chemistry and Technology, Prague, Czech Republic. ³Institute of Biotechnology, Academy of Sciences of the Czech Republic, Prague 142 20, Czech Republic.

Received: 8 January 2015 Accepted: 29 April 2015

Published online: 13 May 2015

References

- DeSantis CE, Lin CC, Mariotto AB, Siegel RL, Stein KD, Kramer JL, et al. Cancer treatment and survivorship statistics, 2014. *CA Cancer J Clin.* 2014;64:252–71.
- DeSantis C, Ma J, Bryan L, Jemal A. Breast cancer statistics, 2013. *CA Cancer J Clin.* 2014;64:52–62.
- Kakarala M, Wicha MS. Implications of the cancer stem-cell hypothesis for breast cancer prevention and therapy. *J Clin Oncol.* 2008;26:2813–20.
- Velasco-Velázquez MA, Homsí N, De La Fuente M, Pestell RG. Breast cancer stem cells. *Int J Biochem Cell Biol.* 2012;44:573–7.
- Kute T, Lack CM, Willingham M, Bishwokama B, Williams H, Barrett K, et al. Development of Herceptin resistance in breast cancer cells. *Cytometry.* 2004;57A:86–93.
- Reya T, Morrison SJ, Clarke MF, Weissman IL. Stem cells, cancer, and cancer stem cells. *Nature.* 2001;414:105–11.
- Wicha MS, Liu S, Dontu G. Cancer stem cells: an old idea—a paradigm shift. *Cancer Res.* 2006;66:1883–90.
- Al-Hajj M, Wicha MS, Benito-Hernandez A, Morrison SJ, Clarke MF. Prospective identification of tumorigenic breast cancer cells. *Proc Natl Acad Sci USA.* 2003;100:3983–8.
- Bonnet D, Dick JE. Human acute myeloid leukemia is organized as a hierarchy that originates from a primitive hematopoietic cell. *Nat Med.* 1997;3:730–7.
- Singh SK, Clarke ID, Terasaki M, Bonn VE, Hawkins C, Squire J, et al. Identification of a cancer stem cell in human brain tumors. *Cancer Res.* 2003;63:5821–8.
- Kim CF, Jackson EL, Woolfenden AE, Lawrence S, Babar I, Vogel S, et al. Identification of bronchioalveolar stem cells in normal lung and lung cancer. *Cell.* 2005;121:823–35.
- Takaishi S, Okumura T, Tu S, Wang SS, Shibata W, Vigneshwaran R, et al. Identification of gastric cancer stem cells using the cell surface marker CD44. *Stem Cells.* 2009;27:1006–20.
- Boman BM, Wicha MS. Cancer stem cells: a step toward the cure. *J Clin Oncol.* 2008;26:2795–9.
- Zhou BB, Zhang H, Damelin M, Geles KG, Grindley JC, Dirks PB. Tumour-initiating cells: challenges and opportunities for anticancer drug discovery. *Nat Rev Drug Discov.* 2009;8:806–23.
- Morrison BJ, Andera L, Reynolds BA, Ralph SJ, Neuzil J. Future use of mitocans against tumour-initiating cells? *Mol Nutr Food Res.* 2009;53:147–53.
- Neuzil J, Dong LF, Rohlena J, Truksa J, Ralph SJ. Classification of mitocans, anti-cancer drugs acting on mitochondria. *Mitochondrion.* 2013;13:199–208.
- Dong LF, Low P, Dyason JC, Wang XF, Prochazka L, Witting PK, et al. α -Tocopheryl succinate induces apoptosis by targeting ubiquinone-binding sites in mitochondrial respiratory complex II. *Oncogene.* 2008;27:4324–35.
- Dong LF, Freeman R, Liu J, Zabalova R, Marin-Hernandez A, Stantic M, et al. Suppression of tumor growth in vivo by the mitocan α -tocopheryl succinate requires respiratory complex II. *Clin Cancer Res.* 2009;15:1593–600.
- Dong LF, Jameson VJ, Tilly D, Cerny J, Mahdavian E, Marin-Hernandez A, et al. Mitochondrial targeting of vitamin E succinate enhances its pro-apoptotic and anti-cancer activity via mitochondrial complex II. *J Biol Chem.* 2011;286:3717–28.
- Dong L-F, Jameson VJA, Tilly D, Prochazka L, Rohlena J, Valis K, et al. Mitochondrial targeting of α -tocopheryl succinate enhances its pro-apoptotic efficacy: A new paradigm for effective cancer therapy. *Free Radic Biol Med.* 2011;50:1546–55.
- Neuzil J, Weber T, Gellert N, Weber C. Selective cancer cell killing by α -tocopheryl succinate. *Brit J Cancer.* 2001;84:87–9.
- Ye XQ, Li Q, Wang GH, Sun FF, Huang GJ, Bian XW, et al. Mitochondrial and energy metabolism-related properties as novel indicators of lung cancer stem cells. *Int J Cancer.* 2011;129:820–31.

23. Guy CT, Webster MA, Schaller M, Parsons TJ, Cardiff RD, Muller WJ. Expression of the neu protooncogene in the mammary epithelium of transgenic mice induces metastatic disease. *Proc Natl Acad Sci USA*. 1992;89:10578–82.
24. Gnaiger E, Steinlechner-Maran R, Méndez G, Eberl T, Margreiter R. Control of mitochondrial and cellular respiration by oxygen. *J Bioenerg Biomembr*. 1995;27:583–96.
25. Weiss S, Dunne C, Hewson J, Wohl C, Wheatley M, Peterson AC, et al. Multipotent CNS stem cells are present in the adult mammalian spinal cord and ventricular neuroaxis. *J Neurosci*. 1996;16:7599–609.
26. Reynolds BA, Weiss S. Generation of neurons and astrocytes from isolated cells of the adult mammalian central nervous system. *Science*. 1992;255:1707–10.
27. Ponti D, Costa A, Zaffaroni N, Pratesi G, Petrangolini G, Coradini D, et al. Isolation and in vitro propagation of tumorigenic breast cancer cells with stem/progenitor cell properties. *Cancer Res*. 2005;65:5506–11.
28. Ricci-Vitiani L, Lombardi DG, Pilozzi E, Biffoni M, Todaro M, Peschle C, et al. Identification and expansion of human colon-cancer-initiating cells. *Nature*. 2007;445:111–5.
29. Zhou ZH, Ping YF, Yu SC, Yi L, Yao XH, Chen JH, et al. A novel approach to the identification and enrichment of cancer stem cells from a cultured human glioma cell line. *Cancer Lett*. 2009;281:92–9.
30. Shackleton M, Vaillant F, Simpson KJ, Stingl J, Smyth GK, Asselin-Labat ML, et al. Generation of a functional mammary gland from a single stem cell. *Nature*. 2006;439:84–8.
31. Ginestier C, Hur MH, Charafe-Jauffret E, Monville F, Dutcher J, Brown M, et al. ALDH1 is a marker of normal and malignant human mammary stem cells and a predictor of poor clinical outcome. *Cell Stem Cell*. 2007;1:555–67.
32. Cariati M, Naderi A, Brown JP, Smalley MJ, Pinder SE, Caldas C, et al. Alpha-6 integrin is necessary for the tumorigenicity of a stem cell-like subpopulation within the MCF7 breast cancer cell line. *Int J Cancer*. 2008;122:298–304.
33. Wright MH, Calcagno AM, Salcido CD, Carlson MD, Ambudkar SV, Varticovski L. Brca1 breast tumors contain distinct CD44⁺/CD24⁻ and CD133⁺ cells with cancer stem cell characteristics. *Breast Cancer Res*. 2008;10:R10.
34. Vaillant F, Asselin-Labat ML, Shackleton M, Forrest NC, Lindeman GJ, Visvader JE. The mammary progenitor marker CD61/3 integrin identifies cancer stem cells in mouse models of mammary tumorigenesis. *Cancer Res*. 2008;68:7711–7.
35. Stapelberg M, Zobalova R, Nguyen M, Walker T, Stantic M, Goodwin J, et al. Indoleamine-2,3-dioxygenase elevated in tumor-initiating cells is suppressed by mitocans. *Free Radic Biol Med*. 2014;67:41–50.
36. Kvinlaug BT, Huntly BJ. Targeting cancer stem cells. *Expert Opin Ther Targets*. 2007;11:915–27.
37. Bansal N, Banerjee D. Tumor initiating cells. *Curr Pharm Biotechnol*. 2009;10:192–6.
38. Guzman ML, Rossi RM, Karnischky L, Li X, Peterson DR, Howard DS, et al. The sesquiterpene lactone parthenolide induces apoptosis of human acute myelogenous leukemia stem and progenitor cells. *Blood*. 2005;105:4163–9.
39. Zhou J, Zhang H, Gu P, Bai J, Margolick JB, Zhang Y. NF-κB pathway inhibitors preferentially inhibit breast cancer stem-like cells. *Breast Cancer Res Treat*. 2008;111:419–27.
40. Smith RA, Hartley RC, Murphy MP. Mitochondria-targeted small molecule therapeutics and probes. *Antiox Redox Signal*. 2011;15:3021–38.
41. Ye XQ, Wang GH, Huang GJ, Bian XW, Qian GS, Yu SC. Heterogeneity of mitochondrial membrane potential: a novel tool to isolate and identify cancer stem cells from a tumor mass? *Stem Cell Rev*. 2011;7:153–60.
42. Sun F, Huo X, Zhai Y, Wang A, Xu J, Su D, et al. Crystal structure of mitochondrial respiratory membrane protein complex II. *Cell*. 2005;121:1043–57.
43. Kluckova K, Bezework-Goleta A, Rohlena J, Dong LF, Neuzil J. Mitochondrial complex II, a novel intriguing target for anti-cancer agents. *Biochim Biophys Acta*. 1827;2013:552–64.
44. Peczkowska M, Cascon A, Prejbisz A, Kubaszek A, Cwikla BJ, Furmanek M, et al. Extra-adrenal and adrenal pheochromocytomas associated with a germline SDHC mutation. *Nat Clin Pract Endocrinol Metab*. 2008;4:111–5.

Submit your next manuscript to BioMed Central and take full advantage of:

- Convenient online submission
- Thorough peer review
- No space constraints or color figure charges
- Immediate publication on acceptance
- Inclusion in PubMed, CAS, Scopus and Google Scholar
- Research which is freely available for redistribution

Submit your manuscript at
www.biomedcentral.com/submit





Original Contributions

Indoleamine-2,3-dioxygenase elevated in tumor-initiating cells is suppressed by mitocans



Michael Stapelberg^{a,*}, Renata Zobalova^{a,b,1}, Maria Nga Nguyen^a, Tom Walker^{a,c}, Marina Stantic^a, Jacob Goodwin^a, Elham Alizadeh Pasdar^a, Thuan Thai^d, Katerina Prokopova^{b,e}, Bing Yan^a, Susan Hall^f, Nicholas de Pennington^c, Shane R. Thomas^d, Gary Grant^f, Jan Stursa^{a,g}, Martina Bajzikova^b, Adrian C.B. Meedeniya^a, Jaroslav Truksa^b, Stephen J. Ralph^a, Olaf Ansorge^c, Lan-Feng Dong^a, Jiri Neuzil^{a,b,**}

^a School of Medical Science, Griffith Health Institute, Griffith University, Southport, 4222 QLD, Australia

^b Institute of Biotechnology, Academy of Sciences of the Czech Republic, Prague 142 20, Czech Republic

^c Department of Neurosurgery, John Radcliffe Hospital, Oxford OX3 9DU, UK

^d Centre for Vascular Research, School of Medical Sciences, University of New South Wales, Sydney, 2052 NSW, Australia

^e Faculty of Science, Charles University, 11000 Prague 1, Czech Republic

^f School of Pharmacy, Griffith Health Institute, Griffith University, Southport, 4222 QLD, Australia

^g Institute of Organic Chemistry and Biochemistry, Academy of Sciences of the Czech Republic, Prague 160 00, Czech Republic

ARTICLE INFO

Article history:

Received 26 May 2013

Received in revised form

2 October 2013

Accepted 2 October 2013

Available online 18 October 2013

Keywords:

IDO

Tumor-initiating cells

Mitocans

Mitochondrially targeted vitamin E succinate

succinate

Free radicals

ABSTRACT

Tumor-initiating cells (TICs) often survive therapy and give rise to second-line tumors. We tested the plausibility of sphere cultures as models of TICs. Microarray data and microRNA data analysis confirmed the validity of spheres as models of TICs for breast and prostate cancer as well as mesothelioma cell lines. Microarray data analysis revealed the Trp pathway as the only pathway upregulated significantly in all types of studied TICs, with increased levels of indoleamine-2,3-dioxygenase-1 (IDO1), the rate-limiting enzyme of Trp metabolism along the kynurenine pathway. All types of TICs also expressed higher levels of the Trp uptake system consisting of CD98 and LAT1 with functional consequences. IDO1 expression was regulated via both transcriptional and posttranscriptional mechanisms, depending on the cancer type. Serial transplantation of TICs in mice resulted in gradually increased IDO1. Mitocans, represented by α -tocopheryl succinate and mitochondrially targeted vitamin E succinate (MitoVES), suppressed IDO1 in TICs. MitoVES suppressed IDO1 in TICs with functional mitochondrial complex II, involving transcriptional and posttranscriptional mechanisms. IDO1 increase and its suppression by VE analogues were replicated in TICs from primary human glioblastomas. Our work indicates that IDO1 is increased in TICs and that mitocans suppress the protein.

© 2013 Elsevier Inc. All rights reserved.

Abbreviations: CHIP, chromatin immunoprecipitation; CII, mitochondrial complex II; EMT, epithelial–mesenchymal transition; ESC, embryonal stem cell; G1, generation 1; GBM, glioblastoma multiforme; HSC, hematopoietic stem cell; IDO, indoleamine-2,3-dioxygenase; LEG, leading-edge gene; miRNA, microRNA; MitoVES, mitochondrially targeted vitamin E succinate; NS, nonsilencing; NSC, neuronal stem cell; RNAi, RNA interference; RNAPOL2, RNA polymerase 2; ROS, reactive oxygen species; SDHC, succinate dehydrogenase subunit C; TF, transcription factor; TIC, tumor-initiating cell; SQR, succinate quinone reductase; α -TOS, α -tocopheryl succinate; USI, ultrasound imaging

* Corresponding author. Fax: +61 2 555 28444.

** Corresponding author at: Griffith University, School of Medical Science and Griffith Health Institute, Parklands Drive, Southport, Queensland 4222, Australia. Fax: +61 2 555 28444.

E-mail addresses: pfm.stapelberg@gmail.com (M. Stapelberg), j.neuzil@griffith.edu.au (J. Neuzil).

¹ These authors contributed equally to this work.

Despite advances in cancer research, neoplastic disease is on the rise [1], one reason being the nature of the tumor environment [2], including the existence of a subpopulation of tumor-initiating cells (TICs)² and their resistance to therapy [3,4]. TICs are “dormant” cells that feature a high level of “stemness” and the propensity to survive for long periods in their niche to give rise to second-line tumors/metastases [5,6]. Therefore, TICs ought to be able to escape tumor surveillance, a process that is not well understood thus far [7], albeit having been relatively well defined for “normal” (non-stem-like) cancer cells [8,9], termed as the “three E’s” (elimination, equilibrium, escape) of tumor immune surveillance [10].

The mechanism for how TICs can escape tumor surveillance may be deduced from what is known about non-stem-like cancer cells [7–9]. The most important denominator of immune tolerance for tumor cells are T lymphocytes that have tumor-killing or -protecting

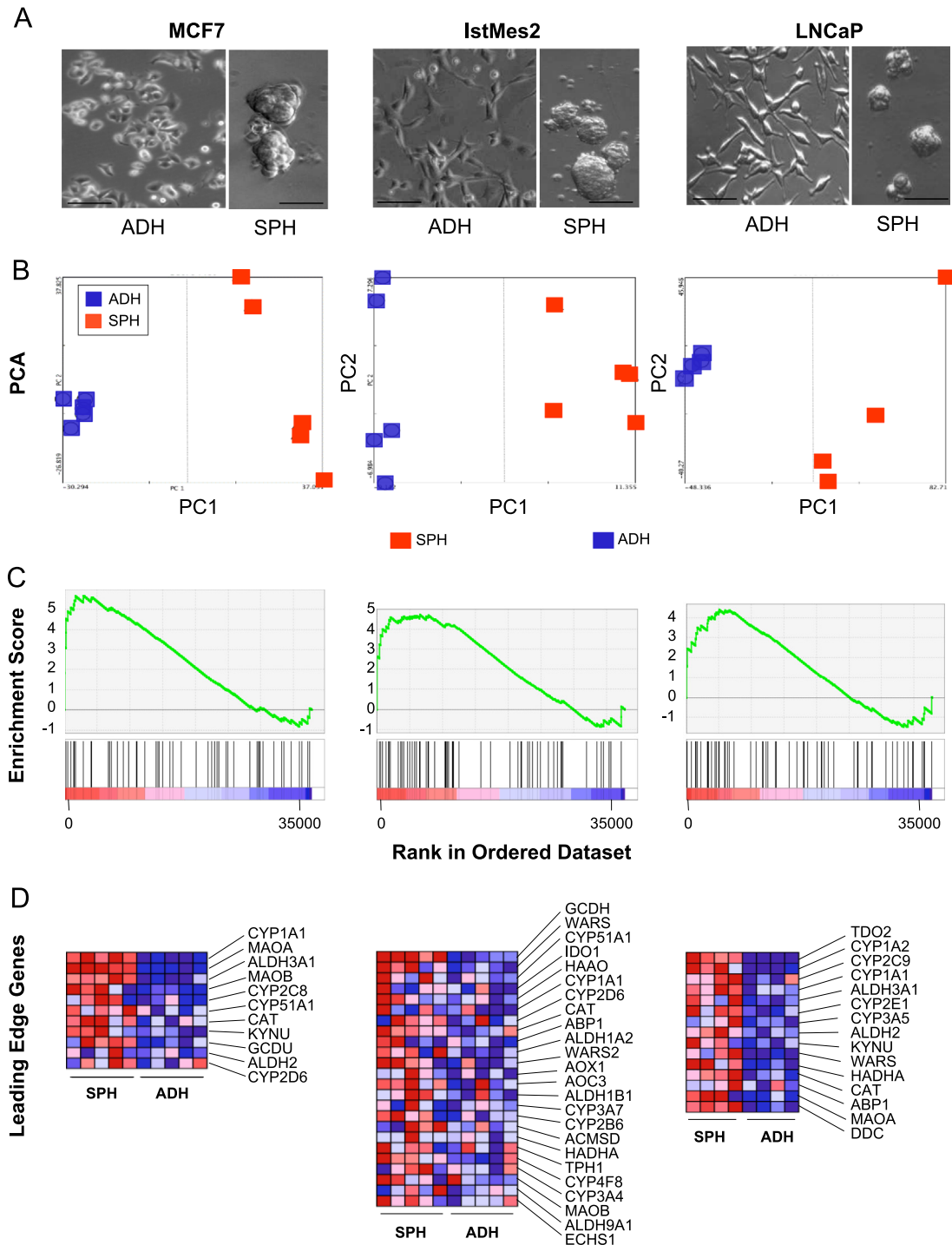


Fig. 1. Microarray analysis documents Trp metabolism increase in TICs. (A) Representative images of adherent and sphere MCF7, IstMes2, and LNCaP cells. (B) PCA of the adherent and sphere cultures of MCF7, IstMes2, and LNCaP cells. (C) GSEA for the Trp pathway in the adherent and sphere cells. (D) LEGs of the Trp pathway; red refers to high and blue to low expression. Detailed description of the analysis is under Materials and methods. Scale bar 50 micrometers (μm).

activity depending on their type in the tumor microenvironment [11,12]. One way by which cancer cells escape the immune system is to increase Trp metabolism mediated by the rate-limiting enzyme indoleamine-2,3-dioxygenase (IDO) [13,14]. This results in the depletion of this essential amino acid from the tumor interstitium, which suppresses cytotoxic T cells and results in naïve T cells maturing into Treg cells [15,16]. Thus, suppression of IDO1 using small molecules has an anti-tumor effect, because it makes cancer cells more susceptible to killing by cells of the immune system [17–19].

Escape from tumor surveillance is inherent to TICs and presents a problem for therapy [20–23]. One reason is that during the development and maturation of TICs in the context of the immune system, the cells develop resistance to killing via the death receptor pathway [7,8]. It is also possible that TICs feature higher levels of Trp metabolism to minimize their vulnerability to the immune system, although this paradigm has not been well characterized thus far [23,24].

In this communication, we report that TICs derived from three different cancer cell lines and from primary glioblastoma

multiforme (GBM) patient biopsies feature higher levels of increased IDO1 expression, using sphere cultures of established and primary cell lines as a model system for stem cell studies, in line with the literature [25,26]. Furthermore, we show that increase in IDO1 can be reversed by agents from the group of mitocans, small molecules with anti-cancer properties acting on mitochondria [27].

Materials and methods

Cell culture

MCF7 and LNCaP cells were obtained from the ATCC and IstMes2 cells from a mesothelioma patient (Torino University Hospital, Italy; epithelial histotype). Primary GBM cells were isolated from biopsies obtained from two patients (B30 and B31; Department of Neurosurgery, John Radcliffe Hospital, Oxford, UK). MCF7, IstMes2, B30, and B31 cells were grown in the Dulbecco's modified Eagle's medium (DMEM), supplemented with 10% fetal bovine serum (FBS), 1% antimycotics and antibiotics, and maintained at 37 °C and 5% CO₂. LNCaP cells were maintained under the same conditions in RPMI 1640 medium supplemented with 10% FBS, 1% antimycotics and antibiotics. MCF7, IstMes2, and LNCaP spheres were cultured in DMEM-F12 medium, with added Neurocult Neural Stem Cell Proliferation Supplement (Stem Cell Technologies), 20 ng/ml rhEGF, 10 ng/ml rhFGF (both Sigma), and 1% antibiotics, and maintained at 37 °C and 5% CO₂. Adherent and sphere cells were treated with 5 μM mitochondrially targeted vitamin E succinate (MitoVES) [28] or 50 μM α-tocopheryl succinate (α-TOS; Sigma), both dissolved in ethanol, for 3 and 6 h, unless specified otherwise.

Gene microarray analysis

Preprocessing, normalization, and principal components analysis (PCA)

The first component of the microarray analysis used the software package BeadStudio to extract the raw expression data. Preprocessing of microarray data was then done using the R software package Linear Models for Microarray Data (LIMMA) [29]. The "normexp" function was used for control background correction, quantile normalization, and log₂ transformation of the raw data [30].

To assess global expression in adherent cells and spheres, we used PCA in the ArrayTrack software environment [31]. PCA uses a mathematical algorithm that reduces the dimensionality of the microarray data while retaining the variation in the data. It reduces the dimensionality by identifying directions, called principal components, along which the variation in the data is maximal [32]. The global gene expression of adherent cells and spheres can then be plotted, making it possible to visually assess similarities and differences between samples.

Gene set enrichment analysis (GSEA)

GSEA was used to assess for stemness in spheres compared to adherent cells. Hematopoietic (HSC), embryonal (ESC) and neural (NSC) stem cell gene sets were derived from an overlap of stemness genes characterized in several microarray studies [33–35] (Fig. 1). To determine the enrichment of HSC, ESC, and NSC gene sets in spheres, all genes expressed on the microarrays were analyzed using GSEA [36]. GSEA was used to assess for stemness by determining whether HSC, ESC, and NSC gene sets were significantly enriched in spheres compared to adherent cells. GSEA was also used to characterize metabolic and signaling pathways enriched in spheres. Pathway analysis of the expression data was

performed using the GSEA implemented in the GSEA Java desktop application version 2.0 and MSigDB (Molecular Signature Database) version 2.0. Pathways derived from the MSigDB on the GSEA Web site were used to assess enrichment in both adherent cells and spheres. GSEA was performed using a total of 880 gene sets containing genes whose products are involved in specific metabolic and signaling pathways. For this study the top 10 up- and downregulated pathways in spheres with a significant enrichment score ($p < 0.05$) and false discovery rate (FDR) ($q < 0.05$) were considered for further interpretation.

The statistical significance (p value) of each gene set was estimated by using phenotype-based permutation analysis using 1000 random permutations. We accepted gene sets with a significant enrichment score (ES) ($p < 0.05$) adjusted for multiple comparisons using the FDR of $q < 0.05$ or very close to $q < 0.05$ for further interpretation. The FDR is a quantity that describes, for a set of tests that are called significant at or above a given level, what proportions are likely to be false positives [37]. Each of the enriched gene sets contained leading edge genes (LEGs). These genes contribute most to the enrichment score of the gene set and therefore are likely to participate in a biological response. We used the default setting signal-to-noise metric ranking in GSEA to rank genes. In this case, LEGs of enriched gene sets are those whose expression correlates with a given phenotype assignment, hence upregulation if $ES > 0$ and downregulation if $ES < 0$. The strength of GSEA and its application to microarray data is that multiple genes belonging to particular gene sets, which are defined based on prior biological knowledge (e.g., genes encoding products in a metabolic pathway, located in the same cytogenetic band, or sharing the same GO category), rather than individual genes, are used to assess for coordinate gene expression between two conditions of interest, bridging microarray data with biological significance.

MicroRNA target prediction and quantitative RT-PCR (qPCR)

MiRNA target predictions for IDO1 were generated using microRNA.org (<http://www.microrna.org>). Briefly, target predictions are performed using the miRanda algorithm, which matches complementarity between miRNAs and a candidate mRNA sequence. The miRNA target sites predicted by miRanda are scored for likelihood of mRNA downregulation using a mirSVR score. We accepted only < iR targets with a mirSVR score of less than -1.0, as scores closer to 0 have a much lower probability of meaningful downregulation of a candidate mRNA. Furthermore, to filter out less-conserved predicted target sites, we used only predicted miRNAs with the highest PhastCons conservation score. The miRNA/IDO1 alignments for these miRNAs derived from microRNA.org are shown in Supplementary Fig. S3A.

Total RNA for miRNA arrays was obtained from MCF7, LNCaP, IstMes2, and GBM adherent cells, spheres, and treated spheres using the miRNeasy Mini Kit (Qiagen). The purified miRNA was reverse transcribed using the RT2 miRNA First Strand Kit (Qiagen). Human miRNome RT2 miRNA PCR arrays were then used to detect the expression of miRNA target predictions for IDO1 using the RT2 SYBR Green ROX qPCR master mix (Qiagen) on an ABI 7900 real-time PCR instrument.

qPCR

RNA was obtained from MCF7, LNCaP, IstMes2, and primary GBM adherent cells, spheres, and treated spheres using the RNeasy Mini Kit. The SuperScript III First-Strand Synthesis System along with random hexamer primers (Life Technologies) were used to reverse transcribe total RNA into cDNA. Custom primers specific for stemness and Trp metabolism genes from the microarray data

were designed using the PCR simulation program Primer3 (Whitehead Institute for Biomedical Research) and the NCBI Primer Design. BLASTN searches confirmed the total gene specificity of the nucleotide sequences chosen for the primers. Primers were then assessed with $2 \times$ Platinum SYBR Green qPCR SuperMix-UDG (Life Technologies) using the Eco qPCR System (Illumina). Each experiment was repeated three times using three biological replicates for each adherent cell, sphere, and α -TOS- and MitoVES-treated sphere groups. Data obtained from the three replicate values were pooled. For each qPCR experiment, the adherent and sphere groups were normalized to the housekeeping gene GAPDH. The change in gene expression was determined using the $\Delta\Delta C_t$ method [38]. For statistical analysis unpaired Student's *t* test was used with $p < 0.05$ compared to the adherent cells being regarded as significant.

Chromatin immunoprecipitation (ChIP) assay

MCF7, IstMes2, LNCaP, and primary GBM adherent cells, spheres, and MitoVES-treated spheres were washed with phosphate-buffered saline (PBS) and cross-linked for 10 min at room temperature in 1% formaldehyde. Cross-linking was stopped by adding 1.25 M glycine to the final concentration of 125 mM. Cells were then centrifuged at 300 g for 10 min at 4 °C and washed in cold PBS. ChIP was performed using the MAGnify Chromatin Immunoprecipitation System (Life Technologies) according to the manufacturer's protocol. Briefly, for each immunoprecipitation, 10^6 cells were lysed, releasing chromatin from the nuclei. Chromatin was then sheared to 200–500 bp fragments by sonication using a UP50H ultrasonic processor (Hielscher) for 25 cycles at 10-s intervals with 40% amplitude. The sheared, cross-linked protein–DNA fragments were then immunoprecipitated with RNA polymerase 2 (RNAPOL2) CTD phospho Ser5 IgG (Active Motif) and non-specific rabbit IgG (Life Technologies) conjugated to Dynabeads Protein A/G. The cross-linking was then reversed, and DNA associated with RNAPOL2 CTD phospho-Ser5 IgG and nonspecific rabbit IgG was isolated by DNA purification using magnetic beads. Finally, isolated DNA was analyzed by qPCR using a standard program with 35 cycles. The following primers were used: GAPDH, forward 5'-TGCACCACCAACTGCTTAGC-3', reverse 5'-GGCATGGAC TGTGGTCATGAG-3'; IDO1 transcription start site (TSS), forward 5'-GCACCAGAGGAGCAGACTACAA-3', reverse 3'-CAAAGCCCACTTCTT-CATCAATATG-5'; IDO1 exon 6, Qiagen manufactured human IDO1 primer Cat. No. 330001 (Qiagen); IDO1 exon 9, forward 5'-AGGCGGAGCTTGACAGTGA-3', reverse 5'-ACGGAGTCCCGCTCTTTA GC-3'. "Fold" enrichment was calculated as the level of the signal over the background. With this method, signals from the ChIP reactions were first divided by signals from the negative rabbit IgG control. This then represented the ChIP signal as the fold increase in the signal relative to the background signal. The ChIP signals were normalized to the housekeeping gene GAPDH using the $\Delta\Delta C_t$ method.

Enzyme-linked immunosorbent assay (ELISA)

The level of the IDO protein in MCF7, LNCaP, IstMes2, and primary GBM adherent cells, spheres, and α -TOS- and MitoVES-treated spheres was assessed using the ELISA kit for human IDO (E91547Hu; Uscn Life Science). Briefly, cells were lysed using whole-cell lysis buffer (9803; Cell Signaling), incubated in a pre-coated 96-well plate for 2 h at 37 °C, and incubated further with Detection Reagent A for 1 h at 37 °C. The wells were then washed and incubated with Detection Reagent B for 30 min at 37 °C, followed by incubation with the TMB substrate solution for 15–20 min at 37 °C. The reaction was stopped using the Stop solution

and the samples were immediately evaluated at 450 nm using a Tecan Infiniti microplate reader.

Western blotting (WB)

MCF7, LNCaP, IstMes2, and primary GBM cells, spheres, and α -TOS- and MitoVES-treated spheres were lysed using whole-cell lysis buffer (9803; Cell Signaling). Cell lysates were separated by SDS-PAGE and transferred to a nitrocellulose membrane, which was incubated with anti-IDO1 IgG (ab55305; Abcam) and anti-LAT1 IgG (5347; Cell Signaling). Anti-actin IgG (clone I-19; Santa Cruz Biotechnology) was used as a loading control. The blots were developed using the ECL kit (Pierce).

Immunocytostaining and flow cytometry

MCF7, LNCaP, IstMes2, and primary GBM adherent cells and spheres were harvested, washed with PBS, and incubated for 30 min at room temperature with neutral-buffered formalin (3.7% paraformaldehyde in PBS, pH 7.4). They were then incubated with anti-CD98 FITC-conjugated IgG1 (clone MEM-108; Exbio) for 60 min on ice. Finally, the cells were assessed by flow cytometry (FACSCalibur; Becton–Dickinson) for populations with high or low fluorescence.

Succinate quinone reductase (SQR) activity assay

The SQR activity of the mitochondrial complex II (CII) was assessed as detailed elsewhere [28] using parental MCF7 cells and MCF7 cells with dysfunctional CII due to low succinate dehydrogenase C (SDHC) (prepared by SDHC RNA interference, RNAi).

Trp uptake assay and HPLC analysis

Corresponding sphere and adherent cells were trypsinized and resuspended in Hanks' balanced salt solution, and 2.5×10^4 cells in 1 ml of buffer were seeded into individual tubes. The assay was initiated by the addition of a radiolabeled Trp cocktail such that the final concentration of radiolabeled L -Trp was 50 nM (1 μ Ci/ml) and of unlabeled L -Trp was 10 μ M. Cells were then incubated for 2–5 min at 37 °C, followed by rapid washing with ice-cold PBS. The cell pellets were lysed with 100% ethanol, the cell lysate was mixed with the scintillation fluid, and the level of radioactive L -Trp present was determined by liquid scintillation counting. L -[5- 3 H (N)]Trp with specific activity of 17.9 Ci/mmol was purchased from PerkinElmer.

The level of Trp in the medium conditioned with adherent and sphere cells was assessed by HPLC as follows. Adherent or sphere cells (10^6 cells per well) were seeded in six-well plates in 3 ml of medium. At 0 or 24 h, 100 μ l of the medium was mixed with 400 μ l of an acetonitrile/2-mercaptoethanol (10 ml/20 μ l) mixture, vortexed, and centrifuged at 12,000 g at 4 °C for 10 min. The supernatant was analyzed by HPLC using the Shimadzu Prominence system equipped with two pumps, a fluorescence detector, and a Phenomenex Gemini-NX C18 (3 μ m, 150 \times 4.6 mm) column. Mobile phase A consisted of a 0.1% glacial acetic acid solution in water, mobile phase B consisted of 100% acetonitrile. An isocratic method using 10% solvent B at 30 °C with a flow rate of 1 ml/min was employed for the elution of Trp. Fluorescence of Trp was monitored at excitation of 285 nm and emission of 360 nm.

Cell viability and reactive oxygen species (ROS) assays

Cell viability was evaluated by the crystal violet method using the standard protocol. In brief, cells were seeded in six-well plates at 10^6 cells per well and treated with MitoVES (5 μ M) and α -TOS

(50 μ M) for 3 and 6 h. The cells were washed and stained with 0.05% crystal violet for 1 h at room temperature. Absorbance at 595 nm was determined using the Tecan Infinity plate reader.

ROS levels were estimated using the MitoSOX probe as follows. Adherent and sphere cells were seeded at 2×10^5 cells per well in 12-well plates and incubated with MitoVES (5 μ M) and α -TOS (50 μ M) for 30, 60, and 120 min. The cells were harvested, incubated with 10 μ M MitoSOX red for 15 min at 37 °C in the dark, and analyzed by flow cytometry (BD LSR Fortessa II). Unstained and untreated samples were used as controls for each condition.

Animal experiments

To prepare tumors, IstMes2 spheres were injected into Balb/c nude mice at 5×10^5 cells per animal suspended in 50% Matrigel in sterile saline. After the tumors reached ~ 100 mm³ as detected by ultrasound imaging (USI; VisualSonics) [39], the mice were sacrificed and tumors excised. They were dissociated into single-cell suspensions, which were used to grow the cells in culture as adherent cells of the first generation of tumors (G1). These cells were converted into the sphere phenotype (see above) and the sphere cells injected into nude mice to form the second generation of tumors (G2). This was repeated two more times to obtain in total four generations of cells, which were then used in the experiments. Animal studies were performed according to the guidelines of the Australian and New Zealand Council for the Care and Use of Animals in Research and Teaching and were approved by the local animal ethics committee.

Statistical analysis

Experimental data are presented as the mean \pm SD. Comparisons between groups were performed using the Mann–Whitney *U* test for unpaired samples and Kruskal–Wallis analysis for multiple comparisons. Statistical calculations were performed using the SPSS statistical package, version 12.0F. Statistical differences of at least $p < 0.05$ were considered statistically significant.

Results

Validation of spheres as a TIC model

We prepared spheres from breast cancer (MCF7), mesothelioma (IstMes2), and prostate cancer cell lines (LNCaP) (Fig. 1A). The adherent and corresponding sphere cells were subjected to microarray analysis using the Illumina HumanHT-12 BeadChip. All microarray data are available at Gene Expression Omnibus (<http://www.ncbi.nlm.nih.gov/geo/>) with Accession No. GSE41980. PCA revealed two separate populations of the adherent and sphere cells for the three lines (Fig. 1B). GSEA based on enrichment of stemness gene sets for NSCs, ESCs, and HSCs verified the increased stemness of sphere cells [33–35]. This is shown in Supplementary Fig. S1A, which also depicts the LEGs. Increased expression of selected LEGs was confirmed by qPCR (Supplementary Fig. S1B).

IDO is upregulated in TICs derived from cell lines and primary biopsies

GSEA of 639 pathways derived from the Molecular Signature Database revealed that the only pathway enhanced in all three types of TICs is Trp metabolism, as shown by the GSEA enrichment plots and LEGs (Fig. 1C and D). The rate-limiting enzyme of Trp metabolism is IDO, which converts L-Trp into N'-formyl kynurenine [40]. We tested the adherent and sphere cells for the levels of both isotypes of IDO, IDO1 and IDO2. Fig. 2A documents that IDO1

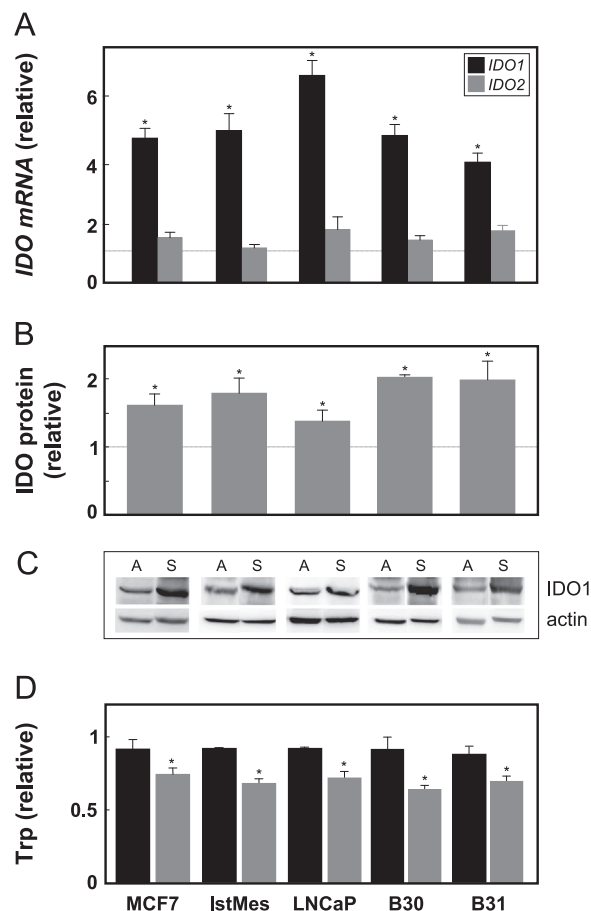


Fig. 2. IDO1 is increased in TICs. MCF7, IstMes2, LNCaP, B30, and B31 adherent and sphere cells were assessed for IDO1 and IDO2 mRNA expression by (A) qPCR, (B) total IDO protein level by ELISA, and (C) IDO1 protein level by WB (A, adherent; S, sphere). (D) Trp was assessed using HPLC in medium conditioned by 24 h cultivation of adherent and sphere cells and is shown relative to its level in the fresh medium (Trp concentration in the adherent cell medium was 8.5 ± 0.1 and 7.6 ± 0.5 μ g/ml). The data are derived from three independent experiments and are represented as mean values \pm SD in the sphere cells relative to their adherent counterpart. *Statistically different data for the adherent and corresponding sphere cells. The images are representative of at least three independent experiments.

mRNA was increased approximately four- to sevenfold in spheres compared to their adherent counterparts for the three cell types, whereas there was little or no change in the level of IDO2 mRNA. This was confirmed at the level of total IDO protein by ELISA and the IDO1 protein by WB (Fig. 2B and C).

Increase in IDO1 should result in the depletion of Trp from the compartment surrounding the cells. To see whether this is the case for TICs, we tested the effect of culturing adherent and sphere cells on the level of Trp in the medium. Fig. 2D clearly documents a decrease in Trp in the medium with sphere cells by ~ 3 μ g/ml in 24 h, whereas the decrease for the adherent cells was only about 1–1.5 μ g/ml.

To determine whether this paradigm also occurs in primary cancer cells, biopsies from two GBM patients (B30 and B31) were analyzed. The histology of the GBM sections is shown in Supplementary Fig. S2. Adherent cells from the biopsies were prepared and these were converted to gliomaspheres, which showed increased expression of several markers of stemness (Supplementary Fig. S2). Fig. 2 documents that the resulting GBM TICs also displayed increased levels of IDO1 but not IDO2, consistent with the results found for the sphere cells derived from the other cancer cell lines.

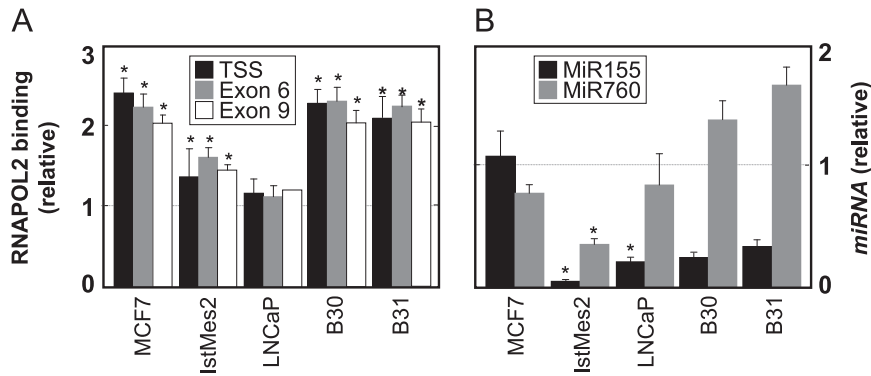


Fig. 3. Expression of IDO1 in TICs is regulated by transcriptional and posttranscriptional mechanisms. (A) Sphere cells were tested for binding of RNAPOL2 to the IDO1 TSS and exon 6/9. (B) MiR155 and MiR760 were evaluated by qPCR in sphere cells. In all cases the ratios of the levels in sphere and adherent cells are shown. The data are derived from three independent experiments and are represented as mean values \pm SD. *Statistically different data for the adherent and corresponding sphere cells.

Increase in IDO1 is regulated at the transcriptional and posttranscriptional levels

We next examined the modulation of increased IDO1 levels in sphere cells. To determine whether the increase in IDO1 was regulated at the transcriptional level, binding of RNAPOL2 to the TSS as well as to exons 6 and 9 (shared in all IDO1 spliced variants) of the IDO1 gene was analyzed by the ChIP assay. Fig. 3A documents an \sim 2-fold increase in binding of RNAPOL2 to the IDO1 TSS and both exons for MCF7 cells, whereas the increase was \sim 1.4-fold for LNCaP cells, and hardly any increase was observed for IstMes2 cells. GBM spheres showed an \sim 2-fold increase in binding of RNAPOL2 to the IDO1 TSS and exons 6 and 9. Possible posttranscriptional regulation of IDO1 involving miRNA was also examined, because analysis of the 3'UTR of the IDO1 mRNA revealed putative binding sites for several miRNAs. These are shown in Supplementary Fig. S3, which also documents expression of miRNAs obtained from miRNA array analysis and qPCR of the cancer cell lines as adherent populations or corresponding spheres. Supplementary Fig. S3C reveals that the activator of the epithelial-mesenchymal transition (EMT), ZEB1, was increased in MCF7, IstMes2, and LNCaP spheres, which was accompanied by regulation of the stemness miRNAs, MiR371, MiR200c, MiR203, and MiR183 [41]. Of the putative miRNAs with a binding site in the IDO1 mRNA 3' UTR, MiR155 was the one whose levels were most reduced in IstMes2, LNCaP, B30, and B31 spheres, whereas MiR760 was lower only in IstMes2 spheres. No change was observed for MiR155 in MCF7 cells or for MiR760 in MCF7 cells and GBM spheres (Fig. 3B). Therefore, it seems that the major regulatory mechanism causing increased expression of IDO1 varies in the different types of cancer cells.

Trp uptake is enhanced in TICs

Because Trp is an essential amino acid, its increased metabolism in TICs would be compensated for by enhancing its uptake by the cells. Hence, the level of expression of the light-chain subunit of the Trp-uptake system LAT1 and its heavy chain CD98 [42] was examined. Microarray data revealed increased expression of both genes in the spheres of all cell types studied (not shown), and this was in most cases confirmed by qPCR (Fig. 4A). In addition, LAT1 and CD98 were also increased at the protein level (Fig. 4B and C). Whether this was reflected by more efficient uptake of Trp by the sphere cells was examined, and we found that in all types of TICs examined, Trp uptake was enhanced by about two- to threefold (Fig. 4D).

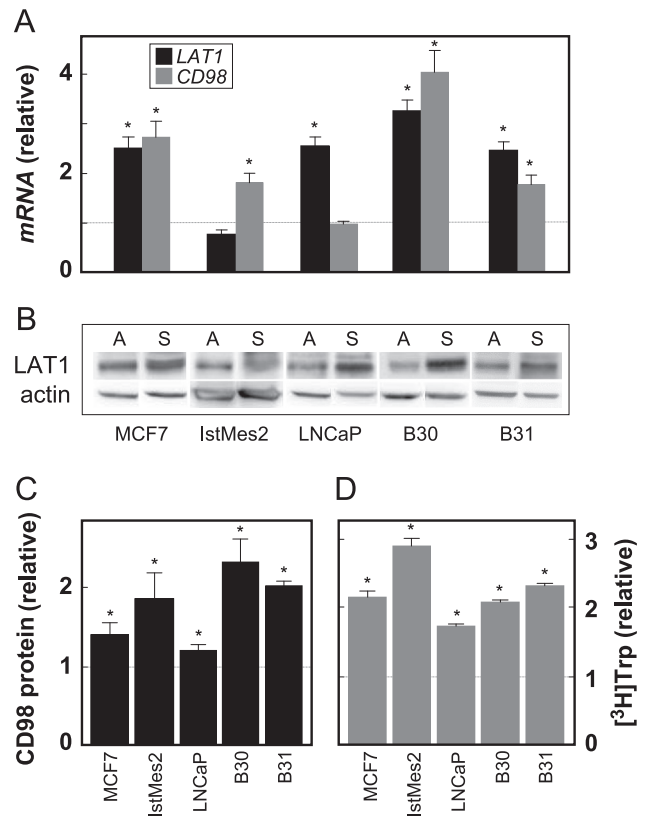


Fig. 4. TICs increase Trp uptake. MCF7, IstMes2, LNCaP, B30, and B31 sphere cells were assessed for (A) LAT1 and CD98 mRNA by qPCR, (B) LAT1 protein by WB, (C) CD98 protein by flow cytometry, and (D) Trp uptake using [³H]Trp. The data are derived from three independent experiments and are represented as mean values \pm SD. *Statistically different data for the adherent and corresponding sphere cells. The images are representative of at least three independent experiments.

Serial transplantation of TICs increases IDO1 level

We next tested whether the levels of IDO1 increase in tumors derived from IstMes2 TICs. Nude mice were injected with the sphere cells and tumors allowed to form. The carcinomas were then used for the preparation of cancer cells that were converted into spheres and these were again grafted into the animals. In this way, four generations (G1 to G4) of tumors were obtained. Fig. 5 (inset) shows that with each generation, the lag time from grafting the cells until the time of first tumor appearance shortened considerably. Correspondingly, the IDO1 mRNA levels increased, such that in G4 it was approximately eightfold higher than in G1, whereas only little change was observed for IDO2 mRNA (Fig. 5).

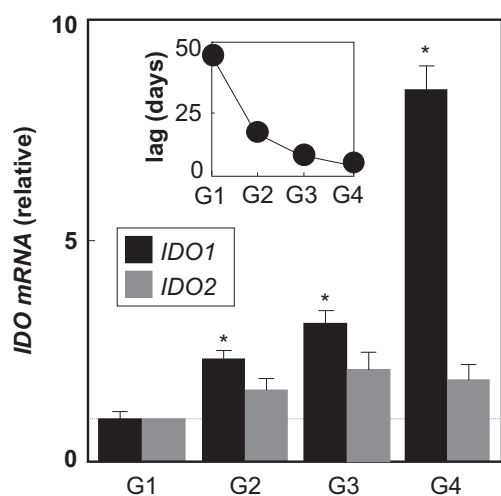


Fig. 5. IDO1 increases in serial tumor transplantations. IstMes2 spheres were injected into nude mice in 50% Matrigel, the resulting tumor (generation 1; G1) was excised at about 100 mm³, and the derived tumor cells were cultured and subsequently converted to spheres, which were then injected into nude mice to obtain the G2 tumor. This process was repeated two more times. In each generation of tumors, IDO1 and IDO2 mRNA was assessed by qPCR. The inset documents the shortening lag time for the appearance of USI-detectable tumors in the individual generations. The data are derived from three independent experiments and are represented as mean values \pm SD. *Statistically different data obtained for individual generations compared with G1 data.

This indicates that with each transplantation of the TICs in nude mice the cells are selected, and this may translate into facilitating escape from immune surveillance, given that nude mice contain interferon, NK cells [43], and NKT cells [44].

Mitocans suppress IDO1 in TICs

Two related mitocans, α -TOS and MitoVES (cf. Fig. 6A for structures) were evaluated for their effects on IDO expression. Fig. 6B documents a strong decrease in the levels of IDO1 mRNA expressed in sphere cells exposed to either 50 μ M α -TOS or 5 μ M MitoVES for 3 and 6 h. A corresponding decrease, albeit less profound, was found at the level of total IDO and IDO1 protein (Fig. 6C and D). The two mitocans did not significantly affect the levels of IDO2 mRNA in MCF7, IstMes2, or LNCaP spheres (Supplementary Fig. S4). Because MitoVES induces apoptosis in cancer cells and generates ROS [28,39,45,46], we tested its effect on the adherent and sphere cells. Supplementary Figs. S5A and S5B indicate that at the levels and times at which MitoVES considerably suppresses IDO1, there was only a low level of toxicity of the agents toward the cells, whereas MitoVES and α -TOS caused a substantial ROS generation already at short periods of time in the sphere cells.

MitoVES suppresses IDO1 at the transcriptional and posttranscriptional levels and by targeting mitochondrial CII

We next studied the effect of the more efficient of the two mitocans, MitoVES, on the binding of RNAPOL2 and on the level of MiR155 and MiR760 in sphere cells. Fig. 7A reveals that the drug suppressed binding of RNAPOL2 in all the cell lines, with the strongest effect in MCF7 spheres. Furthermore, MitoVES profoundly increased MiR155 expression in IstMes2, B30, and B31 spheres and increased MiR760 in IstMes2 and LNCaP spheres. No effect on either miRNA was found for MCF7 spheres (Fig. 7B).

MitoVES acts by targeting the mitochondrial CII to exert its proapoptotic and anti-cancer effects [28,39]. To test whether CII was also relaying the effects of MitoVES to modify the IDO1 level,

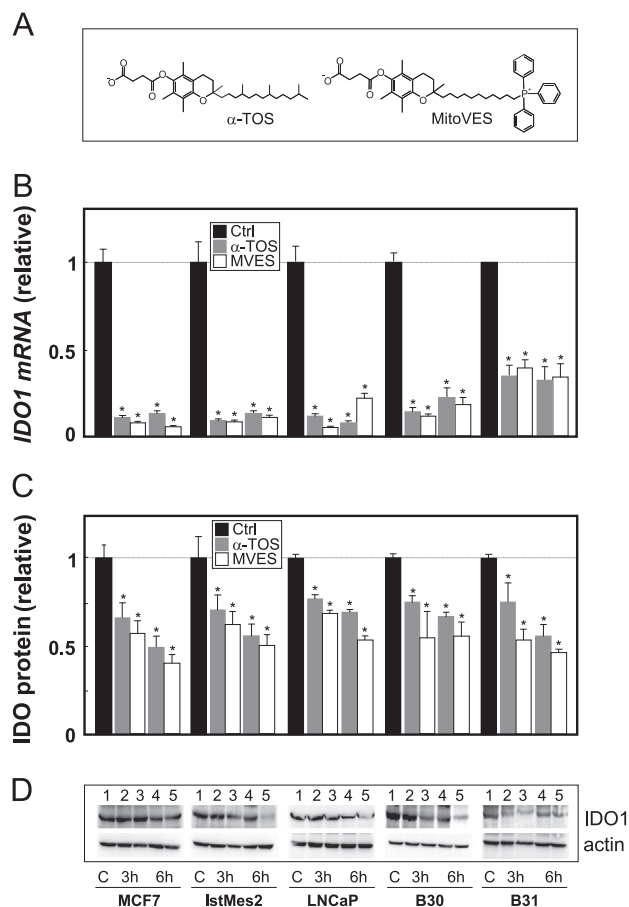


Fig. 6. Mitocans suppress IDO1 in sphere cells. (A) Structures of α -TOS and MitoVES. MCF7, IstMes2, LNCaP, B30, and B31 spheres were exposed for 3 and 6 h to α -TOS (50 μ M) or MitoVES (5 μ M) and assessed for (B) IDO1 mRNA by qPCR, (C) total IDO protein by ELISA, and (D) IDO1 protein by WB (lanes 1, control; 2, α -TOS 3 h; 3, α -TOS 6 h; 4, MitoVES 3 h; 5, MitoVES 6 h). The data are derived from three independent experiments and are represented as mean values \pm SD. *Statistically different data for the treated and control cells. The images are representative of at least three independent experiments.

MCF7 cells with decreased expression of SDHC, one of the four subunits of CII, were prepared using RNAi. Fig. 8A shows that SDHC-targeted shRNA transfection significantly decreased the level of SDHC but not that of the SDHA subunit of CII; it also considerably suppressed the SQR activity of CII (Fig. 8A). Fig. 8B documents that, unlike in the parental or nonsilencing control shRNA-transfected MCF7 cells, SDHC-silenced cells were resistant to the effects of MitoVES on IDO1 expression. Silencing of SDHC itself did not affect the level of IDO1 in the spheres (Supplementary Fig. S5C). Thus, CII seems to transmit the effect of MitoVES on IDO1 levels.

Discussion

An accepted model for the enrichment of cultured cells with TICs is based on growing cancer cells in an anchorage-independent manner, whereby they form spheres [25,26,47]. The three different MCF7, IstMes2, and LNCaP cell lines grew well in culture as both adherent and sphere cells. From gene sets derived for GSEA from published sources [31–33], the microarray data enabled us to validate our sphere cultures as a plausible model of TICs. Using GSEA of metabolic pathways, we identified a number of pathways that were upregulated in two of the three different types of TICs, but the only pathway activated in all three TIC types was Trp

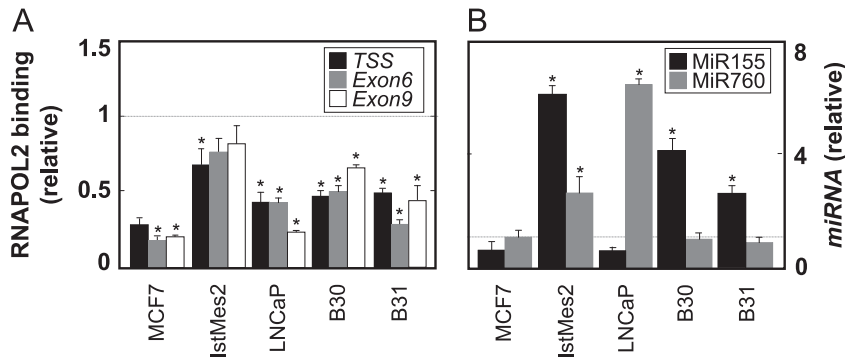


Fig. 7. Suppression of IDO1 in TICs by MitoVES is regulated by transcriptional and posttranscriptional mechanisms. Sphere cells were exposed to MitoVES (5 μ M, 6 h) and tested for (A) the binding of RNAPOL2 to IDO1 TSS and exon 6/9 and for (B) the levels of MiR155 and MiR760 by qPCR. In all cases the ratios of the levels in control and treated sphere cells are shown. The data are derived from three independent experiments and are represented as mean values \pm SD. *Statistically different data for the control and treated sphere cells.

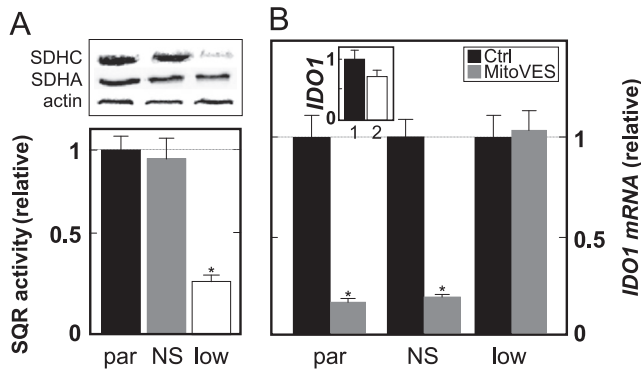


Fig. 8. Functional CII is important for MitoVES suppression of IDO1. (A) Parental (par), NS shRNA-treated, and SDHC shRNA-treated (low) MCF7 cells were assessed for the SDHC/SDHA protein by WB and for SQR activity using a spectrophotometric assay. (B) Parental, NS shRNA-treated, and SDHC shRNA-treated MCF7 cells were exposed to 5 μ M MitoVES for 6 h and IDO1 mRNA was assessed by qPCR. The inset documents the level of IDO1 mRNA in the parental (column 1) and SDHC shRNA-transfected MCF7 cells (column 2). The data are derived from three independent experiments and are represented as mean values \pm SD. *Statistically different data for parental cells and cells transfected with NS shRNA and for cells with low SDHC. The images are representative of at least three independent experiments.

metabolism. This is an intriguing finding, because it is suggestive of an important role of Trp metabolism in TICs, with functional consequences, as previously reported for cancer cells [13–15,48]. We believe that this is the first time that the Trp pathway is shown to be upregulated in TICs.

IDO is the rate-limiting enzyme in the Trp catabolic pathway [14]. Microarray data showed the increase in IDO1 expression in all three types of spheres, and this was also confirmed on the mRNA and protein levels by qPCR and WB, respectively. Furthermore, we observed that the TICs deplete Trp in the surrounding environment with faster kinetics than found for the corresponding adherent cells. Because these data were acquired using cultured cell lines, we also tested whether a similar increase occurred in primary tumor samples. We used cells derived from biopsies from GBM patients that were converted into spheres, which were validated for stemness using a set of markers (CD133, CD24, and ABCG2) routinely used for glioblastoma-initiating cells [49]. Primary gliomaspheres derived from biopsies from two patients confirmed the results with the cell lines, documenting that the increase in IDO expression is a feature of TICs from a variety of sources of different tumor types exemplified both by established cell lines and by primary tissue. We did not observe any discernible change in IDO2 in these spheres. This is consistent with the notion that IDO1 is more important for tumor cell escape and also a preferred target for several inhibitors acting as anti-tumor

agents, at least one of the IDO2 alleles being often lost in cancer patients [48,50].

IDO1 is known to be regulated transcriptionally, the best described pathway involving the IFN γ signaling pathway involving STAT1 and IRF1 [51,52]. Recently, the importance of regulation at the level of miRNA has also been proposed [53]. To understand how IDO1 is regulated in TICs, we first performed the IDO1 gene promoter analysis for putative binding sites of transcription factors (TFs). Supplementary Fig. S3D documents sites for several TFs, including two sites for IRF1. At this stage, we tested for transcriptional regulation of IDO1 by assessing binding of RNAPOL2 to the TSS and exons 6 and 9 of the IDO1 gene and found that the binding was stronger in MCF7 spheres, whereas it did not increase in LNcaP spheres and gliomaspheres.

Trp is an essential amino acid such that its increased metabolism by TICs is expected to be compensated for by its enhanced uptake. There are several systems responsible for Trp uptake, of which the neutral amino acid transporter system L is ubiquitous [42]. It is a dimer consisting of the light chain LAT1 (encoded by SLC7A5) and the heavy chain CD98 (SLC7A8) [54]. Accordingly, our model TICs exert an increase in both proteins in most cases. Functionally, all types of TICs showed higher uptake of Trp, consistent with the increased levels of IDO1. The increased uptake of Trp and IDO activity has been reported [54]. It is plausible to expect that the increased uptake of Trp lowers its level in the tumor microenvironment with functional consequences.

We have established a model of serial transplantation of mesothelioma TICs derived from the IstMes2 cells. Intriguingly, we observed that with each cycle of transplantation of sphere cells into nude mice, the lag time from sphere cell grafting to tumor appearance shortened from the initial \sim 50 days for G1 to < 1 week for G4. Further, we observed that the level of IDO1 increased almost 10-fold over the four generations. This is a very interesting finding, because an increase in a particular gene such as IDO1 has not been reported under these conditions thus far. Conversely, it has been shown for several types of TICs that serial transplantation results in the formation of tumors of similar phenotype and genotype [55,56]. Conceivably, this finding endows IDO1 with considerable pathological importance. Thus, serial transplantation of TICs not only armors the cells with a more aggressive phenotype but also makes them potentially more resistant to the effect of the cells of the immune system.

Suppression of IDO1 is considered to promote the killing of cancer cells by the cells of the immune system, and small molecules have been designed that inhibit IDO at the level of its activity or transcription [17–19,50,57]. We tested whether two mitocans with specific anti-cancer activity, α -TOS and MitoVES [28,39,45,46], lowered IDO in our TIC models. Both agents

suppressed IDO1 at the mRNA and protein levels at different time points and at doses that do not induce apoptosis. No inhibitory effect on IDO2 was observed. Further, we tested the effect of dysfunctional CII, the target of α -TOS and MitoVES for their apoptogenic activity [28,39,45], on the suppression of IDO1 and found the SDHC^{low} cells to be resistant to the effect of MitoVES on IDO1, clearly documenting the role of CII in the process. IDO is regulated by the cellular redox status [51,58]. Therefore, it is possible that MitoVES and α -TOS, reported to generate rapid oxidative stress in cancer cells [28,39] as shown also here, in particular for the sphere cultures, acts by deregulation of IDO homeostasis, linking ROS generation in the spheres via CII as the molecular target for MitoVES [28,39] and IDO1 levels. Further research is needed to confirm this molecular mechanism of action of the mitocan.

It seems that the increase in IDO1 during the shift from the adherent to the sphere phenotype and its suppression by mitocans are regulated at the level of transcription as well as by miRNAs. We found that MitoVES suppressed binding of RNAPOL2 to the IDO1 TSS and exons 6 and 9 in all types of spheres except for those of MCF7 cells. MitoVES also increased the levels of MiR155 in IstMes2 spheres and gliomaspheres and MiR760 in LNCaP spheres. This suggests cell-type-specific effects of the mitocan on transcriptional and posttranscriptional modulation of the expression of IDO1. The transcriptional regulation is consistent with the published data [51,52]. A possible posttranscriptional regulation of IDO1 has been proposed, as reported for MiR181a [53]. Moreover, MiR155 has been shown to regulate the CD4⁺ and Treg responses [59]. A potential cross talk between TFs and miRNAs is indicated by a recent report showing that the TF ZEB1, known to regulate the EMT, suppresses the stemness-inhibiting miRNAs [38], which is consistent with our findings, i.e., documenting that ZEB1 is increased in all types of model TICs (Supplementary Fig. S3C). We are now investigating the precise mechanism for inducing IDO1 expression in TICs as well as for its suppression by mitocans.

In conclusion, we report on an intriguing finding, i.e., that model TICs derived from several unrelated cancer cell lines as well as primary GBM biopsies upregulate their expression of IDO1, the rate-limiting enzyme of Trp metabolism along the kynurenine pathway. This may result in a long-term escape of TICs from immune surveillance [60] and promote their survival to form second-line tumors. Further, mitocans suppress IDO1 levels in TICs, thereby removing their defense to make them more vulnerable to the immune cells, a paradigm that is a subject of our ongoing studies. We believe that this is the first report of its kind and that it has a considerable translational potential [61].

Acknowledgments

This work was supported in part by grants from the Australian Research Council, Cancer Council Queensland, National Health and Medical Research Council of Australia, Clem Jones Foundation, and Czech Science Foundation (P301/10/1937) to J.N.; the Grant Agency of the Charles University (268111) to K.P.; the Czech Science Foundation (P305/12/1708) to J.T.; and a Griffith University Fellowship to L.F.D. This work forms a part of the Ph.D. project of R.Z.

Appendix A. Supporting information

Supplementary data associated with this article can be found in the online version at <http://dx.doi.org/10.1016/j.freeradbiomed.2013.10.003>.

References

- [1] Siegel, R.; Naishadham, D.; Jemal, A. Cancer statistics, 2012. *CA Cancer J. Clin.* **62**:10–29; 2012.
- [2] Hanahan, D.; Weinberg, R. A. The hallmarks of cancer: the next generation. *Cell* **144**:646–674; 2011.
- [3] Clevers, H. The cancer stem cell: premises, promises and challenges. *Nat. Med.* **17**:313–319; 2011.
- [4] Visvader, J. E. Cells of origin in cancer. *Nature* **469**:314–322; 2011.
- [5] Thiery, J. P.; Aclouque, H.; Huang, R. Y.; Nieto, M. A. Epithelial–mesenchymal transitions in development and disease. *Cell* **139**:871–890; 2009.
- [6] Lee, T. K.; Castilho, A.; Cheung, V. C.; Tang, K. H.; Ma, S.; Ng, I. O. CD24⁺ liver tumor-initiating cells drive self-renewal and tumor initiation through STAT3-mediated NANOG regulation. *Cell Stem Cell* **9**:50–63; 2011.
- [7] Qi, Y.; Li, R. M.; Kong, F. M.; Li, H.; Yu, J. P.; Ren, X. B. How do tumor stem cells actively escape from host immunosurveillance? *Biochem. Biophys. Res. Commun.* **420**:699–703; 2012.
- [8] Dunn, G. P.; Bruce, A. T.; Ikeda, H.; Old, L. J.; Schreiber, R. D. Cancer immunoeediting: from immunosurveillance to tumor escape. *Nat. Immunol.* **3**:991–998; 2002.
- [9] Mapara, M. Y.; Sykes, M. Tolerance and cancer: mechanisms of tumor evasion and strategies for breaking tolerance. *J. Clin. Oncol.* **22**:1136–1151; 2004.
- [10] Dunn, G. P.; Old, L. J.; Schreiber, R. D. The three Es of cancer immunoeediting. *Annu. Rev. Immunol.* **22**:329–360; 2004.
- [11] Zou, W. Immunosuppressive networks in the tumour environment and their therapeutic relevance. *Nat. Rev. Cancer* **5**:263–274; 2005.
- [12] Lu, B.; Finn, R. D. T-cell death and cancer immune tolerance. *Cell Death Differ.* **15**:70–79; 2008.
- [13] Munn, D. H.; Mellor, A. L. Indoleamine 2,3-dioxygenase and tumor-induced tolerance. *J. Clin. Invest.* **117**:1147–1154; 2007.
- [14] Prendergast, G. C. Immune escape as a fundamental trait of cancer: focus on IDO. *Oncogene* **27**:3889–3900; 2008.
- [15] Katz, J. B.; Muller, A. J.; Prendergast, G. C. Indoleamine 2,3-dioxygenase in T-cell tolerance and tumoral immune escape. *Immunol. Rev.* **222**:206–221; 2008.
- [16] Löb, S.; Königsrainer, A.; Rammensee, H. G.; Opelz, G.; Terness, P. Inhibitors of indoleamine-2,3-dioxygenase for cancer therapy: can we see the wood for the trees? *Nat. Rev. Cancer* **9**:445–452; 2009.
- [17] Kumar, S.; Malachowski, W. P.; DuHadaway, J. B.; LaLonde, J. M.; Carroll, P. J.; Jaller, D., et al. Indoleamine 2,3-dioxygenase is the anticancer target for a novel series of potent naphthoquinone-based inhibitors. *J. Med. Chem.* **51**:1706–1718; 2008.
- [18] Muller, A. J.; DuHadaway, J. B.; Jaller, D.; Curtis, P.; Metz, R.; Prendergast, G. C. Immuno-therapeutic suppression of indoleamine 2,3-dioxygenase and tumor growth with ethyl pyruvate. *Cancer Res.* **70**:1845–1853; 2010.
- [19] Pilotte, L.; Larrieu, P.; Stroobant, V.; Colau, D.; Dolusic, E.; Frédéric, R., et al. Reversal of tumoral immune resistance by inhibition of tryptophan 2,3-dioxygenase. *Proc. Natl. Acad. Sci. USA* **109**:2497–2502; 2012.
- [20] Liu, G.; Yuan, X.; Zeng, Z.; Tunici, P.; Ng, H.; Abdulkadir, I. R., et al. Analysis of gene expression and chemoresistance of CD133⁺ cancer stem cells in glioblastoma. *Mol. Cancer* **5**:67; 2006.
- [21] Morrison, B. J.; Schmidt, C. W.; Lakhani, S. R.; Reynolds, B. A.; Lopez, J. A. Breast cancer stem cells: implications for therapy of breast cancer. *Breast Cancer Res.* **10**:210; 2008.
- [22] Reiman, J. M.; Knutson, K. L.; Radisky, D. C. Immune promotion of epithelial–mesenchymal transition and generation of breast cancer stem cells. *Cancer Res.* **70**:3005–3008; 2010.
- [23] Zobalova, R.; Prokopova, K.; Stantic, M.; Stapelberg, M.; Dong, L. F.; Ralph, S. J., et al. The potential role of CD133 in immune surveillance and apoptosis: a mitochondrial connection? *Antioxid. Redox Signaling* **15**:2989–3002; 2011.
- [24] Munn, D. H.; Blocking, I. D. O. activity to enhance anti-tumor immunity. *Front. Biosci.* **4**:734–745; 2012.
- [25] Bjornson, C. R.; Rietze, R. L.; Reynolds, B. A.; Magli, M. C.; Vescovi, A. L. Turning brain into blood: a hematopoietic fate adopted by adult neural stem cells in vivo. *Science* **283**:534–537; 1999.
- [26] Charafe-Jauffret, E.; Ginestier, C.; Iovino, F.; Wicinski, J.; Cervera, N.; Finetti, P., et al. Breast cancer cell lines contain functional cancer stem cells with metastatic capacity and a distinct molecular signature. *Cancer Res.* **69**:1302–1313; 2009.
- [27] Neuzil, J.; Dong, L. F.; Rohlena, J.; Truksa, J.; Ralph, S. J. Classification of mitocans, anti-cancer drugs acting on mitochondria. *Mitochondrion* **13**:199–208; 2013.
- [28] Dong, L. F.; Jameson, V. J. A.; Tilly, D.; Cerny, J.; Mahdavian, E.; Marín-Hernández, A., et al. Mitochondrial targeting of vitamin E succinate enhances its pro-apoptotic and anti-cancer activity via mitochondrial complex II. *J. Biol. Chem.* **286**:3717–3728; 2011.
- [29] Wettenhall, J. M.; Smyth, G. K. limmaGUI: a graphical user interface for linear modeling of microarray data. *Bioinformatics* **20**:3705–3706; 2004.
- [30] Ritchie, M. E.; Silver, J.; Oshlack, A.; Holmes, M.; Diyagama, D.; Holloway, A.; Smyth, G. K. A comparison of background correction methods for two-colour microarrays. *Bioinformatics* **23**:2700–2707; 2007.
- [31] Tong, W.; Harris, S.; Cao, X.; Fang, H.; Shi, L.; Sun, H., et al. Development of public toxicogenomics software for microarray data management and analysis. *Mutat. Res.* **549**:241–253; 2004.
- [32] Raychaudhuri, S.; Stuart, J. M.; Altman, R. B. Principal components analysis to summarize microarray experiments: application to sporulation time series. *Pac. Symp. Biocomput* **2000**:455–466; 2000.

- [33] Ramalho-Santos, M.; Yoon, S.; Matsuzaki, Y.; Mulligan, R. C.; Melton, D. A. 'Stemness': transcriptional profiling of embryonic and adult stem cells. *Science* **298**:597–600; 2002.
- [34] Ivanova, N. B.; Dimos, J. T.; Schaniel, C.; Hackney, J. A.; Moore, K. A.; Lemischka, I. R. A stem cell molecular signature. *Science* **298**:601–604; 2002.
- [35] Fortunel, N. O.; Otu, H. H.; Ng, H. H.; Chen, J.; Mu, X.; Chevassut, T., et al. 'Stemness': transcriptional profiling of embryonic and adult stem cells and a stem cell molecular signature. *Science* **302**:393; 2003.
- [36] Subramanian, A.; Tamayo, P.; Mootha, V. K.; Mukherjee, S.; Ebert, B. L.; Gillette, M. A., et al. Gene set enrichment analysis: a knowledge-based approach for interpreting genome-wide expression profiles. *Proc. Natl. Acad. Sci. USA* **102**:15545–15550; 2005.
- [37] Storey, J. D.; Tibshirani, R. Statistical significance for genome-wide studies. *Proc. Natl. Acad. Sci. USA* **100**:9440–9445; 2003.
- [38] Schmittgen, T. D.; Livak, K. J. Analyzing real-time PCR data by the comparative CT method. *Nat. Protoc.* **3**:1101–1108; 2008.
- [39] Dong, L. F.; Jameson, V. J. A.; Tilly, D.; Prochazka, L.; Rohlena, J.; Valis, K., et al. Mitochondrial targeting of α -tocopheryl succinate enhances its pro-apoptotic efficacy: a new paradigm of efficient anti-cancer therapy. *Free Radic. Biol. Med.* **50**:1546–1555; 2011.
- [40] King, N. J.; Thomas, S. R. Molecules in focus: indoleamine 2,3-dioxygenase. *Int. J. Biochem. Cell Biol.* **39**:2167–2172; 2007.
- [41] Wellner, U.; Schubert, J.; Burk, U. C.; Schmalhofer, O.; Zhu, F.; Sonntag, A., et al. The EMT-activator ZEB1 promotes tumorigenicity by repressing stemness-inhibiting microRNAs. *Nat. Cell Biol.* **11**:1487–1495; 2009.
- [42] Devés, R.; Boyd, C. A. Transporters for cationic amino acids in animal cells: discovery, structure, and function. *Physiol. Rev.* **78**; 1998. (487–445).
- [43] Shouval, D.; Rager-Zisman, B.; Quan, P.; Shafritz, D. A.; Bloom, B. R.; Reid, L. M. Role in nude mice of interferon and natural killer cells in inhibiting the tumorigenicity of human hepatocellular carcinoma cells infected with hepatitis B virus. *J. Clin. Invest.* **72**:707–717; 1983.
- [44] Pellicci, D. G.; Hammond, K. J.; Uldrich, A. P.; Baxter, A. G.; Smyth, M. J.; Godfrey, D. I. A natural killer T (NKT) cell developmental pathway involving a thymus-dependent NK1.1-CD4⁺ CD1d-dependent precursor stage. *J. Exp. Med.* **19**:835–844; 2002.
- [45] Dong, L. F.; Low, P.; Dyason, J.; Wang, X. F.; Prochazka, L.; Witting, P. K., et al. α -Tocopheryl succinate induces apoptosis by targeting ubiquinone-binding sites in mitochondrial respiratory complex II. *Oncogene* **27**:4324–4335; 2008.
- [46] Neuzil, J.; Weber, T.; Schröder, A.; Lu, M.; Ostermann, G.; Gellert, N., et al. Induction of cancer cell apoptosis by α -tocopheryl succinate: molecular pathways and structural requirements. *FASEB J.* **15**:403–415; 2001.
- [47] Dontu, G.; Abdallah, W. M.; Foley, J. M.; Jackson, K. W.; Clarke, M. F.; Kawamura, M. J.; Wicha, M. S. In vitro propagation and transcriptional profiling of human mammary stem/progenitor cells. *Genes Dev.* **17**:1253–1270; 2003.
- [48] Muller, A. J.; DuHadaway, J. B.; Donover, P. S.; Sutanto-Ward, E.; Prendergast, G. C. Inhibition of indoleamine 2,3-dioxygenase, an immunoregulatory target of the cancer suppression gene Bin1, potentiates cancer chemotherapy. *Nat. Med.* **11**:312–319; 2005.
- [49] Bao, S.; Wu, Q.; McLendon, R. E.; Hao, Y.; Shi, Q.; Hjelmeland, A. B., et al. Glioma stem cells promote radioresistance by preferential activation of the DNA damage response. *Nature* **444**:756–760; 2006.
- [50] Metz, R.; DuHadaway, J. B.; Kamasani, U.; Laury-Kleintop, L.; Muller, A. J.; Prendergast, G. C. Novel tryptophan catabolic enzyme IDO2 is the preferred biochemical target of the antitumor indoleamine 2,3-dioxygenase inhibitory compound D-1-methyl-tryptophan. *Cancer Res.* **67**:7082–7087; 2007.
- [51] Jeong, Y. I.; Kim, S. W.; Jung, I. D.; Lee, J. S.; Chang, J. H.; Lee, C. M., et al. Curcumin suppresses the induction of indoleamine 2,3-dioxygenase by blocking the Janus-activated kinase-protein kinase C-STAT1 signaling pathway in interferon- γ -stimulated murine dendritic cells. *J. Biol. Chem.* **284**:3700–3708; 2009.
- [52] Ma, X.; Chow, J. M.; Gri, G.; Carra, G.; Gerosa, F.; Wolf, S. F., et al. The interleukin 12 p40 gene promoter is primed by interferon- γ in monocytic cells. *J. Exp. Med.* **183**:147–157; 1996.
- [53] Liu, L.; Wang, Y.; Fan, H.; Zhao, X.; Liu, D.; Hu, Y., et al. MicroRNA-181a regulates local immune balance by inhibiting proliferation and immunosuppressive properties of mesenchymal stem cells. *Stem Cells* **30**:1756–1770; 2012.
- [54] Silk, J. D.; Lakhali, S.; Laynes, R.; Vallius, L.; Karydis, I.; Marcea, C., et al. IDO induces expression of a novel tryptophan transporter in mouse and human tumor cells. *J. Immunol.* **187**:1617–1625; 2011.
- [55] O'Brien, C. A.; Pollett, A.; Gallinger, S.; Dick, J. E. A human colon cancer cell capable of initiating tumour growth in immunodeficient mice. *Nature* **445**:106–110; 2007.
- [56] Zucchi, I.; Astigiano, S.; Bertalot, S.; Sanzone, S.; Cocola, C.; Pelucchi, P., et al. Distinct populations of tumor-initiating cells derived from a tumor generated by rat mammary cancer stem cells. *Proc. Natl. Acad. Sci. USA* **105**:16940–16945; 2008.
- [57] Banerjee, T.; DuHadaway, J. B.; Gaspari, P.; Sutanto-Ward, E.; Munn, D. H.; Mellor, A. L., et al. A key in vivo antitumor mechanism of action of natural product-based brassinins is inhibition of indoleamine 2,3-dioxygenase. *Oncogene* **27**:2851–2857; 2008.
- [58] Thomas, S. R.; Salahifar, H.; Mashima, R.; Hunt, N. H.; Richardson, D. R.; Stocker, R. Antioxidants inhibit indoleamine 2,3-dioxygenase in IFN- γ -activated human macrophages: posttranslational regulation by pyrrolidine dithiocarbamate. *J. Immunol.* **166**:6332–6340; 2001.
- [59] Stahl, H. F.; Fauti, T.; Ullrich, N.; Bopp, T.; Kubach, J.; Rust, W., et al. miR-155 inhibition sensitizes CD4⁺ Th cells for TREG mediated suppression. *PLoS One* **4**:e7158; 2009.
- [60] Fallarino, F.; Grohmann, U.; Vacca, C.; Bianchi, R.; Orabona, C.; Spreca, A., et al. T cell apoptosis by tryptophan catabolism. *Cell Death Differ.* **9**:1069–1077; 2002.
- [61] Frank, N. Y.; Schatton, T.; Frank, M. H. The therapeutic promise of the cancer stem cell concept. *J. Clin. Invest.* **120**:41–50; 2010.

The Potential Role of CD133 in Immune Surveillance and Apoptosis: A Mitochondrial Connection?

Renata Zobalova,^{1,2} Katerina Prokopova,² Marina Stantic,¹ Michael Stapelberg,¹ Lan-Feng Dong,¹
Stephen J. Ralph,¹ Emmanuel Akporiaye,³ and Jiri Neuzil^{1,2}

Abstract

Significance: Recent research has shown that tumors contain a small subpopulation of stem-like cells that are more resistant to therapy and that are likely to produce second-line tumors. **Recent Advances:** Cancer stem-like cells (CSCs) have been characterized by a variety of markers, including, for a number of types of cancer, high expression of the plasma membrane protein CD133, which is also indicative of the increase of stemness of cultured cancer cells growing as spheres. **Critical Issues:** While the function of this protein has not yet been clearly defined, it may have a role in the stem-like phenotype of CSCs that cause (re-)initiation of tumors as well as their propagation. We hypothesize that CD133 selects for CSC survival against not only immunosurveillance mechanisms but also stress-induced apoptosis. **Future Directions:** High level of expression of CD133 may be a useful marker of more aggressive tumors that are recalcitrant toward established therapies. Compelling preliminary data indicate that drugs targeting mitochondria may be utilized as a novel, efficient cancer therapeutic modality. *Antioxid. Redox Signal.* 15, 2989–3002.

Introduction

CARCINOGENESIS RESULTS from accumulation of mutational and genetic changes that alter normal cell growth control and proapoptotic/survival pathways. The newly formed malignant cells are morphologically distinct: they are able to evade apoptosis; proliferate out of control; invade the surrounding tissue; induce angiogenesis; and eventually metastasize (48). During the early stages of carcinogenesis, a variety of intrinsic tumor suppressor mechanisms are ready to trigger apoptosis, repair, or senescence if cellular proliferation and division become abnormal (108). Apoptosis can be triggered in response to a variety of signals induced by cell stress and injury, with mitochondria as key intracellular mediators (21), or in response to ligation of cell-surface death receptors, such as Fas or the tumor necrosis factor-related apoptosis-inducing ligand (TRAIL) (88).

Not all malignant cells are destroyed during the early stages of carcinogenesis. Transformed cells that escape the intrinsic cellular controls for abortive suicide are then subjected to extrinsic tumor suppressor mechanisms. Thus, the immune system functions as an extrinsic tumor suppressor by

detecting and eliminating malignant cells on the basis of tumor-specific antigens (108, 112). Cancer immune surveillance, whereby the immune system identifies cancerous and/or precancerous cells and eliminates them before they can cause harm, is now known as the elimination phase of a broader process that has been termed cancer immunoediting (27, 28). This process is based on the concept that the immune system not only protects the host against cancer formation but also promotes cancer development, and the “three Es” of cancer immunoediting comprise the elimination phase (cancer immunosurveillance), equilibrium phase, and escape phase (29).

In the elimination phase, both the innate and adaptive arms of the immune system work together to detect and eliminate cancer cells that have developed as a result of failed intrinsic tumor suppressor mechanisms (107). The initial stage mainly engages the innate immune system, including macrophages and natural killer (NK) cells that may recognize developing tumors *via* receptor-mediated recognition processes, some of which involve tumor antigen presentation (108). The tumor-activated immune cells then utilize cytotoxic effector mechanisms to kill and eliminate the transformed cells (or cells undergoing malignant transformation). The immune cells

This article was subjected to substantial post-acceptance edits by the author.

¹School of Medical Science, Griffith University, Southport, Australia.

²Molecular Therapy Group, Institute of Biotechnology, Czech Academy of Sciences, Prague, Czech Republic.

³Earle A. Chiles Cancer Research Institute, Portland Providence Medical Center, Portland, Oregon.

also secrete interferons (IFNs), which control tumor growth and amplify the immune response (108). Initially, IFN- γ that is released at the tumor site induces production of chemokines, which recruit cells like macrophages that produce interleukin-12 and NK cells producing more IFN- γ at the tumor site (5). IFN- γ -activated macrophages can induce cancer cell death by releasing products such as reactive oxygen species (ROS) (98). Activated NK cells induce apoptosis in cancer cells by triggering TRAIL- or perforin-dependent pathways (50, 106, 113).

The tumor necrosis factor family member TRAIL is one of the major mediators of antitumor immunity. TRAIL is predominantly expressed by immune cells, particularly of the myeloid lineage, where it is either present on the cell surface as a membrane protein or is secreted in a soluble form to induce apoptosis by binding to cognate death receptors on target (tumor) cells (63, 118). In contrast to other mediators, TRAIL induces apoptosis in various cancer cell types, being generally nontoxic toward normal cells (38). Cancer cell resistance to TRAIL-mediated cell death may be due to up-regulation of the antiapoptotic FLICE-inhibitory protein (FLIP) (40, 55, 123, 132).

ROS are formed as a natural by-product of normal oxygen metabolism. Increase in the level of ROS creates oxidative stress, which causes cell damage with ensuing cell death by way of activating various signaling pathways that, in many cases, converge at apoptosis induction (15, 67). While the signaling mechanisms have not been completely unraveled, mitochondria play a key role in the oxidative stress-induced apoptotic pathways (72). Mitochondria, organelles vital for cellular energy homeostasis, produce ROS in the mitochondrial respiratory chain (13). Recent studies have showed that ROS generation involves complex II of the respiratory chain (1, 71), rendering it very important for apoptosis induction and the ensuing death of cancer cells (3, 23, 25, 75). We have recently designed novel anticancer drugs from the family of mitocans (81, 83) that specifically target mitochondria (the mitochondrial complex II) and that are much more efficient than the corresponding mitochondrial-untargeted compounds, while preserving selectivity for cancer cells (23, 25). These anticancer drugs showed very high efficacy against fast proliferating breast cancer cells as well as their cancer stem-like counterparts, which in our study were represented by spheroid cultures, that is, multicellular structures with stem cell-like characteristics (see below).

If the transformed cells are not fully destroyed during the elimination phase, they then enter into a temporary state of equilibrium with the immune system (28, 29). Here, cancer cells can either remain dormant or continue to evolve by accumulating additional changes, which would allow them to escape detection by the immune system (108, 112).

Taken together, the immune system is for the most part very effective in suppressing cellular transformation and cancer growth *via* the diverse extrinsic mechanisms as described above such that cancer, on average, occurs less than once in a lifetime. This is the case even though many cells in the body exist as potential targets for significant mutational and genetic changes. Nevertheless, cancers do arise in immunocompetent individuals, suggesting that clonally derived populations of cells are able to escape the immune system. These cells that emerge from the selective pressures of the immune system are resistant to immune-induced killing due to reduced immuno-

genicity. Moreover, such cells are often also resistant to many of the currently used anticancer therapies.

The Significance of Emerging Cancer Stem-Like Cells

In the past decade or so, the cancer stem cell hypothesis has been experiencing a resurgence. Various studies have suggested that stem cells may play a vital role in carcinogenesis because cancer stem-like cells (CSCs) (also referred to as tumor-initiating cells) share many crucial characteristics with normal stem cells that have the capacity to repopulate whole tissues (104, 123). These features include the ability to self-renew and differentiate, high levels of telomerase activity, greater capacity for DNA repair, activation of antiapoptotic pathways, and increased membrane transporter activity including the ATP-binding cassette drug transporters (providing for an increased level of drug resistance). In addition, CSCs are able to migrate and metastasize, hence forming secondary tumors that are, as a rule, refractory to established therapeutic modalities (2, 92, 104, 123).

To date, CSCs have been identified in a range of different cancers, including leukemias (8, 62), multiple myeloma (86), neoplasias of the nervous system (90, 104), colorectal, prostate or hepatocellular carcinomas (18, 94, 127), breast cancer (4), melanoma (32), and osteosarcoma (41). Within these tumors the CSCs represent only a small subpopulation, sometimes referred to as the side-population because these cells can actively exclude fluorescent DNA-staining dyes (53). The main problem with CSCs is that, similar to normal stem cells, they share properties that render them relatively resistant to current cancer therapies such as chemotherapy and radiation therapy, thereby promoting their survival. For these reasons they present a considerable problem in cancer management (6, 36, 47).

A variety of markers have been used to characterize CSCs (Table 1). In particular, these include CD133 and CD44 surface proteins and several intrinsic markers (*e.g.*, Oct-4 or ALDH1). Overexpression of CD44 has been found in the CSC population in breast (4), prostate (18), and pancreatic cancer (64). The CD44 protein is involved in cell-cell and cell-matrix interactions, and CD44⁺ breast cancer cells exert more pronounced transforming growth factor- β signaling (102).

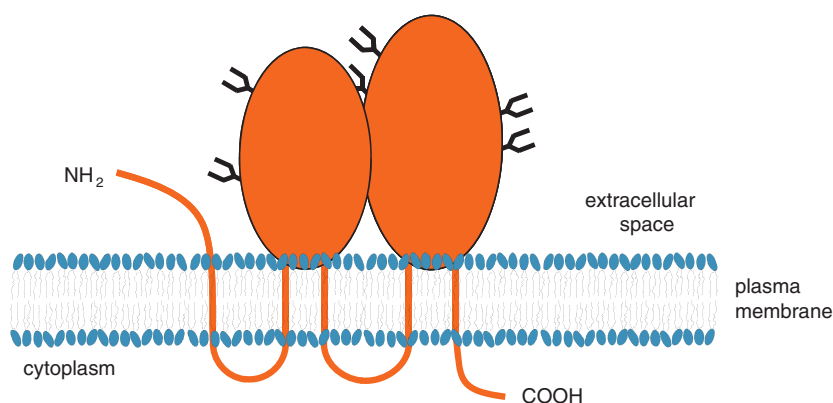
CD133 (Fig. 1), also known as prominin-1 (20, 74), is emerging as an important marker of CSCs identified in many different studies (73, 77, 85, 94, 104, 110, 124). CD133 is highly expressed by a variety of tumor types, including medullo-

TABLE 1. EXAMPLES OF MARKERS FOR DIFFERENT TYPES OF TUMORS

Tumor type	CSC markers	References
Brain	Musashi-1 ⁺ , nestin ⁺ , CD133 ⁺	105
Breast	CD44 ⁺ , CD24 ^{+/low} , ALDH1 ⁺ , CD133 ⁺	4, 42, 124
Colon	CD133 ⁺	84, 94
Hepatocellular	CD133 ⁺	110
Leukemia	CD34 ⁺ , CD38 ⁻ , CD44 ⁺	11
Melanoma	CD20 ⁺ , CD133 ⁺ , ABCG2 ⁺	32, 77
Pancreatic	CD133 ⁺ , ABCG2 ⁺	85
Prostate	CD44 ⁺ , $\alpha_2\beta_1$ ^{high} , CD133 ⁺	18, 73, 87

CSC, cancer stem-like cells.

FIG. 1. The proposed structure of CD133 (Prominin-1) showing the glycosylation sites. (Adapted and modified from refs. 20, 33, 34, 69, 74, 122.) (To see this illustration in color the reader is referred to the web version of this article at www.liebertonline.com/ars).



blastoma (104), glioblastoma (96), colorectal (84), prostate (18), and breast carcinomas (124), as well as mesotheliomas (J.N. *et al.*, unpublished). Given its high level of expression, CD133 has received considerable attention. For example, it has been shown that CD133⁺ cells purified from cultured cancer cells or tumors and transplanted into immunocompromised NOD/SCID mice give rise to carcinomas phenotypically similar to the primary tumors from which they were derived (84, 94, 127). In addition, whereas as many as 10⁷ cultured hepatocarcinoma cells were required to form tumors in NOD/SCID mice, only 10³ or less CD133⁺ cells were required to form tumors (127). Similar results have been obtained using breast CSCs (124). Shmelkov and colleagues have recently demonstrated that CD133⁻ cells can also form tumors in NOD/SCID mice. However, in this study they also showed that CD133⁺ cancer cells have much greater metastatic potential than their CD133⁻ counterparts (103). Even if CD133 may not always be a *bona fide* marker of CSCs, it has a role for suggesting an increase of the level of stemness of cell cultures grown as spheres or, in other words, as a marker of enrichment of sphere cultures in CSCs. Table 2 documents some of the reports proposing a role of CD133 in tumorigenic properties of cancer cells as well as those opposing this notion.

TABLE 2. REPORTS DOCUMENTING THE TUMORIGENIC PROPERTIES OF CD133⁺ CELLS AND THOSE OPPOSING THIS VIEW

Type of tumor	Positive	Negative
Brain tumors	105	
Gliomas, glioblastomas	57, 65, 96	
Medulloblastomas	104	
Breast tumors	124	
Colorectal tumors	35, 84, 94	22, 103
Endometrial cancer	80	
Gallbladder carcinomas	101	
Hepatocellular carcinoma	59, 110, 127	97
Melanomas	77	
Mesotheliomas	J.N. <i>et al.</i> , unpublished	
Non-small-cell lung carcinomas	117	
Oral squamous cell carcinomas	128	
Pancreatic cancer	85	
Prostate cancer	18, 73	89
Ovarian cancer	44	

CD133, Avoidance of Immunosurveillance, and Resistance to Stress-Induced Apoptosis

In this review, we hypothesize that CSCs, escaping elimination by the immune system, are sculpted to efficiently form tumors. This is based on the immunoediting theory and the cancer stem cell theory as well as related studies supporting these paradigms as described in the previous sections. As a result, surviving transformed cells are likely to be selected to exert enhanced levels of stemness. It is also possible that during immunoediting, the pressure of the forces of the immune system causes modifications in cancer cells such that they acquire cancer stem cell-like characteristics, which enable them to survive. This would suggest that CSCs feature low levels of antigen-presenting capacity as well as low levels of NK ligands. In this regard, Wu and colleagues investigated the immunogenicity of CD133⁺ cells in two human astrocytoma and two glioblastoma multiformae samples by flow cytometry and revealed that the majority of CD133⁺ cells do not express detectable major histocompatibility (MHC) Class I or NK cell-activating ligands (125). While MHC Class I expression is required for CD8⁺ T cell-mediated cytotoxicity, the converse is true for NK cells, which recognize and attack cells lacking MHC class I ligands (61, 121). Although CD133⁺ cells do not express MHC Class I ligands, which would make them susceptible to NK-mediated cytotoxicity, the absence of NK cell-activating ligands on CD133⁺ cells could contribute to their escape from immune surveillance by these innate immune cells.

Accordingly, studies on embryonic stem (ES) cell immunogenicity revealed that ES cells are immune-privileged as well and are readily transplanted across MHC barriers without or with only minimal immunosuppression (26, 31, 59). Hence, it would appear that CSCs share properties similar to stem cells, including ES cells. It is, therefore, also possible that the immune system fails to recognize these cells as a potential threat since their malignant status remains undetected.

CSCs and the Role of CD133

CD133 expression is not just restricted to CSCs in that, for example, both CD133⁺ and CD133⁻ metastatic colon cancer cells are equally capable of initiating tumors (103). It would appear more likely that CD133 expression represents a transient state that CSCs are capable of undergoing. Thus, the CD133⁺ population in the normal intestinal crypt is part of a larger stem cell/transit amplifying progenitor compartment that is susceptible to neoplastic transformation after which

CD133 expression reduces to a small percentage of cancer cells (131). Notwithstanding, whether CD133 expression is essential for the emergence of tumors remains unclear.

Thus far, the exact role of CD133 in CSCs has not been resolved. However, CD133 family molecules show a highly restricted localization on plasma membrane protrusions of epithelial and other cell types (hence the name "prominin-1"), where they are associated with cholesterol-rich lipid rafts, indicating a role in the organization of plasma membrane topology (19, 20, 76, 95, 122). The inclusion in cholesterol lipid rafts, which are important for cell growth signaling, is consistent with the association of CD133 with important stem cell growth signaling pathways. As well as being a stem cell marker (74), CD133 has been proposed to be involved in several signaling pathways (76, 115), including the Notch pathway (30, 111) and the related sonic HEDGEHOG/GLI pathway (17), which are of significant importance in normal stem cell as well as CSC proliferation and self-renewal. A role for CD133 in signal transduction is consistent with the observations that the protein is phosphorylated on cytoplasmic tyrosine residues 828 and 852 of CD133 in human cancer cells by Src and Fyn tyrosine kinases (10). Recently, a link between the Notch pathway and CD133 has been corroborated by findings that blocking the Notch pathway (using an inhibitor of γ -secretase) promoted down-regulation of CD133, which then resulted in prevention of such cells to form spheres and tumors in immunocompromized animals (30, 111). Moreover, we have observed that CD133-positive mesothelioma cells, grown as mesospheres, are also typified by increased Notch expression. We also found higher expression of CD47 in mesospheres (J.N. *et al.*, unpublished), a marker of resistance of cancer cells to be phagocytosed by macrophages that may protect CSCs from the immune system (14, 56), further suggesting a link between CD133 expression and the propensity of such cells to evade the immune surveillance.

CD133 is likely also involved in adaptive changes in cellular bioenergetic metabolism, providing the CSCs with increased survival advantages. Thus, CD133 expression is greatly increased in the presence of high glucose, whose uptake is facilitated by CD133 (130). It has now been documented that CD133 also represents a state of hypoxic induction in CSCs and may be indicative of a side population of stem cells, thereby transient in nature depending on the prevailing microenvironment and conditions these cells are exposed to and influenced by (68, 109). Consistent with this role, CD133-expressing CSC populations have been commonly observed to show greater proliferative potential than their CD133⁻ counterparts (7, 125). Further, increased exposure to hypoxia results in stabilization of the hypoxia-inducible factor-1 α (HIF-1 α) and is linked to the increase in the level of CD133 (43, 70, 109). Hypoxia-induced activation of HIF-1 α and the increase in the expression of CD133 requires activation of the kinase Akt. Another piece of evidence linking CD133 to Akt signaling comes from a recent article by Takenobu *et al.* (114), who showed that knocking down CD133 in neuroblastoma cells deregulated the Akt as well as mitogen-activated protein (MAP) kinase pathway and, interestingly, resulted in much slower growth of tumors in nude mice than found for the parental cells. In these studies, CD133 was also found to enhance the survival of the neuroblastoma cells in spheres, further linking CD133 to the stemness phenotype. Since Akt is a central regulator of the survival pathways, promoting survival and

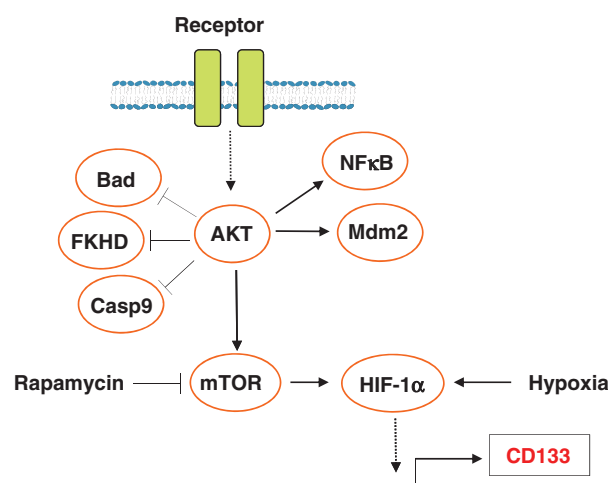


FIG. 2. Possible link between resistance of cancer stem-like cells (CSCs) to apoptosis and the level of CD133. Within the hypoxic microenvironment of pretumorous mass or carcinoma, HIF-1 α becomes stabilized, which is linked to increased expression of CD133. This process requires the activation of the central prosurvival kinase Akt, which is responsive, generally, to mitogenic signaling. Akt itself suppresses the activity/activation of the proapoptotic pathways *via* phosphorylating the Bcl-2 family protein Bad, caspase-9, and members of the forkhead (FKHD) transcription factors, such as FoxO1 that is involved in transcriptional activation of the Bcl-2 family member Noxa (120). Akt also activates several important prosurvival pathways, involving the transcription factor NF- κ B, the Mdm2 protein suppressing the function of p53, and the molecular target of rapamycin (mTOR). mTOR positively controls the function of hypoxia-inducible factor-1 α (HIF-1 α), further promoting the expression of CD133. Although not completely understood at present, these notions provide a possible explanation of the association of CD133 with the prosurvival/antiapoptotic status of CD133-positive cancer cells (adapted from ref. 68). (To see this illustration in color the reader is referred to the web version of this article at www.liebertonline.com/ars).

proliferation while suppressing apoptosis, we propose an emerging picture linking the high level of CD133 and increased resistance to apoptosis (Fig. 2). Further, the increased activity of HIF-1 α and higher expression of CD133 connects this phenotype to the mitochondrial bioenergetics, since HIF-1 is known as a regulator of a variety of mitochondrial bioenergetics pathways as well as a sensor of oxygen (93, 99).

As indicated above, high levels of CD133 expression have been associated with resistance of CSCs to apoptosis (6, 17, 36, 37). This is directly supported by the observation that down-regulation of CD133 sensitizes cancer cells to apoptosis (17). Analysis of CD133⁺ and CD133⁻ glioma cell lines prepared from primary human glioblastoma cells identified a number of genes differentially expressed in the two subpopulations (65). The analysis showed that the antiapoptotic proteins Bcl-2, Bcl-x_L, FLIP, and members of the inhibitors of apoptosis family of proteins (c-IAP1, c-IAP2, XIAP, and survivin) were highly up-regulated in CD133⁺ cells, whereas the expression of the proapoptotic protein Bax was slightly down-regulated when compared to their CD133⁻ counterparts. Of all the up-regulated genes, FLIP exerted the highest expression with up to 300-fold increase in the CD133⁺ cells when compared to the CD133⁻ cells (Table 3). This is of great interest, since FLIP (as

TABLE 3. EXAMPLES OF DIFFERENTIALLY EXPRESSED APOPTOSIS-ASSOCIATED GENES IN CD133⁺ AND CD133⁻ GLIOBLASTOMA CELLS (ADAPTED FROM REF. 65)

Gene name	Fold change between CD133 ⁺ and CD133 ⁻ cells
FLIP	294 ± 26
cIAP1	39 ± 3.5
XIAP	21.9 ± 2.2
Bcl-2	13.9 ± 1
Bcl-x _L	5.6 ± 4
cIAP2	3 ± 0.3
Survivin	1.6 ± 0.1
Bax	0.33 ± 0.03

discussed above) is an inhibitor of death receptor-induced apoptosis (55, 116). Its increased expression could be a consequence of acquisition of the malignant phenotype of cells, requiring an advantage to survive the tumor immune surveillance.

Further support for the survival-promoting effects of CD133 on CSCs stems from studies where CD133⁺ cells were also found to be resistant to cytotoxic chemotherapeutic drugs, including etoposide, paclitaxel, temozolomide, and carboplatin, whereas their autologous CD133⁻ counterparts were susceptible to these agents (65). Despite the new insights into CSCs, the reasons for their resilience to therapy are not well understood. However, recent research has indicated possible molecular determinants underlying this resistance (119). Several studies have shown that CSCs, epitomized in this case by CD133⁺ cells, exhibit increased expression of antiapoptotic proteins (FLIP, Bcl-2, Bcl-x_L, and the IAP family members) and a low level of expression of proapoptotic proteins (including Bax) (57, 65, 100). We reported that CD133^{high} subpopulations of cancer cells (including both Jurkat T lymphoma and breast cancer cells) possess high

levels of the antiapoptotic protein FLIP relative to their CD133^{low} counterparts, which makes them resistant to TRAIL-mediated apoptosis (132). By contrast, we found that CD133^{low} cells were more susceptible to killing by TRAIL. This result can be reconciled with the notion that TRAIL-induced apoptosis is one of the key mechanisms by which the immune system eliminates transforming cells. In addition, the TRAIL-dependent apoptotic cascade primarily affects malignant cells and, as a rule, has only marginal effects, if any, on normal (nonmalignant) cells (63). However, this is not the case for CSCs (or at least for CD133^{high} cancer cells), as we have demonstrated. Nevertheless, down-regulation of FLIP in CD133^{high} Jurkat T lymphoma or breast cancer cells caused their sensitization to apoptosis induced by TRAIL in both cell types (132). This finding is further corroborated by results of another report documenting that down-regulation of FLIP in TRAIL-resistant melanoma cells was sufficient to make these cells susceptible to the apoptogen (40).

In a separate study on CSCs, we observed that stress in the form of nutrient deprivation, cell crowding, or hypoxia results in apoptosis induction (J.N. *et al.*, unpublished). Interestingly, the surviving population showed an increased expression of CD133 in agreement with similar findings of others (43). We also observed that exposure of cancer cells growing in monolayer cultures to the same stresses results in rapid up-regulation of CD133 such that the resulting cells were also protected from apoptosis for extended periods of time. These processes, involving differential expression of CD133, may signify more general properties of CSCs, since we observed similar findings with diverse cancer cells, including Jurkat T lymphoma, breast cancer, and mesothelioma cell lines (J.N. *et al.*, unpublished). This suggests that either the cells that survive already display the phenotype of CSCs or that the pressure of the stressful environment favors cancer cell populations acquiring increased cancer stem cell-like properties to survive. This latter possibility has been re-

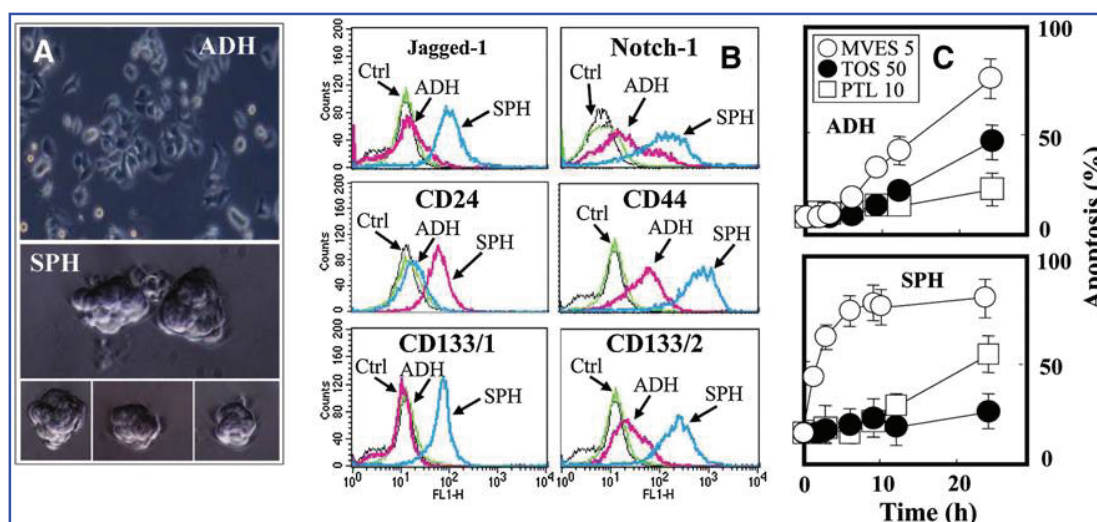


FIG. 3. Breast cancer stem-like cells are susceptible to mitochondrially targeted vitamin E succinate (MitoVES). MCF7 cells were grown as adherent cells (ADH) or spheres (SPH) (A) and assessed for the expression of several CSC markers, including CD133 (both isotypes), CD44, CD24, Jagged-1, and Notch-1 (B). The adherent and sphere cells were exposed to α -tocopheryl succinate (α -TOS), its mitochondrially targeted analog (MitoVES), or pathenolide (PTL) at the concentrations (μ M) and times shown, and assessed for apoptosis induction (C). (To see this illustration in color the reader is referred to the web version of this article at www.liebertonline.com/ars).

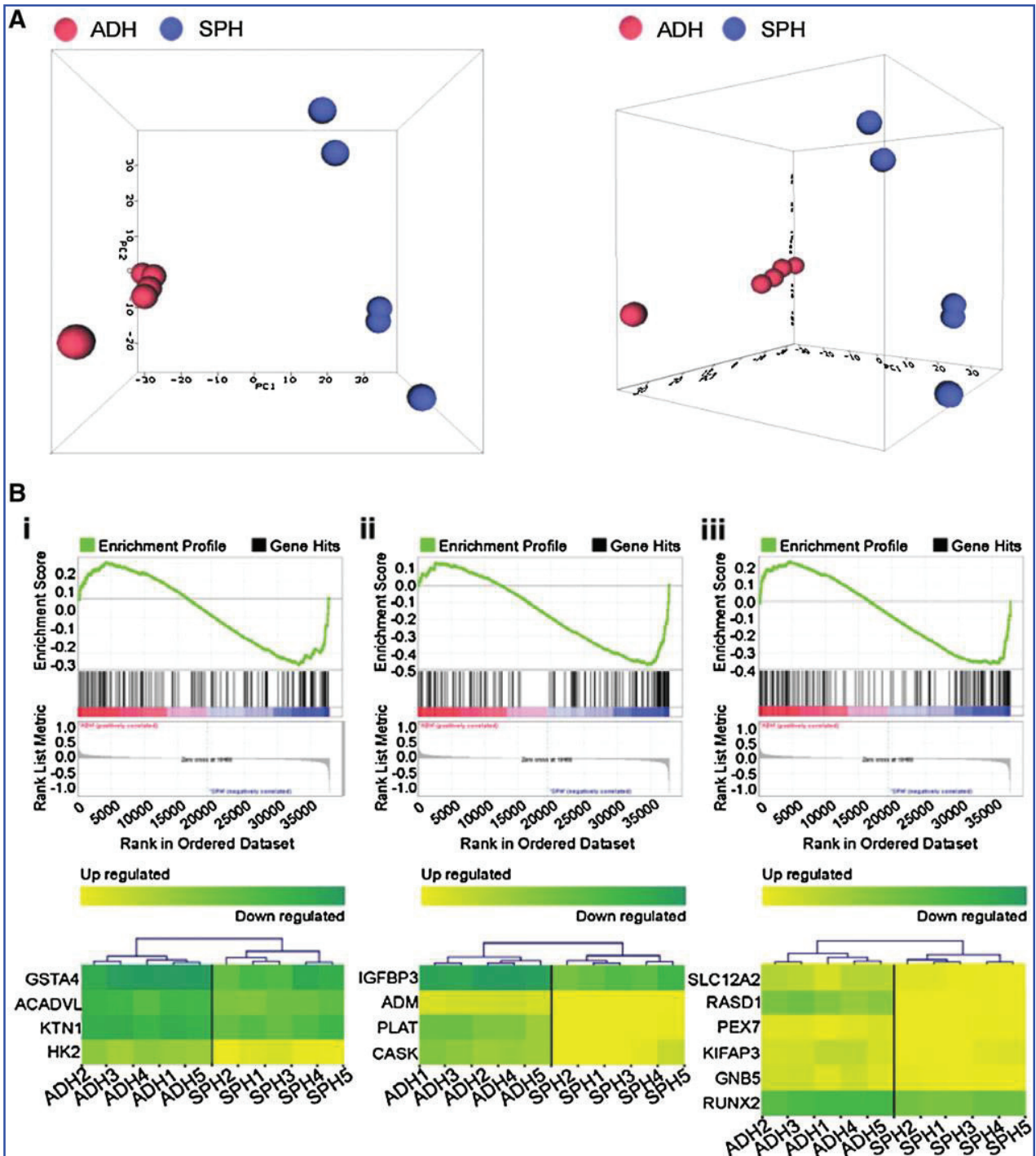


FIG. 4. Microarray data characterize mammospheres as a phenotype with increased stemness. (A) Principle components analysis of adherent (ADH) and mammosphere (SPH) MCF7 cells shows that each phenotype clusters together. Principle components analysis projections are represented in a two-dimensional (left) and a three-dimensional (right) manner. (B) Gene set enrichment analysis plots show enrichment of (i) embryonic stem cell ($p=0.044$, false discovery rate [FDR]=0.046), (ii) neuronal stem cell ($p=0.001$, FDR=0.006), and (iii) hematopoietic stem cell ($p=0.075$, FDR=0.085) gene sets in mammosphere but not adherent cultures. Each vertical line on the enrichment plot represents a probe in the corresponding gene set. The left to right position of vertical lines indicates the relative position genes from ESC, NSC, and HSC gene sets within the rank-ordered list of the 37,805 probes present on the HumanHT-12 BeadChip. The first probe on the left represents the most upregulated probe in adherent samples and the last on the right represents the most upregulated probe in the sphere forming samples. Probes in the middle are not differentially expressed. (To see this illustration in color the reader is referred to the web version of this article at www.liebertonline.com/ars).

cently supported by the studies of Griguer and colleagues, who showed that CD133 expression was up-regulated in response to stress by hypoxia or by mitochondrial respiratory inhibition using rotenone (43). This finding can be reconciled with the reported high level stabilization of HIF-1 α under normoxic conditions in CD34⁺ and CD133⁺ hematopoietic stem cells, probably *via* increased levels of (mitochondrial) ROS generation, suggesting that the cells are undergoing adaptation to promote their enhanced survival propensity (91).

Hence, cancer cell selection by the immune system or prevailing conditions (*e.g.*, oxidative or hypoxic stress) leads to their acquisition of increased level of stemness, epitomized by elevated CD133 expression, being more difficult to efficiently eliminate using current therapies. These cells are also capable of forming second-line tumors, clonally derived from the resistant CD133⁺ CSCs, and such carcinomas are expected to be much more difficult to treat.

Where to from Here?

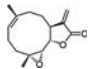
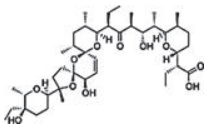
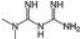
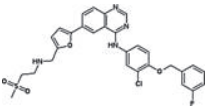
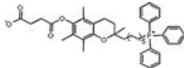
As stated above, CD133 may be either a factor that selects cancer cells (possibly with high levels of stemness) for survival, or readily increases when cancer cells are challenged by stressful/unfavorable selection pressures leading to increased CD133 expression associated with greater resistance of cancer cell subpopulations to the stress (in very broad terms). It is unclear at this stage, though, whether there is a causal (or, better, functional) link between the level of CD133 and resistance of cancer cells to stress, most likely involving mitochondria. Based on the evidence presented here, we more strongly favor a role for expression of CD133 in the induction of apoptosis-regulating genes such that CSCs exhibit greater likelihood of survival. We also believe it more plausible that malignant cells develop resistance during immunoediting to escape immunosurveillance first, and then CSCs with initially low levels of CD133 emerge that rapidly increases when the cells are challenged by the en-

suing unfavorable or stressful growth conditions. However, although unlikely, current data cannot completely rule out a concomitant increase of CD133 and acquisition of a resistant phenotype.

It is unlikely that the selection of CSCs that survive the challenge (including immunosurveillance or, later on, stress) is a random, uncoordinated process. However, the molecular basis is not known whereby CSCs are selected for survival, and one would reason that CD133 is not the only key element that dictates the very early cellular responses to the selection pressure(s). Understanding how cells are selected is not only of fundamental importance for our understanding of those events occurring within cancer cell populations, but it also has far-reaching implications for clinical applications to anticancer therapy. Thus, we propose that CD133 remains a valid marker for predicting subpopulation of cancer cells that will show enhanced survival to immune and other stressful challenges. This is supported, for example, by findings that CD133⁺ cells isolated from tumors show much greater resistance to apoptosis than their CD133⁻ counterparts (12, 16, 65). Approaches that focus on targeting CD133, such as therapy resulting in its down-regulation and the consequential enhanced susceptibility of these cells to apoptosis, both mediated *via* the death receptor and mitochondrial mechanisms (17), are warranted.

Gene therapy is, scientifically, a very elegant, although challenging approach. Silencing of the expression of the CD133 gene in experimental animals, such as transgenic mice with spontaneously generated tumors, may prove superior in preventing selection of CD133⁺ cancer cell resistance to apoptosis during the process of immunoediting. On the practical level, however, this can be difficult to achieve due to potential effects on other bystander cells that are not the desired target. Such approaches ought to be first tested in animals with experimental tumors, such as transgenic, immunocompetent mice with spontaneously arising tumors. In these models, stable transfection with a plasmid or a viral

TABLE 4. EXAMPLES OF COMPOUNDS THAT KILL CANCER STEM-LIKE CELLS

Name	Structure	Type of tumor	Mechanism of action	Reference
Parthenolide		Leukemia Breast cancer Prostate cancer	Inhibition of NF κ B	46, 49, 58
Salinomycin		Breast cancer	Potassium ionophore	45
Metformin		Breast cancer	Effect on energy metabolism	52
Lapatinib		Breast cancer	Dual inhibitor of receptor tyrosine kinases	60
MitoVES		Breast cancer, mesothelioma	Generation of ROS by targeting complex II	J.N. <i>et al.</i> , unpublished

MitoVES, mitochondrially targeted vitamin E succinate; ROS, reactive oxygen species.

vector carrying *CD133* shRNA targeted to the tumor-prone tissue could be tested. This approach, if successful, will provide direct evidence for the pathophysiological role of *CD133* and indicate a possibility of gene therapy to eliminate malignant *CD133*⁺ cells.

Another way for dealing with *CD133*⁺ cancer cells is to design pharmacological agents that would kill such cells with high efficacy and selectivity without affecting normal cells. To date, only several compounds have been published and shown to possess these features, a prime example being parthenolide (PTL), a drug isolated from the plant feverfew with *NFκB* inhibitory activity (51). PTL was found to be relatively efficient in killing leukemia stem cells (46, 49) and, also, breast CSCs represented by mammospheres (MS) de-

rived from breast cancer cell lines (129). The latter include MS derived from the human breast cancer cell line MCF7, which were resistant to a range of established anticancer agents. We observed similar susceptibility of MCF7 cell-derived MS to PTL in our laboratory, and have also found that these MS exhibited high level of expression of both isoforms of *CD133* relative to their adherent counterparts (J.N. *et al.*, unpublished). High-throughput screening using *CD44*^{high}/*CD24*^{low} cells uncovered salinomycin as an efficient agent that exerted selective toxicity toward breast CSCs, although a relationship to the level of *CD133* has not been documented (45).

We have recently designed novel anticancer drugs from the family of mitocans (81–83), epitomized by the mi-

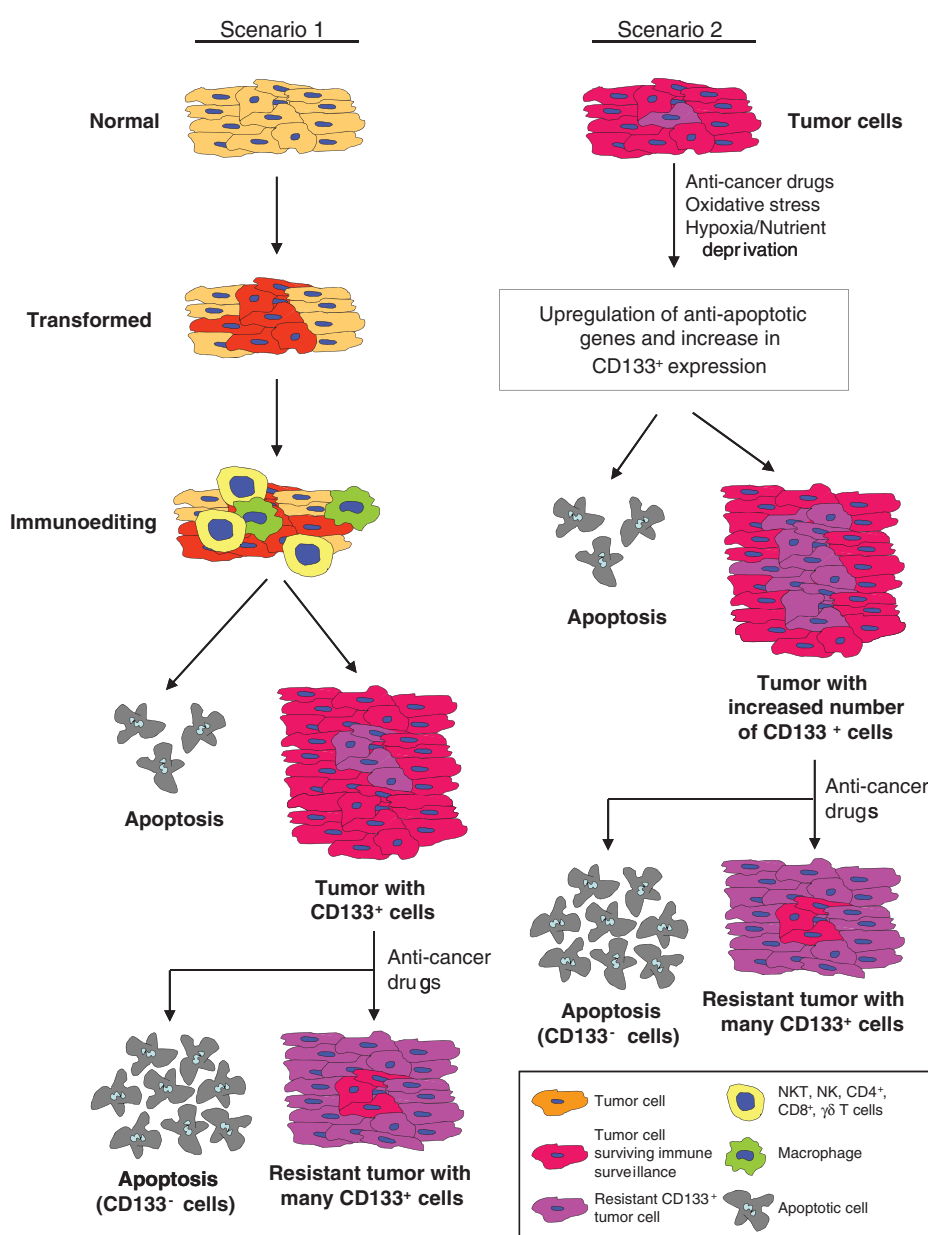


FIG. 5. *CD133* selects cancer cells for resistance to apoptosis.

We propose two scenarios describing the origin of the resistant, *CD133*⁺ cancer (stem-like) cells in tumors. Scenario 1 involves the role of the immune system, which, *via* the process of immunoeediting, selects cells that are resistant to immune surveillance or escape being intercepted and eliminated by the immune system. These cells form a tumor with low number of *CD133*⁺ cancer cells. Upon challenge of the tumor with anticancer drugs, the *CD133*⁻ cells are killed *via* apoptosis, unless they can respond rapidly by up-regulating *CD133* and antiapoptotic genes (plus, most likely, down-regulating proapoptotic genes). The *CD133*⁺ cells survive and the resulting tumor will be highly enriched in these apoptosis-resistant cells. Scenario 2 is very similar to Scenario 1. However, it is based on results obtained largely with cell lines. Accordingly, tumor cells, when under the pressure of oxidative stress, anticancer drugs or hypoxia (most likely in combination with nutrient deprivation), rapidly up-regulate expression of *CD133* in a subpopulation of the cells, and this is associated with differential regulation of apoptosis-modulating genes. Therefore, in the forthcoming therapy, the intervention causes killing of non-resistant cells, whereas the resistant (*CD133*⁺) cells survive and constitute the majority of cells within the resulting tumor, highly recalcitrant to anticancer agents (adapted from ref. 108). (To see this illustration in color the reader is referred to the web version of this article at www.liebertonline.com/ars).

tochondrially targeted vitamin E succinate. These agents specifically target mitochondria and are much more efficient than the corresponding mitochondrial-untargeted parental compounds, while preserving selectivity for cancer cells (24). Mitochondrially targeted compounds exert very high efficacy not only against fast proliferating cancer cells, but also against their cancer stem-like counterparts typified by high levels of CD133 expression and grown as spheres (Figs. 3 and 4) (J.N. *et al.*, unpublished). Therefore, mitocans show substantial promise to be developed into anticancer drugs that can efficiently kill the recalcitrant CD133⁺ cells, and we are currently investigating the molecular mechanism of susceptibility of CSCs to certain mitocans, with a special focus on mitochondrially targeted vitamin E succinate. A representative list of compounds that have been suggested to kill CSCs, often with increased level of expression of CD133, is shown in Table 4, with some of these agents acting at the level of mitochondria.

Even though CD133 seems to be the most important marker of wide interest at the moment for many CSC types, there is a possibility that other CSC markers may play significant roles in carcinogenesis and in the evasion of the immune system. Nevertheless, we believe that the escape mechanisms of cells presenting CD133 or CD44 and other markers should be very similar if not the same as that of the cancer cells (CSCs) that we have discussed here as being capable of evading the immune surveillance. Targeting of these CSCs [found, *e.g.*, in breast cancer (4), prostate cancer (18), and pancreatic cancer (64)] should also be the same as for CSCs that express the CD133 marker. Since not much is known about the function of CD44, in particular its role in CSCs, CD44 might not be the best target. However, targeting CSCs with pharmacological agents should have a similar affect (31). For example, in a recent study, we found that mitocans (23, 81, 83) showed a considerable efficacy against CD44⁺ CSCs represented by MS (J.N. *et al.*, unpublished). Therefore, this approach also appears promising for CSCs that are characterized by markers other than CD133 (78). Collectively, while CD133 appears the most wide-spread marker of CSCs and a potential target for therapeutic approach (or, rather, targeting mitochondria of CD133-positive cells), other markers should not be excluded.

Conclusions and Future Perspectives

We present here a hypothesis according to which the surface receptor CD133 selects cancer cells to survive immunosurveillance as well as stress-induced apoptotic challenges. This hypothesis is two-pronged (Fig. 5): (i) Pre-cancerous cells are under immunosurveillance, and the cells that emerge from the process of immunoediting are resistant to killing by apoptotic inducers, many of which are established anticancer agents. This population of CSCs shows high level of CD133 expression. (ii) Within cancer cells (including cancer cell lines), there are subpopulations (or a subpopulation) that, upon being challenged with inducers of apoptosis (stress, anticancer agents, *etc.*), will rapidly increase CD133 expression and, associated with this, up-regulation of anti-apoptotic and down-regulation of proapoptotic genes.

Regardless of whether CD133 is functionally linked to resistance of cancer cells to apoptosis or is co-upregulated in cancer cells with a more pronounced stemness phenotype,

typified by the propensity to escape killing by apoptosis, high levels of CD133 expression may be considered a marker of more aggressive and more resistant tumors (126). To overcome such resistance, new methodological approaches need to be developed. One approach that appears plausible, given the initial results, is mitochondrial targeting. A class of novel agents is being developed that act on mitochondria and that are modified so that they accumulate in these organelles. These agents, tagged with cationic group (9), are being proved as more efficient in killing cancer cells than their untagged counterparts (9, 24). Whether such compounds are efficient in killing CSCs represented by CD133^{high} populations, as indicated by our initial results (either alone or in combination with other agents), is yet to be fully documented, although our pilot data are encouraging.

One plausible approach to efficient tumor therapy can be documented by the following example. We have used microarray analysis to characterize the stemness of several types of cancer cells grown as spheres, including breast and prostate cancer as well as malignant mesotheliomas, all with increased level of CD133 in the sphere phenotype (J.N. *et al.*, unpublished). This resulted in the confirmation of increased stemness in all three types of cancer. We found that of the upregulated pathways the three types of CSCs shared the tryptophan metabolism (represented by increased expression of indoleamine-2,3-dioxygenase, IDO). This finding would imply that CSCs deplete their neighborhood of tryptophan. In this manner, they may protect themselves from being killed by cells of the immune system (66, 79). Thus, inhibitors of IDO are being tested as anticancer agents (39, 54). We dare speculate that a highly efficient way to kill CSCs with high levels of CD133 may be accomplished by a combinatorial treatment of such cells with agents like mitochondrially targeted compounds (mitocans) and inhibitors of IDO. In other words, a drug that has high propensity of killing cancer cells by targeting their mitochondria in combination with agents that may enhance the tumor immune surveillance may present the magic bullet of optimal anticancer therapeutic modality, hitting the Achilles' heel of cancer.

Acknowledgments

J.N. was supported in part by grants from the Australian Research Council, the Cancer Council (Queensland), and the Grant Agency of the Czech Republic (204/08/0811, 305/07/1008); E.A. was supported in part by the Fullbright Fellowship; R.Z. was supported in part by a Ph.D. scholarship from the National Breast Cancer Foundation of Australia.

References

1. Adam-Vizi V and Chinopoulos C. Bioenergetics and the formation of mitochondrial reactive oxygen species. *Trends Pharmacol Sci* 27: 639–645, 2006.
2. Aguirre-Ghiso JA. Models, mechanisms and clinical evidence for cancer dormancy. *Nat Rev Cancer* 7: 834–846, 2007.
3. Albayrak T, Albayrak T, Scherhammer V, Schoenfeld N, Braziulis E, Mund T, Bauer MK, Scheffler IE, and Grimm S. The tumor suppressor cybL, a component of the respiratory chain, mediates apoptosis induction. *Mol Biol Cell* 4: 3082–3096, 2003.

4. Al-Hajj M, Wicha MS, Benito-Hernandez A, Morrison SJ, and Clarke MF. Prospective identification of tumorigenic breast cancer cells. *Proc Natl Acad Sci U S A* 100: 3983–3988, 2003.
5. Bancroft GJ, Schreiber RD, and Unanue ER. Natural immunity: a T-cell independent pathway of macrophage activation, defined in the scid mouse. *Immunol Rev* 124: 5–24, 1991.
6. Bao S, Wu Q, McLendon RE, Hao Y, Shi Q, Hjelmeland AB, Dewhirst MW, Bigner DD, and Rich JN. Glioma stem cells promote radioresistance by preferential activation of the DNA damage response. *Nature* 444: 756–760, 2006.
7. Beier D, Hau P, Proescholdt M, Lohmeier A, Wischhusen J, Oefner PJ, Aigner L, Brawanski A, Bogdahn U, and Beier CP. CD133⁺ and CD133⁻ glioblastoma-derived cancer stem cells show differential growth characteristics and molecular profiles. *Cancer Res* 67: 4010–4015, 2007.
8. Bhatia M, Bonnet D, Murdoch B, Gan OI, and Dick JE. A newly discovered class of human hematopoietic cells with SCID-repopulating activity. *Nat Med* 4: 1038–1045, 1998.
9. Biassutto L, Dong LF, Neuzil J, and Zoratti M. Mitochondrially targeted anti-cancer drugs. *Mitochondrion* 10: 670–681, 2010.
10. Boivin D, Labbé D, Fontaine N, Lamy S, Beaulieu E, Gingras D, and Béliveau R. The stem cell marker CD133 (prominin-1) is phosphorylated on cytoplasmic tyrosine-828 and tyrosine-852 by src and fyn tyrosine kinases. *Biochemistry* 48: 3998–4007, 2009.
11. Bonnet D and Dick JE. Human acute myeloid leukemia is organized as a hierarchy that originates from a primitive hematopoietic cell. *Nat Med* 3: 730–737, 1997.
12. Capper D, Gaiser T, Hartmann C, Habel A, Mueller W, Herold-Mende C, von Deimling A, and Siegelin MD. Stem-cell-like glioma cells are resistant to TRAIL/Apo2L and exhibit down-regulation of caspase-8 by promoter methylation. *Acta Neuropathol* 117: 445–456, 2009.
13. Chakraborti T, Das S, Mondal M, Roychoudhury S, and Chakraborti S. Oxidant, mitochondria and calcium: an overview. *Cell Signal* 11: 77–85, 1999.
14. Chan KS, Espinosa I, Chao M, Wong D, Ailles L, Diehn M, Gill H, Presti J Jr., Chang HY, van de Rijn M, Shortliffe L, and Weissman IL. Identification, molecular characterization, clinical prognosis, and therapeutic targeting of human bladder tumor-initiating cells. *Proc Natl Acad Sci U S A* 106: 14016–14021, 2009.
15. Chandra J, Samali A, and Orrenius S. Triggering and modulation of apoptosis by oxidative stress. *Free Radic Biol Med* 29: 323–333, 2000.
16. Chen YC, Hsu HS, Chen YW, Tsai TH, How CK, Wang CY, Hung SC, Chang YL, Tsai ML, Lee YY, Ku HH, and Chiou SH. Oct-4 expression maintains cancer stem-like properties in lung cancer-derived CD133-positive cells. *PLoS ONE* 3: e2637, 2008.
17. Clement V, Sanchez P, de Tribolet N, Radovanovic L, Ruiz I, and Altaba A. HEDGEHOG-GLI1 signaling regulates human glioma growth, cancer stem cell self-renewal, and tumorigenicity. *Curr Biol* 17: 165–172, 2007.
18. Collins AT, Berry PA, Hyde C, Stower MJ, and Maitland NJ. Prospective identification of tumorigenic prostate cancer stem cells. *Cancer Res* 65: 10946–10951, 2005.
19. Corbeil D, Marzesco AM, Wilsch-Bräuninger M, and Huttner WB. The intriguing links between prominin-1 (CD133), cholesterol-based membrane microdomains, remodeling of apical plasma membrane protrusions, extra-cellular membrane particles, and (neuro)epithelial cell differentiation. *FEBS Lett* 584: 1659–1664, 2010.
20. Corbeil D, Roper F, Fargeas CA, Joester A, and Huttner WB. Prominin: a story of cholesterol, plasma membrane protrusions and human pathology. *Traffic* 2: 82–91, 2001.
21. Danial NN and Korsmeyer SJ. Cell death: critical control points. *Cell* 116: 205–219, 2004.
22. Dittfeld C, Dietrich A, Peickert S, Hering S, Baumann M, Grade M, Ried T, and Kunz-Schughart LA. CD133 expression is not selective for tumor-initiating or radioresistant cell populations in the CRC cell line HCT-116. *Radiother Oncol* 94: 375–383, 2010.
23. Dong LF, Freeman R, Liu J, Zobalova R, Marin-Hernandez A, Stantic M, Rohlena J, Valis K, Rodriguez-Enriquez S, Butcher B, Goodwin J, Brunk UT, Witting PK, Moreno-Sanchez R, Scheffler IE, Ralph SJ, and Neuzil J. Suppression of tumour growth *in vivo* by the mitocan α -tocopheryl succinate requires respiratory complex II. *Clin Cancer Res* 15: 1593–1600, 2009.
24. Dong LF, Jameson VJA, Tilly D, Cerny J, Mahdavian E, Marín-Hernández A, Hernández-Esquivel L, Rodríguez-Enríquez S, Stursa J, Witting PK, Stantic B, Rohlena J, Truksa J, Kluckova K, Dyason JC, Ledvina M, Salvatore BA, Moreno-Sánchez R, Coster MJ, Ralph SJ, Smith RAJ, and Neuzil J. Mitochondrial targeting of vitamin E succinate enhances its pro-apoptotic and anti-cancer activity via mitochondrial complex II. *J Biol Chem* 286: 3717–3728, 2011.
25. Dong LF, Low P, Dyason J, Wang XF, Prochazka L, Witting PK, Freeman R, Swettenham E, Valis K, Liu J, Zobalova R, Turanek J, Spitz DR, Domann FE, Scheffler IE, Ralph SJ, and Neuzil J. α -Tocopheryl succinate induces apoptosis by targeting ubiquinone-binding sites in mitochondrial respiratory complex II. *Oncogene* 27: 4324–4335, 2008.
26. Drukker M, Katz G, Urbach A, Schuldiner M, Markel G, Itskovitz-Eldor J, Reubinoff B, Mandelboim O, and Benvenisty N. Characterization of the expression of MHC proteins in human embryonic stem cells. *Proc Natl Acad Sci U S A* 99: 9864–9869, 2002.
27. Dunn GP, Bruce AT, Ikeda H, Old LJ, and Schreiber RD. Cancer immunoediting: from immunosurveillance to tumor escape. *Nat Immunol* 3: 991–998, 2008.
28. Dunn GP, Old LJ, and Schreiber RD. The immunobiology of cancer immunosurveillance and immunoediting. *Immunity* 21: 137–148, 2004.
29. Dunn GP, Old LJ, and Schreiber RD. The three Es of cancer immunoediting. *Annu Rev Immunol* 22: 329–360, 2004.
30. Fan X, Khaki L, Zhu TS, Soules ME, Talsma CE, Gul N, Koh C, Zhang J, Li YM, Maciaczyk J, Nikkhah G, Dimeco F, Piccirillo S, Vescovi AL, and Eberhart CG. Notch pathway blockade depletes CD133-positive glioblastoma cells and inhibits growth of tumor neurospheres and xenografts. *Stem Cells* 28: 5–16, 2010.
31. Fändrich F, Lin X, Chai GX, Schulze M, Ganten D, Bader M, Holle J, Huang DS, Parwaresch R, Zavazava N, and Binas B. Pre-implantation-stage stem cells induce long-term allogeneic graft acceptance without supplementary host conditioning. *Nat Med* 8: 107–108, 2002.
32. Fang D, Nguyen TK, Leishear K, Finko R, Kulp AN, Hotz S, Van Belle PA, Xu X, Elder DE, and Herlyn M. A tumorigenic subpopulation with stem cell properties in melanomas. *Cancer Res* 65: 9328–9337, 2005.
33. Fargeas CA, Corbeil D, and Huttner WB. AC133 antigen, CD133, prominin-1, prominin-2, etc.: prominin family gene

- products in need of a rational nomenclature. *Stem Cells* 21: 506–508, 2003.
34. Fargeas CA, Fonseca A-V, Huttner WB, and Corbeil D. Prominin-1 (CD133)-from progenitor cells to human diseases. *Future Lipidol* 1: 213–225, 2006.
 35. Ferrand A, Sandrin MS, Shulkes A, and Baldwin GS. Expression of gastrin precursors by CD133-positive colorectal cancer cells is crucial for tumour growth. *Biochim Biophys Acta* 1793: 477–488, 2009.
 36. Frank NY, Margaryan A, Huanget Y, Schatton T, Waaga-Gasser AM, Gasser M, Sayegh MH, Sadee W, and Frank MH. ABCB5-mediated doxorubicin transport and chemoresistance in human malignant melanoma. *Cancer Res* 65: 4320–4333, 2005.
 37. Frank NY, Schatton T, and Frank MH. The therapeutic promise of the cancer stem cell concept. *J Clin Invest* 120: 41–50, 2010.
 38. French LE and Tschopp J. The TRAIL to selective tumour death. *Nat Med* 5: 146–147, 1999.
 39. Gaspari P, Banerjee T, Malachowski WP, Muller AJ, Prendergast GC, DuHadaway J, Bennett S, and Donovan AM. Structure-activity study of brassinin derivatives as indoleamine 2,3-dioxygenase inhibitors. *J Med Chem* 49: 684–692, 2006.
 40. Geserick P, Drewniok C, Hupe M, Haas TL, Diessenbacher P, Sprick MR, Schön MP, Henkler F, Gollnick H, Walczak H, and Leverkus M. Suppression of cFLIP is sufficient to sensitize human melanoma cells to TRAIL- and CD95L-mediated apoptosis. *Oncogene* 27: 3211–3220, 2008.
 41. Gibbs CP, Kukekov VG, Reith JD, Tchigrinova O, Suslov ON, Scott EW, Ghivizzani SC, Ignatova TN, and Steindler DA. Stem-like cells in bone sarcomas: implications for tumorigenesis. *Neoplasia* 7: 967–976, 2005.
 42. Ginestier C, Hur MH, Charafe-Jauffret E, Monville F, Dutcher J, Brown M, Jacquemier J, Viens P, Kleer CG, Liu S, Schott A, Hayes D, Birnbaum D, Wicha MS, and Dontu G. ALDH1 is a marker of normal and malignant human mammary stem cells and a predictor of poor clinical outcome. *Cell Stem Cell* 1: 555–567, 2007.
 43. Griguer CE, Oliva CR, Gobin E, Gobin E, Marcorelles P, Benos DJ, Lancaster JR, and Gillespie GY. CD133 is a marker of bioenergetic stress in human glioma. *PLoS ONE* 3: e3655, 2008.
 44. Guo R, Wu Q, Liu F, and Wang Y. Description of the CD133+ subpopulation of the human ovarian cancer cell line OVCAR3. *Oncol Rep* 25: 141–146, 2011.
 45. Gupta PB, Onder TT, Jiang G, Tao K, Kuperwasser C, Weinberg RA, and Lander ES. Identification of selective inhibitors of cancer stem cells by high-throughput screening. *Cell* 138: 645–659, 2009.
 46. Guzman L, Rossi RM, Karnischky L, Li X, Peterson DR, Howard DS, and Jordan CT. The sesquiterpene lactone parthenolide induces apoptosis of human acute myelogenous leukemia stem and progenitor cells. *Blood* 105: 4163–4169, 2005.
 47. Hambardzumyan D, Squartro M, and Holland EC. Radiation resistance and stem-like cells in brain tumors. *Cancer Cell* 10: 454–456, 2006.
 48. Hanahan D and Weinberg RA. The hallmarks of cancer. *Cell* 144: 646–674, 2011.
 49. Hassane DC, Guzman ML, Corbett C, Li X, Abboud R, Young F, Liesveld JL, Carroll M, and Jordan CT. Discovery of agents that eradicate leukemia stem cells using an *in silico* screen of public gene expression data. *Blood* 111: 5654–5662, 2008.
 50. Hayakawa Y, Kelly JM, Westwood JA, Darcy PK, Diefenbach A, Raulet D, and Smyth MJ. Cutting edge: tumor rejection mediated by NKG2D receptor-ligand interaction is dependent upon perforin. *J Immunol* 169: 5377–5381, 2002.
 51. Hehner SP, Hofmann TG, Dröge W, and Schmitz ML. The anti-inflammatory sesquiterpene lactone parthenolide inhibits NF- κ B by targeting the I κ B kinase complex. *J Immunol* 163: 5617–5623, 1999.
 52. Hirsch HA, Iliopoulos D, Tschlis PN, and Struhl K. Metformin selectively targets cancer stem cells, and acts together with chemotherapy to block tumor growth and prolong remission. *Cancer Res* 69: 7507–7511, 2009.
 53. Hirschmann-Jax C, Foster AE, Wulf GG, Nuchtern JG, Jax TW, Gobel U, Goodell MA, and Brenner MK. A distinct “side population” of cells with high drug efflux capacity in human tumor cells. *Proc Natl Acad Sci U S A* 101: 14228–14233, 2004.
 54. Hou DY, Muller AJ, Sharma MD, DuHadaway J, Banerjee T, Johnson M, Mellor AL, Prendergast GC, and Munn DH. Inhibition of indoleamine 2,3-dioxygenase in dendritic cells by stereoisomers of 1-methyl-tryptophan correlates with antitumor responses. *Cancer Res* 67: 792–801, 2007.
 55. Irmeler M, Thome M, Hahne M, Schneider P, Hofmann K, Steiner V, Bodmer JL, Schröter M, Burns K, Mattmann C, Rimoldi D, French LE, and Tschopp J. Inhibition of death receptor signals by cellular FLIP. *Nature* 388: 190–195, 1997.
 56. Jaiswal S, Jamieson CH, Pang WW, Park CY, Chao MP, Majeti R, Traver D, van Rooijen N, and Weissman IL. CD47 is upregulated on circulating hematopoietic stem cells and leukemia cells to avoid phagocytosis. *Cell* 138: 271–285, 2009.
 57. Jin F, Zhao L, Zhao HY, Guo SG, Feng J, Jiang XB, Zhang SL, Wei YJ, Fu R, and Zhao JS. Comparison between cells and cancer stem-like cells isolated from glioblastoma and astrocytoma on expression of anti-apoptotic and multidrug resistance-associated protein genes. *Neuroscience* 154: 541–550, 2008.
 58. Kawasaki BT, Hurt EM, Kalathur M, Duhagon MA, Milner JA, Kim YS, and Farrar WL. Effects of the sesquiterpene lactone parthenolide on prostate tumor-initiating cells: an integrated molecular profiling approach. *Prostate* 69: 827–837, 2009.
 59. Kohga K, Tatsumi T, Takehara T, Tsunematsu H, Shimizu S, Yamamoto M, Sasakawa A, Miyagi T, and Hayashi N. Expression of CD133 confers malignant potential by regulating metalloproteinases in human hepatocellular carcinoma. *J Hepatol* 52: 872–879, 2010.
 60. Korkaya H and Wicha MS. HER2, Notch, and breast cancer stem cells: targeting an axis of evil. *Clin Cancer Res* 15: 1845–1847, 2009.
 61. Lanier LL. NK cell recognition. *Annu Rev Immunol* 23: 225, 2005.
 62. Lapidot T, Sirard C, Vormoor J, Haas TL, Diessenbacher P, Sprick MR, Schön MP, Henkler F, Gollnick H, Walczak H, and Leverkus M. A cell initiating human acute myeloid leukaemia after transplantation into SCID mice. *Nature* 367: 645–648, 1994.
 63. LeBlanc HN and Ashkenazi A. Apo2L/TRAIL and its death and decoy receptors. *Cell Death Differ* 10: 66–75, 2003.
 64. Li C, Heidt DG, Dalerba P, Burant CF, Zhang L, Adsay V, Wicha M, Clarke MF, and Simeone DM. Identification of

- pancreatic cancer stem cells. *Cancer Res* 67: 1030–1037, 2007.
65. Liu G, Yuan X, Zeng Z, Tunici P, Ng H, Abdulkadir IR, Lu L, Irvin D, Black KL, and Yu JS. Analysis of gene expression and chemoresistance of CD133⁺ cancer stem cells in glioblastoma. *Mol Cancer* 5: 1476–1498, 2006.
 66. Löb S, Königsrainer A, Rammensee HG, Opelz G, and Terness P. Inhibitors of indoleamine-2,3-dioxygenase for cancer therapy: can we see the wood for the trees? *Nat Rev Cancer* 9: 445–452, 2009.
 67. Mascareno E, El-Shafei M, Maulik N, Sato M, Guo Y, Das DK, and Siddiqui MA. JAK/STAT signaling is associated with cardiac dysfunction during ischemia and reperfusion. *Circulation* 104: 325–329, 2001.
 68. Matsumoto K, Arao T, Tanaka K, Kaneda H, Kudo K, Fujita Y, Tamura D, Aomatsu K, Tamura T, Yamada Y, Saijo N, and Nishio K. mTOR signal and HIF-1 α regulate CD133 expression in cancer cells. *Cancer Res* 69: 7160–7164, 2009.
 69. Maw MA, Corbeil D, Koch J, Hellwig A, Wilson-Wheeler JC, Bridges RJ, Kumaramanickavel G, John S, Nancarrow D, Röper K, Weigmann A, Huttner WB, and Denton MJ. A frameshift mutation in prominin (mouse)-like 1 causes human retinal degeneration. *Hum Mol Genet* 9: 27–34, 2000.
 70. McCord AM, Jamal M, Shankavaram UT, Lang FF, Camphausen K, and Tofilon PJ. Physiologic oxygen concentration enhances the stem-like properties of CD133⁺ human glioblastoma cells *in vitro*. *Mol Cancer Res* 7: 489–497, 2009.
 71. McLennan HR and Degli Esposti M. The contribution of mitochondrial respiratory complexes to the production of reactive oxygen species. *J Bioenerg Biomembr* 32: 153–162, 2000.
 72. Mignotte B and Vayssiere JL. Mitochondria and apoptosis. *Eur J Biochem* 252: 1–15, 1998.
 73. Miki J, Furusato B, Li H, Gu Y, Takahashi H, Egawa S, Sesterhenn IA, McLeod DG, Srivastava S, and Rhim JS. Identification of putative stem cell markers, CD133 and CXCR4, in hTERT-immortalized primary nonmalignant and malignant tumor-derived human prostate epithelial cell lines and in prostate cancer specimens. *Cancer Res* 67: 3153–3161, 2007.
 74. Miraglia S, Godfrey W, Yin AH, Atkins K, Warnke R, Holden JT, Bray RA, Waller EK, and Buck DW. A novel five-transmembrane hematopoietic stem cell antigen: isolation, characterization, and molecular cloning. *Blood* 90: 5013–5021, 1997.
 75. Miyadera H, Shiomi K, Ui H, Yamaguchi Y, Masuma R, Tomoda H, Miyoshi H, Osanai A, Kita K, and Omura S. Atpenins, potent and specific inhibitors of mitochondrial complex II (succinate-ubiquinone oxidoreductase). *Proc Natl Acad Sci U S A* 100: 473–477, 2003.
 76. Mizrak D, Brittan M, and Alison MR. CD133: molecule of the moment. *J Pathol* 214: 3–9, 2008.
 77. Monzani E, Facchetti F, Galmozzi E, Corsini E, Benetti A, Cavazzin C, Gritti A, Piccinini A, Porro D, Santinami M, Invernici G, Parati E, Alessandri G, and La Porta CA. Melanoma contains CD133 and ABCG2 positive cells with enhanced tumorigenic potential. *Eur J Cancer* 43: 935–946, 2007.
 78. Morrison BJ, Andera L, Reynolds BA, Ralph SJ, and Neuzil J. Future use of mitocans against tumour-initiating cells? *Mol Nutr Food Res* 53: 147–153, 2009.
 79. Munn DH and Mellor AL. Indoleamine 2,3-dioxygenase and tumor-induced tolerance. *J Clin Invest* 117: 1147–1154, 2007.
 80. Nakamura M, Kyo S, Zhang B, Zhang X, Mizumoto Y, Takakura M, Maida Y, Mori N, Hashimoto M, Ohno S, and Inoue M. Prognostic impact of CD133 expression as a tumor-initiating cell marker in endometrial cancer. *Hum Pathol* 41: 1516–1529, 2010.
 81. Neuzil J, Dong LF, Ramanathapuram L, Hahn T, Chladova M, Wang XF, Zobalova R, Prochazka L, Gold M, Freeman R, Turanek J, Akporiaye ET, Dyason JC, and Ralph SJ. Vitamin E analogues: a novel group of mitocans, anti-cancer agents that act by targeting mitochondria. *Mol Aspects Med* 28: 607–645, 2007.
 82. Neuzil J, Stantic M, Zobalova R, Chladova M, Wang XF, Dong LF, Prochazka L, Andera L, and Ralph SJ. Tumour-initiating cells vs. cancer “stem” cells and CD133: what’s in the name? *Biochem Biophys Res Commun* 355: 855–859, 2007.
 83. Neuzil J, Tomasetti M, Zhao Y, Dong LF, Birringer M, Wang XF, Low P, Wu K, Salvatore BA, and Ralph SJ. Vitamin E analogs, a novel group of “mitocans”, as anti-cancer agents: the importance of being redox-silent. *Mol Pharmacol* 71: 1185–1199, 2007.
 84. O’Brien CA, Pollett A, Gallinger S, and Dick JE. A human colon cancer cell capable of initiating tumour growth in immunodeficient mice. *Nature* 445: 106–110, 2007.
 85. Olempska M, Eisenach PA, Ammerpohl O, Ungefroren H, Fandrich F, and Kalthoff H. Detection of tumor stem cell markers in pancreatic carcinoma cell lines. *Hepatobiliary Pancreat Dis Int* 6: 92–97, 2007.
 86. Park CH, Bergsagel DE, and McCulloch EA. Mouse myeloma tumour stem cells: a primary cell culture assay. *J Natl Cancer Inst* 46: 411–422, 1971.
 87. Patrawala L, Calhoun T, Schneider-Broussard R, Li H, Bhatia B, Tang S, Reilly JG, Chandra D, Zhou J, Claypool K, Coghlan L, and Tang DG. Highly purified CD44⁺ prostate cancer cells from xenograft human tumors are enriched in tumorigenic and metastatic progenitor cells. *Oncogene* 25: 1696–1708, 2006.
 88. Peter ME and Krammer PH. The CD95(APO-1/Fas) DISC and beyond. *Cell Death Differ* 10: 26–35, 2003.
 89. Pfeiffer MJ and Schalken JA. Stem cell characteristics in prostate cancer cell lines. *Eur Urol* 57: 246–254, 2010.
 90. Piccirillo SG, Reynolds BA, Zanetti N, Lamorte G, Binda E, Broggi G, Brem H, Olivi A, Dimeco F, and Vescovi AL. Bone morphogenetic proteins inhibit the tumorigenic potential of human brain tumour-initiating cells. *Nature* 444: 761–765, 2006.
 91. Piccoli C, D’Aprile A, Ripoli M, Scrima R, Boffoli D, Tabilio A, and Capitanio N. The hypoxia-inducible factor is stabilized in circulating hematopoietic stem cells under normoxic conditions. *FEBS Lett* 581: 3111–3119, 2007.
 92. Polyak K and Hahn WC. Roots and stems: stem cells in cancer. *Nat Med* 11: 296–298, 2006.
 93. Ralph SJ, Rodríguez-Enríquez S, Neuzil J, Saavedra E, and Moreno-Sánchez R. The causes of cancer revisited: “Mitochondrial malignancy” and ROS-induced oncogenic transformation—why mitochondria are targets for cancer therapy. *Mol Asp Med* 31: 145–170, 2010.
 94. Ricci-Vitiani L, Lombardi DG, Pilozzi E, Ricci-Vitiani L, Lombardi DG, and Pilozzi E. Identification and expansion of human colon-cancer-initiating cells. *Nature* 445: 111–115, 2007.
 95. Röper K, Corbeil D, and Huttner WB. Retention of prominin in microvilli reveals distinct cholesterol-based lipid micro-domains in the apical plasma membrane. *Nat Cell Biol* 2: 582–592, 2000.

96. Salmaggi A, Boiardi A, Gelati M, Russo A, Calatozzolo C, Ciusani E, Sciacca FL, Ottolina A, Parati EA, La Porta C, Alessandri G, Marras C, Croci D, and De Rossi M. Glioblastoma-derived tumorspheres identify a population of tumor stem-like cells with angiogenic potential and enhanced multidrug resistance phenotype. *Glia* 54: 850–860, 2006.
97. Salnikov AV, Kusumawidjaja G, Rausch V, Bruns H, Gross W, Khamidjanov A, Ryschich E, Gebhard MM, Moldenhauer G, Büchler MW, Schemmer P, and Herr I. Cancer stem cell marker expression in hepatocellular carcinoma and liver metastases is not sufficient as single prognostic parameter. *Cancer Lett* 275: 185–193, 2009.
98. Schreiber RD, Pace JL, Russell SW, Altman A, and Katz DH. Macrophage-activating factor produced by a T cell hybridoma: physicochemical and biosynthetic resemblance to γ -interferon. *J Immunol* 131: 826–832, 1983.
99. Semenza GL. HIF-1: upstream and downstream of cancer metabolism. *Curr Opin Genet Dev* 20: 51–56, 2010.
100. Shervington A and Lu C. Expression of multidrug resistance genes in normal and cancer stem cells. *Cancer Invest* 26: 535–542, 2008.
101. Shi C, Tian R, Wang M, Wang X, Jiang J, Zhang Z, Li X, He Z, Gong W, and Qin R. CD44⁺ CD133⁺ population exhibits cancer stem cell-like characteristics in human gallbladder carcinoma. *Cancer Biol Ther* 10: 1182–1190, 2010.
102. Shipitsin M, Campbell LL, Argani P, Weremowicz S, Bloushtain-Qimron N, Yao J, Nikolskaya T, Serebryiskaya T, Beroukhim R, Hu M, Halushka MK, Sukumar S, Parker LM, Anderson KS, Harris LN, Garber JE, Richardson AL, Schnitt SJ, Nikolsky Y, Gelman RS, and Polyak K. Molecular definition of breast tumor heterogeneity. *Cancer Cell* 11: 259–273, 2007.
103. Shmelkov SV, Butler JM, Hooper AT, Hormigo A, Kushner J, Milde T, St. Clair R, Baljevic M, White I, Jin DK, Chadburn A, Murphy AJ, Valenzuela DM, Gale NW, Thurston G, Yancopoulos GD, D'Angelica M, Kemeny N, Lyden D, and Rafii S. CD133 expression is not restricted to stem cells, and both CD133⁺ and CD133⁻ metastatic colon cancer cells initiate tumors. *J Clin Invest* 118: 2111–2120, 2008.
104. Singh SK, Clarke ID, Terasaki M, Haas TL, Diessenbacher P, Sprick MR, Schön MP, Henkler F, Gollnick H, Walczak H, and Leverkus M. Identification of a cancer stem cell in human brain tumors. *Cancer Res* 63: 5821–5828, 2003.
105. Singh SK, Hawkins C, Clarke ID, Squire JA, Bayani J, Hide T, Henkelman RM, Cusimano MD, and Dirks PB. Identification of human brain tumour initiating cells. *Nature* 432: 396–401, 2004.
106. Smyth MJ, Cretney E, Takeda K, Wiltrot RH, Sedger LM, Kayagaki N, Yagita H, and Okumura K. Tumor necrosis factor-related apoptosis-inducing ligand (TRAIL) contributes to interferon γ -dependent natural killer cell protection from tumor metastasis. *J Exp Med* 193: 661–670, 2001.
107. Smyth MJ, Crowe NY, Hayakawa Y, Takeda K, Yagita H, and Godfrey DI. NKT cells-conductors of tumor immunity? *Curr Opin Immunol* 14: 165–171, 2002.
108. Smyth MJ, Dunn GP, and Schreiber RD. Cancer immunosurveillance and immunoediting: the roles of immunity in suppressing tumor development and shaping tumor immunogenicity. *Adv Immunol* 90: 1–50, 2006.
109. Soeda A, Park M, Lee D, Mintz A, Androutsellis-Theotokis A, McKay RD, Engh J, Iwama T, Kunisada T, Kassam AB, Pollack IF, and Park DM. Hypoxia promotes expansion of the CD133-positive glioma stem cells through activation of HIF-1 α . *Oncogene* 28: 3949–3959, 2009.
110. Suetsugu A, Nagaki M, Aoki H, Motohashi T, Kunisada T, and Moriwaki H. Characterization of CD133⁺ hepatocellular carcinoma cells as cancer stem/progenitor cells. *Biochem Biophys Res Commun* 351: 820–824, 2006.
111. Sullivan JP, Spinola M, Dodge M, Raso MG, Behrens C, Gao B, Schuster K, Shao C, Larsen JE, Sullivan LA, Honorio S, Xie Y, Scaglioni PP, DiMaio JM, Gazdar AF, Shay JW, Wistuba II, and Minna JD. Aldehyde dehydrogenase activity selects for lung adenocarcinoma stem cells dependent on notch signaling. *Cancer Res* 70: 9937–9948, 2010.
112. Swann JB and Smyth MJ. Immune surveillance of tumors. *J Clin Invest* 117: 1137–1146, 2007.
113. Takeda K, Hayakawa Y, Smyth MJ, Kayagaki N, Yamaguchi N, Kakuta S, Iwakura Y, Yagita H, and Okumura K. Involvement of tumor necrosis factor-related apoptosis-inducing ligand in surveillance of tumor metastasis by liver natural killer cells. *Nat Med* 7: 94–100, 2001.
114. Takenobu H, Shimozato O, Nakamura T, Ochiai H, Yamaguchi Y, Ohira M, Nakagawara A, and Kamijo T. CD133 suppresses neuroblastoma cell differentiation via signal pathway modification. *Oncogene* 30: 97–105, 2011.
115. Tang C, Ang BT, and Pervaiz S. Cancer stem cell: target for anti-cancer therapy. *FASEB J* 21: 1–9, 2007.
116. Thome M, Schneider P, Hofmann K, Schneider P, Hofmann K, Steiner V, Bodmer JL, Schröter M, Burns K, Mattmann C, Rimoldi D, French LE, and Tschopp J. Viral FLICE-inhibitory proteins (FLIPs) prevent apoptosis induced by death receptors. *Nature* 386: 517–521, 1997.
117. Tirino V, Camerlingo R, Franco R, Malanga D, La Rocca A, Viglietto G, Rocco G, and Pirozzi G. The role of CD133 in the identification and characterisation of tumour-initiating cells in non-small-cell lung cancer. *Eur J Cardiothorac Surg* 36: 446–453, 2009.
118. Tomasetti M, Andera L, Alleva R, Borghi B, Neuzil J, and Procopio A. α -Tocopheryl succinate induces DR4 and DR5 expression by a p53-dependent route: implication for sensitisation of resistant cancer cells to TRAIL apoptosis. *FEBS Lett* 580: 1925–1931, 2006.
119. Ursini-Siegel J, Schade B, and Cardiff RD. Insights from transgenic mouse models of ERBB2-induced breast cancer. *Nat Rev Cancer* 7: 389–397, 2007.
120. Valis K, Prochazka L, Boura E, Chladova M, Obsil T, Rohlena J, Truksa J, Dong LF, Ralph SJ, and Neuzil J. Hippo/Mst1 stimulates transcription of NOXA in a FoxO1-dependent manner. *Cancer Res* 71: 946–954, 2011.
121. Vivier E, Raulet DH, Moretta A, Caligiuri MA, Zitvogel L, Lanier LL, Yokoyama WM, and Ugolini S. Innate or adaptive immunity? The example of natural killer cells. *Science* 331: 44–49, 2011.
122. Weigmann A, Corbeil D, Hellwig A, and Huttner WB. Prominin, a novel microvilli-specific polytopic membrane protein of the apical surface of epithelial cells, is targeted to plasmalemmal protrusions of non-epithelial cells. *Proc Natl Acad Sci U S A* 94: 12425–12430, 1997.
123. Wicha MS, Liu S, and Dontu G. Cancer stem cells: an old idea—a paradigm shift. *Cancer Res* 66: 1883–1890, 2006.
124. Wright MH, Calcagno AM, Salcido CD, Carlson MD, Ambudkar SV, and Varticovski L. Brca1 breast tumors contain distinct CD44⁺/CD24⁻ and CD133⁺ cells with cancer stem cell characteristics. *Breast Cancer Res* 10: R10, 2008.
125. Wu A, Wiesner S, Xiao J, Ericson K, Chen W, Hall WA, Low WC, and Ohlfest JR. Expression of MHC I and NK

- ligands on human CD133⁺ glioma cells: possible targets of immunotherapy. *J Neurooncol* 83: 121–131, 2007.
126. Yan X, Ma L, Yi D, Yoon JG, Diercks A, Foltz G, Price ND, Hood LE, and Tian Q. A CD133-related gene expression signature identifies an aggressive glioblastoma subtype with excessive mutations. *Proc Natl Acad Sci U S A* 108: 1591–1596, 2011.
 127. Yin S, Li J, Hu C, Chen X, Yao M, Yan M, Jiang G, Ge C, Xie H, Wan D, Yang S, Zheng S, and Gu J. CD133 positive hepatocellular carcinoma cells possess high capacity for tumorigenicity. *Int J Cancer* 120: 1436–1442, 2007.
 128. Zhang Q, Shi S, Yen Y, Brown J, Ta JQ, and Le AD. A subpopulation of CD133(+) cancer stem-like cells characterized in human oral squamous cell carcinoma confer resistance to chemotherapy. *Cancer Lett* 289: 151–160, 2010.
 129. Zhou J, Zhang H, Gu P, Bai J, Margolick JB, and Zhang Y. NF- κ B pathway inhibitors preferentially inhibit breast cancer stem-like cells. *Breast Cancer Res Treat* 111: 419–427, 2008.
 130. Zhu G, Chang Y, Zuo J, Dong X, Zhang M, Hu G, and Fang F. Fudenine, a C-terminal truncated rat homologue of mouse prominin, is blood glucose-regulated and can up-regulate the expression of GAPDH. *Biochem Biophys Res Commun* 281: 951–956, 2001.
 131. Zhu L, Gibson P, Currie DS, Tong Y, Richardson RJ, Bayazitov IT, Poppleton H, Zakharenko S, Ellison DW, and Gilbertson RJ. Prominin 1 marks intestinal stem cells that are susceptible to neoplastic transformation. *Nature* 457: 603–607, 2009.
 132. Zabalova R, McDermott L, Stantic M, Prokopova K, Dong LF, and Neuzil J. CD133-positive cells are resistant to TRAIL due to up-regulation of FLIP. *Biochem Biophys Res Commun* 373: 567–571, 2008.

Address correspondence to:

Prof. Jiri Neuzil
 Apoptosis Research Group
 School of Medical Science and Griffith Health Institute
 Griffith University
 Southport QLD 4222
 Australia

E-mail: j.neuzil@griffith.edu.au

Date of first submission to ARS Central, November 18, 2010; date of final revised submission, April 10, 2011; date of acceptance, April 19, 2011.

Abbreviations Used

CSC = cancer stem-like cell
 ES = embryonic stem
 FDR = false discovery rate
 FLIP = FLICE-inhibitory protein
 HIF-1 α = hypoxia-inducible factor-1 α
 IDO = indoleamine 2,3-dioxygenase
 IFN = interferon
 MHC = major histocompatibility
 MitoVES = mitochondrially targeted vitamin E succinate
 MS = mammospheres
 NK = natural killer
 PTL = parthenolide
 ROS = reactive oxygen species
 TOS = tocopheryl succinate
 TRAIL = tumor necrosis factor-related apoptosis-inducing ligand

Drugs that Kill Cancer Stem-like Cells

Renata Zobalova,^{1,2} Marina Stantic,¹ Michael Stapelberg,¹
Katerina Prokopova,² Lanfeng Dong,¹ Jaroslav Truksa² and Jiri Neuzil^{1,2}

¹*Apoptosis Research Group, School of Medical Science and Griffith Health Institute,
Griffith University, Southport, Qld,*

²*Molecular Therapy Group, Institute of Biotechnology,
Academy of Sciences of the Czech Republic, Prague,*

¹*Australia,*

²*Czech Republic*

1. Introduction

The hallmarks of cancer include processes like self-sufficiency for growth signals, insensitivity to growth-inhibitory (anti-growth) signals, evasion of programmed cell death (apoptosis), unlimited replicative potential, sustained angiogenesis, and tissue invasion and metastasis (Hanahan & Weinberg, 2000). Recent research dictates that these definitions, while valid, ought to be enriched. That is, we should also consider tumours as a heterogeneous 'collection of cancer cells' with a hierarchy. This 'hierarchical hypothesis' tells us that tumours contain a minute (sometimes very small) sub-set of cells with distinct properties from the bulk of the tumour mass (D'Amour & Gage, 2002; Visvader & Lindeman, 2008; Visvader, 2009). These cells feature certain characteristics inherent to stem cells, including the capacity of self-renewal, asymmetric division and differentiation. They have also a very high propensity to form tumours. Therefore these cells are referred to as cancer stem cells (CSC) or cancer stem-like cells or, better, tumour-initiating cells (TICs). The terminology, while not too important, may be misleading though, since the term 'cancer stem cells' implies that we are dealing with true stem cells, which is not possible to reconcile with at this stage, perhaps even more so, since the origin of CSCs is not exactly known.

Recent evidence, rather circumstantial, indicates that CSCs may have developed during the stage of tumour immunoediting (Dunn *et al.*, 2002, 2004a). According to this concept, the immune system is actively involved in tumour initiation as well as progression, and this became known as the principle of 'three Es', involving the phases of 'elimination', 'equilibrium' and 'escape' (Dunn *et al.*, 2004b). The elimination phase of the process of immunoediting is responsible for the detection and elimination of cells that became malignant, usually due to the failure of their tumour suppressor mechanisms (Smyth *et al.*, 2002). The selection of such CSCs is depicted schematically in Figure 1. Here, certain cells, possibly with slightly different properties than the bulk of the cell population, survive the pressure of the immune system, while most of the cells are eliminated by the cells of the immune system such as the cytotoxic T lymphocytes (CTLs) (Schreiber *et al.*, 1983; Bancroft *et al.*, 1991; Smyth *et al.*, 2001; Takeda *et al.*, 2001; Hayakawa *et al.*, 2002). These cells then give rise to a tumour. Upon therapeutic intervention, many cells of the tumour are induced into

apoptosis and die, while some survive and give rise to 'second-line' tumours with acquired resistance to the 'first-line' treatment, vastly complicating further therapy and making the prognosis very grim (Neuzil *et al.*, 2007; Visvader & Lindeman, 2008; Alison *et al.*, 2010; McDermott & Wicha, 2010).

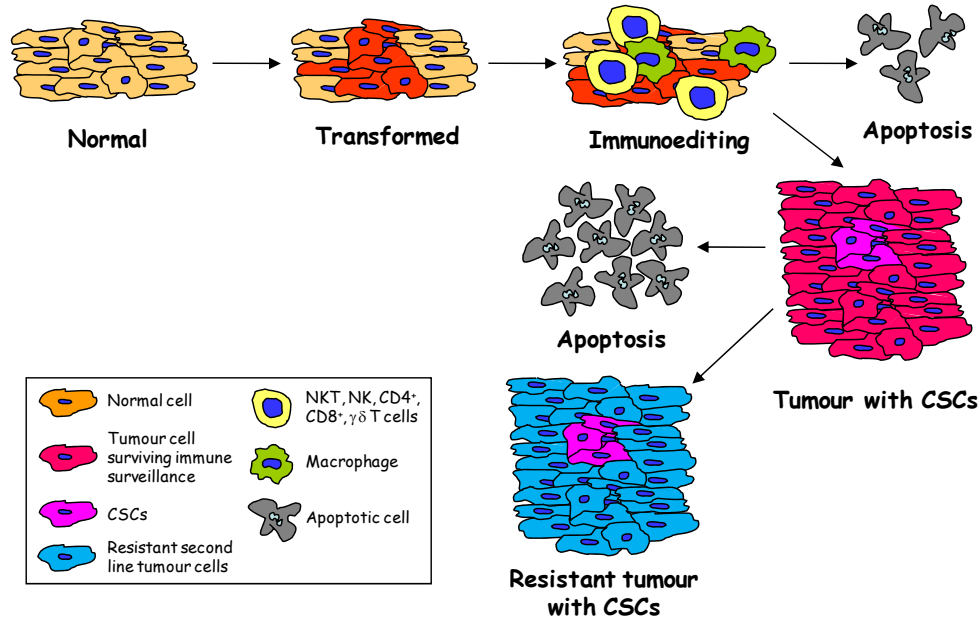


Fig. 1. Possible selection of CSCs during cancer cell immunoediting and their contribution to the resistance of tumours to therapy. During the process of malignant conversion, several cells that carry mutations escape the elimination phase of the process of immunoediting, which involves a variety of cells of the immune system, such as natural killer cells, natural killer T cells, cytotoxic T cells or macrophages. These 'selected' cells form a tumour with relatively low number of CSCs. Upon challenge of the tumour with anti-cancer drugs, majority of the cells are killed via apoptosis, while the CSCs survive. They then start differentiating and proliferating to give rise to 'second-line' tumours with higher resistance to therapy, making them very hard to eliminate. The percentage of CSCs in the 'second-line' tumours is similar to that in the primary tumour.

2. Identification of cancer stem-like cells

CSCs have been, thus far, identified in a great number of tumours. Thus, CSCs have been described in multiple myelomas (Park *et al.*, 1971) and in leukemias (Lapidot *et al.*, 1994; Bhatia *et al.*, 1998), after which they were also discovered in the neoplastic diseases of the nervous system (Singh *et al.*, 2003; Piccirillo *et al.*, 2006), colon cancer (Ricci-Vitiani *et al.*, 2007), prostate cancer (Collins *et al.*, 2005), hepatocarcinomas (Yin *et al.*, 2007), breast cancer (Al-Hajj *et al.*, 2003), melanomas (Fang *et al.*, 2005; Schatton *et al.*, 2008) and osteosarcomas (Gibbs *et al.*, 2005), and we have recently identified CSCs in the context of malignant mesotheliomas (Neuzil *et al.*, unpublished data).

One of the most vexing problems in the study of CSCs is their identification. A number of markers of CSCs or the combination thereof, varying, more-or-less, from cancer type to cancer type, have been described. Of the 'markers' used to define CSCs, many are cell surface proteins that endow the sub-set of CSCs with specific properties, and some have been involved in functional differences of CSCs when compared to the fast-proliferating, more differentiated cancer cells. However, different markers or their combinations have been proposed to characterize CSCs even within the same type of tumour. For example, breast cancer CSCs have been typified by the genotype CD44⁺/CD24⁻/ALDH (Ginestier *et al.*, 2007; Charafe-Jauffret *et al.*, 2009). We found breast cancer CSCs also upregulating CD133, while the CD24 status varies (Neuzil *et al.*, unpublished data). Similarly, ovarian carcinoma stem cells have been described as CD44⁺/CD117⁺ (Zhang *et al.*, 2008) or CD133⁺ (Baba *et al.*, 2009).

Probably the most frequently used markers of CSCs are the surface proteins CD24, CD44, CD47, CD133, the level of expression of aldehyde dehydrogenase (ALDH), and the presence of the so-called 'side-population'. These markers have been used to characterize CSCs from a variety of tumour types, although the use of some of these markers has been challenged. This controversy has been proposed, for example, for the probably most frequently used CSC marker CD133, with Shmelkov *et al.* (2008) having reported that metastatic colon cancer cells exert comparable tumour-initiating capacity regardless of the CD133 status.

While the glycoprotein CD24 has been shown to be downregulated in CSCs of some types of breast cancer, CD44 appears to be consistently upregulated in breast cancer CSCs (Al-Hajj *et al.*, 2003; Ginestier *et al.*, 2007; Charafe-Jauffret *et al.*, 2009) as well as CSCs of prostate (Collins *et al.*, 2005), pancreatic (Patrawala *et al.*, 2006; Li *et al.*, 2007), ovarian (Zhang *et al.*, 2008; Alvero *et al.*, 2009), colorectal (Du *et al.*, 2008) and liver cancer (Yang *et al.*, 2008). CD44 has been earlier identified as a receptor for hyaluronic acid, whose engagement may result in the activation of TGFβ signalling, promoting the pro-survival, anti-apoptotic pathways (Shipitsin *et al.*, 2007).

Over the last few years, CD133 has been utilized most frequently as a marker of CSCs (Corbeil *et al.*, 2001; Miraglia *et al.*, 2007; Neuzil *et al.*, 2007; Tang *et al.*, 2007). The types of tumours that are typified by CSCs that exert high level of CD133 include such diverse neoplasias as breast cancer, colon cancer, tumours of the nervous system, etc. It is rather surprising that not too much is known about the function of the protein. CD133, also known as prominin-1, was first discovered in hematopoietic stem cells (Corbeil *et al.*, 2001; Miraglia *et al.*, 2007). It was shown that CD133⁺ cells have the propensity to form tumours in NOD/SCID mice even when low numbers of such cells were xenografted (Ricci-Vitiani *et al.*, 2007; Yin *et al.*, 2007; O'Brian *et al.*, 2007; Wright *et al.*, 2008). Even though Shmelkov *et al.* (2008) reported that in their hands, CD133⁻ cells are also capable of tumour initiation in immunocompromised mice, they showed that CD133⁺ colon cancer cells exert much greater metastatic potential than their CD133⁻ counterparts. Thus, regardless the reports doubting the usefulness of CD133 as a stem cell marker, prominin-1 can be used as a marker for the increase in the 'stemness' of the cell subpopulation, in particular in combination with other markers, such as CD44 and CD24.

A considerable problem in studying CSCs is, besides their identification, their maintenance in culture. For example, we studied CD133⁺ Jurkat cells from 'mixed' pre-separation population of the cells following their separation by immunomagnetic sorting, and found that the CD133^{high} sub-population (over 60% CD133 positivity) reverted to the 'mixed' population phenotype with some 20% CD133-positive cells within several days after placing

the sorted cells to the serum-containing medium (Zobalova *et al.*, 2009). This gives only a relatively short time window for subsequent studies, and the results obtained with such cells are difficult to interpret.

Probably the best option for studying CSCs of solid tumours *in vitro* is maintaining cancer cells in spheres, growing them under conditions that prevent their adhesion. The basic feature of such conditions is the absence of serum and supplementation of the medium with growth factors, including FGF2 and EGF (Vescovi *et al.*, 2006). Keeping cells in such a medium maintains their stem-like properties for extended periods of time, and we have found that such conditions result in sphere cell phenotype for breast and prostate cancer as well as mesotheliomas (Neuzil *et al.*, unpublished data). Using microarray analysis approach, we confirmed an overall increase in the 'stemness signature' of such cultures, i.e. enrichment in markers of several types of stem cells, including the hematopoietic, embryonic and neural stem cell gene sets (Ramalho-Santos *et al.*, 2002; Ivanova *et al.*, 2002; Fortunel *et al.*, 2003). This approach also makes it possible to characterise in a global as well as more focused manner the features of CSCs, including the pathways that become activated. For example, we found that for breast and prostate cancer as well as mesothelioma spheres, the tryptophan pathway was the most activated of all pathways whose activation was common to the three types of CSCs, indicating a mechanism how such cells may survive for prolonged periods of time in the niche (Neuzil *et al.*, unpublished data). This also suggests that inhibitors of indoleamine-2,3-dioxygenase (IDO), a key enzyme in the conversion of tryptophan to N-formyl kynurenin, may be useful for promoting killing of CSCs (see below).

3. Compounds that kill cancer stem-like cells

Numerous studies have documented resistance of CSCs to established therapeutic modalities, including radiation therapy as well as chemotherapy. The reasons are multiple and include altered expression of genes that are important for initiation, progression and execution of apoptosis, activation of the survival pathways, and upregulation of transmembrane proteins that promote survival as well as activation of the DNA repair machinery. Increased resistance has been shown for many types of CSCs, including leukemic (Essers & Trumpp, 2010), brain (Bao *et al.*, 2006; Liu *et al.*, 2006; Hambardzumyan *et al.*, 2006; Dirks 2010), pancreatic (Lonardo *et al.*, 2010), breast (McDermott & Wicha, 2010), melanoma (Frank *et al.*, 2003, 2005) as well as colon CSCs (Boman & Huang, 2008).

Liu *et al.* (2006) found that CD133⁺ glioblastoma cells isolated from primary tumours were highly enriched in the products of genes that provide cells with survival advantage, which includes the anti-apoptotic genes Bcl-2, Bcl-x_L, four members of the IAP family (c-IAP2, XIAP, NIAP and survivin) and, most notably the protein FLIP, while the expression of the apoptosis-promoting Bax was decreased. The caspase-8 inhibitor FLIP was upregulated up to 300-fold, pointing to its importance. The pattern of genes over-expressed in the CSCs suggests that the cells are well protected from induction and execution of both the intrinsic apoptosis mechanism (Bcl-2, Bcl-x_L) as well as against the extrinsic pathway (FLIP). Moreover, the IAP family proteins inhibit the possible activation of multiple caspases. We found that CD133^{high} cells, both Jurkat and MCF7, featured high level of expression of FLIP. This conferred their resistance to the immunological inducer of apoptosis TRAIL, which could be overcome by knocking down the FLIP protein using siRNA (Zobalova *et al.*, 2008). Several types of CSCs have been reported to upregulate ABC pumps that make them

resistant to various chemotherapeutics. For example, ABCG5 has been shown to be upregulated in melanoma CSCs (Frank *et al.*, 2003, 2005). Cells with high level of expression of members of the ABC pumps are classified as the so-called 'side-population', and these cells have been shown to possess a high re-populating activity when injected into NOD/SCID mice (Bhatia *et al.*, 1998).

Finding efficient modalities to kill CSCs is undoubtedly of paramount importance and is a focus of intensive research. Thus far, the results are not particularly encouraging, although several potentially promising agents have been described (Table I). The first and probably best characterized is the sesquiterpene lactone parthenolide, a natural product isolated from medicinal plants including *Tanacetum parthenium* (feverfew) that has been initially found to inhibit the transcription factor NF κ B (Bork *et al.*, 1997), by way of inhibiting activation of the inhibitory components of the transcription factor (Hehner *et al.*, 1998). However, it has been suggested that induction of apoptosis by parthenolide may be independent of inhibition of NF κ B activation (Anderson & Bejcek, 2008). Since parthenolide proved efficient in suppressing the proliferation and inducing apoptosis of leukemia stem cells (Guzman *et al.*, 2005a,b, 2007), a number of sesquiterpene lactones have been synthesized and tested as anti-cancer drugs (Ghantous *et al.*, 2010). Parthenolide as a compound efficient in killing leukemia stem cells was confirmed using high-throughput, *in silico* screening (Hassane *et al.*, 2008). The drug is now in Phase I clinical trial for several types of leukemia (<http://www.globenewswire.com/newsroom/news.html?d=158480>). Recently, breast CSCs as well as prostate CSCs have been reported as targets for parthenolide (Liu *et al.*, 2008; Zhou *et al.*, 2008; Kawasaki *et al.*, 2009).

The mechanism(s) by which parthenolide kills CSCs is still obscure. Guzman *et al.* (2005b, 2007) reported that an analogue of parthenolide, dimethylamino-parthenolide, was very efficient in killing primary leukemic stem cells, which was replicated in pre-clinical models. It was found that induction of apoptosis in leukemia CSCs included generation of reactive oxygen species (ROS), inhibition of NF κ B activation and activation of p53. An effect on NF κ B was also proposed for inhibition of breast cancer CSCs by parthenolide as well as by other known inducers of the transcription factor, including pyrrolidinedithiocarbamate, using the mammosphere model of CSCs (Zhou *et al.*, 2008). In prostate CSCs, parthenolide has been shown to exert also other activities than inhibition of NF κ B or generation of ROS, which include inhibition of a variety of non-receptor and receptor tyrosine kinases as well as a number of transcription factors, such as C/EBP α , FRA-1, HOXA-4, c-Myb, Snail, SP1, etc. (Kawasaki *et al.*, 2009). Of considerable clinical interest is combination of parthenolide with established anti-cancer agents. To this effect, Liu *et al.* (2008) reported that the combination of long-circulating (stealth) liposomes carrying parthenolide with those containing vinorelbine fully inhibited xenografts derived in immunocompromised mice from MCF7 cells. In cultured MCF7 cells sorted for the 'side-population' with high tumour-initiating potential, the combination of the two drugs exerted a very good anti-proliferative effect.

High-throughput *in silico* screening has been used recently in a search for compounds that would efficiently kill breast CSCs. This resulted in discovery of the well known agent salinomycin as an anti-CSC drug (Gupta *et al.*, 2009), with a potential clinical application (Rowan, 2009). This agent was some 100-fold more efficient in lowering the proportion of CSCs in the cancer cell population than the established anti-cancer agent paclitaxel. Analysis of breast tumour xenografts in mice treated with salinomycin revealed that the agent promoted differentiation of the tumour cells and down-regulation of the breast CSC marker

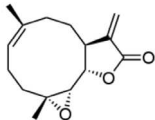
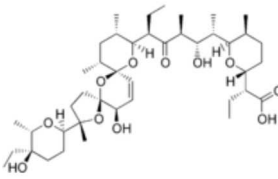
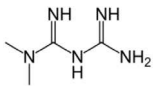
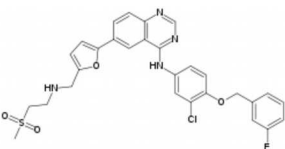
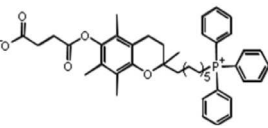
Name	Structure	Type of tumour	Mechanism of action	Reference
Parthenolide		Leukemia Breast cancer Prostate cancer	Inhibition of NFκB	Guzman et al., 2005b, 2007; Hassane et al., 2008; Liu et al., 2008; Zhou et al., 2008; Kawasaki et al., 2009
Salinomycin		Breast cancer	Potassium ionophore	Gupta et al., 2009; Fuchs et al., 2009, 2010; Riccioni et al., 2010
Metformin		Breast cancer	Effect on energy metabolism	Hirsch et al., 2009; Vazquez-Martin et al., 2010a,b; Martin-Castillo et al., 2010
Lapatinib		Breast cancer	Dual inhibitor of receptor tyrosine kinases	Korkaya et al., 2009; Magnifico et al., 2009; Diaz et al., 2010o
MitoVES		Breast cancer, mesothelioma	Generation of ROS by targeting complex II	Neuzil et al., unpublished

Table I. Small molecules killing cancer stem-like cells.

genes. A follow-up publication documented that salinomycin induces apoptosis in resistant cells, such as those expressing high levels of Bcl-2 and p-glycoprotein (Fuchs *et al.*, 2009). Similar findings were also reported by Riccioni *et al.* (2010). Multidrug resistance, mediated by the ABC transporter proteins, was overcome by salinomycin in leukemic stem-like cells, inducing the resilient cells into apoptosis (Fuchs *et al.*, 2010). Salinomycin, a potassium ionophore, is a product of the bacterium *Streptomyces albus* (Miyazaki *et al.*, 1974), and has been used for a long time in poultry industry. A potential problem with the clinical application of the agent is its relatively high toxicity (Li *et al.*, 2010) that may jeopardize its use in human medicine, quelling somewhat the enthusiasm for the future use of the agent.

Metformin is an oral anti-diabetic drug from the biguanide class, which has been used clinically as an efficient first-line agent against type 2 diabetes (Crandall *et al.*, 2008). Recently this drug was reported to target breast CSCs and, when combined with doxorubicin, prevent growth of tumours as well as their remission (Hirsch *et al.*, 2009). Another study documented that metformin could efficiently inhibit proliferation of breast CSCs refractory to the HER2-targeting agent Herceptin (trastuzumab) as well as their self renewal (Vazquez-Martin *et al.*, 2010a). Since metformin acts by interfering with the energy metabolism of cells, it may inhibit self-maintenance of mitotically competent cells acting as a caloric restriction mimetic (Martin-Castillo *et al.*, 2010; Vazquez-Martin *et al.*, 2010b; Nguyen *et al.*, 2010).

A considerable problem in cancer management is encountered in the case of HER2-high breast cancer (Slamon *et al.*, 1989). To this effect, the agent lapatinib has been applied as a drug of choice for Herceptin-resistant, metastatic breast cancer cells (Burriss *et al.*, 2005). This dual receptor tyrosine kinase inhibitor (suppressing the activation of HER2/erbB2 and EGFR) has been suggested to suppress the growth of CSCs in the context of HER2-high breast and lung tumours (Magnifico *et al.*, 2009; Korkaya and Wicha, 2009; Diaz *et al.*, 2010). Several of the above agents reported to suppress tumour growth and, in some cases, prolong the remission-free period in experimental animals, act by inducing generation of ROS. In this context, we have been studying a class of anti-cancer drugs from the group of vitamin E analogues, epitomized by the redox-silent α -tocopheryl succinate (α -TOS) (Figure 2B) (Neuzil *et al.*, 2001; Weber *et al.*, 2002). This agent acts by targeting the mitochondrial complex II (CII), whereby causing generation of high levels of ROS, which then induce apoptosis by destabilizing the mitochondrial outer membrane (Dong *et al.*, 2008, 2009), by promoting the formation of the Bak channel in mitochondria (Prochazka *et al.*, 2010; Valis *et al.*, in press). To enhance the activity of the vitamin E analogue, we modified the agent by its tagging with the positively charged triphenylphosphonium (TPP⁺) group, as suggested for a variety of redox-active compounds (Smith & Murphy, 2005; Biassutto *et al.*, 2010), generating mitochondrially targeted vitamin E succinate (MitoVES) (Figure 2B). As indicated in Figure 2A, such TPP⁺-modified compounds move across most biological membranes. Upon crossing the mitochondrial inner membrane (MIM) with the negative potential on the matrix face, the agent is trapped and gradually accumulates in this compartment so that its local concentration is considerably increased. In the case of MitoVES, with its target CII within the MIM, such approach can be expected to maximize its biological activity. Indeed, we found that MitoVES was 1-2 log more efficient in killing cancer cells than the untargeted counterpart (α -TOS), which was paralleled by an effect on experimental cancer, including colon cancer and HER2-high breast cancer (Dong *et al.*, 2011). We have recently found that MitoVES is very efficient in apoptosis induction in a breast cancer CSC model represented by mammospheres, which feature cells with enhanced level of stemness and which can be characterized as CD44^{high}/CD133^{high}/CD24^{low}/Jagged-1^{high} (Figure 3A,B). In fact, MitoVES was more efficient in killing the mammosphere cells than did the untargeted α -TOS and than parthenolide, probably thus far the best characterized agent toxic to CSCs (Figure 3C) (Neuzil *et al.*, unpublished data). While the mechanism is not clear at this stage and much more work needs to be done, agents like MitoVES may present a substantial promise for the development of compounds that will efficiently eradicate not only the bulk of the tumour cells but, more importantly, also the highly recalcitrant CSCs, whereby minimizing the probability of tumour remission.

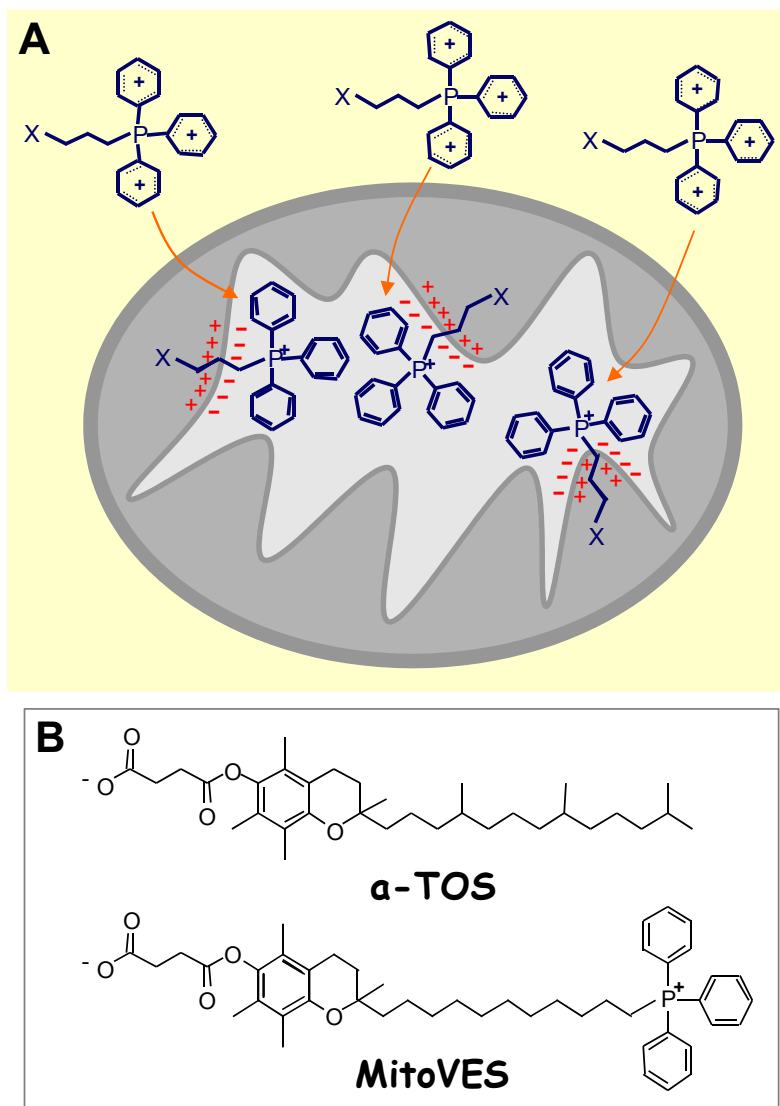


Fig. 2. **Principle of mitochondrial targeting.** A. Addition of a cationic, triphenylphosphonium (TPP^+) group to hydrophobic compounds, with the charge on the phosphorus delocalised on the flanking phenyl groups, causes their relatively free movement across biological membranes. Once in the mitochondrial matrix with the negative potential on the matrix face of the mitochondrial inner membrane (MIM), the TPP^+ group anchors the compound at the matrix-MIM interface, with increased concentration of the agent in this compartment. This is important for enhancing the bioactivity of agents, whose target is in the proximity of the interface. B. The structures are shown of the untargeted α -tocopheryl succinate (α -TOS) and the mitochondrially targeted vitamin E succinate (MitoVES).

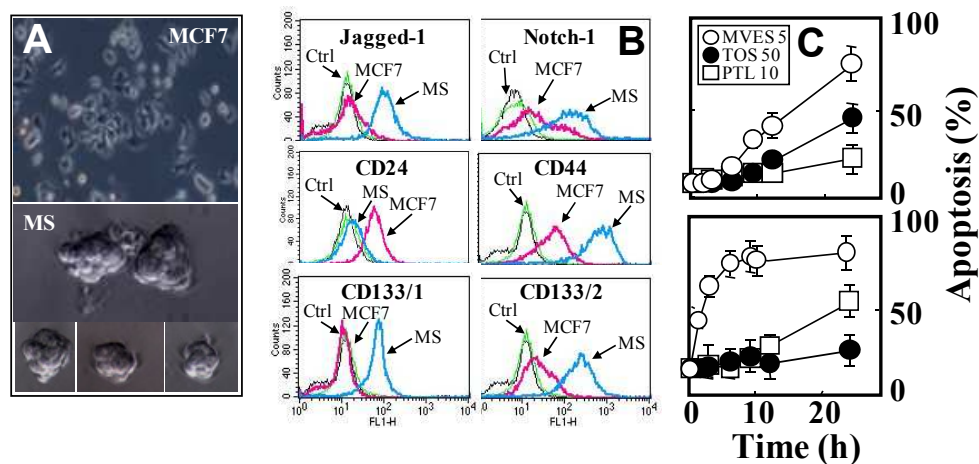


Fig. 3. MitoVES is efficient in killing mammosphere cells. A. The breast cancer cells (line MCF7) were cultured as adherent cells (MCF7) or as mammospheres (MS). B. Flow cytometric analysis characterized the adherent MCF7 cells as CD24^{high}/CD44^{low}/CD133^{low}, while the MS cells were CD24^{low}/CD44^{high}/CD133^{high}. We also found MCF7 cells low in expression of the stemness marker Jagged-1, which was increased in the MS cultures. Both CD133 isotypes were analysed here. C. The adherent MCF7 cells (top panel) and their mammosphere counterparts (lower panel) were exposed to 50 μ M α -tocopheryl succinate (TOS), 10 μ M parthenolide (PTL) or 5 μ M mitochondrially targeted vitamin E succinate, MitoVES (MVES), for the time periods indicated and the cells analysed for apoptosis level.

4. Conclusions

Cancer is now number one reason for the demise of human patients, having surpassed the number of deaths linked to cardiovascular diseases (Twombly, 2005), and the trend appears rather grim (Jemal *et al.*, 2010). A factor contributing to this negative outlook is undoubtedly the hierarchical structure of tumours with a subset of cells with tumour-initiating properties. These cells share some features with stem cells, while they are tumour cells in that they are malignant. Experiments, in which CSCs were isolated from xenografts and used to give rise to a tumour in a serial manner, documented that, although more-or-less pure CSCs were used to initiate the tumour, the percentage of cells with stem-like properties were kept very similar in each subsequent experimental animal. This suggests that tumours are endowed with a level of plasticity and 'memory', which dictates that cells are always present in the tumour whose role is to make sure that the total population of cancer cells will not be eradicated. This 'memory', however, also includes additional mutations such that the 'second-line' tumours, derived from the CSCs that survived the therapeutic intervention, is resistant to the 'first-line' treatment, which considerably jeopardizes any therapeutic modalities applicable to such patients.

While every tumour has different properties, cancer cells also share many features. This may well be true also for CSCs from different types of tumours. Finding such common traits may help discover the Achilles' heel of CSCs and, subsequently, devise efficient therapeutic

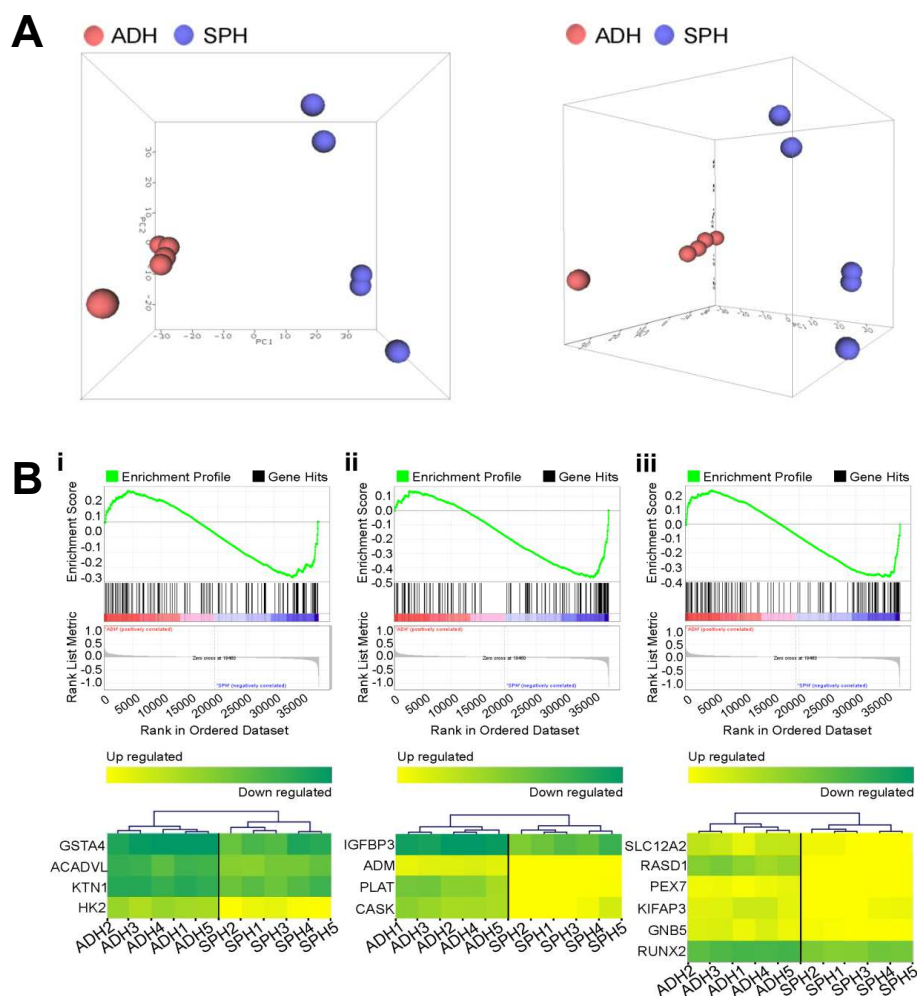


Fig. 4. Microarray data characterise mammospheres as a phenotype with increased stemness. A. Principle components analysis (PCA) of adherent (ADH) and mammosphere (SPH) MCF7 cell cultures shows that each phenotype clusters together. PCA projections are represented in 2D (left) and 3D (right) manner. B. Gene set enrichment analysis (GSEA) plots show enrichment of (i) embryonic stem cell (ESC) ($p = 0.044$, $FDR = 0.046$), (ii) neuronal stem cell (NSC) ($p = 0.001$, $FDR = 0.006$) and (iii) hematopoietic stem cell (HSC) ($p = 0.075$, $FDR = 0.085$) gene sets in mammosphere but not adherent cultures. Each vertical line on the enrichment plot represents a probe in the corresponding gene set. The left to right position of vertical lines indicates the relative position genes from ESC, NSC and HSC gene sets within the rank-ordered list of the 37,805 probes present on the HumanHT-12 BeadChip. The first probe on the left represents the most upregulated probe in adherent samples and the last on the right represents the most upregulated probe in the sphere-forming samples. Probes in the middle are not differentially expressed.

approaches. There are studies that attempted to characterize the global difference of gene expression in fast-proliferating tumour cells and the corresponding CSCs, and such studies have been useful for confirming the stemness features of the cells (Ivanova *et al.*, 2002; Ramalho-Santoz *et al.*, 2002; Fortunel *et al.*, 2003) or to characterize specific properties of CSCs (Birnie *et al.*, 2008).

We have attempted to use microarray analysis to characterize the stemness of several types of cancer cells grown as spheres, including breast and prostate cancer as well as malignant mesotheliomas (Figure 4) (Neuzil *et al.*, unpublished data). Using this approach, we identified increased stemness in all three types of cancer. Moreover, the tools of bioinformatics allow us to search for features that are shared by the different types of model CSC cultures. We found that the three types of CSCs share certain pathways, including glycolysis and oxidative phosphorylation, which suggests that the use of agents like MitoVES (*cf.* Figure 3) may be a way how to kill such cells. Further and probably most intriguingly, we found that of all the shared pathways that are upregulated in the three types of CSCs, tryptophan metabolism (represented by increased expression of IDO) is the most activated pathway. This is a highly interesting result, which suggests that CSCs are endowed with activity that results in lowering the level of tryptophan in their 'neighborhood'. Depletion of tryptophan (especially due to upregulation of IDO) is one way how cancer cells may protect themselves from the immune surveillance, providing the cancer cells with both passive and active defense mechanisms (Munn & Melor, 2008; Löb *et al.*, 2009), and inhibitors of IDO, such as brassinin or 1-methyl tryptophan, are being considered as anti-cancer drugs (Gaspari *et al.*, 2006; Hou *et al.*, 2007).

It is therefore very tempting to speculate that a highly efficient way to eradicate tumour cells, including the fast-proliferating ones and the resistant CSCs, may be the combination of agents like MitoVES that would kill the bulk of the tumour cells, while the IDO inhibitor would allow for the cells of the immune system to attack the remaining tumour cells, likely those with higher level of 'stemness'. Although a lot of work remains to be done, we propose that such a strategy may be potentially developed and applied in the clinic to minimize the probability of cancer relapse.

5. References

- Al-Hajj, M., Wicha, M.S., Benito-Hernandez, A., Morrison, S.J. & Clarke, M.F. (2003) Prospective identification of tumorigenic breast cancer cells. *Proc Natl Acad Sci USA* 100, 3983-3988.
- Alison, M.R., Islam, S. & Wright, N.A. (2010) Stem cells in cancer: instigators and propagators? *J Cell Sci* 123, 2357-2368.
- Alvero, A.B., Chen, R., Fu, H.H., Montagna, M., Schwartz, P.E., Rutherford, T., Silasi, D.A., Steffensen, K.D., Waldstrom, M., Visintin, I. & Mor, G. (2009) Molecular phenotyping of human ovarian cancer stem cells unravels the mechanisms for repair and chemoresistance. *Cell Cycle* 8, 158-166.
- Anderson, K.N. & Bejcek, B.E. (2008) Parthenolide induces apoptosis in glioblastomas without affecting NF- κ B. *J Pharmacol Sci* 106, 318-320.
- Baba, T., Convery, P.A., Matsumura, N., Whitaker, R.S., Kondoh, E., Perry, T., Huang, Z., Bentley, R.C., Mori, S., Fujii, S., Marks, J.R., Berchuck, A. & Murphy, S.K. (2009) Epigenetic regulation of CD133 and tumorigenicity of CD133⁺ ovarian cancer cells. *Oncogene* 28, 209-218.

- Bancroft, G.J., Schreiber, R.D. & Unanue, E.R. (1991) Natural immunity: A T-cell independent pathway of macrophage activation, defined in the scid mouse. *Immunol Rev* 124, 5-24.
- Bao, S., Wu, Q., McLendon, R.E., Hao, Y., Shi, Q., Hjelmelad, A.B., Dewhirst, M.W., Bigner, D.D. & Rich, J.N. (2006) Glioma stem cells promote radioresistance by preferential activation of the DNA damage response. *Nature* 444, 756-760.
- Bhatia, M., Bonnet, D., Murdoch, B., Gan, O.I. & Dick, J.E. (1998) A newly discovered class of human hematopoietic cells with SCID-repopulating activity. *Nat Med* 4, 1038-1045.
- Biassutto, L., Dong, L.F., Zoratti, M. & Neuzil, J. (2010) Mitochondrially targeted anti-cancer drugs. *Mitochondrion* 10, 670-681.
- Birnie, R., Bryce, S.D., Roome, C., Dussupt, V., Droop, A., Lang, S.H., Berry, P.A., Hyde, C.F., Lewis, J.L., Stower, M.J., Maitland, N.J. & Collins, A.T. (2008) Gene expression profiling of human prostate cancer stem cells reveals a pro-inflammatory phenotype and the importance of extracellular matrix interactions. *Genome Biol* 9, R83.
- Boman, B.M. & Huang, E. (2008) Human colon cancer stem cells: a new paradigm in gastrointestinal oncology. *J Clin Oncol* 26, 2828-2838.
- Bork, P.M., Schmitz, M.L., Kuhnt, M., Escher, C. & Heinrich, M. (1997) Sesquiterpene lactone containing Mexican Indian medicinal plants and pure sesquiterpene lactones as potent inhibitors of transcription factor NF- κ B. *FEBS Lett* 402, 85-90.
- Burris, H.A., Hurwitz, H.I., Dees, E.C., Dowlati, A., Blackwell, K.L., O'Neil, B., Marcom, P.K., Ellis, M.J., Overmoyer, B., Jones, S.F., Harris, J.L., Smith, D.A., Koch, K.M., Stead, A., Mangum, S. & Spector, N.L. (2005) Phase I safety, pharmacokinetics, and clinical activity study of lapatinib (GW572016), a reversible dual inhibitor of receptor tyrosine kinases, in heavily pretreated patients with metastatic carcinomas. *J Clin Oncol* 23, 5305-5313.
- Charafe-Jauffret, E., Ginestier, C., Iovino, F., Wicinski, J., Cervera, N., Finetti, P., Hur, M.H., Diebel, M.E., Monville, F., Dutcher, J., Brown, M., Viens, P., Xerri, L., Bertucci, F., Stassi, G., Dontu, G., Birnbaum, D. & Wicha, M.S. (2009) Breast cancer cell lines contain functional cancer stem cells with metastatic capacity and a distinct molecular signature. *Cancer Res* 69, 1302-1313.
- Collins, A.T., Berry, P.A., Hyde, C., Stower, M.J. & Maitland, N.J. (2005) Prospective identification of tumorigenic prostate cancer stem cells. *Cancer Res* 65, 10946-10951.
- Corbeil, D., Roper, F., Fargeas, C.A., Joester, A. & Huttner, W.B. (2001) Prominin: a story of cholesterol, plasma membrane protrusions and human pathology. *Traffic* 2, 82-91.
- Crandall, J.P., Knowler, W.C., Kahn, S.E., Marrero, D., Florez, J.C., Bray, G.A., Haffner, S.M., Hoskin, M. & Nathan, D.M. (2008) The prevention of type 2 diabetes. *Nat Clin Pract Endocrinol Metab* 4, 382-393.
- D'Amour, K.A. & Gage, F.H. (2002) Are somatic stem cells pluripotent or lineage-restricted? *Nat Med* 8, 213-214.
- Diaz, R., Nguewa, P.A., Parrondo, R., Perez-Stable, C., Manrique, I., Redrado, M., Catena, R., Collantes, M., Penuelas, I., Diaz-Gonzalez, J.A. & Calvo, A. (2010) Antitumour and antiangiogenic effect of the dual EGFR and HER-2 tyrosine kinase inhibitor lapatinib in a lung cancer model. *BMC Cancer* 10, 188.
- Dirks, P.B. (2010) Brain tumour stem cells: The cancer stem cell hypothesis writ large. *Mol Oncol* 4, 420-430.

- Dong, L.F., Freeman, R., Liu, J., Zabalova, R., Marin-Hernandez, A., Stantic, M., Rohlena, J., Rodriguez-Enriquez, S., Valis, K., Butcher, B., Goodwin, J., Brunk, U.T., Witting, P.K., Moreno-Sanchez, R., Scheffler, I.E., Ralph, S.J. & Neuzil, J. (2009) Suppression of tumour growth *in vivo* by the mitocan α -tocopheryl succinate requires respiratory complex II. *Clin Cancer Res* 15, 1593-1600.
- Dong, L.F., Low, P., Dyason, J., Wang, X.F., Prochazka, L., Witting, P.K., Freeman, R., Swettenham, E., Valis, K., Liu, J., Zabalova, R., Turanek, J., Spitz, D.R., Domann, F.E., Scheffler, I.E., Ralph, S.J. & Neuzil, J. (2008) α -Tocopheryl succinate induces apoptosis by targeting ubiquinone-binding sites in mitochondrial respiratory complex II. *Oncogene* 27, 4324-4335.
- Dong, L.F., Jameson, V.J.A., Tilly, D., Cerny, J., Mahdavian, E., Marín-Hernández, A., Hernández-Esquivel, L., Rodríguez-Enriquez, S., Witting, P.K., Stantic, B., Rohlena, J., Truksa, J., Kluckova, K., Dyason, J.C., Salvatore, B.A., Moreno-Sánchez, R., Coster, M.J., Ralph, S.J., Smith, R.A.J., & Neuzil, J. (2011) Mitochondrial targeting of vitamin E succinate enhances its pro-apoptotic and anti-cancer activity via mitochondrial complex II. *J Biol Chem* 286, 3717-3728.
- Du, L., Wang, H., He, L., Zhang, J., Ni, B., Wang, X., Jin, H., Cahuzac, N., Mehrpour, M., Lu, Y. & Chen, Q. (2008) CD44 is of functional importance for colorectal cancer stem cells. *Clin Cancer Res* 14, 6751-6760.
- Dunn, G.P., Bruce, A.T., Ikeda, H., Old, L.J. & Schreiber, R.D. (2002) Cancer immunoediting: From immunosurveillance to tumour escape. *Nat Immunol* 3, 991-998.
- Dunn, G.P., Old, L.J. & Schreiber, R.D. (2004a) The immunobiology of cancer immunosurveillance and immunoediting. *Immunity* 21, 137-148.
- Dunn, G.P., Old, L.J. & Schreiber, R.D. (2004b) The three Es of cancer immunoediting. *Annu Rev Immunol* 22, 329-360.
- Essers, M.A.G. & Trumpp, A. (2010) Targeting leukemic stem cells by breaking their dormancy. *Mol Oncol* 4, 443-450.
- Fang, D., Nguyen, T.K., Leishear, K., Finko, R., Kulp, A.N., Hotz, S., Van Belle, P.A., Xu, X., Elder, D.E. & Herlyn, M. (2005) A tumorigenic subpopulation with stem cell properties in melanomas. *Cancer Res* 65:9328-9337.
- Fortunel, N.O., Out, H.H., Ng, H.H., Chen, J., Mu, X., Chevassut, T., Li, X., Joseph, M., Bailey, C., Hatzfeld, J.A., Hatzfeld, A., Usta, F., Vega, V.B., Long, P.M., & Libermann, T.A., & Lim, B. (2003) *Science* 302, 393.
- Frank, N.Y., Pendse, S.S., Lapchak, P.H., Margaryan, A., Shlain, D., Doeing, C., Sayegh, M.H. & Frank, M.H. (2003) Regulation of progenitor cell fusion by ABCB5 P-glycoprotein, a novel human ATP-binding cassette transporter. *J Biol Chem* 278, 47156-47165.
- Frank, N.Y., Margaryan, A., Huang, Y., Schatton, T., Waaga-Gasser, A.M., Gasser, M., Sayegh, M.H., Sadee, W. & Frank, M.H. (2005) ABCB5-mediated doxorubicin transport and chemoresistance in human malignant melanoma. *Cancer Res* 65, 4320-4333.
- Fuchs, D., Daniel, V., Sadeghi, M., Opelz, G. & Naujokat, C. (2010) Salinomycin overcomes ABC transporter-mediated multidrug and apoptosis resistance in human leukemia stem cell-like KG-1a cells. *Biochem Biophys Res Commun* 394, 1098-1104.

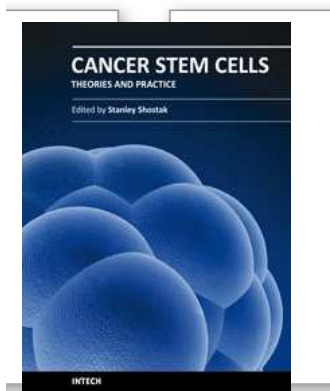
- Fuchs, D., Heinold, A., Opelz, G., Daniel, V. & Naujokat, C. (2009) Salinomycin induces apoptosis and overcomes apoptosis resistance in human cancer cells. *Biochem Biophys Res Commun* 390, 743-749.
- Gaspari, P., Banerjee, T., Malachowski, W.P., Muller, A.J., Prendergast, G.C., DuHadaway, J., Bennett, S. & Donovan, A.M. (2006) Structure-activity study of brassinin derivatives as indoleamine 2,3-dioxygenase inhibitors. *J Med Chem* 49, 684-692.
- Ghantous, A., Gali-Muhtasib, H., Vuorela, H., Saliba, N.A. & Darwiche, N. (2010) What made sesquiterpene lactones reach cancer clinical trials? *Drug Discov Today* 15, 668-678.
- Gibbs, C.P., Kukekov, V.G., Reith, J.D., Tchigrinova, O., Suslov, O.N., Scott, E.W., Ghivizzani, S.C., Ignatova, T.N. & Steindler, D.A. (2005) Stem-like cells in bone sarcomas: implications for tumorigenesis. *Neoplasia* 7, 967-976.
- Ginestier, C., Hur, M.H., Charafe-Jauffret, E., Monville, F., Dutcher, J., Brown, M., Jacquemier, J., Viens, P., Kleer, C.G., Liu, S., Schott, A., Hayes, D., Birnbaum, D., Wicha, M.S. & Dontu, G. (2007) ALDH1 is a marker of normal and malignant human mammary stem cells and a predictor of poor clinical outcome. *Cell Stem Cell* 1, 555-567.
- Gupta, P.B., Onder, T.T., Jiang, G., Tao, K., Kuperwasser, C., Weinberg, R.A. & Lander, E.S. (2009) Identification of selective inhibitors of cancer stem cells by high-throughput screening. *Cell* 138, 645-659.
- Guzman, M.L. & Jordan, C.T. (2005a) Feverfew: weeding out the root of leukaemia. *Expert Opin Biol Ther* 5, 1147-1152.
- Guzman, M.L., Rossi, R.M., Karnischky, L., Li, X., Peterson, D.R., Howard, D.S. & Jordan, C.T. (2005b) The sesquiterpene lactone parthenolide induces apoptosis of human acute myelogenous leukemia stem and progenitor cells. *Blood* 105, 4163-4169.
- Guzman, M.L., Rossi, R.M., Neelakantan, S., Li, X., Corbett, C.A., Hassane, D.C., Becker, M.W., Bennett, J.M., Sullivan, E., Lachowicz, J.L., Vaughan, A., Sweeney, C.J., Matthews, W., Carroll, M., Liesveld, J.L., Crooks, P.A. & Jordan, C.T. (2007) An orally bioavailable parthenolide analog selectively eradicates acute myelogenous leukemia stem and progenitor cells. *Blood* 110, 4427-4435.
- Hambardzumyan, D., Squartro, M. & Holland, E.C. (2006) Radiation resistance and stem-like cells in brain tumours. *Cancer Cell* 10, 454-456.
- Hanahan, D. & Weinberg, R.A. (2000) The hallmarks of cancer. *Cell* 100, 57-70.
- Hassane, D.C., Guzman, M.L., Corbett, C., Li, X., Abboud, R., Young, F., Liesveld, J.L., Carroll, M. & Jordan, C.T. (2008) Discovery of agents that eradicate leukemia stem cells using an in silico screen of public gene expression data. *Blood* 111, 5654-5662.
- Hayakawa, Y., Kelly, J.M., Westwood, J.A., Darcy, P.K., Diefenbach, A., Raulet, D. & Smyth, M.J. (2002) Cutting edge: Tumour rejection mediated by NKG2D receptor-ligand interaction is dependent upon perforin. *J Immunol* 169, 5377-5381.
- Hehner, S.P., Heinrich, M., Bork, P.M., Vogt, M., Ratter, F., Lehmann, V., Schulze-Osthoff, K., Dröge, W. & Schmitz, M.L. (1998) Sesquiterpene lactones specifically inhibit activation of NF- κ B by preventing the degradation of I κ B- α and I κ B- β . *J Biol Chem* 273, 1288-1297.
- Hemmati, H.D., Nakano, I., Lazareff, J.A., Masterman-Smith, M., Geschwind, D.H., Bronner-Fraser, M. & Kornblum, H.I. (2003) Cancerous stem cells can arise from pediatric brain tumours. *Proc Natl Acad Sci USA* 100, 15178-15183.

- Hirsch, H.A., Iliopoulos, D., Tsichlis, P.N. & Struhl, K. (2009) Metformin selectively targets cancer stem cells, and acts together with chemotherapy to block tumour growth and prolong remission. *Cancer Res* 69, 7507-7511.
- Hou, D.Y., Muller, A.J., Sharma, M.D., DuHadaway, J., Banerjee, T., Johnson, M., Mellor, A.L., Prendergast, G.C. & Munn, D.H. (2007) Inhibition of indoleamine 2,3-dioxygenase in dendritic cells by stereoisomers of 1-methyl-tryptophan correlates with antitumour responses. *Cancer Res* 67, 792-801.
- Ivanova, N.B., Dimos, J.T., Schaniel, C., Hackney, J.A., Moore, K.A. & Lemischka, I.R. (2002) A stem cell molecular signature. *Science* 298, 601-604.
- Jemal, A., Siegel, R., Xu, J. & Ward, E. (2010) Cancer statistics, 2010. *CA Cancer J Clin* 60, 277-300.
- Kawasaki, B.T., Hurt, E.M., Kalathur, M., Duhagon, M.A., Milner, J.A., Kim, Y.S. & Farrar, W.L. (2009) Effects of the sesquiterpene lactone parthenolide on prostate tumour-initiating cells: An integrated molecular profiling approach. *Prostate* 69, 827-837.
- Korkaya, H. & Wicha, M.S. (2009) HER2, Notch, and breast cancer stem cells: targeting an axis of evil. *Clin Cancer Res* 15, 1845-1847.
- Lapidot, T., Sirard, C., Vormoor, J., Haas, T.L., Diessenbacher, P., Sprick, M.R., Schön, M.P., Henkler, F., Gollnick, H., Walczak, H. & Leverkus, M. (1994) A cell initiating human acute myeloid leukaemia after transplantation into SCID mice. *Nature* 367, 645-648.
- Li, C., Heidt, D.G., Dalerba, P., Burant, C.F., Zhang, L., Adsay, V., Wicha, M., Clarke, M.F. & Simeone, D.M. (2007) Identification of pancreatic cancer stem cells. *Cancer Res* 67, 1030-1037.
- Li, Y., Fang, J., Wu, S., Ma, K., Li, H., Yan, X. & Dong, F. (2010) Identification and quantification of salinomycin in intoxicated human plasma by liquid chromatography-electrospray tandem mass spectrometry. *Anal Bioanal Chem* 398, 955-961.
- Liu, G., Yuan, X., Zeng, Z., Tunici, P., Ng, H., Abdulkadir, I.R., Lu, L., Irvin, D., Black, K.L. & Yu, J.S. (2006) Analysis of gene expression and chemoresistance of CD133⁺ cancer stem cells in glioblastoma. *Mol Cancer* 5, 1476-1498.
- Liu, Y., Lu, W.L., Guo, J., Du, J., Li, T., Wu, J.W., Wang, G.L., Wang, J.C., Zhang, X. & Zhang, Q. (2008) A potential target associated with both cancer and cancer stem cells: a combination therapy for eradication of breast cancer using vinorelbine stealthy liposomes plus parthenolide stealthy liposomes. *J Control Release* 129, 18-25.
- Löb, S., Königsrainer, A., Rammensee, H.G., Opelz, G. & Terness, P. (2009) Inhibitors of indoleamine-2,3-dioxygenase for cancer therapy: can we see the wood for the trees? *Nat Rev Cancer* 9, 445-452.
- Lonardo, E., Hermann, P.C. & Heeschen, C. (2010) Pancreatic cancer stem cells - update and future perspective. *Mol Oncol* 4, 431-442.
- Magnifico, A., Albano, L., Campaner, S., Delia, D., Castiglioni, F., Gasparini, P., Sozzi, G., Fontanella, E., Menard, S. & Tagliabue, E. (2009) Tumour-initiating cells of HER2-positive carcinoma cell lines express the highest oncoprotein levels and are trastuzumab-sensitive. *Clin Cancer Res* 15, 306-313.
- Martin-Castillo, B., Vazquez-Martin, A., Oliveras-Ferraros, C. & Menendez, J.A. (2010) Metformin and cancer: Doses, mechanisms and the dandelion and hormetic phenomena. *Cell Cycle*, in press.

- McDermott, S.P. & Wicha, M.S. (2010) Targeting breast cancer stem cells. *Mol Oncol* 4, 404-419.
- Miraglia, S., Godfrey, W., Yin, A.H., Atkins, K., Warnke, R., Holden, J.T., Bray, R.A., Waller, E.K. & Buck, D.W. (2007) A novel five-transmembrane hematopoietic stem cell antigen: isolation, characterization, and molecular cloning. *Blood* 90, 5013-5021.
- Miyazaki, Y., Shibuya, M., Sugawara, H., Kawaguchi, O. & Hirsoe, C. (1974) Salinomycin, a new polyether antibiotic. *J Antibiot* 27, 814-821.
- Munn, D.H. & Mellor, A.L. (2007) Indoleamine 2,3-dioxygenase and tumour-induced tolerance. *J Clin Invest* 117, 1147-1154.
- Murphy, M.P. & Smith, R. (2007) Targeting antioxidants to mitochondria by conjugation to lipophilic cations. *Annu Rev Pharmacol Toxicol* 47, 629-656.
- Neuzil, J., Stantic, M., Zobalova, R., Chladova, M., Wang, X.F., Dong, L.F., Prochazka, L., Andera, L. & Ralph, S.J. (2007) Tumour-initiating cells vs. cancer 'stem' cells and CD133: What's in the name? *Biochem Biophys Res Commun* 355, 855-859.
- Neuzil, J., Weber, T., Schröder, A., Lu, M., Ostermann, G., Gellert, N., Mayne, G.C., Olejnicka, B., Nègre-Salvayre, A., Sticha, M., Coffey, R.J. & Weber, C. (2001) Induction of apoptosis in cancer cells by α -tocopheryl succinate: Molecular pathways and structural requirements. *FASEB J* 15, 403-415.
- Nguyen, N.P., Almeida, F.S., Chi, A., Nguyen, L.M., Cohen, D., Karlsson, U. & Vinh-Hung, V. (2010) Molecular biology of breast cancer stem cells: potential clinical applications. *Cancer Treat Rev* 36, 485-491.
- O'Brien, C.A., Pollett, A., Gallinger, S. & Dick, J.E. (2007) A human colon cancer cell capable of initiating tumour growth in immunodeficient mice. *Nature* 445, 106-110.
- Park, C.H., Bergsagel, D.E. & McCulloch, E.A. (1971) Mouse myeloma tumour stem cells: a primary cell culture assay. *J Natl Cancer Inst* 46, 411-422.
- Patrawala, L., Calhoun, T., Schneider-Broussard, R., Li, H., Bhatia, B., Tang, S., Reilly, J.G., Chandra, D., Zhou, J., Claypool, K., Coghlan, L. & Tang, D.G. (2006) Highly purified CD44+ prostate cancer cells from xenograft human tumours are enriched in tumorigenic and metastatic progenitor cell *Oncogene* 25, 1696-1708.
- Piccirillo, S.G., Reynolds, B.A., Zanetti, N., Lamorte, G., Binda, E., Broggi, G., Brem, H., Olivi, A., Dimeco, F. & Vescovi, A.L. (2006) Bone morphogenetic proteins inhibit the tumorigenic potential of human brain tumour-initiating cells. *Nature* 444, 761-765.
- Prochazka, L., Dong, L.F., Valis, K., Freeman, R., Ralph, S.J., Turanek, J. & Neuzil, J. (2010) α -Tocopheryl succinate causes mitochondrial permeabilization by preferential formation of Bak channel. *Apoptosis* 15, 782-794.
- Ramalho-Santos, M., Yoon, S., Matsuzaki, Y., Mulligan, R.C. & Melton, D.A. (2002) "Stemness": transcriptional profiling of embryonic and adult stem cells. *Science* 298, 597-600.
- Ricci-Vitiani, L., Lombardi, D.G., Pilozzi, E., Ricci-Vitiani, L., Lombardi, D.G. & Pilozzi, E. (2007) Identification and expansion of human colon-cancer-initiating cells. *Nature* 445, 111-115.
- Riccioni, R., Dupuis, M.L., Bernabei, M., Petrucci, E., Pasquini, L., Mariani, G., Cianfriglia, M. & Testa, U. (2010) The cancer stem cell selective inhibitor salinomycin is a p-glycoprotein inhibitor. *Blood Cells Mol Dis* 45, 86-92.
- Rowan, K. (2009) High-throughput screening finds potential killer for cancer stem cells. *J Natl Cancer Inst* 101, 1438-1439.

- Schatton, T., Murphy, G.F., Frank, N.Y., Yamaura, K., Waaga-Gasser, A.M., Gasser, M., Zhan, Q., Jordan, S., Duncan, L.M., Weishaupt, C., Fuhlbrigge, R.C., Kupper, T.S., Sayegh, M.H. & Frank, M.H. (2008) Identification of cells initiating human melanomas. *Nature* 451, 345-349.
- Schreiber, R.D., Pace, J.L., Russell, S.W., Altman, A. & Katz, D.H. (1983) Macrophage-activating factor produced by a T cell hybridoma: Physicochemical and biosynthetic resemblance to γ -interferon. *J Immunol* 131, 826-832.
- Shipitsin, M., Campbell, L.L., Argani, P., Weremowicz, S., Bloushtain-Qimron, N., Yao, J., Nikolskaya, T., Serebryiskaya, T., Beroukhim, R., Hu, M., Halushka, M.K., Sukumar, S., Parker, L.M., Anderson, K.S., Harris, L.N., Garber, J.E., Richardson, A.L., Schnitt, S.J., Nikolsky, Y., Gelman, R.S. & Polyak K: Molecular definition of breast tumour heterogeneity. *Cancer Cell* 11, 259-273.
- Shmelkov, S.V., Butler, J.M., Hooper, A.T., Hormigo, A., Kushner, J., Milde, T., St Clair, R., Baljevic, M., White, I., Jin, D.K., Chadburn, A., Murphy, A.J., Valenzuela, D.M., Gale, N.W., Thurston, G., Yancopoulos, G.D., D'Angelica, M., Kemeny, N., Lyden, D. & Rafii, S. (2008) CD133 expression is not restricted to stem cells, and both CD133+ and CD133- metastatic colon cancer cells initiate tumours. *J Clin Invest* 118, 2111-2120.
- Singh, S.K., Clarke, I.D., Terasaki, M., Haas, T.L., Diessenbacher, P., Sprick, M.R., Schön, M.P., Henkler, F., Gollnick, H., Walczak, H. & Leverkus, M. (2003) Identification of a cancer stem cell in human brain tumours. *Cancer Res* 63, 5821-5828.
- Slamon, D.J., Godolphin, W., Jones, L.A., Holt, J.A., Wong, S.G., Keith, D.E., Levin, W.J., Stuart, S.G., Udove, J. & Ullrich, A. (1989) Studies of the HER-2/neu proto-oncogene in human breast and ovarian cancer. *Science* 244, 707-712.
- Smyth, M.J., Cretney, E., Takeda, K., Wiltout, R.H., Sedger, L.M., Kayagaki, N., Yagita, H. & Okumura, K. (2001) Tumour necrosis factor-related apoptosis-inducing ligand (TRAIL) contributes to interferon γ -dependent natural killer cell protection from tumour metastasis. *J Exp Med* 193, 661-670.
- Smyth, M.J., Crowe, N.Y., Hayakawa, Y., Takeda, K., Yagita, H. & Godfrey, D.I. (2002) NKT cells-conductors of tumour immunity? *Curr Opin Immunol* 14, 165-171.
- Takeda, K., Hayakawa, Y., Smyth, M.J., Kayagaki, N., Yamaguchi, N., Kakuta, S., Iwakura, Y., Yagita, H. & Okumura, K. (2001) Involvement of tumour necrosis factor-related apoptosis-inducing ligand in surveillance of tumour metastasis by liver natural killer cells. *Nat Med* 7, 94-100.
- Tang, C., Ang, B.T. & Pervaiz, S. (2007) Cancer stem cell: target for anti-cancer therapy. *FASEB J* 21, 1-9.
- Twombly, R. (2005) Cancer surpasses heart disease as leading cause of death of all but the very elderly. *J Natl Cancer Inst* 97, 330-331.
- Valis, K., Prochazka, L., Boura, E., Chladova, M., Obsil, T., Rohlena, J., Truksa, J., Dong, L.F., Ralph, S.J. & Neuzil, J. Hippo/Mst1 stimulates transcription of NOXA in a FoxO1-dependent manner. *Cancer Res*, in press.
- Vazquez-Martin, A., Oliveras-Ferraros, C., Barco, S.D., Martin-Castillo, B. & Menendez, J.A. (2010a) The anti-diabetic drug metformin suppresses self-renewal and proliferation of trastuzumab-resistant tumour-initiating breast cancer stem cells. *Breast Cancer Res Treat*, in press.

- Vazquez-Martin, A., Oliveras-Ferraros, C., Cufi, S., Martin-Castillo, B. & Menendez, J.A. (2010b) Metformin and energy metabolism in breast cancer: From insulin physiology to tumour-initiating stem cells. *Curr Mol Med* 10, 674-691.
- Vescovi, A.L., Galli, R., & Reynolds, B.A. (2006) Brain tumour stem cells. *Nat Rev Cancer* 6, 425-436.
- Visvader, J.E. (2009) Keeping abreast of the mammary epithelial hierarchy and breast tumourigenesis. *Genes Dev* 23, 2563-2577.
- Visvader, J.E. & Lindeman, G.J. (2008) Cancer stem cells in solid tumours: accumulating evidence and unresolved questions. *Nat Rev Cancer* 8, 755-768.
- Weber, T., Lu, M., Andera, L., Lahm, H., Gellert, N., Fariss, M.W., Korinek, V., Sattler, W., Ucker, D.S., Terman, A., Schröder, A., Erl, W., Brunk, U., Coffey, R.J., Weber, C. & Neuzil, J. (2002) Vitamin E succinate is a potent novel anti-neoplastic agent with high tumour selectivity and cooperativity with tumour necrosis factor-related apoptosis-inducing ligand (TRAIL, Apo2L) in vivo. *Clin Cancer Res* 8, 863-869.
- Wright, M.H., Calcagno, A.M., Salcido, C.D., Carlson, M.D., Ambudkar, S.V. & Varticovski, L. (2007) Brca1 breast tumours contain distinct CD44⁺/CD24⁻ and CD133⁺ cells with cancer stem cell characteristics. *Breast Cancer Res* 10, R10.
- Yang, Z.F., Ho, D.W., Ng, M.N., Lau, C.K., Yu, W.C., Ngai, P., Chu, P.W., Lam, C.T., Poon, R.T. & Fan, S.T. (2008) Significance of CD90⁺ cancer stem cells in human liver cancer. *Cancer Cell* 13, 153-166.
- Yin, S., Li, J., Hu, C., Chen, X., Yao, M., Yan, M., Jiang, G., Ge, C., Xie, H., Wan, D., Yang, S., Zheng, S. & Gu, J. (2007) CD133 positive hepatocellular carcinoma cells possess high capacity for tumourigenicity. *Int J Cancer* 120, 1436-1442.
- Zhang, S., Belch, C., Chan, M.W., Lai, H.C., Matei, D., Schilder, J.M., Yan, P.S., Huang, T.H. & Nephew, K.P. (2008) Identification and characterization of ovarian cancer-initiating cells from primary human tumours. *Cancer Res* 68, 4311-4320.
- Zhou, J., Zhang, H., Gu, P., Bai, J., Margolick, J.B. & Zhang, Y (2008) NF- κ B pathway inhibitors preferentially inhibit breast cancer stem-like cells. *Breast Cancer Res Treat* 111, 419-427.
- Zobalova, R., McDermott, L., Stantic, M., Prokopova, K., Dong, L.F. & Neuzil, J. (2008) CD133-positive cancer cells are resistant to TRAIL due to upregulation of FLIP. *Biochem Biophys Res Commun* 373, 567-571.



Cancer Stem Cells Theories and Practice

Edited by Prof. Stanley Shostak

ISBN 978-953-307-225-8

Hard cover, 442 pages

Publisher InTech

Published online 22, March, 2011

Published in print edition March, 2011

Cancer Stem Cells Theories and Practice does not 'boldly go where no one has gone before!' Rather, Cancer Stem Cells Theories and Practice boldly goes where the cutting edge of research theory meets the concrete challenges of clinical practice. Cancer Stem Cells Theories and Practice is firmly grounded in the latest results on cancer stem cells (CSCs) from world-class cancer research laboratories, but its twenty-two chapters also tease apart cancer's vulnerabilities and identify opportunities for early detection, targeted therapy, and reducing remission and resistance.

How to reference

In order to correctly reference this scholarly work, feel free to copy and paste the following:

Renata Zobalova, Marina Stantic, Michael Stapelberg, Katerina Prokopova, Lanfeng Dong, Jaroslav Truksa and Jiri Neuzil (2011). Drugs that Kill Cancer Stem-like Cells, Cancer Stem Cells Theories and Practice, Prof. Stanley Shostak (Ed.), ISBN: 978-953-307-225-8, InTech, Available from:
<http://www.intechopen.com/books/cancer-stem-cells-theories-and-practice/drugs-that-kill-cancer-stem-like-cells>

INTECH
open science | open minds

InTech Europe

University Campus STeP Ri
Slavka Krautzeka 83/A
51000 Rijeka, Croatia
Phone: +385 (51) 770 447
Fax: +385 (51) 686 166
www.intechopen.com

InTech China

Unit 405, Office Block, Hotel Equatorial Shanghai
No.65, Yan An Road (West), Shanghai, 200040, China
中国上海市延安西路65号上海国际贵都大饭店办公楼405单元
Phone: +86-21-62489820
Fax: +86-21-62489821

5. DISSCUSSION

Utilization of mitochondria as a target for anti-cancer treatment has been neglected for a long time. However, in light of recent development in the fields of mitochondrial bioenergetics, the role of reactive oxygen species and apoptosis induction by mitochondria, these organelles are emerging as the prime target for novel therapeutic strategies. Based on the considerable heterogeneity within cancer cells of a tumour, it is becoming increasingly clear that targeting of a single gene or a signalling pathway is unlikely to bring a benefit on a large scale. Mitochondria in this context represent an intriguing option for cancer therapy for several reasons. (i) Mitochondria represent a stable target, functional in vast majority of cancers (Ralph et al., 2010). (ii) Mitochondria in cancer cells differ from mitochondria in normal cells (Koppenol et al., 2011). (iii) Mitochondria are reservoirs for apoptosis-promoting molecules, such as cyt c and caspase proteases, important for induction and execution of cell death (Galluzzi et al., 2012).

Tamoxifen is the first-line therapy of ER-positive breast cancer. However, as many as 50% of patients develop resistance to treatment. One of the common reasons for this resistance is overexpression of the *HER2* oncogene. The main mode of tamoxifen action is its anti-ER activity. In addition, tamoxifen has been shown to act as an inhibitor of CI of the ETC, although at supra-pharmacological doses (Moreira et al., 2006).

Based on the above considerations, we designed a mitochondrially targeted derivative of tamoxifen, MitoTam, by tagging the parental molecule with the TPP⁺ group. As expected, this caused accumulation of the modified tamoxifen in mitochondria, specifically at the IMM. Mitochondrial localization of tamoxifen had striking functional consequences.

(i) The anti-cancer efficacy of the drug was increased by at least an order of magnitude. At the therapeutic doses, MitoTam did not cause toxic side-effects. (ii) The efficacy was particularly high for the HER2^{high} subtype, which is resistant to tamoxifen. (iii) The main molecular targets identified were CI-dependent respiration and the respiratory supercomplexes.

We have detected a substantial generation of ROS after MitoTam treatment, whereas tamoxifen did not induce ROS production. These ROS were functionally relevant, as N-acetyl cysteine (NAC) ROS scavenger treatment protected from MitoTam-induced cell death. MitoTam treatment suppressed CI-dependent respiration and CI-CIII enzymatic activity, whereas its effect on CII-dependent respiration and CII-CIII activity was negligible. Moreover, molecular modelling approach suggested the interaction of MitoTam with the ubiquinone-binding pocket of CI. In such position, MitoTam would interfere with electron flow through CI, leading to excessive ROS generation, in line with the experimental observations. A similar mode of action was shown earlier for MitoVES, which interacts with ubiquinone-binding site of CII (Dong et al., 2011a; Kluckova et al., 2015). Such interaction is strongly dependent on the length of the carbon chain linker connecting the TPP⁺ moiety and the functional group (Truksa et al., 2015).

MitoTam was particularly efficient in eliminating HER2^{high} breast cancer cells and tumours, in stark contrast to the parental compound. We showed that HER2^{high} cells and tumours express more CI, engage in increased respiration through CI and have more assembled respiratory SCs. Overexpression of HER2 sensitized cells to MitoTam regardless of its ER status, as both ER-dependent MCF7 cells and ER-independent MDA-MB-231 cells became sensitive after HER2 overexpression. Therefore, the enhancement of CI respiration and the level of SCs is a plausible reason for HER2^{high} cell sensitivity.

MitoTam treatment disrupted SCs more prominently in the HER2^{high} situation, and HER2^{high} cells generated more mitochondrial ROS after MitoTam exposure. This is consistent with the notion that SCs enhance the effectivity of electron flow through respiratory complexes and facilitate a barrier against electron leakage. Therefore, higher SCs in HER2^{high} cells give support to enhanced respiration, which has fatal consequences in case of their disruption by MitoTam.

The results discussed above indicate that HER2 overexpression directly sensitized mitochondria to MitoTam. Several oncogenes have been reported to localize to mitochondria at some stage (Rohlenova et al., 2016a). Recently, Ding et al. (2012) reported existence of a mitochondrial fraction of HER2 and suggested its involvement in the enhancement of glycolysis. We have confirmed mitochondrial presence of HER2 in HER2-overexpressing cells in independent models. Using electron and super-resolution microscopy as well as biochemical approaches, we showed that HER2 in mitochondria is localized at the IMM. We have tested various aspects of glycolysis, as it would be feasible that if glycolysis was not induced as a compensatory mechanism upon decline of OXPHOS, it could also account for the sensitivity of HER2^{high} cells to MitoTam. Nevertheless, although we observed an increase in glucose uptake and lactate production in response to MitoTam treatment, we have not found significant differences between HER2^{high} and HER2^{low} cells. In addition, MitoTam treatment did not reduce ATP levels in any of the sublines. This indicates that glycolytic compensation cannot explain the increased sensitivity of HER2^{high} cells to MitoTam. In contrast, we consistently found increased respiration in HER2^{high} cells and tumours. Localized at the IMM, mitochondrial HER2 is ideally placed to engage in interaction with the ETC. In our system, we indeed observed increased respiration and SC assembly when mitochondrial HER2 was present, in

contrast to Ding et al, who focused mainly on changes in glycolysis. It should be noted that we also observed some increase in glycolysis when HER2 is high. To provide evidence that mitochondrial HER2 sensitizes HER2^{high} cells to MitoTam, we used two independent approaches. First, using siRNA against mtHSP70, a protein implicated in transport of HER2 to mitochondria (Ding et al., 2012), we were able to decrease the level of mitochondrial HER2. Silencing of mtHSP70 de-sensitized HER2^{high} cells to MitoTam, but did not affect the sensitivity of HER2^{low} cells. Second, we prepared a set of *HER2* constructs with increased and decreased ability to translocate into mitochondria and, consistently, increased mitochondrial localization was clearly connected with increased sensitivity to the drug and *vice versa*.

Both MitoTam and MitoVES are drugs targeting mitochondrial bioenergetics. As such, these drugs are able to control the metabolic heterogeneity of a tumour. It was repeatedly shown that the aggressive, resistant populations of tumour cells feature increased mitochondrial respiration. In our study, the aggressive HER2^{high} breast cancer cells also displayed increased respiration and higher level of respiratory SCs, which made them susceptible to MitoTam, while resistant to tamoxifen.

CSCs are recognized as one of the possible reasons of tumour resistance. We and others (Yan et al., 2015; Ye et al., 2011) have shown that CSCs possess higher $\Delta\Psi_{m,i}$ than the bulk tumour cells. In our study CSCs derived from mouse NeuTL breast cancer cells, although resistant to established therapeutics paclitaxel and doxorubicin were sensitive to MitoVES (Yan et al., 2015). MitoVES not only eliminated the CSC population via apoptosis induction, but the treatment also affected the tumour microenvironment. In CSCs derived from cancer cell lines as well as from patient tumour samples, we found up-regulated the tryptophan degradation pathway including indoleamine-2,3-dioxygenase 1

(IDO1), its rate-limiting enzyme. Depletion of tryptophan, as a result of increased uptake, and the accumulation of its metabolites is recognized as one of the mechanisms of cancer cell escape from the immune surveillance, as it leads to the inhibition of cytotoxic T cells and favours a switch to regulatory T cells (Liu et al., 2009). Nonetheless, MitoVES treatment suppressed IDO1 at the mRNA and protein levels. The effect was apparent using sub-apoptotic doses of MitoVES, and is likely connected with the increased oxidative stress as MitoVES was not effective in cells with dysfunctional CII, its molecular target, and IDO1 has been shown to be regulated by redox status (Thomas et al., 2001). This suggests an additional mechanism how ETC-directed compounds such as MitoVES deal with CSCs, via inducing their increased exposure to the immune system (Stapelberg et al., 2014).

According to the CSC theory, CSCs stand at the origin of tumour metastases, and we detected significantly decreased number of metastatic cells in the lung and of circulating tumour cells in mice with experimental mammary carcinoma treated with MitoTam. In an *in vitro* sphere model of CSCs, pre-incubation of cells with MitoTam, but not with tamoxifen, completely precluded the sphere formation (Rohlenova et al., 2016b). Therefore, both MitoTam and MitoVES are efficient against CSCs derived from various cell lines. The notion of CSCs, as a resistant sub-population of tumour with diverted metabolic needs perhaps describes them more accurately than classification according to the surface markers, as was presented in the Introduction. As such, CSCs and other ‘OXPHOS-addicted’ resistant sub-populations are introduced as a plausible target for the mitochondrially targeted agents presented herein.

To summarize, functional OXPHOS is essential for tumour initiation, while treatment-resistant populations of cancer cells are increasingly viewed as ‘OXPHOS-addicted’. Classical inhibitors such as rotenone (CI inhibitor), antimycin A (CIII inhibitor) or

potassium cyanate (CIV inhibitor) show systemic toxicity and are therefore unsuitable for therapy. On the other hand, the efficacy of known non-toxic inhibitors, such as the anti-diabetic drug metformin, did not bring as yet substantial benefit for cancer patients (Kordes et al., 2015; Reni et al., 2016). Therefore, there is an eminent need for effective agents, which would selectively target OXPHOS in cancer cells. Such a need may be fulfilled by the mitochondrially targeted compounds, epitomized by MitoVES and MitoTam. It is of note that the same principle of TPP⁺ modification of an existing anti-cancer drug has recently also been applied to metformin in our laboratory (Boukalova et al., submitted), as well as by others (Cheng et al., 2016), showing auspicious results. This indicates that the phenomenon of targeting ETC-directed anti-cancer drug to mitochondria, where they are in close proximity to their molecular targets, represents a promising approach, which may improve therapy of some hard-to-treat cancer types in the future.

The research in agents such as MitoTam or MitoVES has been hampered by the lack of suitable *in vivo* models more closely approximating the situation in a human tumour. Fortunately, the recent development of patient-derived xenografts (PDX) represents better option for testing the efficacy of novel cancer therapeutics than traditional testing of human cancer cell lines xenografts. Although it is important to keep in mind that PDX are still a model of an extremely complex disease, the variability of different patient samples and its maintenance in the form of tumours in an *in vivo* microenvironment have a potential to deliver responses much closer to the clinical situation. PDX sample can be implanted either subcutaneously or orthotopically, in the case of breast cancer PDXs directly into the mice mammary fat pad, into a natural microenvironment. This strategy may help to design personalized therapy for individual patients, such as testing of different treatment regimes. Moreover, with PDXs, it would be possible to test not only biomarkers, but also the

functional properties of a tumour, such as its respiratory activity. Overall, complex PDX models would more closely recapitulate the extremely heterogeneous nature of cancer, including the molecular landscape and resistance/sensitivity status which may help develop new strategies of treatment without inducing resistance to therapy.

Future plans based on the research summarized in this thesis will address the efficacy of MitoTam in PDX models of breast cancer. We plan to extend our focus from HER2^{high} breast cancer also to the triple-negative breast cancer subtype. This subtype has clinically extremely poor prognosis, with no targeted treatment available for patients diagnosed with this pathology. Interestingly, in contrast to other subtypes including HER2^{high} breast cancer samples, when implanted as a PDX, triple negative tumour samples show very high success rates of implantation. According to our preliminary data, although HER2^{high} cells are exceptionally sensitive to MitoTam, the agent efficiently suppresses also HER2-negative cells and it may therefore represent a novel therapeutic option for this hard-to-treat disease.

Another research line, derived from the presented research will address the mitochondrial fraction of HER2. The presence of HER2 in mitochondria was published in 2012 in a single report (Ding et al., 2012). In our work, we document, that mitochondrial HER2 is linked with the increased susceptibility of HER2^{high} cells to MitoTam (Rohlenova et al., 2016a; Rohlenova et al., 2016b). However, the precise function of this tyrosine kinase in mitochondria and its interaction partners remain to be elucidated. These questions are the main focus of the next publication planned by the author of this thesis.

6. CONCLUSIONS

This PhD project aimed to introduce new means to overcome resistance of breast cancer to therapy. Cells possessing stemness properties are recognized as one of the reasons for resistance to traditional therapy, and as a source of metastatic dissemination. Recently, these cells as well as other resistant sub-populations have been shown to comprise specific metabolic characteristics, such as high dependency on OXPHOS. In this thesis I document that these features are targetable by anti-cancer agents acting at mitochondrial ETC.

We established an *in vitro* model of mammary CSCs, the mammosphere culture in serum-free condition. We demonstrated that this model generates cell population with stemness properties and uncovered one of the molecular mechanisms, by which CSCs hide from the immune system by up-regulating the system of tryptophan uptake. Using MitoVES, an experimental anti-cancer agent developed in our laboratory in the past, we were able not only to eliminate CSCs with high efficacy, but also to suppress the Trp degradation machinery. Hence, we showed a potential mechanism for CSCs exposure to the immune system.

The main task of the author of the presented thesis was to characterise the newly synthesized agent, the TPP⁺ targeted tamoxifen, referred to as MitoTam. Mitochondrial targeting of tamoxifen enhanced its anti-cancer efficacy and broadened the spectrum of its applicability, as MitoTam is, unlike the parental compound, highly effective in HER2 overexpressing cells. The efficacy of MitoTam was confirmed *in vivo* using several mouse models, and, importantly, the drug proved to be well tolerated when administered to experimental animals.

We were successful to uncover the molecular mechanism of MitoTam's action. The respiratory complex I and its supercomplex assembly were identified as the principal targets. The efficacy of MitoTam is based on the induction of ROS production by inhibition of CI and, as a feedback loop, more ROS are produced because of the disruption of SCs. Moreover, we were able to uncover the basis for the unexpected sensitivity of HER2^{high} cells to MitoTam, which are otherwise resistant to tamoxifen. We showed that this phenomenon is dependent on the presence of a fraction of the HER2 protein in mitochondria.

MitoTam passed the official pre-clinical testing and a clinical trial is planned to start later in 2016/early 2017. This gives the agent a very high translational status. Thus, we present here a novel anti-cancer therapeutic; we were able not only to describe its basic scientific aspects, but also to successfully bring the drug to potential clinical use.

Coming back to the title of this thesis, "Targeting mitochondria to overcome the resistance of breast cancer to therapy", we show that mitochondrially-targeted agents directed at the ETC act by several distinct mechanisms that, in cooperation, provide the means to effectively overcome this resistance. By exploring these mechanisms we have contributed not only to the expansion of basic scientific knowledge, but also put forward a novel approach to breast cancer therapy potentially applicable in the clinical settings. Together, the aims of the presented research, as stated above, have been met.

7. REFERENCES

Acin-Perez, R., Bayona-Bafaluy, M. P., Fernandez-Silva, P., Moreno-Loshuertos, R., Perez-Martos, A., Bruno, C., Moraes, C. T., and Enriquez, J. A. (2004). Respiratory complex III is required to maintain complex I in mammalian mitochondria. *Mol Cell* **13**, 805-815.

Acin-Perez, R., and Enriquez, J. A. (2014). The function of the respiratory supercomplexes: the plasticity model. *Biochim Biophys Acta* **1837**, 444-450.

Acin-Perez, R., Fernandez-Silva, P., Peleato, M. L., Perez-Martos, A., and Enriquez, J. A. (2008). Respiratory active mitochondrial supercomplexes. *Mol Cell* **32**, 529-539.

Adam-Vizi, V., and Chinopoulos, C. (2006). Bioenergetics and the formation of mitochondrial reactive oxygen species. *Trends Pharmacol Sci* **27**, 639-645.

Adlam, V. J., Harrison, J. C., Porteous, C. M., James, A. M., Smith, R. A., Murphy, M. P., and Sammut, I. A. (2005). Targeting an antioxidant to mitochondria decreases cardiac ischemia-reperfusion injury. *FASEB J* **19**, 1088-1095.

Al-Hajj, M., Wicha, M. S., Benito-Hernandez, A., Morrison, S. J., and Clarke, M. F. (2003). Prospective identification of tumorigenic breast cancer cells. *Proc Natl Acad Sci U S A* **100**, 3983-3988.

Balsa, E., Marco, R., Perales-Clemente, E., Szklarczyk, R., Calvo, E., Landazuri, M. O., and Enriquez, J. A. (2012). NDUFA4 is a subunit of complex IV of the mammalian electron transport chain. *Cell Metab* **16**, 378-386.

Bayir, H., and Kagan, V. E. (2008). Bench-to-bedside review: Mitochondrial injury, oxidative stress and apoptosis--there is nothing more practical than a good theory. *Crit Care* **12**, 206.

Bhola, P. D., and Letai, A. (2016). Mitochondria-Judges and Executioners of Cell Death Sentences. *Mol Cell* **61**, 695-704.

Bienert, G. P., Moller, A. L., Kristiansen, K. A., Schulz, A., Moller, I. M., Schjoerring, J. K., and Jahn, T. P. (2007). Specific aquaporins facilitate the diffusion of hydrogen peroxide across membranes. *J Biol Chem* **282**, 1183-1192.

Birsoy, K., Wang, T., Chen, W. W., Freinkman, E., Abu-Remaileh, M., and Sabatini, D. M. (2015). An Essential Role of the Mitochondrial Electron Transport Chain in Cell Proliferation Is to Enable Aspartate Synthesis. *Cell* **162**, 540-551.

Boerner, J. L., Demory, M. L., Silva, C., and Parsons, S. J. (2004). Phosphorylation of Y845 on the epidermal growth factor receptor mediates binding to the mitochondrial protein cytochrome c oxidase subunit II. *Mol Cell Biol* **24**, 7059-7071.

Bollu, L. R., Ren, J., Blessing, A. M., Katreddy, R. R., Gao, G., Xu, L., Wang, J., Su, F., and Weihua, Z. (2014). Involvement of de novo synthesized palmitate and mitochondrial EGFR in EGF induced mitochondrial fusion of cancer cells. *Cell Cycle* **13**, 2415-2430.

Bonnet, S., Archer, S. L., Allalunis-Turner, J., Haromy, A., Beaulieu, C., Thompson, R., Lee, C. T., Lopaschuk, G. D., Puttagunta, L., Bonnet, S., *et al.* (2007). A mitochondria-K⁺ channel axis is suppressed in cancer and its normalization promotes apoptosis and inhibits cancer growth. *Cancer Cell* **11**, 37-51.

Brand, M. D. (2016). Mitochondrial generation of superoxide and hydrogen peroxide as the source of mitochondrial redox signaling. *Free Radic Biol Med*.

Calvo, S. E., Clauser, K. R., and Mootha, V. K. (2016). MitoCarta2.0: an updated inventory of mammalian mitochondrial proteins. *Nucleic Acids Res* **44**, D1251-1257.

Campbell, P. J., Yachida, S., Mudie, L. J., Stephens, P. J., Pleasance, E. D., Stebbings, L. A., Morsberger, L. A., Latimer, C., McLaren, S., Lin, M. L., *et al.* (2010). The patterns and dynamics of genomic instability in metastatic pancreatic cancer. *Nature* **467**, 1109-1113.

Cardinale, D., Colombo, A., Torrisi, R., Sandri, M. T., Civelli, M., Salvatici, M., Lamantia, G., Colombo, N., Cortinovis, S., Dessanai, M. A., *et al.* (2010). Trastuzumab-induced cardiotoxicity: clinical and prognostic implications of troponin I evaluation. *J Clin Oncol* **28**, 3910-3916.

Cecchini, G. (2003). Function and structure of complex II of the respiratory chain. *Annu Rev Biochem* **72**, 77-109.

Collins, A. T., Berry, P. A., Hyde, C., Stower, M. J., and Maitland, N. J. (2005). Prospective identification of tumorigenic prostate cancer stem cells. *Cancer Res* **65**, 10946-10951.

D'Uva, G., Aharonov, A., Lauriola, M., Kain, D., Yahalom-Ronen, Y., Carvalho, S., Weisinger, K., Bassat, E., Rajchman, D., Yifa, O., *et al.* (2015). ERBB2 triggers mammalian heart regeneration by promoting cardiomyocyte dedifferentiation and proliferation. *Nat Cell Biol* **17**, 627-638.

Dalerba, P., Dylla, S. J., Park, I. K., Liu, R., Wang, X., Cho, R. W., Hoey, T., Gurney, A., Huang, E. H., Simeone, D. M., *et al.* (2007). Phenotypic characterization of human colorectal cancer stem cells. *Proc Natl Acad Sci U S A* **104**, 10158-10163.

Davies, K. M., Anselmi, C., Wittig, I., Faraldo-Gomez, J. D., and Kuhlbrandt, W. (2012). Structure of the yeast F1Fo-ATP synthase dimer and its role in shaping the mitochondrial cristae. *Proc Natl Acad Sci U S A* **109**, 13602-13607.

Dawson, S. J., Makretsov, N., Blows, F. M., Driver, K. E., Provenzano, E., Le Quesne, J., Baglietto, L., Severi, G., Giles, G. G., McLean, C. A., *et al.* (2010). BCL2 in breast cancer: a favourable prognostic marker across molecular subtypes and independent of adjuvant therapy received. *Br J Cancer* **103**, 668-675.

Demory, M. L., Boerner, J. L., Davidson, R., Faust, W., Miyake, T., Lee, I., Huttemann, M., Douglas, R., Haddad, G., and Parsons, S. J. (2009). Epidermal growth factor receptor translocation to the mitochondria: regulation and effect. *J Biol Chem* **284**, 36592-36604.

DeSantis, C. E., Lin, C. C., Mariotto, A. B., Siegel, R. L., Stein, K. D., Kramer, J. L., Alteri, R., Robbins, A. S., and Jemal, A. (2014). Cancer treatment and survivorship statistics, 2014. *CA Cancer J Clin* **64**, 252-271.

Ding, Y., Liu, Z., Desai, S., Zhao, Y., Liu, H., Pannell, L. K., Yi, H., Wright, E. R., Owen, L. B., Dean-Colomb, W., *et al.* (2012). Receptor tyrosine kinase ErbB2 translocates into mitochondria and regulates cellular metabolism. *Nat Commun* **3**, 1271.

Dong, L. F., Jameson, V. J., Tilly, D., Cerny, J., Mahdavian, E., Marin-Hernandez, A., Hernandez-Esquivel, L., Rodriguez-Enriquez, S., Stursa, J., Witting, P. K., *et al.* (2011a). Mitochondrial targeting of vitamin E succinate enhances its pro-apoptotic and anti-cancer activity via mitochondrial complex II. *J Biol Chem* **286**, 3717-3728.

Dong, L. F., Jameson, V. J., Tilly, D., Prochazka, L., Rohlena, J., Valis, K., Truksa, J., Zobalova, R., Mahdavian, E., Kluckova, K., *et al.* (2011b). Mitochondrial targeting of alpha-tocopheryl succinate enhances its pro-apoptotic efficacy: a new paradigm for effective cancer therapy. *Free Radic Biol Med* **50**, 1546-1555.

Eramo, A., Lotti, F., Sette, G., Pilozzi, E., Biffoni, M., Di Virgilio, A., Conticello, C., Ruco, L., Peschle, C., and De Maria, R. (2008). Identification and expansion of the tumorigenic lung cancer stem cell population. *Cell Death Differ* **15**, 504-514.

Fruehauf, J. P., and Meyskens, F. L., Jr. (2007). Reactive oxygen species: a breath of life or death? *Clin Cancer Res* **13**, 789-794.

Galluzzi, L., Bravo-San Pedro, J. M., Vitale, I., Aaronson, S. A., Abrams, J. M., Adam, D., Alnemri, E. S., Altucci, L., Andrews, D., Annicchiarico-Petruzzelli, M., *et al.* (2015). Essential versus accessory aspects of cell death: recommendations of the NCCD 2015. *Cell Death Differ* **22**, 58-73.

Galluzzi, L., Kepp, O., Trojel-Hansen, C., and Kroemer, G. (2012). Mitochondrial control of cellular life, stress, and death. *Circ Res* **111**, 1198-1207.

Gane, E. J., Weilert, F., Orr, D. W., Keogh, G. F., Gibson, M., Lockhart, M. M., Frampton, C. M., Taylor, K. M., Smith, R. A., and Murphy, M. P. (2010). The mitochondria-targeted anti-oxidant mitoquinone decreases liver damage in a phase II study of hepatitis C patients. *Liver Int* **30**, 1019-1026.

Gerlinger, M., Rowan, A. J., Horswell, S., Larkin, J., Endesfelder, D., Gronroos, E., Martinez, P., Matthews, N., Stewart, A., Tarpey, P., *et al.* (2012). Intratumor heterogeneity and branched evolution revealed by multiregion sequencing. *N Engl J Med* **366**, 883-892.

Ginestier, C., Hur, M. H., Charafe-Jauffret, E., Monville, F., Dutcher, J., Brown, M., Jacquemier, J., Viens, P., Kleer, C. G., Liu, S., *et al.* (2007). ALDH1 is a marker of normal and malignant human mammary stem cells and a predictor of poor clinical outcome. *Cell Stem Cell* **1**, 555-567.

Hackenbrock, C. R., Chazotte, B., and Gupte, S. S. (1986). The random collision model and a critical assessment of diffusion and collision in mitochondrial electron transport. *J Bioenerg Biomembr* **18**, 331-368.

Hahn, A., Parey, K., Bublitz, M., Mills, D. J., Zickermann, V., Vonck, J., Kuhlbrandt, W., and Meier, T. (2016). Structure of a Complete ATP Synthase Dimer Reveals the Molecular Basis of Inner Mitochondrial Membrane Morphology. *Mol Cell*.

Han, D., Antunes, F., Canali, R., Rettori, D., and Cadenas, E. (2003). Voltage-dependent anion channels control the release of the superoxide anion from mitochondria to cytosol. *J Biol Chem* **278**, 5557-5563.

Higaki, Y., Mikami, T., Fujii, N., Hirshman, M. F., Koyama, K., Seino, T., Tanaka, K., and Goodyear, L. J. (2008). Oxidative stress stimulates skeletal muscle glucose uptake through a phosphatidylinositol 3-kinase-dependent pathway. *Am J Physiol Endocrinol Metab* **294**, E889-897.

Holmstrom, K. M., and Finkel, T. (2014). Cellular mechanisms and physiological consequences of redox-dependent signalling. *Nat Rev Mol Cell Biol* **15**, 411-421.

Hynes, N. E., and Lane, H. A. (2005). ERBB receptors and cancer: the complexity of targeted inhibitors. *Nat Rev Cancer* **5**, 341-354.

Chacko, B. K., Reily, C., Srivastava, A., Johnson, M. S., Ye, Y., Ulasova, E., Agarwal, A., Zinn, K. R., Murphy, M. P., Kalyanaraman, B., and Darley-Usmar, V. (2010). Prevention of diabetic nephropathy in Ins2(+/-)(AkitaJ) mice by the mitochondria-targeted therapy MitoQ. *Biochem J* **432**, 9-19.

Chance, B., and Williams, G. R. (1955). A simple and rapid assay of oxidative phosphorylation. *Nature* **175**, 1120-1121.

Chandel, N. S., McClintock, D. S., Feliciano, C. E., Wood, T. M., Melendez, J. A., Rodriguez, A. M., and Schumacker, P. T. (2000). Reactive oxygen species generated at mitochondrial complex III stabilize hypoxia-inducible factor-1alpha during hypoxia: a mechanism of O2 sensing. *J Biol Chem* **275**, 25130-25138.

Chen, Q., and Lesnefsky, E. J. (2006). Depletion of cardiolipin and cytochrome c during ischemia increases hydrogen peroxide production from the electron transport chain. *Free Radic Biol Med* **40**, 976-982.

Cheng, G., Zielonka, J., Ouari, O., Lopez, M., McAllister, D., Boyle, K., Barrios, C. S., Weber, J. J., Johnson, B. D., Hardy, M., *et al.* (2016). Mitochondria-Targeted Analogues of Metformin Exhibit Enhanced Antiproliferative and Radiosensitizing Effects in Pancreatic Cancer Cells. *Cancer Res* **76**, 3904-3915.

Chiarugi, P., and Fiaschi, T. (2007). Redox signalling in anchorage-dependent cell growth. *Cell Signal* **19**, 672-682.

Ishikawa, K., Takenaga, K., Akimoto, M., Koshikawa, N., Yamaguchi, A., Imanishi, H., Nakada, K., Honma, Y., and Hayashi, J. (2008). ROS-generating mitochondrial DNA mutations can regulate tumor cell metastasis. *Science* **320**, 661-664.

Iwata, S., Lee, J. W., Okada, K., Lee, J. K., Iwata, M., Rasmussen, B., Link, T. A., Ramaswamy, S., and Jap, B. K. (1998). Complete structure of the 11-subunit bovine mitochondrial cytochrome bc1 complex. *Science* **281**, 64-71.

Keefe, D. L. (2002). Trastuzumab-associated cardiotoxicity. *Cancer* **95**, 1592-1600.

Khalique, L., Ayhan, A., Weale, M. E., Jacobs, I. J., Ramus, S. J., and Gayther, S. A. (2007). Genetic intra-tumour heterogeneity in epithelial ovarian cancer and its implications for molecular diagnosis of tumours. *J Pathol* **211**, 286-295.

Kluckova, K., Sticha, M., Cerny, J., Mracek, T., Dong, L., Drahota, Z., Gottlieb, E., Neuzil, J., and Rohlena, J. (2015). Ubiquinone-binding site mutagenesis reveals the role of mitochondrial complex II in cell death initiation. *Cell Death Dis* **6**, e1749.

- Koopman, W. J., Willems, P. H., and Smeitink, J. A. (2012). Monogenic mitochondrial disorders. *N Engl J Med* **366**, 1132-1141.
- Koppenol, W. H., Bounds, P. L., and Dang, C. V. (2011). Otto Warburg's contributions to current concepts of cancer metabolism. *Nat Rev Cancer* **11**, 325-337.
- Kordes, S., Pollak, M. N., Zwinderman, A. H., Mathot, R. A., Weterman, M. J., Beeker, A., Punt, C. J., Richel, D. J., and Wilmink, J. W. (2015). Metformin in patients with advanced pancreatic cancer: a double-blind, randomised, placebo-controlled phase 2 trial. *Lancet Oncol* **16**, 839-847.
- Kovarova, N., Mracek, T., Nuskova, H., Holzerova, E., Vrbacky, M., Pecina, P., Hejzlarova, K., Kluckova, K., Rohlena, J., Neuzil, J., and Houstek, J. (2013). High molecular weight forms of mammalian respiratory chain complex II. *PLoS One* **8**, e71869.
- Lapidot, T., Sirard, C., Vormoor, J., Murdoch, B., Hoang, T., Caceres-Cortes, J., Minden, M., Paterson, B., Caligiuri, M. A., and Dick, J. E. (1994). A cell initiating human acute myeloid leukaemia after transplantation into SCID mice. *Nature* **367**, 645-648.
- Lee, S. R., Yang, K. S., Kwon, J., Lee, C., Jeong, W., and Rhee, S. G. (2002). Reversible inactivation of the tumor suppressor PTEN by H₂O₂. *J Biol Chem* **277**, 20336-20342.
- Lemarie, A., Huc, L., Pazarentzos, E., Mahul-Mellier, A. L., and Grimm, S. (2011). Specific disintegration of complex II succinate:ubiquinone oxidoreductase links pH changes to oxidative stress for apoptosis induction. *Cell Death Differ* **18**, 338-349.
- Li, C., Heidt, D. G., Dalerba, P., Burant, C. F., Zhang, L., Adsay, V., Wicha, M., Clarke, M. F., and Simeone, D. M. (2007). Identification of pancreatic cancer stem cells. *Cancer Res* **67**, 1030-1037.
- Li, C., Wu, J. J., Hynes, M., Dosch, J., Sarkar, B., Welling, T. H., Pasca di Magliano, M., and Simeone, D. M. (2011). c-Met is a marker of pancreatic cancer stem cells and therapeutic target. *Gastroenterology* **141**, 2218-2227 e2215.
- Lindstrom, L. S., Karlsson, E., Wilking, U. M., Johansson, U., Hartman, J., Lidbrink, E. K., Hatschek, T., Skoog, L., and Bergh, J. (2012). Clinically used breast cancer markers such as estrogen receptor, progesterone receptor, and human epidermal growth factor receptor 2 are unstable throughout tumor progression. *J Clin Oncol* **30**, 2601-2608.
- Liu, X., Kim, C. N., Yang, J., Jemmerson, R., and Wang, X. (1996). Induction of apoptotic program in cell-free extracts: requirement for dATP and cytochrome c. *Cell* **86**, 147-157.

- Liu, X., Newton, R. C., Friedman, S. M., and Scherle, P. A. (2009). Indoleamine 2,3-dioxygenase, an emerging target for anti-cancer therapy. *Curr Cancer Drug Targets* **9**, 938-952.
- Lonardo, E., Cioffi, M., Sancho, P., Sanchez-Ripoll, Y., Trabulo, S. M., Dorado, J., Balic, A., Hidalgo, M., and Heeschen, C. (2013). Metformin targets the metabolic achilles heel of human pancreatic cancer stem cells. *PLoS One* **8**, e76518.
- Madjd, Z., Mehrjerdi, A. Z., Sharifi, A. M., Molanaei, S., Shahzadi, S. Z., and Asadi-Lari, M. (2009). CD44+ cancer cells express higher levels of the anti-apoptotic protein Bcl-2 in breast tumours. *Cancer Immun* **9**, 4.
- Martindale, J. L., and Holbrook, N. J. (2002). Cellular response to oxidative stress: signaling for suicide and survival. *J Cell Physiol* **192**, 1-15.
- Meyer, B., Wittig, I., Trifilieff, E., Karas, M., and Schagger, H. (2007). Identification of two proteins associated with mammalian ATP synthase. *Mol Cell Proteomics* **6**, 1690-1699.
- Meyer, M. J., Fleming, J. M., Lin, A. F., Hussnain, S. A., Ginsburg, E., and Vonderhaar, B. K. (2010). CD44posCD49fhiCD133/2hi defines xenograft-initiating cells in estrogen receptor-negative breast cancer. *Cancer Res* **70**, 4624-4633.
- Miraglia, S., Godfrey, W., Yin, A. H., Atkins, K., Warnke, R., Holden, J. T., Bray, R. A., Waller, E. K., and Buck, D. W. (1997). A novel five-transmembrane hematopoietic stem cell antigen: isolation, characterization, and molecular cloning. *Blood* **90**, 5013-5021.
- Modica-Napolitano, J. S., and Aprille, J. R. (1987). Basis for the selective cytotoxicity of rhodamine 123. *Cancer Res* **47**, 4361-4365.
- Moreira, P. I., Custodio, J., Moreno, A., Oliveira, C. R., and Santos, M. S. (2006). Tamoxifen and estradiol interact with the flavin mononucleotide site of complex I leading to mitochondrial failure. *J Biol Chem* **281**, 10143-10152.
- Moreno-Lastres, D., Fontanesi, F., Garcia-Consuegra, I., Martin, M. A., Arenas, J., Barrientos, A., and Ugalde, C. (2012). Mitochondrial complex I plays an essential role in human respirasome assembly. *Cell Metab* **15**, 324-335.
- Moreno-Sanchez, R., Hernandez-Esquivel, L., Rivero-Segura, N. A., Marin-Hernandez, A., Neuzil, J., Ralph, S. J., and Rodriguez-Enriquez, S. (2013). Reactive oxygen species are generated by the respiratory complex II--evidence for lack of contribution of the reverse electron flow in complex I. *FEBS J* **280**, 927-938.

- Murphy, M. P. (2008). Targeting lipophilic cations to mitochondria. *Biochim Biophys Acta* **1777**, 1028-1031.
- Naresh, A., Thor, A. D., Edgerton, S. M., Torkko, K. C., Kumar, R., and Jones, F. E. (2008). The HER4/4ICD estrogen receptor coactivator and BH3-only protein is an effector of tamoxifen-induced apoptosis. *Cancer Res* **68**, 6387-6395.
- Neupert, W., and Herrmann, J. M. (2007). Translocation of proteins into mitochondria. *Annu Rev Biochem* **76**, 723-749.
- Neuzil, J., Dong, L. F., Rohlena, J., Truksa, J., and Ralph, S. J. (2013). Classification of mitocans, anti-cancer drugs acting on mitochondria. *Mitochondrion* **13**, 199-208.
- Nogueira, V., Park, Y., Chen, C. C., Xu, P. Z., Chen, M. L., Tonic, I., Unterman, T., and Hay, N. (2008). Akt determines replicative senescence and oxidative or oncogenic premature senescence and sensitizes cells to oxidative apoptosis. *Cancer Cell* **14**, 458-470.
- Okoh, V. O., Garba, N. A., Penney, R. B., Das, J., Deoraj, A., Singh, K. P., Sarkar, S., Felty, Q., Yoo, C., Jackson, R. M., and Roy, D. (2015). Redox signalling to nuclear regulatory proteins by reactive oxygen species contributes to oestrogen-induced growth of breast cancer cells. *Br J Cancer* **112**, 1687-1702.
- Orsucci, D., Mancuso, M., Ienco, E. C., LoGerfo, A., and Siciliano, G. (2011). Targeting mitochondrial dysfunction and neurodegeneration by means of coenzyme Q10 and its analogues. *Curr Med Chem* **18**, 4053-4064.
- Pasdar, E. A., Smits, M., Stapelberg, M., Bajzikova, M., Stantic, M., Goodwin, J., Yan, B., Stursa, J., Kovarova, J., Sachaphibulkij, K., *et al.* (2015). Characterisation of mesothelioma-initiating cells and their susceptibility to anti-cancer agents. *PLoS One* **10**, e0119549.
- Pavlova, N. N., and Thompson, C. B. (2016). The Emerging Hallmarks of Cancer Metabolism. *Cell Metab* **23**, 27-47.
- Perillo, B., Sasso, A., Abbondanza, C., and Palumbo, G. (2000). 17beta-estradiol inhibits apoptosis in MCF-7 cells, inducing bcl-2 expression via two estrogen-responsive elements present in the coding sequence. *Mol Cell Biol* **20**, 2890-2901.
- Pfeiffer, T., Schuster, S., and Bonhoeffer, S. (2001). Cooperation and competition in the evolution of ATP-producing pathways. *Science* **292**, 504-507.

Prochazka, L., Koudelka, S., Dong, L. F., Stursa, J., Goodwin, J., Neca, J., Slavik, J., Ciganek, M., Masek, J., Kluckova, K., *et al.* (2013). Mitochondrial targeting overcomes ABCA1-dependent resistance of lung carcinoma to alpha-tocopheryl succinate. *Apoptosis* **18**, 286-299.

Quinlan, C. L., Perevoshchikova, I. V., Hey-Mogensen, M., Orr, A. L., and Brand, M. D. (2013). Sites of reactive oxygen species generation by mitochondria oxidizing different substrates. *Redox Biol* **1**, 304-312.

Quintana, E., Shackleton, M., Foster, H. R., Fullen, D. R., Sabel, M. S., Johnson, T. M., and Morrison, S. J. (2010). Phenotypic heterogeneity among tumorigenic melanoma cells from patients that is reversible and not hierarchically organized. *Cancer Cell* **18**, 510-523.

Ralph, S. J., Rodriguez-Enriquez, S., Neuzil, J., and Moreno-Sanchez, R. (2010). Bioenergetic pathways in tumor mitochondria as targets for cancer therapy and the importance of the ROS-induced apoptotic trigger. *Mol Aspects Med* **31**, 29-59.

Reni, M., Dugnani, E., Cereda, S., Belli, C., Balzano, G., Nicoletti, R., Liberati, D., Pasquale, V., Scavini, M., Maggiora, P., *et al.* (2016). (Ir)relevance of Metformin Treatment in Patients with Metastatic Pancreatic Cancer: An Open-Label, Randomized Phase II Trial. *Clin Cancer Res* **22**, 1076-1085.

Ricci-Vitiani, L., Lombardi, D. G., Pilozzi, E., Biffoni, M., Todaro, M., Peschle, C., and De Maria, R. (2007). Identification and expansion of human colon-cancer-initiating cells. *Nature* **445**, 111-115.

Ricci, J. E., Munoz-Pinedo, C., Fitzgerald, P., Bailly-Maitre, B., Perkins, G. A., Yadava, N., Scheffler, I. E., Ellisman, M. H., and Green, D. R. (2004). Disruption of mitochondrial function during apoptosis is mediated by caspase cleavage of the p75 subunit of complex I of the electron transport chain. *Cell* **117**, 773-786.

Roesch, A., Vultur, A., Bogeski, I., Wang, H., Zimmermann, K. M., Speicher, D., Korbel, C., Laschke, M. W., Gimotty, P. A., Philipp, S. E., *et al.* (2013). Overcoming intrinsic multidrug resistance in melanoma by blocking the mitochondrial respiratory chain of slow-cycling JARID1B(high) cells. *Cancer Cell* **23**, 811-825.

Rohlena, J., Dong, L. F., and Neuzil, J. (2013). Targeting the mitochondrial electron transport chain complexes for the induction of apoptosis and cancer treatment. *Curr Pharm Biotechnol* **14**, 377-389.

Rohlenova, K., Neuzil, J., and Rohlena, J. (2016a). The role of Her2 and other oncogenes of the PI3K/AKT pathway in mitochondria. *Biol Chem* **397**, 607-615.

Rohlenova, K., Sachaphibulkij, K., Stursa, J., Bezawork-Geleta, A., Blecha, J., Endaya, B., Werner, L., Cerny, J., Zobalova, R., Goodwin, J., *et al.* (2016b). Selective disruption of respiratory supercomplexes as a new strategy to suppress Her2-high breast cancer. *Antioxid Redox Signal*.

Sancho, P., Burgos-Ramos, E., Tavera, A., Bou Kheir, T., Jagust, P., Schoenhals, M., Barneda, D., Sellers, K., Campos-Olivas, R., Grana, O., *et al.* (2015). MYC/PGC-1alpha Balance Determines the Metabolic Phenotype and Plasticity of Pancreatic Cancer Stem Cells. *Cell Metab* **22**, 590-605.

Shmelkov, S. V., Butler, J. M., Hooper, A. T., Hormigo, A., Kushner, J., Milde, T., St Clair, R., Baljevic, M., White, I., Jin, D. K., *et al.* (2008). CD133 expression is not restricted to stem cells, and both CD133+ and CD133- metastatic colon cancer cells initiate tumors. *J Clin Invest* **118**, 2111-2120.

Schagger, H. (2002). Respiratory chain supercomplexes of mitochondria and bacteria. *Biochim Biophys Acta* **1555**, 154-159.

Schagger, H., Cramer, W. A., and von Jagow, G. (1994). Analysis of molecular masses and oligomeric states of protein complexes by blue native electrophoresis and isolation of membrane protein complexes by two-dimensional native electrophoresis. *Anal Biochem* **217**, 220-230.

Schagger, H., and Pfeiffer, K. (2000). Supercomplexes in the respiratory chains of yeast and mammalian mitochondria. *EMBO J* **19**, 1777-1783.

Schnitt, S. J. (2010). Classification and prognosis of invasive breast cancer: from morphology to molecular taxonomy. *Mod Pathol* **23 Suppl 2**, S60-64.

Schriewer, J. M., Peek, C. B., Bass, J., and Schumacker, P. T. (2013). ROS-mediated PARP activity undermines mitochondrial function after permeability transition pore opening during myocardial ischemia-reperfusion. *J Am Heart Assoc* **2**, e000159.

Schuh, A., Becq, J., Humphray, S., Alexa, A., Burns, A., Clifford, R., Feller, S. M., Grocock, R., Henderson, S., Khrebtukova, I., *et al.* (2012). Monitoring chronic lymphocytic leukemia progression by whole genome sequencing reveals heterogeneous clonal evolution patterns. *Blood* **120**, 4191-4196.

Siebels, I., and Drose, S. (2013). Q-site inhibitor induced ROS production of mitochondrial complex II is attenuated by TCA cycle dicarboxylates. *Biochim Biophys Acta* **1827**, 1156-1164.

Siegel, R. L., Miller, K. D., and Jemal, A. (2016). Cancer statistics, 2016. *CA Cancer J Clin* **66**, 7-30.

Silva, I. A., Bai, S., McLean, K., Yang, K., Griffith, K., Thomas, D., Ginestier, C., Johnston, C., Kueck, A., Reynolds, R. K., *et al.* (2011). Aldehyde dehydrogenase in combination with CD133 defines angiogenic ovarian cancer stem cells that portend poor patient survival. *Cancer Res* **71**, 3991-4001.

Singh, S. K., Clarke, I. D., Terasaki, M., Bonn, V. E., Hawkins, C., Squire, J., and Dirks, P. B. (2003). Identification of a cancer stem cell in human brain tumors. *Cancer Res* **63**, 5821-5828.

Smart, C. E., Morrison, B. J., Saunus, J. M., Vargas, A. C., Keith, P., Reid, L., Wockner, L., Askarian-Amiri, M., Sarkar, D., Simpson, P. T., *et al.* (2013). In vitro analysis of breast cancer cell line tumourspheres and primary human breast epithelia mammospheres demonstrates inter- and intrasphere heterogeneity. *PLoS One* **8**, e64388.

Smerage, J. B., Budd, G. T., Doyle, G. V., Brown, M., Paoletti, C., Muniz, M., Miller, M. C., Repollet, M. I., Chianese, D. A., Connelly, M. C., *et al.* (2013). Monitoring apoptosis and Bcl-2 on circulating tumor cells in patients with metastatic breast cancer. *Mol Oncol* **7**, 680-692.

Smith, R. A., Porteous, C. M., Gane, A. M., and Murphy, M. P. (2003). Delivery of bioactive molecules to mitochondria in vivo. *Proc Natl Acad Sci U S A* **100**, 5407-5412.

St-Pierre, J., Buckingham, J. A., Roebuck, S. J., and Brand, M. D. (2002). Topology of superoxide production from different sites in the mitochondrial electron transport chain. *J Biol Chem* **277**, 44784-44790.

Stapelberg, M., Zobalova, R., Nguyen, M. N., Walker, T., Stantic, M., Goodwin, J., Pasdar, E. A., Thai, T., Prokopova, K., Yan, B., *et al.* (2014). Indoleamine-2,3-dioxygenase elevated in tumor-initiating cells is suppressed by mitocans. *Free Radic Biol Med* **67**, 41-50.

Stewart, J. M., Shaw, P. A., Gedye, C., Bernardini, M. Q., Neel, B. G., and Ailles, L. E. (2011). Phenotypic heterogeneity and instability of human ovarian tumor-initiating cells. *Proc Natl Acad Sci U S A* **108**, 6468-6473.

Stroh, A., Anderka, O., Pfeiffer, K., Yagi, T., Finel, M., Ludwig, B., and Schagger, H. (2004). Assembly of respiratory complexes I, III, and IV into NADH oxidase supercomplex stabilizes complex I in *Paracoccus denitrificans*. *J Biol Chem* **279**, 5000-5007.

Sullivan, L. B., Gui, D. Y., Hosios, A. M., Bush, L. N., Freinkman, E., and Vander Heiden, M. G. (2015). Supporting Aspartate Biosynthesis Is an Essential Function of Respiration in Proliferating Cells. *Cell* **162**, 552-563.

Sun, F., Huo, X., Zhai, Y., Wang, A., Xu, J., Su, D., Bartlam, M., and Rao, Z. (2005). Crystal structure of mitochondrial respiratory membrane protein complex II. *Cell* **121**, 1043-1057.

- Sundaresan, M., Yu, Z. X., Ferrans, V. J., Irani, K., and Finkel, T. (1995). Requirement for generation of H₂O₂ for platelet-derived growth factor signal transduction. *Science* **270**, 296-299.
- Tait, S. W., and Green, D. R. (2010). Mitochondria and cell death: outer membrane permeabilization and beyond. *Nat Rev Mol Cell Biol* **11**, 621-632.
- Tait, S. W., and Green, D. R. (2012). Mitochondria and cell signalling. *J Cell Sci* **125**, 807-815.
- Tan, A. S., Baty, J. W., Dong, L. F., Bezawork-Geleta, A., Endaya, B., Goodwin, J., Bajzikova, M., Kovarova, J., Peterka, M., Yan, B., *et al.* (2015). Mitochondrial genome acquisition restores respiratory function and tumorigenic potential of cancer cells without mitochondrial DNA. *Cell Metab* **21**, 81-94.
- Thomas, S. R., Salahifar, H., Mashima, R., Hunt, N. H., Richardson, D. R., and Stocker, R. (2001). Antioxidants inhibit indoleamine 2,3-dioxygenase in IFN-gamma-activated human macrophages: posttranslational regulation by pyrrolidine dithiocarbamate. *J Immunol* **166**, 6332-6340.
- Tormos, K. V., Anso, E., Hamanaka, R. B., Eisenbart, J., Joseph, J., Kalyanaraman, B., and Chandel, N. S. (2011). Mitochondrial complex III ROS regulate adipocyte differentiation. *Cell Metab* **14**, 537-544.
- Toyokuni, S., Okamoto, K., Yodoi, J., and Hiai, H. (1995). Persistent oxidative stress in cancer. *FEBS Lett* **358**, 1-3.
- Truksa, J., Dong, L. F., Rohlena, J., Stursa, J., Vondrusova, M., Goodwin, J., Nguyen, M., Kluckova, K., Rychtarcikova, Z., Lettlova, S., *et al.* (2015). Mitochondrially targeted vitamin E succinate modulates expression of mitochondrial DNA transcripts and mitochondrial biogenesis. *Antioxid Redox Signal* **22**, 883-900.
- Tsujimoto, Y., and Shimizu, S. (2007). Role of the mitochondrial membrane permeability transition in cell death. *Apoptosis* **12**, 835-840.
- Tsukihara, T., Aoyama, H., Yamashita, E., Tomizaki, T., Yamaguchi, H., Shinzawa-Itoh, K., Nakashima, R., Yaono, R., and Yoshikawa, S. (1996). The whole structure of the 13-subunit oxidized cytochrome c oxidase at 2.8 Å. *Science* **272**, 1136-1144.
- Uchida, N., Buck, D. W., He, D., Reitsma, M. J., Masek, M., Phan, T. V., Tsukamoto, A. S., Gage, F. H., and Weissman, I. L. (2000). Direct isolation of human central nervous system stem cells. *Proc Natl Acad Sci U S A* **97**, 14720-14725.

Vaillant, F., Merino, D., Lee, L., Breslin, K., Pal, B., Ritchie, M. E., Smyth, G. K., Christie, M., Phillipson, L. J., Burns, C. J., *et al.* (2013). Targeting BCL-2 with the BH3 mimetic ABT-199 in estrogen receptor-positive breast cancer. *Cancer Cell* **24**, 120-129.

Vander Heiden, M. G., Cantley, L. C., and Thompson, C. B. (2009). Understanding the Warburg effect: the metabolic requirements of cell proliferation. *Science* **324**, 1029-1033.

Viale, A., Pettazzoni, P., Lyssiotis, C. A., Ying, H., Sanchez, N., Marchesini, M., Carugo, A., Green, T., Seth, S., Giuliani, V., *et al.* (2014). Oncogene ablation-resistant pancreatic cancer cells depend on mitochondrial function. *Nature* **514**, 628-632.

Vidal, G. A., Naresh, A., Marrero, L., and Jones, F. E. (2005). Presenilin-dependent gamma-secretase processing regulates multiple ERBB4/HER4 activities. *J Biol Chem* **280**, 19777-19783.

Vinothkumar, K. R., Zhu, J., and Hirst, J. (2014). Architecture of mammalian respiratory complex I. *Nature* **515**, 80-84.

Wallace, D. C. (2012). Mitochondria and cancer. *Nat Rev Cancer* **12**, 685-698.

Wang, Y. C., Morrison, G., Gillihan, R., Guo, J., Ward, R. M., Fu, X., Botero, M. F., Healy, N. A., Hilsenbeck, S. G., Phillips, G. L., *et al.* (2011). Different mechanisms for resistance to trastuzumab versus lapatinib in HER2-positive breast cancers--role of estrogen receptor and HER2 reactivation. *Breast Cancer Res* **13**, R121.

Warburg, O. (1925). The Metabolism of Carcinoma Cells. *The Journal of Cancer Research* **9**, 148-163.

Warburg, O. (1956). On the origin of cancer cells. *Science* **123**, 309-314.

Ward, P. S., and Thompson, C. B. (2012). Metabolic reprogramming: a cancer hallmark even warburg did not anticipate. *Cancer Cell* **21**, 297-308.

Weinberg, F., Hamanaka, R., Wheaton, W. W., Weinberg, S., Joseph, J., Lopez, M., Kalyanaraman, B., Mutlu, G. M., Budinger, G. R., and Chandel, N. S. (2010). Mitochondrial metabolism and ROS generation are essential for Kras-mediated tumorigenicity. *Proc Natl Acad Sci U S A* **107**, 8788-8793.

Wilkens, V., Kohl, W., and Busch, K. (2013). Restricted diffusion of OXPHOS complexes in dynamic mitochondria delays their exchange between cristae and engenders a transitory mosaic distribution. *J Cell Sci* **126**, 103-116.

- Wirth, C., Brandt, U., Hunte, C., and Zickermann, V. (2016). Structure and function of mitochondrial complex I. *Biochim Biophys Acta* **1857**, 902-914.
- Wittig, I., and Schagger, H. (2008). Structural organization of mitochondrial ATP synthase. *Biochim Biophys Acta* **1777**, 592-598.
- Wright, M. H., Calcagno, A. M., Salcido, C. D., Carlson, M. D., Ambudkar, S. V., and Varticovski, L. (2008). Brca1 breast tumors contain distinct CD44+/CD24- and CD133+ cells with cancer stem cell characteristics. *Breast Cancer Res* **10**, R10.
- Yan, B., Stantic, M., Zobalova, R., Bezawork-Geleta, A., Stapelberg, M., Stursa, J., Prokopova, K., Dong, L., and Neuzil, J. (2015). Mitochondrially targeted vitamin E succinate efficiently kills breast tumour-initiating cells in a complex II-dependent manner. *BMC Cancer* **15**, 401.
- Yanamala, N., Kapralov, A. A., Djukic, M., Peterson, J., Mao, G., Klein-Seetharaman, J., Stoyanovsky, D. A., Stursa, J., Neuzil, J., and Kagan, V. E. (2014). Structural re-arrangement and peroxidase activation of cytochrome c by anionic analogues of vitamin E, tocopherol succinate and tocopherol phosphate. *J Biol Chem* **289**, 32488-32498.
- Ye, X. Q., Li, Q., Wang, G. H., Sun, F. F., Huang, G. J., Bian, X. W., Yu, S. C., and Qian, G. S. (2011). Mitochondrial and energy metabolism-related properties as novel indicators of lung cancer stem cells. *Int J Cancer* **129**, 820-831.
- Zhang, J., Khvorostov, I., Hong, J. S., Oktay, Y., Vergnes, L., Nuebel, E., Wahjudi, P. N., Setoguchi, K., Wang, G., Do, A., *et al.* (2011). UCP2 regulates energy metabolism and differentiation potential of human pluripotent stem cells. *EMBO J* **30**, 4860-4873.
- Zhang, S., Balch, C., Chan, M. W., Lai, H. C., Matei, D., Schilder, J. M., Yan, P. S., Huang, T. H., and Nephew, K. P. (2008). Identification and characterization of ovarian cancer-initiating cells from primary human tumors. *Cancer Res* **68**, 4311-4320.
- Zhang, X., Fryknas, M., Hernlund, E., Fayad, W., De Milito, A., Olofsson, M. H., Gogvadze, V., Dang, L., Pahlman, S., Schughart, L. A., *et al.* (2014). Induction of mitochondrial dysfunction as a strategy for targeting tumour cells in metabolically compromised microenvironments. *Nat Commun* **5**, 3295.
- Zickermann, V., Wirth, C., Nasiri, H., Siegmund, K., Schwalbe, H., Hunte, C., and Brandt, U. (2015). Structural biology. Mechanistic insight from the crystal structure of mitochondrial complex I. *Science* **347**, 44-49.

Zobalova, R., McDermott, L., Stantic, M., Prokopova, K., Dong, L. F., and Neuzil, J. (2008). CD133-positive cells are resistant to TRAIL due to up-regulation of FLIP. *Biochem Biophys Res Commun* **373**, 567-571.

Zobalova, R., Prokopova, K., Stantic, M., Stapelberg, M., Dong, L. F., Ralph, S. J., Akporiaye, E., and Neuzil, J. (2011). The potential role of CD133 in immune surveillance and apoptosis: a mitochondrial connection? *Antioxid Redox Signal* **15**, 2989-3002.

Zu, X. L., and Guppy, M. (2004). Cancer metabolism: facts, fantasy, and fiction. *Biochem Biophys Res Commun* **313**, 459-465.